

The Effects of Air Pollution on Respiratory Bacteria

Thesis submitted for the degree of

Doctor of Philosophy

at the University of Leicester

By

Shane J. K. Hussey BSc (Hons)

Department of Genetics

University of Leicester

2016

Abstract

The Effects of Air Pollution on Respiratory Bacteria

By Shane Hussey

Particulate Matter (PM), a major component of air pollution, is associated with a variety of cardiorespiratory diseases including acute lower respiratory tract infections. It is well established that PM has detrimental effects on the host, causing tissue damage, oxidative stress, and modulating the immune system. However there has been extremely limited research into the effects of PM on bacteria, the organisms responsible for the respiratory infections associated with PM exposure.

This project investigated whether Black Carbon (BC), a major component of PM produced as a by-product of fossil fuel combustion, directly affects respiratory tract bacteria. Two model opportunistic pathogens of the respiratory tract were chosen for this investigation, *Streptococcus pneumoniae* and *Staphylococcus aureus*.

BC was found to alter biofilm formation, structure, matrix composition, and functioning, of both *S. pneumoniae* and *S. aureus*, as well as inhibiting planktonic growth. Interestingly, these effects were strain-dependent. Furthermore, BC promoted dissemination of *S. pneumoniae* from the nasopharynx to the lower respiratory tract in an *in vivo* murine colonisation model. BC was not observed to alter the respiratory tract microbiota in this project, however a variety of limitations which may have prevented a definitive conclusion being reached are presented.

This study provides the first evidence to show that bacteria are directly affected by PM, and thereby suggests that the adverse health effects of PM may not only be due to effects on host tissues, but that modulation of bacterial behaviour may also have a role. The findings of this study therefore show the potential importance of this overlooked field.

Acknowledgements

Firstly I would like to thank my primary supervisor, Dr. Julie Morrissey. Thank you for all your support and guidance throughout my PhD, reading countless drafts of reports and my thesis, and for putting up with me, particularly when I'd threaten to run away before every presentation. Thank you for taking me on four years ago (even though I know you only did it as Peter made you).

Next I would like to thank Prof. Peter Andrew, Prof. Julian Ketley, Prof. Paul Monks, and Dr. Chris Bayliss. Thank you for all your support and insight over the last few years in supervisory and thesis committee meetings. Peter, you were my undergraduate supervisor and convinced me to apply for this PhD four years ago, so without you I wouldn't be here now. Peter, Paul, and Julian, our supervisor meetings have given me a thick skin, you were all truly terrifying to argue against.

I would also like to thank everyone in Adrian lab 121, especially Becky, Vickesh, Jo, Jamie, Rich, and Adam. Becky and Vickesh, you both helped me when I had no idea what I was doing, listened to me whinge, and got me through the first couple of years (until you both unfairly abandoned me when you finished your PhDs).

Natalie Allcock and Stefan Hyman, thank you for letting me hide out in your lab playing with your electron microscopes, and taking the time to teach me. Stefan, you are missed.

To my family, specifically my sister Fern, thank you for supporting me and taking an interest in my work, even if you didn't really know what I was doing.

Finally, Joe, you have supported me through every step of my PhD and I couldn't have done it without you. You let me complain about lab work, give you daily updates about my thesis writing, and listened even when you had no idea what I was talking about. Thank you for being there for me.

Contents

Abstract	i
Acknowledgements	ii
List of Tables	xi
List of Figures	xii
Abbreviations	xv
Chapter 1. Introduction	1
1.1. Particulate Matter	2
1.1.1. Size range and deposition of particulate matter	3
1.1.2. Primary and secondary particles.....	5
1.1.3. Generation of particulate matter.....	5
1.1.4. Current particulate matter exposure guidelines.....	6
1.1.5. Black Carbon.....	8
1.2. Increased morbidity and mortality caused by exposure to particulate matter	12
1.2.1. Variation in disease associations.....	13
1.3. Diseases associated with particulate matter exposure	15
1.3.1. Respiratory infections and alterations in respiratory health associated with particulate matter exposure.....	16
1.4. The impact of reducing particulate matter emissions.....	17
1.5. Mechanisms by which particulate matter causes disease	17
1.5.1. Cardiovascular effects.....	17
1.5.2. Respiratory effects.....	18

1.5.3. Specific mechanisms for alterations in host susceptibility to respiratory infection	19
1.6. Bacteria associated with particulate matter	21
1.7. The respiratory tract microbiota.....	23
1.8. <i>Streptococcus pneumoniae</i>	23
1.8.1. Virulence determinants of <i>S. pneumoniae</i>	25
1.9. <i>Staphylococcus aureus</i>	27
1.9.1. The <i>S. aureus</i> genome and Methicillin-Resistant <i>S. aureus</i>	28
1.9.2. Virulence determinants of <i>S. aureus</i>	30
1.10. Bacterial biofilm formation.....	31
1.10.1. Pneumococcal biofilms.....	34
1.10.2. <i>S. aureus</i> biofilms	36
1.11. Effects of particulate matter on microbiota diversity	39
1.12. Effects of particulate matter and other inhaled compounds on bacterial phenotypes	40
1.13. Aims and Objectives.....	43
Chapter 2. Materials and Methods.....	44
2.1. Bacterial strains and growth conditions.....	44
2.2. Black Carbon.....	44
2.1. Growth media.....	46
2.1.1. Blood Agar	46
2.1.2. Brain Heart Infusion broth (BHI).....	47
2.1.3. Brain Heart Infusion Serum Broth	47
2.1.4. Chelexed RPMI (CRPMI).....	47

2.1.5. DNase Agar.....	47
2.1.6. Luria-Bertani (LB) Broth.....	47
2.1.7. Luria-Bertani Agar (LA).....	47
2.1.8. Phosphate Buffered Saline (PBS).....	47
2.1.9. Todd Hewitt Broth (THB).....	48
2.1.10. Todd Hewitt Broth + Yeast Extract (THY)	48
2.1.11. Tryptic Soy Broth (TSB).....	48
2.2. CFU growth analysis	48
2.3. Exoprotein analysis	48
2.3.1. Haemolysis, DNase, and Lipase activity	48
2.3.2. Quantitative haemolysis activity assay	49
2.4. Biofilm analysis.....	50
2.4.1. Staining method.....	50
2.4.2. Quantification of biofilm viability.....	50
2.4.3. DNaseI and proteinase K degradation of biofilms	51
2.4.4. Biofilm antibiotic tolerance	53
2.5. Microscopy	53
2.5.1. Scanning Electron Microscopy	53
2.5.2. Transmission Electron Microscopy and biofilm thickness.....	54
2.6. Protein extraction and protein gels.....	55
2.6.1. Protein extraction.....	55
2.6.2. Standardisation of protein concentrations.....	55
2.6.3. 1D SDS-PAGE	56

2.7. Pneumococcal colonisation model.....	56
2.7.1. Preparation of pneumococci.....	57
2.7.2. Intranasal dosing procedure	59
2.7.3. Disease sign scoring	59
2.7.4. Culling mice	61
2.7.5. Collection of blood, bronchoalveolar lavages, and nasal lavages to determine bacterial load and for microbiota investigations.....	61
2.7.6. Determination of bacterial load.....	62
2.7.7. Tissue collection for histopathology.....	62
2.7.8. Tissue processing and analysis for histopathology	63
2.8. Statistical analysis of <i>in vitro</i> and pneumococcal colonisation data	63
2.9. Ion torrent sample preparation and analysis	64
2.9.1. DNA extractions.....	64
2.9.2. Polymerase Chain Reaction (PCR).....	66
2.9.3. Agarose gel electrophoresis	66
2.9.4. Gel extraction	68
Chapter 3. The effect of BC on growth, virulence, and biofilm formation of <i>S. aureus</i> and <i>S. pneumoniae</i>.....	69
3.1. Introduction.....	69
3.1.1. Bacterial species and strains used in this research	69
3.2. The effect of BC on bacterial growth.....	70
3.2.1. Effects of BC on growth of <i>S. aureus</i>	70
3.2.2. Effects of BC on growth of <i>S. pneumoniae</i>	74
3.3. Effect of BC on virulence factors.....	77

3.3.1. BC has no effect on haemolysis	77
3.3.2. BC has no effect on DNase or lipase secretion	79
3.4. Effect of BC on biofilm formation.....	79
3.4.1. Biofilm formation assay choice.....	79
3.4.2. Variation in biofilm formation under different environmental conditions ..	84
3.4.3. BC alters biofilm formation in a strain dependent manner.....	88
3.5. Discussion.....	92
3.5.1. BC alters bacterial growth and viability	92
3.5.2. BC has no effect on the virulence factors tested	95
3.5.3. Variation in biofilm formation in the absence of BC	97
3.5.4. BC alters biofilm formation	98
3.5.5. Future investigations into the mechanisms of BC effects.....	100
3.5.6. Conclusions.....	100
Chapter 4. Further investigations into BC-induced biofilm alterations	101
4.1. Introduction.....	101
4.2. BC alters biofilm architecture	102
4.3. Further analysis of biofilm structural modifications	110
4.3.1. BC increases biofilm thickness	110
4.3.2. Association of bacteria with BC in biofilms	112
4.4. Biofilm architectural modifications are not just due to the physical presence of BC particles	112
4.5. Biofilm alterations are observed within two hours of attachment	115
4.6. BC does not alter the protein expression profile of biofilm cells	119

4.7. The biofilm extracellular matrix	119
4.7.1. BC does not alter biofilm degradation by DNaseI	121
4.7.2. BC alters biofilm degradation by proteinase K.....	123
4.8. Biofilms formed in the presence of BC display an altered tolerance to antibiotics	123
4.9. Discussion.....	127
4.9.1. BC alters pneumococcal biofilm structures	127
4.9.2. BC alters <i>S. aureus</i> biofilm structures	130
4.9.3. Mechanisms of biofilm induced modifications.....	131
4.9.4. Biofilm alterations are also observed after 2 hours attachment	132
4.9.5. BC alters biofilm matrix composition	133
4.9.6. BC alters antibiotic tolerance of biofilms	136
4.9.7. Conclusions.....	138

Chapter 5. Effects of BC on pneumococcal colonisation and the respiratory tract microbiota **139**

5.1. Introduction.....	139
5.2. Establishing lung pathology of BC	140
5.3. Optimising inoculation volume for pneumococci and BC	145
5.4. Murine colonisation model	145
5.4.1. Pneumococcal colonisation of the murine respiratory tract.....	147
5.4.2. Pathological effects of pneumococcal colonisation and BC inhalation.....	148
5.5. Microbiota investigations	156
5.5.1. DNA extraction protocol choice.....	156
5.5.2. Initial tests for diversity showed potential contamination issues.....	157

5.5.3. Amplification of microbial DNA	159
5.5.4. Ion Torrent output and initial processing.....	161
5.5.5. Elimination of contamination.....	162
5.5.6. Sequences identified	166
5.5.7. Alpha Diversity	174
5.5.8. Beta Diversity and Non-metric Multidimensional Scaling.....	176
5.5.9. Statistical analysis	179
5.6. Discussion.....	180
5.6.1. Preliminary work for the murine colonisation model.....	180
5.6.2. BC causes pneumococci to spread to the LRT.....	182
5.6.3. Potential mechanisms for the BC-induced spread of pneumococci to the lungs	186
5.6.4. The effect of pneumococcal colonisation and BC inhalation on the respiratory tract microbiota.....	188
5.6.5. The composition of the murine respiratory tract microbiota	189
5.6.6. Limitations of microbiota assessment, and potential sources of bias and error	191
5.6.7. Conclusions.....	197
Chapter 6. Final Discussion	198
6.1. Limitations of investigations in this project	203
6.2. Additional future research	205
6.3. Conclusions.....	206

Appendices	207
Appendix 1. UK cities breaching the World Health Organisation annual mean guidelines for PM ₁₀ in 2013.....	207
Appendix 2. UK cities breaching the World Health Organisation annual mean guidelines for PM _{2.5} in 2013	208
Appendix 3. Initial processing of ion torrent data from main investigation.	209
Appendix 4. Construction of relative abundance bar charts.....	216
Appendix 5. Statistical analysis of ion torrent data – alpha diversity.....	220
Appendix 6. Beta diversity and ordinations.	223
Appendix 7. Statistical analysis of ion torrent data – Adonis and betadisper.	225
Appendix 8. Statistical analysis of ion torrent data – Multiple testing in Phyloseq.....	227
Appendix 9. Statistical analysis of ion torrent data – DeSeq2.	228
Appendix 10. Analysis for preliminary ion torrent test.	230
Appendix 11. Full sequences of 334R and 8F primers used in this study	235
Appendix 12. Biofilm formation of <i>S. aureus</i> in various environmental conditions.....	239
Appendix 13. Biofilm formation of <i>S. pneumoniae</i> in various environmental conditions.....	240
Appendix 14. Examples showing the consistency of the effect of BC on biofilm formation in different environmental conditions.	241
Appendix 15. Percent reduction in SH1000 biofilm viability due to DNaseI degradation.	242
 Bibliography.....	 244

List of Tables

Table 1-1. Deposition of particles in the respiratory tract.....	4
Table 1-2. Increased mortality due to long and short-term exposure to PM.....	14
Table 2-1. Bacterial strains used.....	45
Table 2-2. Scoring for disease severity in mice.....	60
Table 3-1. Significant differences between biofilm, planktonic, and loosely adherent bacteria	87
Table 5-1. The 14 most abundant families identified in sequencing of the murine respiratory tract microbiota, after removal of contaminants	170

List of Figures

Figure 1-1. Size range of Particulate Matter particles	4
Figure 1-2. Annual mean exposure to PM ₁₀ in urban areas 2008-2013	7
Figure 1-3. Annual mean exposure to PM _{2.5} in urban areas 2008-2013	7
Figure 1-4. Global distribution of black carbon in 2007.....	10
Figure 1-5. Stages of biofilm formation.....	32
Figure 2-1. Protocol for the enumeration of bacterial viability of biofilms.....	52
Figure 2-2. Protocol for assessing the impact of black carbon on pneumococcal colonisation of the MF1 mouse nasopharynx.....	58
Figure 2-3. Flow diagram depicting sample preparation for analysis of the mouse respiratory tract microbiota nasopharynx.....	65
Figure 2-4. Overview of the 16S DNA sequence	67
Figure 3-1. The effect of black carbon on growth of <i>S. aureus</i> over the period of 1 to 8 hours.....	72
Figure 3-2. The effect of black carbon on viability of <i>S. aureus</i> after 24 hours co-incubation	73
Figure 3-3. The effect of black carbon on growth of <i>S. pneumoniae</i> over the period of 1 to 8 hours.....	75
Figure 3-4. The effect of black carbon on viability of <i>S. pneumoniae</i> after 24 hours co-incubation	76
Figure 3-5. The effect of black carbon on haemolysis.....	78
Figure 3-6. The effect of black carbon on DNase and lipase activity	80
Figure 3-7. Biofilms stained with crystal violet	82
Figure 3-8. Biofilm structure	83
Figure 3-9. Biofilm formation of <i>S. aureus</i> and <i>S. pneumoniae</i> strains.....	86
Figure 3-10. The effect of black carbon on <i>S. aureus</i> biofilms.....	89
Figure 3-11. The effect of black carbon on <i>S. pneumoniae</i> biofilms.....	91

Figure 4-1. Black Carbon imaged by Scanning Electron Microscopy	103
Figure 4-2. The effect of black carbon on bacterial biofilm architecture.	104
Figure 4-3. The effect of black carbon on <i>S. pneumoniae</i> PR201 biofilm architecture	106
Figure 4-4. The effect of black carbon on <i>S. aureus</i> SH1000 biofilm architecture.....	107
Figure 4-5. The effect of black carbon on <i>S. aureus</i> USA300 biofilm architecture....	108
Figure 4-6. The effect of black carbon on <i>S. aureus</i> Newman biofilm architecture ...	109
Figure 4-7. The effect of black carbon on biofilm thickness	111
Figure 4-8. The association between black carbon and bacteria in biofilms	113
Figure 4-9. Quartz imaged by Scanning Electron Microscopy	114
Figure 4-10. Quartz has no effect on biofilm architecture	116
Figure 4-11. The effect of BC on bacterial attachment to a surface	118
Figure 4-12. BC had no detectable effect on the protein profile of biofilm bacteria...	120
Figure 4-13. The effect of black carbon on biofilm matrix DNA	122
Figure 4-14. The effect of black carbon on biofilm matrix protein.....	124
Figure 4-15. Antibiotic tolerance of control and BC-formed biofilms.....	126
Figure 5-1. Penetration of black carbon into the lungs immediately after intranasal inoculation	141
Figure 5-2. Penetration of black carbon into alveoli immediately after intranasal inoculation	142
Figure 5-3. Persistence of black carbon in the lungs at 7 days post-inoculation.....	143
Figure 5-4. Comparison of black carbon persistence in the lungs at 7 days post-inoculation.	144
Figure 5-5. Bacterial load recovered after intranasal inoculation with <i>S. pneumoniae</i> D39	146
Figure 5-6. The effect of black carbon on pneumococcal colonisation of the respiratory tract of MF1 mice.....	149

Figure 5-7. Histological analysis of lungs, nares, cervical lymph nodes, and spleen at 7 days post-inoculation	150
Figure 5-8. Histological analysis of lungs, nares, cervical lymph nodes, and spleen at 14 days post-inoculation	153
Figure 5-9. Microbiota profiles of the upper and lower respiratory tracts of naïve MF1 mice.....	158
Figure 5-10. Example agarose gel of PCR amplifying microbial 16S DNA from mouse nasal lavages.....	160
Figure 5-11. Microbiota profiles of the negative PCR reaction controls and negative extraction controls.....	163
Figure 5-12. Microbiota profiles of the upper and lower respiratory tracts of mice prior to removal of contaminants	165
Figure 5-13. Microbiota profiles of the murine upper respiratory tract at 7 and 14 days post-inoculation	168
Figure 5-14. Microbiota profiles of the murine lower respiratory tract at 7 and 14 days post-inoculation	169
Figure 5-15. Microbiota profiles of the murine upper respiratory tract at 7 and 14 days post-inoculation, facetted by phylum.....	172
Figure 5-16. Microbiota profiles of the murine lower respiratory tract at 7 and 14 days post-inoculation, facetted by phylum.....	173
Figure 5-17. Alpha diversity analysis	175
Figure 5-18. Non-metric Multidimensional Scaling (NMDS) analysis of the upper respiratory tract microbiota profiles of MF1 mice subjected to Bray-Curtis similarity coefficient transformation	177
Figure 5-19. Non-metric Multidimensional Scaling (NMDS) analysis of the lower respiratory tract microbiota profiles of MF1 mice subjected to Bray-Curtis similarity coefficient transformation	178
Figure 6-1. Proposed effects of black carbon (BC) on bacteria	199

Abbreviations

°C	Degrees centigrade
Agr	Accessory Gene Regulator
AM	Alveolar Macrophages
ANOVA	Analysis Of Variance
ATCC	American Type Culture Collection
BC	Black Carbon
BHI	Brain Heart Infusion
bp / Mbp	base pair/Megabase pair
BSA	Bovine Serum Albumin
CA-MRSA	Community Acquired MRSA
CAP	Community Acquired Pneumonia
CF	Cystic Fibrosis
CO ₂	Carbon dioxide
COPD	Chronic Obstructive Pulmonary Disease
CFU	Colony Forming Units
CRPMI	Chelexed RPMI
DEPs	Diesel Exhaust Particles
dH ₂ O	Distilled water
DNA	deoxyribonucleic acid
dNTPs	deoxyribonucleotide triphosphates
eDNA	Extracellular DNA
H ₂ O ₂	Hydrogen Peroxide
HA-MRSA	Healthcare Associated MRSA
HCl	Hydrochloric Acid
IL	Interleukin
IMS	Industrial Methylated Spirits
INF	Interferon
LA	Luria-Bertani Agar
LB Broth	Luria-Bertani Broth

LRR fixation	Lysine-acetate-based formaldehyde-glutaraldehyde ruthenium red-osmium fixation
LRT	Lower Respiratory Tract
MRSA	Methicillin Resistant <i>S. aureus</i>
MSSA	Methicillin Sensitive <i>S. aureus</i>
NaCl	Sodium chloride
NanA/NanB/NanC	Pneumococcal Neuraminidase A/B/C
ng / µg / mg / g	nanogram / microgram / milligram / gram
NK cells	Natural Killer cells
nl / µl / ml / l	nanolitre / microlitre / millilitre / litre
nm / µm / mm / cm	nanometre / micrometre / millimetre / centimetre
nM / µM / mM / M	nanoMolar / microMolar / miniMolar / Molar
NCTC	National Collection of Type Cultures (UK)
Nuc/Nuc2	<i>S. aureus</i> nuclease 1/2
OD	Optical Density
PAFr	Platelet-Activating Factor receptor
PBS	Phosphate Buffered Saline
PCR	Polymerase Chain Reaction
PIA	<i>S. aureus</i> Polysaccharide Intercellular Adhesin
Ply	Pneumolysin
PM	Particulate Matter
PM ₁₀	Particulate Matter with a diameter less than 10 µm
PM _{10-2.5}	Particulate Matter with a diameter between 10 and 2.5 µm
PM _{2.5}	Particulate Matter with a diameter less than 2.5 µm
PM _{0.1}	Particulate Matter with a diameter less than 100 nm
PNAG	Polymeric N-acetylglucosamine
rbf	Protein Regulator of Biofilm Formation
rRNA	Ribosomal Ribonucleic Acid
RNA	Ribonucleic Acid
RNS	Reactive Nitrogen Species
ROS	Reactive Oxygen Species
RPMI	Roswell Park Memorial Institute – 1640 (medium)

<i>rpm</i>	Revolutions Per Minute
Sar	Staphylococcal Accessory Gene Regulator
SasG	<i>S. aureus</i> Surface protein G
SCC(<i>mec</i>)	Staphylococcal Cassette Chromosome (<i>mec</i>)
SD	Standard Deviation
SDS-PAGE	Sodium Dodecyl Sulphate Poly-Acrylamide Gel Electrophoresis
SEM	Standard Error of the Mean
SEM	Scanning Electron Microscopy
SpA	Staphylococcal Protein A
SpxB	Pyruvate oxidase
ST	Sequence Type
TEM	Transmission Electron Microscopy
TNF	Tumour Necrosis Factor
TSB	Tryptic Soy Broth
THB	Todd Hewitt Broth
THY	Todd Hewitt Broth + 0.5 % (w/v) Yeast Extract
UFP	Ultra-Fine Particles
UHL	University Hospitals of Leicester
UOL	University of Leicester
URT	Upper Respiratory Tract
UV	Ultraviolet
V	Volt
v/v	Volume by volume
w/v	Weight by volume

Chapter 1. Introduction

Particulate matter (PM) is a major component of air pollution associated with causing and exacerbating a variety of cardiorespiratory health problems, thereby increasing morbidity and mortality (Xu *et al.* 2016; Thurston & Lippmann 2015; WHO 2014d; Janssen *et al.* 2012). The leading agents of PM-induced mortality are Ischaemic Heart Disease (IHD), stroke, Chronic Obstructive Pulmonary Disease (COPD), lung cancer, and acute lower respiratory tract infections (Costello *et al.* 2016; Shah *et al.* 2015; Cui *et al.* 2015; WHO 2014d; WHO 2007). In order to establish how PM causes disease, past research has investigated the effects of PM on eukaryotic cells and tissues (Provost *et al.* 2016; Aztatzi-Aguilar *et al.* 2015; Zhao *et al.* 2014; Janssen *et al.* 2012). PM has been found to have a variety of effects on the cardiovascular and respiratory systems, with the major disease causing mechanisms identified being the induction of oxidative stress and inflammation (Longhin *et al.* 2016; De Prins *et al.* 2014; Zhao *et al.* 2012; Mazzoli-Rocha *et al.* 2010).

In contrast to research into effects on the host however, there is extremely limited research into the direct effect of PM on bacteria, the organisms responsible for the respiratory infections associated with PM. Furthermore, bacterial infections have a role in the exacerbations of other respiratory tract diseases including COPD and asthma (Erkan *et al.* 2008; Pelaia *et al.* 2006). Therefore the aim of this study was to determine whether bacteria are affected by PM, for the purpose of elucidating an aspect of how PM may cause respiratory disease, specifically respiratory tract infections. Black Carbon (BC) is a major component of PM and was used to model PM in this research. The opportunistic pathogens *Streptococcus pneumoniae* and *Staphylococcus aureus* were used as model organisms as these are important respiratory pathogens which cause major burdens of disease worldwide.

This chapter will discuss PM and BC, the health effects of these pollutants, known mechanisms for these health effects, research into effects on bacteria, and key aspects of the biology of *S. pneumoniae* and *S. aureus*. The first results chapter will describe the initial characterisation of how BC alters key phenotypes of *S. pneumoniae* and *S. aureus*, including growth and biofilm formation. The second results chapter will further

investigate how BC alters biofilm formation, structure, and functioning. The third results chapter will then describe the investigation of the effect of BC on *in vivo* colonisation of *S. pneumoniae*, and on the respiratory tract microbiota. These findings are used to propose that the morbidity and mortality associated with PM exposure are not solely due to effects on host tissues, but also results from direct alterations of respiratory tract bacteria.

1.1. Particulate Matter

Air pollution is responsible for 7 million deaths per year, equating to an eighth of all global deaths (WHO 2014a; WHO 2012). This makes it the single largest environmental health risk worldwide (WHO 2014a; WHO 2012). The major constituents of air pollution are Particulate Matter (PM), ozone, nitrogen dioxide, and sulphur dioxide (Kelly & Fussell 2012; Kelly & Fussell 2011; WHO 2006a). However, in reality, air pollution encompasses a diverse range of pollutants that are heterogeneous in space and time, depending on the sources from which the pollutants originate and the level of anthropogenic activity (Kelly & Fussell 2012; Air Quality Expert Group 2012; Kelly & Fussell 2011; WHO 2006a). Therefore although it is possible to discuss the major contributors to air pollution, it should be noted that there is variation in personal exposure based on geography and lifestyle (Gu *et al.* 2015; WHO 2006b).

PM is one of the most harmful components of air pollution and the leading agent of air pollution-associated mortality (WHO 2014a; WHO 2014d; WHO 2012). Indeed, of the 7 million deaths caused by air pollution each year, 3.7 million deaths are caused by exposure to PM (WHO 2014d). PM exposure is associated with increased respiratory and cardiovascular morbidity and mortality (Costello *et al.* 2016; Shah *et al.* 2015; WHO 2014d; Janssen *et al.* 2012; Brunekreef & Forsberg 2005). Diseases range from minor illnesses and exacerbations of existing conditions such as asthma and COPD, to severe illnesses and premature mortality (Thurston & Lippmann 2015; Kelly & Fussell 2012). However, in order to discuss the damaging effects of PM, the specific components of PM responsible for this toxicity must first be described.

1.1.1. Size range and deposition of particulate matter

PM itself is an umbrella term which refers to condensed phase (solid or liquid) particles suspended in the atmosphere (Kelly & Fussell 2012; Air Quality Expert Group 2012; Air Quality Expert Group 2005). These particles range in size from hundreds of micrometres to a few nanometres, and are divided based on particle size, as illustrated in Figure 1-1 (Heal *et al.* 2012; Kelly & Fussell 2012; Air Quality Expert Group 2012; Air Quality Expert Group 2005). As can be seen in Figure 1-1, particle size is conventionally indicated by adding the size range in μm after “PM”. For example, PM_{10} refers to all particles smaller than 10 μm in diameter, and $\text{PM}_{10-2.5}$ describes particles between 10 and 2.5 μm . An alternative convention also exists which describes particles as coarse, fine, and ultrafine, which is also represented in Figure 1-1. Unfortunately some studies vary in the use of these nomenclatures. For example, the term “coarse particles” is often used to refer to just the $\text{PM}_{10-2.5}$ component of coarse particles (Qiu *et al.* 2014; Kan *et al.* 2007; Lipsett *et al.* 2006). Therefore it is important to determine how each study defines PM before assessing the conclusions reached.

Particle size is directly linked to the length of time particles can remain suspended in the atmosphere, which impacts the distance they can travel and therefore the number of people that may be potentially exposed. Fine and ultrafine particles can travel over 100 km and so there is a greater potential for higher background levels of these particles over large areas (Heal *et al.* 2012; Kelly & Fussell 2012; Air Quality Expert Group 2012). Particle size also impacts deposition within the respiratory tract, as shown in Table 1-1, however there is interpersonal variation in inspiration flow rate and volume, which also influences the location of deposition (Kelly & Fussell 2012; Heal *et al.* 2012; Peters *et al.* 2006). Furthermore, approximately 15 % of particles between 1 μm and 100 nm do not deposit in the airways at all, being too large to deposit by diffusion and too small to deposit by impaction or sedimentation on the epithelial tissues (Briant & Lippmann 1993; Briant & Lippmann 1992).

Site deposition and particle composition also affect clearance mechanisms. Notably, ultrafine particles (UFPs) and soluble components of $\text{PM}_{2.5}$ that reach the alveoli can enter the bloodstream (Lippmann 2014). These particles can then be translocated by the

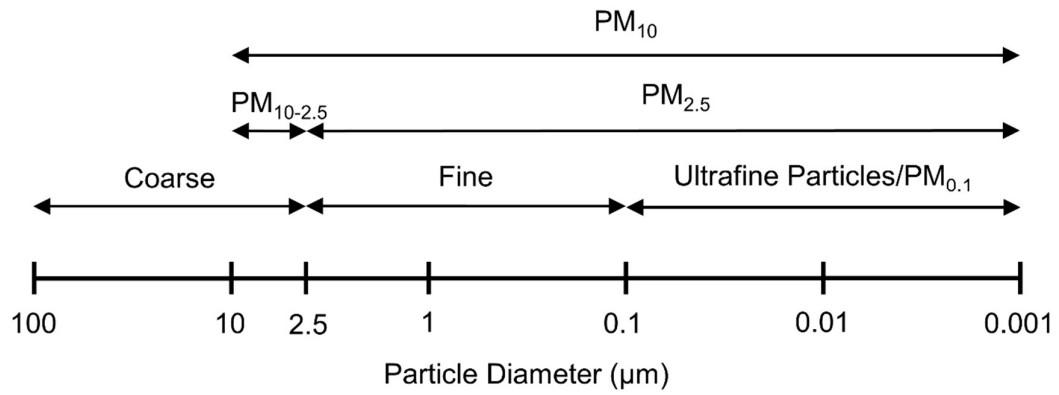


Figure 1-1. Size range of Particulate Matter particles

Table 1-1. Deposition of particles in the respiratory tract

Particle size	Depth of deposition in the respiratory tract
Coarse particles - larger than 10 µm	Nasopharynx
Coarse particles - PM _{10-2.5}	Primary bronchi
Fine particles	Terminal bronchioles and alveoli
Ultrafine Particles	Alveoli, particles may also cross the interstitium between the lung and bloodstream

blood to other organs where they may be retained long-term and have a higher potential toxicity (Peters *et al.* 2006). In contrast, the majority of insoluble particles that reach the lower respiratory tract are phagocytosed by alveolar macrophages and dendritic cells within weeks (Thurston & Lippmann 2015; Peters *et al.* 2006). These may then be cleared by mucociliary clearance or may be carried to lymph nodes, allowing these particles to also penetrate through the lungs (Thurston & Lippmann 2015; Peters *et al.* 2006). The majority of poorly soluble coarse particles are carried to the larynx where they are then swallowed (Lippmann 2014). Therefore it is clear that particle size is important in determining the distance particles may spread after release, inhalation, deposition, and clearance, all of which have a role in determining potential health effects.

1.1.2. Primary and secondary particles

PM can be generated by both man-made and natural processes. Man-made sources include fossil fuel combustion, industrial processes, construction, and biomass burning (Kelly & Fussell 2012). Natural sources include volcanic ash, wind-blown dust, sea salt, soil particles, the products of forest fires, pollen, and microbes (Kelly & Fussell 2012). Furthermore, PM is comprised of both primary particles released directly from a source, and secondary particles formed through atmospheric reactions (Kelly & Fussell 2012; Heal *et al.* 2012; Air Quality Expert Group 2012; Air Quality Expert Group 2005). Primary particles include Black Carbon (BC), sodium chloride, and trace metals (Kelly & Fussell 2012; Air Quality Expert Group 2012). Secondary particles include sulphates and nitrates, such as ammonium sulphate and ammonium nitrate formed by the oxidation of sulphur dioxide (SO₂), nitrogen oxides (NO and NO₂), and ammonia (NH₃) (Kelly & Fussell 2012; Air Quality Expert Group 2012). Coarse particles tend to be made up of primary particles whereas fine and ultrafine particles tend to be secondary particles (Kelly & Fussell 2012).

1.1.3. Generation of particulate matter

In general, developing countries are responsible for a greater burden of PM emissions than developed countries (USEPA 2012). In the developing world, substantial levels of

PM are released in biomass burning and combustion of biofuels in the home for heating and cooking, and from open biomass burning, for example in agriculture (Philip *et al.* 2014; Mazzoli-Rocha *et al.* 2010). In the developed world, the main contributors to the release of PM are road transport, commercial and domestic fuel use, and industrial processes (Salisbury *et al.* 2015; Kelly & Fussell 2012). In fact, road traffic emissions make up 30-50 % of urban PM_{2.5} above background rural levels in the UK (Air Quality Expert Group 2012). Within road transport, diesel exhaust fumes are a much greater contributor to PM than petrol fumes (Kelly & Fussell 2012; Riedl & Diaz-Sanchez 2005; Shah *et al.* 2004). In the long-term, diesel emissions have been steadily rising in the UK due to the increase in traffic and the general switch to diesel engines, and diesel exhaust particles (DEPs) now account for a significant proportion of urban PM (Salisbury *et al.* 2015). However the impact of diesel engines is now recognised, and progress has been made in reducing diesel emissions since the introduction of stricter emission regulations in 1992 (Salisbury *et al.* 2015).

1.1.4. Current particulate matter exposure guidelines

Current World Health Organization (WHO) guidelines recommend that the annual mean levels of PM₁₀ and PM_{2.5} should not exceed 20 µg/m³ and 10 µg/m³, respectively (WHO 2006b). Despite legislation to reduce PM emissions, both PM₁₀ and PM_{2.5} levels are above these guidelines in many countries, as shown in Figures 1-2 and 1-3 (Heal *et al.* 2012; Air Quality Expert Group 2012; WHO 2006a). Indeed, in low- and middle income countries, 98 % of cities which have a population over 100,000 exceed these guidelines, whereas in high-income countries 56 % of these cities exceed guidelines (WHO 2016). Importantly, PM released into the atmosphere is not restricted to national borders. This is therefore one of the reasons that a concerted international effort is required to tackle air pollution, and means that PM released in one country can impact people over a wider geographical area.

There has been a long term decrease in UK PM levels since 1970, mainly due to a general reduction in coal use. In particular, there has been a substantial reduction in emissions from power stations due to a shift towards use of natural gas, nuclear, and renewable energy, as well as improved emission control systems (Salisbury *et al.* 2015;

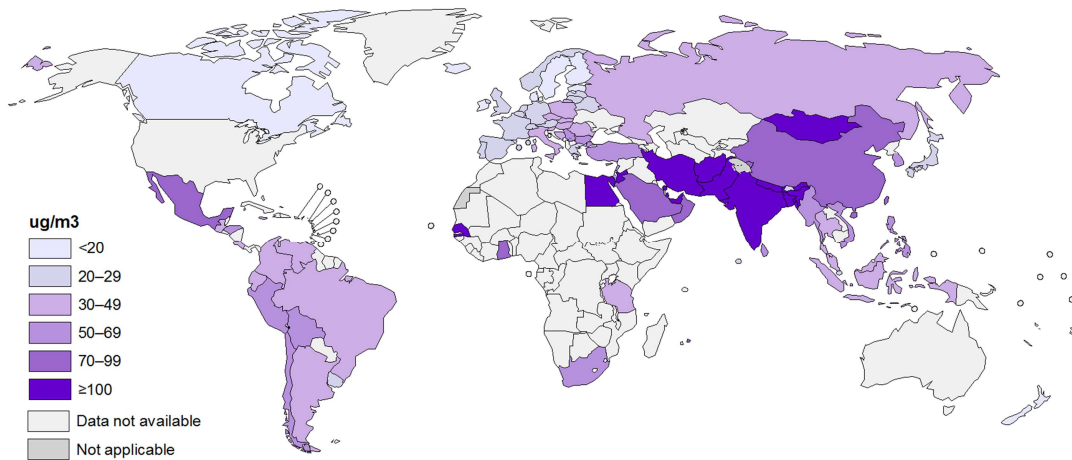


Figure 1-2. Annual mean exposure to PM₁₀ in urban areas 2008-2013. Adapted from the Global Health Observatory Map Gallery, World Health Organization (WHO 2014e)

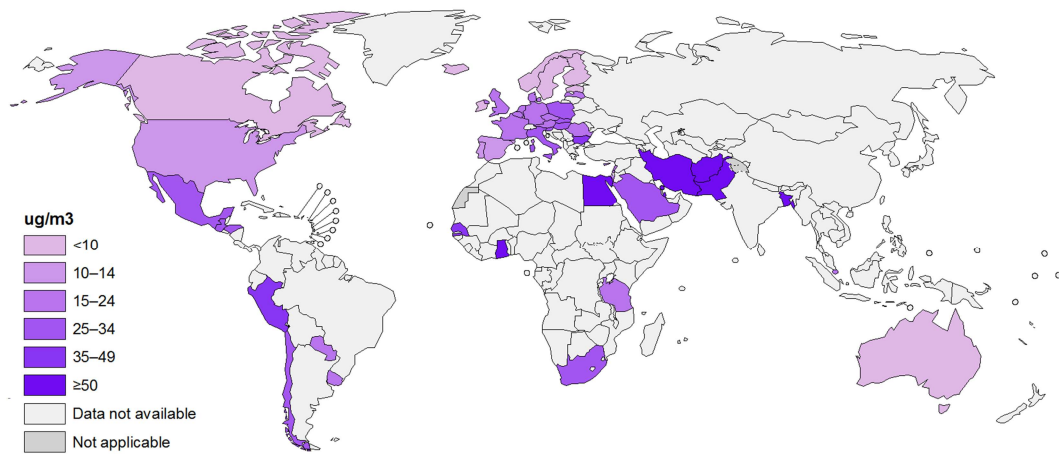


Figure 1-3. Annual mean exposure to PM_{2.5} in urban areas 2008-2013. Adapted from the Global Health Observatory Map Gallery, World Health Organization (WHO 2014f)

Thistlethwaite *et al.* 2012). Since 1970, UK PM₁₀ levels have fallen by 73 % and PM_{2.5} levels have fallen by 76 % (DEFRA 2015). The average concentration of PM₁₀ in the UK in 2014 was 19 µg/m³, and the average concentration of PM_{2.5} was 12.5 µg/m³ (DEFRA 2016; WHO 2014b). These UK average values therefore breach the WHO PM_{2.5} guidelines, but are just within the PM₁₀ guidelines. Indeed, specific UK cities which exceed PM guidelines are given in Appendices 1 and 2, and show that in 2013, only 10 cities exceeded guidelines for PM₁₀ whereas 39 cities exceeded those for PM_{2.5} (WHO 2016).

In addition to annual mean exposure limits, the 24-hour mean concentrations of PM₁₀ and PM_{2.5} should not exceed 50 µg/m³ and 25 µg/m³, respectively (WHO 2006b). These recommendations aim to limit the harmful effects of short-term high pollution events, but are also often regularly exceeded (Zhou *et al.* 2015). Currently, ambient levels of PM in China are some of the highest worldwide, and severe smog events in Beijing have been associated with PM_{2.5} levels of over 800 µg/m³, over 32 times the WHO recommended limit (He *et al.* 2016; Zhou *et al.* 2015; Guo *et al.* 2013).

In reality, both the annual and 24-hour mean concentration limits for PM₁₀ and PM_{2.5} are not entirely safe, and adverse health effects are observed at concentrations well below current guidelines. Indeed, a lower threshold below which health effects are not observed has never been identified (Beelen *et al.* 2014; WHO 2006a). Therefore current efforts attempt to reduce PM exposure as far as practically possible, but even at these levels, PM causes morbidity and mortality.

1.1.5. Black Carbon

Black Carbon (BC) is an important component of global PM (Janssen *et al.* 2012; USEPA 2012; Air Quality Expert Group 2012). Indeed, BC is such a major PM constituent that it is often used as a proxy when assessing PM levels and health effects (Invernizzi *et al.* 2011). BC is a collective term for airbourne carbon-based particles formed through the incomplete combustion of fossil fuels, biofuels, and biomass (Butterfield *et al.* 2015; Ni *et al.* 2014; Janssen *et al.* 2012). Once released, BC is stable in the atmosphere for days to weeks (B. Li *et al.* 2015; Butterfield *et al.* 2015;

Invernizzi *et al.* 2011; Schulz *et al.* 2006). BC contributes to climate change by absorbing solar radiation and warming the atmosphere, and is second only to CO₂ in terms of causing global warming (Ni *et al.* 2014; Air Quality Expert Group 2012; Shrestha *et al.* 2010). BC also causes a variety of serious health problems (Samoli *et al.* 2016; Y. Li *et al.* 2015; Ostro *et al.* 2014; Janssen *et al.* 2012).

The vast majority of BC sources are anthropogenic, with the only natural source being natural biomass burning, for example in forest fires (Schleicher *et al.* 2013). In the developed world, the major source of BC is fuel combustion in transportation, particularly from diesel engines (USEPA 2012; Kelly & Fussell 2012). In contrast, in the developing world the two major sources of BC are open biomass burning, for example burning of agricultural waste, and the residential burning of biomass for heat and cooking (USEPA 2012). Additional sources of BC include industrial processes and power stations (Philip *et al.* 2014; Janssen *et al.* 2012; USEPA 2012; Air Quality Expert Group 2012). Urban environments and industrialised regions are particularly associated with high levels of BC (Philip *et al.* 2014; Invernizzi *et al.* 2011), which is a serious issue as the majority of the world's population (~3.5 billion people) live in urban areas, and this is expected to increase to ~6.3 billion by 2050 (WMO/IGAC 2012).

Europe and North America combined account for only about 13 % of global BC emissions, whereas developing countries are responsible for ~80 % (USEPA 2012; Cofala *et al.* 2007; Bond *et al.* 2007). The biggest global contributors to BC are China (~30 % of emissions) and India (~10 % of emissions) as seen in Figure 1-4, and there has been a marked increase in BC emissions from these countries over the past few decades (Philip *et al.* 2014; Wang *et al.* 2014; Ni *et al.* 2014; R. Wang *et al.* 2012; Air Quality Expert Group 2012; Sloss 2012). In China, emissions increased each year since 1949, but began to level off in the mid 1990's (Ni *et al.* 2014; R. Wang *et al.* 2012).

The UK Black Carbon Network, managed by the Department for Environment, Food, and Rural Affairs (DEFRA), monitors hourly BC levels at 20 locations across the UK (Butterfield *et al.* 2015; Air Quality Expert Group 2012). BC concentrations have been stable since monitoring began in 2006 (Butterfield *et al.* 2015). In 2014, BC levels from

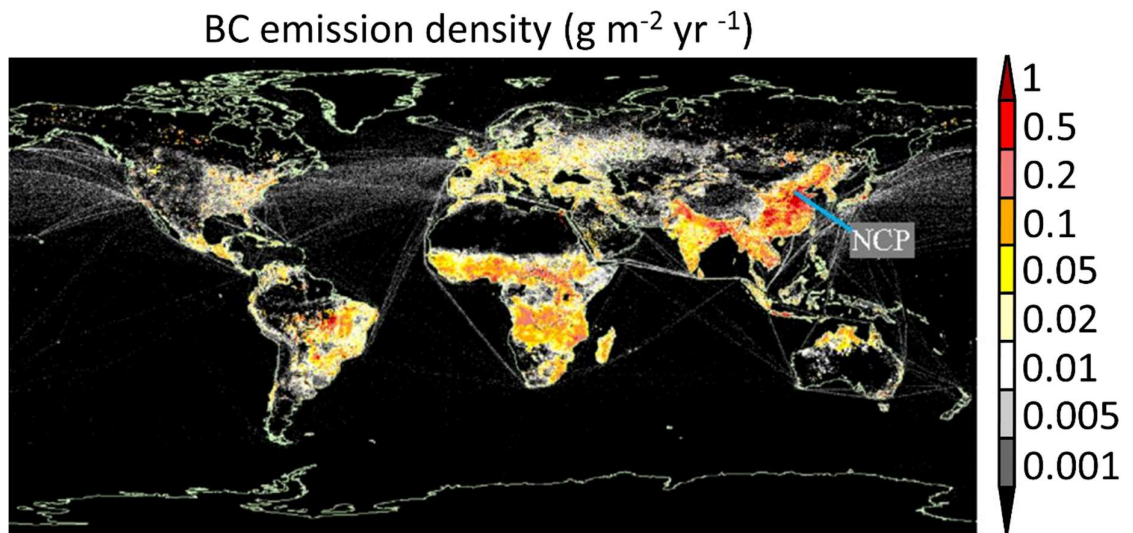


Figure 1-4. Global distribution of black carbon in 2007. Adapted from - Exposure to ambient black carbon derived from a unique inventory and high-resolution model by Wang *et al.* (2014). NCP – North China Plain, one of the areas with highest BC emissions worldwide.

1 to 7 $\mu\text{g}/\text{m}^3$ were measured across the UK, and the country-wide average was 1.6 $\mu\text{g}/\text{m}^3$ (Butterfield *et al.* 2015). In general, higher concentrations were recorded at the roadside in comparison to other urban environments.

Factors which are particularly important in determining individual BC exposure include commuting, local industrial activity, time spent outside, and the background level of exposure at home and in the workplace (Nieuwenhuijsen *et al.* 2015; B. Li *et al.* 2015; Schleicher *et al.* 2013; Dons *et al.* 2012; WHO 2006b). Generally, the greatest exposure is encountered on weekdays during commutes between the home and workplace, during which commuters can receive up to 30 % of their daily dose of BC (Nieuwenhuijsen *et al.* 2015; B. Li *et al.* 2015; Butterfield *et al.* 2015; Dons *et al.* 2012). The method of commuting also impacts exposure. The highest levels of BC are encountered in travel by car and underground systems, but interestingly, the highest doses of BC are inhaled when walking and cycling (B. Li *et al.* 2015; Vilcassim *et al.* 2014; Dons *et al.* 2012; Nwokoro *et al.* 2012). This is due to the close proximity to road traffic when walking and cycling, in combination with the increased duration of exposure and inhalation rate in comparison to during travel by car, bus, and on the underground (B. Li *et al.* 2015; Dons *et al.* 2012; Nwokoro *et al.* 2012). Therefore traffic management schemes which reduce the amount of vehicles and limit their movement are useful tools in reducing exposure (Invernizzi *et al.* 2011), and may benefit those commuters travelling by multiple methods.

Particle size and compounds absorbed onto particles are the main factors that influence health effects of BC (Ni *et al.* 2014; Janssen *et al.* 2012). BC particles range in size and may fall within PM_{10} , $\text{PM}_{2.5}$, and even the UFP size fractions of PM (Shrestha *et al.* 2010), and may also aggregate to create particles of larger sizes (B. Li *et al.* 2015). Particle size affects the distance that particles may be transported, as well as deposition in the respiratory tract as discussed in Section 1.1.1 (Kelly & Fussell 2012; Heal *et al.* 2012; Shrestha *et al.* 2010; Peters *et al.* 2006). The composition of BC varies depending on its source, with particles associated with a variety of compounds present during and after combustion (Ni *et al.* 2014; Kelly & Fussell 2012; Janssen *et al.* 2012; Shrestha *et al.* 2010; Koelmans *et al.* 2006). For example, diesel exhaust fumes are characterised by a carbon core and may be coated with metals including iron, zinc, nickel, chromium,

vanadium, lead, and copper, organic compounds including polycyclic aromatic hydrocarbons, and other compounds present during the combustion process (Kelly & Fussell 2012). Additional components that may adhere to BC include potentially carcinogenic compounds such as polychlorinated dibenzodioxins (PCDDs) (Ni *et al.* 2014; Kelly & Fussell 2012; Shrestha *et al.* 2010; Koelmans *et al.* 2006). Therefore BC can act as a carrier particle allowing diverse compounds to come into contact with the respiratory system (Janssen *et al.* 2012). It can be difficult to separate the health effects of adsorbed toxic species from each other, and this must be taken into account when interpreting the effects of BC on health (Kelly & Fussell 2012).

1.2. Increased morbidity and mortality caused by exposure to particulate matter

Developing countries carry a greater burden of mortality associated with PM exposure than developed countries. In 2012, ~88 % of the 3.7 million deaths caused by PM exposure occurred in low- and middle-income countries (WHO 2014d). The Western Pacific and Southeast Asia were most adversely affected, accounting for 1.67 million and 0.9 million deaths, respectively, whereas 200,000 deaths occurred in Europe (WHO 2014d). Smog episodes, which are regularly experienced in Asia, carry the greatest associations with mortality. For example, the severe smog episodes experienced during January 2013 in Beijing, China, caused a 12-22 % increase in cardiovascular and respiratory mortality (Zhou *et al.* 2015). By modelling ambient BC concentrations and combining these with data on exposed populations, the risk of mortality, health effects, and numbers of deaths, it has been estimated that BC alone caused 14,000 premature deaths in the US in 2010, as well as hundreds of thousands of cases of illnesses, particularly respiratory disease (Y. Li *et al.* 2015). Background levels of BC in London have also been correlated with a 2.72 % increase in respiratory mortality (Samoli *et al.* 2016).

Meta-analyses of epidemiological studies have calculated the increase in mortality caused by each 10 $\mu\text{g}/\text{m}^3$ increase in PM, and are summarised in Table 1-2. These data show that long-term exposure to PM carries a higher mortality risk than short-term exposure. Interestingly, some studies have found even more significant associations

than those given in Table 1-2. For example, a 71 % increase in cardiopulmonary mortality has been associated with long-term exposure to traffic-derived pollution (Anderson *et al.* 2012; Hoek *et al.* 2002).

In addition to assessing the number of deaths and increased mortality caused by PM exposure, it is possible to assess the years of life lost, which gives more weight to the premature deaths of young people. Exposure to ambient PM₁₀ and PM_{2.5} in Beijing results in a reduction in lifespan of 15.8 years (Guo *et al.* 2013). However, PM levels in Beijing are some of the highest worldwide as discussed in Section 1.1.4 (He *et al.* 2016; Zhou *et al.* 2015; Guo *et al.* 2013). The annual mean concentrations of ambient PM₁₀ and PM_{2.5} in the city of Ningbo, China, are 84 µg/m³ and 60 µg/m³, respectively (He *et al.* 2016). Therefore PM levels in Ningbo exceed WHO guidelines and are high in comparison to most European cities, however are lower than in Beijing (He *et al.* 2016; Guo *et al.* 2013). PM₁₀ in Ningbo is associated with a reduction in lifespan of 4.27 years, whilst exposure to PM_{2.5} is associated with a reduction in lifespan by 2.97 years (He *et al.* 2016). In contrast, on average PM exposure reduces life expectancy by 8.6 months in Europe (Brugha & Grigg 2014; COMEAP 2009).

1.2.1. Variation in disease associations

For completeness in an assessment of the literature, it is necessary to comment that investigations often identify variation in the link between PM and disease. Indeed, some studies have found no statistically significant link between PM and adverse health effects (Tuan *et al.* 2015; Guarnieri *et al.* 2015; MacIntyre *et al.* 2014; Anderson *et al.* 2001). This is generally accepted to be due to differences in particle size, composition, and individual differences in exposure and inhalation (Thomson *et al.* 2015; Hoek *et al.* 2013). Furthermore, climate has been identified as a modifier of PM induced mortality, with a lower mortality identified in warmer temperatures (Sun *et al.* 2015). This may be due to an increased time spent outdoors in cooler weather, altered industrial activity between different seasons, and changes in winds between seasons bringing varied PM compositions from different locations (Sun *et al.* 2015). This research highlights the complexity of the effect of PM, and the importance of the pollutant mixture in determining toxicity. Currently, attempts are being made to assess the impact of

Table 1-2. Increased mortality due to long and short-term exposure to PM. This table combines data from meta-analyses of epidemiological studies which assess the effect of Particulate Matter (PM) on mortality (Lu *et al.* 2015; Hoek *et al.* 2013), as well as investigations using mathematical models which combine data on PM levels with mortality across geographical regions to estimate increases in mortality from PM exposure (Shi *et al.* 2016; Chen *et al.* 2012; Zanobetti & Schwartz 2009; Zeka *et al.* 2005). In general, long-term exposure is defined as exposure of a year or more, whereas short-term exposures are defined as increases in PM levels for up to 2-days.

Particle size	Increase in mortality per 10 µg/m³ increase in pollutant	Reference
Long-term exposure		
PM ₁₀	24 %	(Lu <i>et al.</i> 2015)
PM _{2.5}	6-7 %	(Shi <i>et al.</i> 2016; Hoek <i>et al.</i> 2013)
Short-term exposure		
PM ₁₀	0.35-0.45 %	(Lu <i>et al.</i> 2015; Chen <i>et al.</i> 2012; Zeka <i>et al.</i> 2005)
PM _{2.5}	0.36-2.3 %	(Shi <i>et al.</i> 2016; Lu <i>et al.</i> 2015; Zanobetti & Schwartz 2009)

individual PM components on disease, such as the effect of BC alone, in order to provide a better understanding of the relationship between different components and ill health (Y. Li *et al.* 2015; Darrow *et al.* 2014; Qiu *et al.* 2014).

1.3. Diseases associated with particulate matter exposure

Both short-term and long-term exposure to PM can result in adverse health effects, increasing both cardiovascular and respiratory morbidity and mortality (Thurston & Lippmann 2015; Faustini *et al.* 2012). Ischaemic Heart Disease (IHD) (Costello *et al.* 2016) and stroke (Shah *et al.* 2015) are the leading agents of PM induced mortality, followed by COPD, lung cancer (Cui *et al.* 2015), and acute lower respiratory tract infections (WHO 2014d; WHO 2007). The effect of PM on respiratory tract infections is focused on in Section 1.3.1. Approximately 5 % of all lung cancer deaths and 3 % of cardiopulmonary deaths are attributed to PM globally (WHO 2013). Specifically, there is a strong relationship between PM exposure and risk of myocardial infarction (Cai *et al.* 2016; Mustafic *et al.* 2012) and heart failure (Shah *et al.* 2013).

Other health effects related to PM exposure include a link to infertility (Mahalingaiah *et al.* 2016; Nieuwenhuijsen *et al.* 2014) and decreased sperm motility (Hammoud *et al.* 2010). There is also an association with lower birthweights caused by antenatal exposure (Sun *et al.* 2016), diabetes (Hansen *et al.* 2016), and deep vein thrombosis and pulmonary embolisms (Kloog *et al.* 2015). Interestingly, PM exposure may more adversely affect certain populations than others. Women (Guo *et al.* 2013; Hoek *et al.* 2013; Taylor & Nakai 2012), particularly post-menopausal and pregnant women (Mannucci *et al.* 2015; Miller *et al.* 2007), the elderly over 65 years old (Mannucci *et al.* 2015; Ostro *et al.* 2014; Guo *et al.* 2013), children under 5 years old (Martinelli *et al.* 2013; Taylor & Nakai 2012), those from socially deprived backgrounds (Morelli *et al.* 2016; Hoek *et al.* 2013), the immunocompromised, and those with prior illnesses such as COPD (Faustini *et al.* 2012) and Cystic Fibrosis (CF) (Psoter *et al.* 2015), are particularly at risk.

1.3.1. Respiratory infections and alterations in respiratory health associated with particulate matter exposure

High PM and BC levels are significantly associated with emergency department visits and hospitalisation for upper and lower respiratory tract infections, including pneumonia, and increasing mortality from respiratory diseases (Xu *et al.* 2016; Chang *et al.* 2015; Brugha & Grigg 2014; MacIntyre *et al.* 2014; Qiu *et al.* 2014; Darrow *et al.* 2014; Gittins *et al.* 2013; Janssen *et al.* 2012). Importantly, it is now recognised that current research may even underestimate mortality from pneumonia caused by PM exposure (Gittins *et al.* 2013). Furthermore both PM_{2.5} and BC exacerbate existing respiratory conditions such as asthma (Deng *et al.* 2015; Brauer *et al.* 2007; Brauer *et al.* 2002), CF (Psoter *et al.* 2015; Goeminne *et al.* 2013), and COPD (Xu *et al.* 2016; Cortez-Lugo *et al.* 2015; Qiu *et al.* 2014; Darrow *et al.* 2014). PM is also implicated in the development, not just exacerbation, of asthma (Deng *et al.* 2015).

Children (Brugha & Grigg 2014; Darrow *et al.* 2014; Qiu *et al.* 2014; MacIntyre *et al.* 2014), women (Brugha & Grigg 2014; Qiu *et al.* 2014), the elderly (Qiu *et al.* 2014), and those with underlying medical conditions (Psoter *et al.* 2015) are particularly vulnerable to respiratory tract infections caused by exposure to PM. In the developing world, burning of biomass in the home significantly increases the risk of developing acute respiratory tract infections, which is a greater risk factor for women and children, who spend more of their in the home (Taylor & Nakai 2012; Smith *et al.* 2011). Antenatal PM exposure is also linked to increasing vulnerability of children to respiratory infections after birth (Jedrychowski *et al.* 2013). Furthermore, exposure to PM_{2.5} and BC reduces lung function which may most adversely affect children and the elderly (Paulin & Hansel 2016; Deng *et al.* 2015; Zhang *et al.* 2015; Hwang *et al.* 2015; Lepeule *et al.* 2014). *Pseudomonas aeruginosa* is a key pathogen for CF patients, and morbidity and mortality are increased the earlier this bacterium is acquired (Nixon *et al.* 2001). It has been shown that a 10 µg/m³ increase in PM_{2.5} exposure increases the risk of children with CF acquiring *P. aeruginosa* by 24 % (Psoter *et al.* 2015). This clearly shows the detrimental impact PM has on increasing the susceptibility of these patients to colonisation by *P. aeruginosa*.

1.4. The impact of reducing particulate matter emissions

Reductions in PM levels have both health and environmental benefits (Thurston & Lippmann 2015; Dominici *et al.* 2015). For example the reduction in PM air pollution from 2008 to 2010 in the Netherlands correlated with an increase in respiratory function of residents living in low vehicle emission zones (Boogaard *et al.* 2013). Furthermore in 1990, the black smoke concentration in Ireland dropped by 35.6 $\mu\text{g}/\text{m}^3$ and correlated with a 15.5 % decrease in respiratory mortality and a 10.3 % decrease in cardiovascular mortality (Clancy *et al.* 2002). However there are also underappreciated economic benefits. It is predicted that reducing PM_{2.5} levels by 10 $\mu\text{g}/\text{m}^3$ in Denmark, which is at comparable levels to that in the UK (WHO 2014f), would save the healthcare system €0.1 – 2.6 million per 100,000 inhabitants in the treatment of coronary heart disease, stroke, COPD, and lung cancer (Sætterstrøm *et al.* 2012). It is also estimated that healthcare costs associated with PM₁₀ in Beijing, China, were \$31 billion in 2012 and that a reduction in PM would substantially reduce this cost (Yin *et al.* 2015).

1.5. Mechanisms by which particulate matter causes disease

1.5.1. Cardiovascular effects

The most salient effect of PM is the triggering of oxidative stress and inflammation, which increase the risk of myocardial infarction (Mustafic *et al.* 2012), heart failure (Shah *et al.* 2013), and stroke (Shah *et al.* 2015). PM and BC cause significant increases in atherosclerosis and arterial stiffness via oxidative stress and inflammation (Provost *et al.* 2016; Patel *et al.* 2011; Vlachopoulos *et al.* 2005; Sun *et al.* 2005), mediated by inflammatory cytokines including IL-6, TNF- α , C-reactive protein (CRP) (Hoffmann *et al.* 2009; R ckerl *et al.* 2006). In addition, PM increases levels of procoagulants, such as fibrinogen and plasminogen activator fibrinogen inhibitor-1, increasing coagulation and platelet activation (Snow *et al.* 2014; Chuang *et al.* 2007; R ckerl *et al.* 2006). These effects therefore provide a potential mechanism for the cause of cardiovascular disease (Provost *et al.* 2016; Fang *et al.* 2012). Increases in vascular stiffness may not result in visible alterations in health for healthy individuals,

but may be of greater clinical importance in those with a higher risk of cardiovascular disease (Provost *et al.* 2016).

PM also induces the overexpression of two key endocrine systems, the Renin-Angiotensin-Aldosterone system (RAAS), and the Kallikrein-Kinin system (KKS) (Aztatzi-Aguilar *et al.* 2015). These systems control vasoconstriction and cardiac muscle contraction through vasoactive peptides, promote the production of superoxide anion radicals, and are involved in inflammation, regulated by IL-1 β , IL-6, TNF- α , and Interferon- γ (INF- γ) (Aztatzi-Aguilar *et al.* 2015). Importantly, RAAS and KKS are overexpressed during inflammation and cardiovascular disease, providing another potential mechanism by which PM causes disease (Aztatzi-Aguilar *et al.* 2015).

PM and BC increase both systolic and diastolic blood pressure, which may be due to altered autonomic nervous system functioning and the induction of systemic inflammation and oxidative stress, causing endothelial dysfunction (Liang *et al.* 2014). Additionally, PM and BC increase heart rate variability, heart weight, expression of hypertrophic markers, and cholesterol levels (Bind *et al.* 2016; Ohlwein *et al.* 2016; Ying *et al.* 2015; Liang *et al.* 2014), as well as circulating white blood cells, lipids, fibrinogen, and certain interleukins (Yeatts *et al.* 2007; Brook 2004). PM and BC also decrease cardiac stroke volume and output (Bind *et al.* 2016; Ying *et al.* 2015; Liang *et al.* 2014). Notably, these effects are more strongly associated with long-term PM exposure (Liang *et al.* 2014).

1.5.2. Respiratory effects

Oxidative stress and inflammation are also the major mechanisms responsible for the adverse respiratory health effects of PM (Longhin *et al.* 2016; De Prins *et al.* 2014; Rosa *et al.* 2014; Zhao *et al.* 2012). In the respiratory tract, both PM and BC may generate oxidative stress, inflammation, and may be mutagenic (Xie *et al.* 2010; Folkmann *et al.* 2009; Yang *et al.* 2009; Renwick 2004; Gallagher *et al.* 2003). PM also alters the expression of genes involved in metabolism, inflammatory responses, and oxidative stress in epithelial cells, and alters epithelial cell morphology (Longhin *et al.* 2016). Pro-inflammatory effects are caused by the release of specific inflammatory

mediators including IL-1 β , IL-5, IL-6, IL-8, IL-12, TNF- α , and INF- γ from epithelial cells, and IL-1 β , IL-8, and TNF- α release from macrophages and NK cells (Longhin *et al.* 2016; Wang *et al.* 2015; Mannucci *et al.* 2015; Kumar *et al.* 2015; Cho *et al.* 2014; Zhao *et al.* 2012; Yin *et al.* 2002). General inflammatory changes include subepithelial widening, inflammatory cell infiltration and vascular space widening, and decreased expression of epithelial sodium channel subunits (Park *et al.* 2014). Accompanying this, PM also triggers the release of H₂O₂ from epithelial cells (Cho *et al.* 2014), further contributing to oxidative stress.

Importantly, released inflammatory mediators penetrate into the bloodstream where they may act systemically (Wang *et al.* 2015; Mannucci *et al.* 2015; Yin *et al.* 2002). In addition, UFPs and soluble components of PM_{2.5} also penetrate into the bloodstream and are transported systemically, exerting effects on a wide range of tissues (Lippmann 2014). Furthermore, PM modulates the autonomic nervous system which further contributes to systemic inflammation and oxidative stress (Brook 2004). Therefore the effects of PM may act additively or synergistically, and there is a complex interplay once PM exposure has begun. Inflammation and oxidative stress may therefore set off a signalling cascade which causes further systemic inflammation and exacerbates any pulmonary and cardiovascular conditions (Uski *et al.* 2012; Zhao *et al.* 2012; Brook 2004; Li *et al.* 2004).

1.5.3. Specific mechanisms for alterations in host susceptibility to respiratory infection

Both *in vitro* and *in vivo* studies have shown that PM alters host susceptibility to respiratory infection by bacteria (Zhao *et al.* 2014; Tellabati *et al.* 2010; Harrod 2004; Yin *et al.* 2003; Yin *et al.* 2002) and viruses (Clifford *et al.* 2015; Müller *et al.* 2013), although this research is still in relatively early stages. In the lungs, PM reduces ciliary beat frequency inhibiting efficient clearance of particles and bacteria (Nel 2005).

Although PM-induced inflammation is associated with an increase in polymorphonuclear neutrophils and macrophages in the respiratory tract (Noël *et al.* 2015; Steenhof *et al.* 2014; Graff *et al.* 2009; Li *et al.* 2004), PM also reduces the oxidative burst capacity of macrophages (Rylance *et al.* 2015). Furthermore alveolar

macrophages (AM) become loaded with PM and BC upon exposure, reducing the ability of these cells to effectively phagocytose bacteria (Zhao *et al.* 2012; Tellabati *et al.* 2010; Lundborg *et al.* 2007; Zhou & Kobzik 2007; Renwick 2004). DEPs also impair immune effector cell maturation and macrophage cytokine release (Chaudhuri *et al.* 2012). These effects thereby reduce resistance to infection (Klumper *et al.* 2015; Graff *et al.* 2009; Li *et al.* 2004).

Culturing of A459 airway epithelial cells and human primary bronchial epithelial cells with PM₁₀ and PM_{2.5} has been shown to enhance subsequent adhesion of *S. pneumoniae* to these cells, after the removal of the PM (Mushtaq *et al.* 2011). This occurred in a dose-dependent manner and varied depending on PM source. The mechanism for this effect was an increase in host PAFr expression mediated by oxidative stress (Mushtaq *et al.* 2011), which is known to enhance bacterial adhesion (Gilley & Orihuela 2014; Sanchez *et al.* 2011). Other potential sources of increased adhesion, such as cell death, were excluded in this study (Mushtaq *et al.* 2011).

Pre-exposure to PM_{2.5} has also been found to significantly increase susceptibility of rats to a subsequent intranasal infection with *S. aureus* (Zhao *et al.* 2014). This was identified to be associated with increases in pathology, inflammatory cells, levels of IL-6 and TNF- α , depressed macrophage phagocytosis, and decreased recruitment of Natural Killer (NK) cells (Zhao *et al.* 2014). Adoptive transfer of NK cells from unexposed rats increased the ability of PM-exposed rats to clear *S. aureus*, suggesting that in this model, impairment of the NK cell response by PM_{2.5} was a critical mechanism in PM-induced susceptibility to infection (Zhao *et al.* 2014).

In addition, prior exposure to DEPs has been shown to increase later susceptibility of rats and mice to *Listeria monocytogenes* and *P. aeruginosa*, respectively (Harrod 2004; Yin *et al.* 2003; Yin *et al.* 2002). Prior exposure to DEPs transiently reduced clearance of *L. monocytogenes* and was characterised by significantly decreased phagocytosis and reduced secretion of IL-1 β , IL-12, and TNF- α (Yin *et al.* 2002). Mechanisms by which DEPs were found to increase susceptibility to infection with *P. aeruginosa* include the impairment of bacterial clearance, lung inflammation and pathology, and morphologic changes in the lung epithelium (Harrod 2004). Effects on bacterial clearance were

concentration dependent, with higher doses having a greater inhibitory effect (up to a higher threshold) (Harrod 2004). Interestingly, this impaired clearance of *P. aeruginosa* was only identified with acute exposure to DEPs for one week, whereas exposure for six months had no effect on susceptibility to infection (Harrod 2004).

In contrast to the majority of research in this area, one study has found that BC actually increased resistance to pneumococcal infection (Tellabati *et al.* 2010). In comparison to non-treated controls, pre-treatment of mice with two doses of ultrafine-BC reduced bacterial load and decreased susceptibility to pneumococcal pneumonia upon subsequent challenge. In the study by Tellabati *et al.* (2010), BC exposure caused carbon loading of AM. Carbon-laden AM have also been observed in the bronchoalveolar lavage fluid of humans exposed to smoke from burning biomass, who are known to be more susceptible to pneumonia (Fullerton *et al.* 2009). It has also been repeatedly shown that PM-and BC-laden AM have a decreased ability to phagocytose *S. pneumoniae* (Lundborg *et al.* 2007; Zhou & Kobzik 2007; Renwick 2004). Therefore it is surprising that carbon-laden macrophages were identified in this study, but that BC increased resistance to pneumococcal infection (Tellabati *et al.* 2010). The mechanism for this increased resistance was not identified in the research by Tellabati *et al.* (2010).

1.6. Bacteria associated with particulate matter

In addition to chemical components of PM, there are biological elements. Up to 25 % of aerosols may be of biological origin, consisting of fragments of microbes, pollen, and plant and animal debris (Jalava *et al.* 2016; Jaenicke 2005; Heinrich *et al.* 2003). For example, Gram-negative bacterial endotoxins have been identified in PM, and are interestingly more prevalent in coarse PM compared to fine PM (Gangamma 2014; Heinrich *et al.* 2003). However it has recently become appreciated that entire microbes, rather than simply fragments, may also be suspended with these particulates, and much less is known about the microbiological component of PM in comparison to the chemical components (Cao *et al.* 2014; Alghamdi *et al.* 2014).

One study using culture based methods identified bacteria and fungi associated with both PM₁₀ and PM_{2.5}, with a greater bacterial load associated with the former, and

notable daily variation (Alghamdi *et al.* 2014). Unfortunately no taxonomic classification of bacteria was presented in the investigation by Alghamdi *et al.* (2014). However sequenced-based investigations have revealed more information about the microbial airborne composition. One critical investigation into microbial diversity during a smog event in Beijing in 2013 revealed that bacteria were the most abundant microorganism, contributing 81 % and 86 % to the total microbial component of PM₁₀ and PM_{2.5}, respectively (Cao *et al.* 2014). This was followed by eukaryota at 18 % and 13 %, respectively, with archaea and viruses contributing less than 1 % (Cao *et al.* 2014). Over 85 % of bacteria identified were associated with terrestrial and faecal environments (Cao *et al.* 2014). The most abundant phyla identified in this study were *Actinobacteria*, *Proteobacteria*, *Chloroflexi*, *Firmicutes*, *Bacteroidetes*, and *Euryarchaeota* (Cao *et al.* 2014).

In fact, *Proteobacteria*, *Firmicutes*, and *Actinobacteria* have been repeatedly identified as the most abundant phyla of PM-associated microbes (Gou *et al.* 2016; Gandolfi *et al.* 2015; Yamaguchi *et al.* 2014; Robertson *et al.* 2013; Franzetti *et al.* 2011). *Bacteroidetes*, *Acidobacteria*, *Cyanobacteria*, *Chloroflexi*, and *Deinococcus-Thermus* have also been detected at lower abundances, as well as a variety of other phyla with more minor contributions (Gou *et al.* 2016; Yamaguchi *et al.* 2014; Gangamma 2014; Robertson *et al.* 2013). The exact abundance of each phylum has been found to vary dependent on the location and timing of collection (Yamaguchi *et al.* 2014; Franzetti *et al.* 2011), and depending on the composition of the PM studied (Gandolfi *et al.* 2015). Importantly, key pathogens have been identified associated with PM including *Pseudomonas*, *Staphylococcus*, and *S. pneumoniae* (Gou *et al.* 2016; Cao *et al.* 2014; Gangamma 2014). Therefore as well as bacteria being potentially affected by PM in the host, bacteria can be delivered to a host in conjunction with PM. This means that a host may be confronted with damage from PM at the same time that microbes, including opportunistic pathogens, are introduced into the respiratory tract.

1.7. The respiratory tract microbiota

The sum of all microorganisms present in a specific site or system are collectively described as the microbiota (Huang *et al.* 2013). Although this term encompasses all microbes, including bacteria, viruses, fungi, archaea, and protozoa, it is often used to describe just the bacterial component, which is the meaning used in this thesis. The term ‘microbiome’ is often incorrectly used in the place of ‘microbiota’ (Dickson *et al.* 2014; Beck *et al.* 2012), however in reality, the microbiome refers to the genes and genomes of the microbiota, rather than the microorganisms themselves (Huang *et al.* 2013).

The role of the human respiratory tract microbiota in health and disease is an emerging research area gaining greater recognition (Huang *et al.* 2013; Beck *et al.* 2012). The field has been revolutionised in recent years through the use of sequence-based analysis such as 16S rRNA gene sequencing (Dickson *et al.* 2014; Charlson *et al.* 2011). The upper respiratory tract harbours a distinct microbiota which substantially varies from person to person, and is a main site of entry for colonising microbes, including opportunistic pathogens (Bogaert *et al.* 2011; Charlson *et al.* 2011; Frank *et al.* 2010). Until recently the bacterial density and diversity of the lower respiratory tract has been underappreciated. The microbiota of the lungs generally mirrors the diversity of the upper airways, but holds far fewer microbes (Dickson & Huffnagle 2015; Dickson *et al.* 2014; Charlson *et al.* 2011). Therefore the respiratory tract contains a homogenous microbiota that progressively decreases in biomass from the upper airways down to the lower respiratory tract. Common bacteria of the respiratory tract microbiota include the genera *Streptococcus*, *Staphylococcus*, *Haemophilus*, *Neisseria*, *Pseudomonas*, *Fusobacteria*, and *Veillonella* (Vernatter & Pirofski 2013; Beck *et al.* 2012), and as well as harbouring commensals, opportunistic pathogens may be members of the microbiota.

1.8. *Streptococcus pneumoniae*

S. pneumoniae (the pneumococcus) is a Gram-positive coccus which asymptotically colonises the nasopharynx of the human respiratory tract (Shak *et al.* 2013b; Hogberg

et al. 2007). An estimated 30-88 % of children are colonised with *S. pneumoniae*, but carriage declines to 5-20 % in adults (Wyllie *et al.* 2014; Shak *et al.* 2013b; Mook-kanamori *et al.* 2011; Lanie *et al.* 2007; Hussain *et al.* 2005; Bogaert *et al.* 2004). Nasopharyngeal colonisation may be transient, lasting for weeks to months before bacteria are cleared, or instead of clearance, carriage may progress to infection (Gritzfeld *et al.* 2014; Kadioglu *et al.* 2008). Therefore the colonised nasopharynx acts as a reservoir from which pneumococci can spread and cause disease (Bogaert *et al.* 2004; Bogaert *et al.* 2001).

The pneumococcus may infect a variety of sites within a host, including both the upper and lower respiratory tract. The most common non-invasive diseases associated with pneumococcal infection are acute otitis media (an infection of the middle-ear), sinusitis, and bronchitis (Kadioglu *et al.* 2008). However it is also able to cause a variety of more serious invasive diseases such as pneumonia, bacteraemia, and meningitis, which carry much higher mortality rates than non-invasive disease (Shak *et al.* 2013b; Vernatter & Pirofski 2013; Mook-kanamori *et al.* 2011). Indeed, 50 % of community-acquired pneumonia (CAP) cases in developing countries result in death, compared to 20 % in developed countries (Bogaert *et al.* 2004). Furthermore, up to 60 % of CAP survivors develop long-term complications such as hearing loss and neurological deficits (Koedel *et al.* 2002). Mortality from pneumococcal meningitis ranges from 18 % to 37 %, and 20 % to 30 % of survivors experience cognitive impairments (Weisfelt *et al.* 2006; van de Beek *et al.* 2004; Kastenbauer & Pfister 2003; van de Beek *et al.* 2002). Young children, the elderly, and those with immunodeficiencies are most at risk of pneumococcal disease (O'Brien *et al.* 2009; Bogaert *et al.* 2004; Koedel *et al.* 2002). In particular, *S. pneumoniae* causes around 1 million deaths per year in HIV-negative children under 5 years old, representing ~11 % of all deaths in this age group (O'Brien *et al.* 2009; Bogaert *et al.* 2004).

Importantly, prior establishment of nasopharyngeal colonisation and carriage is vital before a pneumococcal infection can occur (Simell *et al.* 2012; Weiser 2010).

Therefore factors which influence colonisation can impact the possibility of later development of disease. The exact mechanisms which promote the transfer from colonisation to infection are not yet fully understood, however co-infection with certain

viruses, including respiratory syncytial virus (RSV) and influenza A virus, have been implicated in this switch, and viral infection often precedes or occurs alongside pneumococcal infection (Smith *et al.* 2014; Pettigrew *et al.* 2014; Chertow & Memoli 2013; Marks *et al.* 2013; Launes *et al.* 2012).

1.8.1. Virulence determinants of *S. pneumoniae*

Arguably the most important pneumococcal virulence factor is the capsule, the polysaccharide outermost layer of the cell (Shainheit *et al.* 2014). The capsule encloses and protects the pneumococcal cell, is generally covalently attached to the cell wall, and depending on the strain, may be 200-400 nm thick (Sorensen *et al.* 1990; Sorensen *et al.* 1988). The capsule is negatively charged and repulses the sialic acid residues of mucus, preventing entrapment in mucus layer of the nasopharynx during colonisation (Nelson *et al.* 2007). In addition, the capsule prevents bacteria being detected by the host immune system by shielding underlying surface molecules (Nelson *et al.* 2007). Once pneumococci have passed through the mucus layer, capsule expression is reduced, exposing surface molecules to allow adhesion to the host epithelium and enable biofilm formation (Shainheit *et al.* 2014; Sanchez *et al.* 2011; Munoz-Elias *et al.* 2008; Hammerschmidt *et al.* 2005). During infection however, capsule expression is increased, which is thought to assist bacteria to evade opsonisation and phagocytosis (Shainheit *et al.* 2014; Hava *et al.* 2003). Pneumococcal capsules are biochemically distinct, depending on the nature of the polysaccharide repeat unit and enzymes involved in its production, and distinguish the 91 serotypes of *S. pneumoniae* (Calix *et al.* 2012; Weinberger *et al.* 2009; Bentley *et al.* 2006). Encapsulated and unencapsulated pneumococci exist, both of which are recovered from clinical samples, however unencapsulated strains are more often associated with infections such as conjunctivitis, whereas encapsulated strains are associated with more severe infections (Valentino *et al.* 2014; Crum *et al.* 2004; Martin *et al.* 2003; Catterall 1999).

In addition to the capsule, pneumolysin (Ply) is a vital pneumococcal virulence factor with roles in colonisation, infection, and inflammation (Harvey *et al.* 2011; Berry *et al.* 1999; Canvin *et al.* 1995; Walker *et al.* 1987). Ply oligomerises in cholesterol-containing membranes, disrupting cell functioning or causing cytolysis, depending on

the concentration (Marshall *et al.* 2015; Harvey *et al.* 2011; Marriott *et al.* 2008; Tilley *et al.* 2005). Ply may facilitate colonisation by inducing the expression of adhesion molecules on the host cell surface, but may also activate complement, which is in part due to stimulating the release of Interleukin-1 β (IL-1 β), tumour necrosis factor- α (TNF- α), and leukotriene C₄ (Cruse *et al.* 2010; Marriott *et al.* 2008).

Three groups of pneumococcal cell-surface proteins are linked to the cell wall; choline-binding proteins, lipoproteins, and covalently linked proteins (Bergmann & Hammerschmidt 2006). The choline binding proteins include Surface Protein A (PspA), which aids in colonisation and interferes with complement (Parker *et al.* 2009; King *et al.* 2006), and autolysin (LytA), which is reported to be responsible for Ply release, causing cell lysis under specific environmental conditions (Mitchell *et al.* 1997; Benton *et al.* 1997; Canvin *et al.* 1995). It has also been reported that Ply may be released in the absence of LytA-induced autolysis, however the nonautolytic release mechanism remains unidentified (Price *et al.* 2012; Balachandran *et al.* 2001).

Pneumococcal neuraminidases are thought to aid in colonisation by exposing receptors for adherence, and Neuraminidase A (NanA) has been shown to be important in biofilm formation (Xu *et al.* 2011; Parker *et al.* 2009). NanA and NanB are involved in the removal and metabolism of sialic acid, respectively, and the genes encoding these neuraminidases, *nanA* and *nanB*, are found in 100 % and 96 % of *S. pneumoniae* strains, respectively (Gualdi *et al.* 2012; Xu *et al.* 2011; Xu *et al.* 2008; Pettigrew *et al.* 2006). In contrast, *nanC* is present in only 51 % of strains (Pettigrew *et al.* 2006). NanC is a regulator of the neuraminidases NanA and NanB, and has two functions (Hayre *et al.* 2012; Xu *et al.* 2011; Pettigrew *et al.* 2006). The first is producing an intermediate metabolic compound (2-deoxy-2,3-didehydro-N-acetylneuraminic acid) which acts as a neuraminidase inhibitor, and the second function is hydrating this inhibitor when the substrate is depleted (Hayre *et al.* 2012; Xu *et al.* 2011; Pettigrew *et al.* 2006).

Bacteriocins are antimicrobial peptides used to inhibit or kill other bacteria.

Pneumococci have at least four bacteriocin systems which regulate killing of other pneumococcal strains (Miller *et al.* 2016; Kjos *et al.* 2016; Hoover *et al.* 2015; Bogaardt *et al.* 2015; Guiral *et al.* 2005). As multiple pneumococcal strains may

cocolonise the nasopharynx at the same time, bacteriocin production is a competition strategy which has the potential to impact the duration of carriage of different strains, and thereby impact disease progression. There is considerable variation between the bacteriocins produced by different strains, therefore putative immunity genes are thought to defend against the bacteriocins of other strains, and prevent bacteriocin-associated suicide (Miller *et al.* 2016; Bogaardt *et al.* 2015).

It is clear that *S. pneumoniae* is an important global pathogen, able to cause a variety of non-invasive and invasive diseases, including severe respiratory infections such as pneumonia. This results in *S. pneumoniae* being responsible for a considerable number of deaths each year. This is in part due to the array of effective virulence factors *S. pneumoniae* carries, as well as its ability to survive in diverse environments within the human host. The range of ecological niches pneumococci can survive in, and the diseases it may cause, is a testament to the adaptability of this organism. The importance of this pathogen, its colonisation of the respiratory tract (where it may interact with PM), and the respiratory infections it is able to cause, make *S. pneumoniae* a suitable model organism in this research.

1.9. *Staphylococcus aureus*

S. aureus is a Gram-positive coccus which colonises the skin and mucosal membranes (Wertheim *et al.* 2005). All skin and mucous membranes may be colonised, however carriage in the nasal passages, particularly the nares, is most common. Approximately 20 % of people are consistently colonised in this site, with 30-80 % being intermittently colonised at some point in their lives (Edwards *et al.* 2012; Liu 2009; van Belkum *et al.* 2009; Wertheim *et al.* 2005; Kluytmans *et al.* 1997).

As well as being a commensal, *S. aureus* causes a wide range of infections ranging from minor skin infections to invasive diseases including pneumonia, septicaemia, meningitis, and endocarditis (Porto *et al.* 2013; Park *et al.* 2013; Edwards *et al.* 2012; Durai *et al.* 2010; Wertheim *et al.* 2005). In fact, *S. aureus* is the leading cause of infectious endocarditis in most western countries, which is often an aggressive and fatal infection (Fernández Guerrero *et al.* 2009; Fowler *et al.* 2005; Sanabria *et al.* 1990).

The majority of *S. aureus* infections following colonisation are known to be caused by the same strain, therefore colonisation is a significant risk factor for infection (Balm *et al.* 2013; Safdar & Bradley 2008; Huang *et al.* 2008; Wertheim *et al.* 2005).

1.9.1. The *S. aureus* genome and Methicillin-Resistant *S. aureus*

It is estimated that 75 % of the 2.8 Mbp genome of *S. aureus* encodes the highly conserved core genome. This core genome contains the seven house-keeping genes which determine separation of strains into sequence types (ST) within clonal complexes (CC) (Lindsay & Holden 2006; Feil *et al.* 2003; Enright *et al.* 2000). The remaining 25 % of the genome encodes additional genes acquired through horizontal gene transfer (HGT) (Lindsay & Holden 2006). Therefore *S. aureus* strains show a huge genetic diversity. *S. aureus* HGT involves mobile genetic elements including plasmids, bacteriophages, and Staphylococcal cassette chromosomes (SCC) (Malachowa & DeLeo 2010).

β -lactam antibiotics including penicillin, oxacillin, and methicillin have historically been the front-line treatments for infections by Gram-positive pathogens including *S. aureus*. However, constant antibiotic exposure and sub-lethal antibiotic treatment promote the development of antibiotic resistance (Andersson & Hughes 2014). For example, penicillin was introduced in the 1940s and penicillin resistant *S. aureus* were reported as early as 1942 (Rammelkamp & Maxon 1942). Methicillin-Resistant *S. aureus* (MRSA) first emerged in the 1960s, soon after the introduction of methicillin in 1961 (Lowy 2003; Jevons *et al.* 1963). Since then, MRSA strains have become a major cause of infections worldwide (WHO 2014c; Köck *et al.* 2010).

The *mecA* gene, which is carried on the SCC_{mec} cassette and is acquired through horizontal gene transfer, confers the MRSA phenotype (ECDC 2015; Durai *et al.* 2010; Ito *et al.* 2009; Palavecino 2007). *mecA* encodes for PBP2a, a variant penicillin-binding protein which has a low affinity for β -lactams, providing resistance to β -lactam antibiotics including methicillin (ECDC 2015; Durai *et al.* 2010; Palavecino 2007). The level of methicillin resistance depends on the amount of PBP2a production, which is influenced by a variety of genetic factors (ECDC 2015). This antibiotic resistance makes MRSA infections more difficult to treat than infections caused by Methicillin

Sensitive *S. aureus* (MSSA) strains (ECDC 2015; Durai *et al.* 2010; Palavecino 2007). Therefore MRSA are associated with more invasive infections and higher mortality rates than MSSAs (Porto *et al.* 2013; Park *et al.* 2013; Edwards *et al.* 2012). However it is important to note that MRSA infections add to, rather than replace, MSSA infections, therefore increasing the overall burden of disease (ECDC 2015). The MRSA problem is further exacerbated by the recent development of resistance to last-line antibiotics including vancomycin, daptomycin, and linezolid, highlighting the current shortage of appropriate antibiotic choices (Stefani *et al.* 2015; Yue *et al.* 2014; Gardete & Tomasz 2014; Gu *et al.* 2013).

Over 50 % of clinical staphylococcal cultures in the USA are MRSA (WHO 2014c; Kavanagh *et al.* 2013). In contrast, MRSA levels are generally much lower in Europe, particularly Northern Europe, where levels have been decreasing over the last 10 years (PHE 2016; ECDC 2015; WHO 2014c; Public Health England 2013). Less than 1-3 % of invasive *S. aureus* isolates are currently reported to be methicillin resistant in Scandinavia and the Netherlands, but higher levels of 10-25 % are reported for the UK, Germany, Spain, and France (ECDC 2015; WHO 2014c). There has been a reduction in MRSA infections in the UK over the last decade, which may be attributed to the implementation of hand-washing for hospital staff and visitors, mupirocin decolonisation for MRSA positive individuals, more effective environmental disinfection, and a reduction in ciprofloxacin prescriptions. MRSA strains display high ciprofloxacin resistance due to historical use, therefore it has been hypothesised that the reduction in ciprofloxacin prescriptions reduced the selective pressure for MRSA infections (Knight *et al.* 2012). In contrast to the rest of Europe, 25 % to greater than 50 % of *S. aureus* isolates are reported to be methicillin resistant in countries of Southern Europe including Portugal, Italy, and Greece (ECDC 2015; WHO 2014c).

Initially MRSA infections were almost exclusively associated with hospital exposure, referred to as Healthcare Associated MRSA (HA-MRSA). HA-MRSA infections are most common in immunocompromised individuals and those with implanted medical devices which require antibiotic therapy (Liu 2009). However in the past few years hyper virulent MRSA strains have emerged which are able to cause disease in otherwise healthy individuals outside of the healthcare setting, referred to as

Community Acquired MRSA (CA-MRSA) (Gupta *et al.* 2015; Sowash & Uhlemann 2014; David & Daum 2010; DeLeo *et al.* 2010; M. D. King *et al.* 2006). CA-MRSA strains are particularly associated with skin and soft tissue infections (SSTI) and currently CA-MRSA are a major healthcare issue worldwide (Gupta *et al.* 2015). In the USA in particular, CA-MRSA infections are an epidemic becoming increasingly problematic with the emergence of strain USA300, and incidences of CA-MRSA cases are higher than with HA-MRSA strains (Liu 2009; M. D. King *et al.* 2006).

The combinations of six classes of *mec* gene complexes and eight types of *ccr* (cassette chromosome recombinase) gene complexes within *SCCmec* allow the separation of eleven *SCCmec* types (Ito *et al.* 2009). Typically, HA-MRSA strains are associated with the larger *SCCmec* types I, II, and III, whereas CA-MRSAs tend to have the smaller *SCCmec* types IV and V (David & Daum 2010; Diederens & Kluytmans 2006). In addition, CA-MRSA strains often carry the *lukSF-PV* genes encoding the Panton–Valentine leukocidin toxin (David & Daum 2010). Interestingly, it has been reported that carriage of the larger *SCCmec* type II carries a fitness burden which is not evident with the smaller *SCCmec* type IV (Knight *et al.* 2013).

1.9.2. Virulence determinants of *S. aureus*

S. aureus virulence factors can be divided into cell surface and secreted factors (Costa *et al.* 2013). Two important cell surface virulence factors are Staphylococcal Protein A (SpA) and capsular polysaccharides. SpA binds to Immunoglobulin G (IgG), interferes with opsonisation and phagocytosis, and binds to the receptor for TNF- α , reducing proinflammatory signalling (Zecconi & Scali 2013; Costa *et al.* 2013). The capsular polysaccharides reduce phagocytosis and enhance colonisation (Costa *et al.* 2013). Therefore both are key factors in colonisation and the avoidance of bacterial killing.

Important secreted virulence factors include haemolysins and various exoproteins such as nucleases (Nuc and Nuc2) and lipases (Costa *et al.* 2013). *S. aureus* strains may produce 4 distinct haemolysins (α , β , δ , and γ), which cause lysis in a wide range of cells (Huseby *et al.* 2007; Dinges *et al.* 2000). These haemolysins are important for colonisation and virulence, altering interactions with the host immune system and

disease progression (Huseby *et al.* 2007; Dinges *et al.* 2000). Specifically, strains which produce high levels of α -haemolysin are associated with more invasive diseases (Stulik *et al.* 2014; Huseby *et al.* 2007; Dinges *et al.* 2000). The main roles of the nucleases are in the disruption of neutrophil extracellular traps (NETs) and the modulation of biofilm formation (Lister & Horswill 2014; Kiedrowski *et al.* 2014). In addition, nucleases degrade DNA released into the *in vivo* environment by killed bacteria, preventing its action as an immunostimulant via toll-like receptors (Kiedrowski *et al.* 2014; Lister & Horswill 2014; Ishii & Akira 2006). Lipases are involved in interference with granulocytes, macrophages, and platelets, and inactivating bacteriocidal lipids, and are upregulated in biofilms and during deep-tissue infections (Hu *et al.* 2012). This array of diverse virulence factors explains the ability of *S. aureus* to infect and manipulate a wide range of environments, mediating its survival within the host.

It is clear that *S. aureus* is an important global pathogen. The diversity of sites which *S. aureus* can colonise, the array of diseases it can cause, and its variety of virulence determinants all show the adaptability of this organism. This is partially due to the ability of this bacterium to effectively assess and respond to its environment with a complex system of gene expression regulation. The importance of respiratory tract colonisation as a risk factor for the development of disease, and the role of *S. aureus* in respiratory infections, make *S. aureus* a suitable model organism in this research.

1.10. Bacterial biofilm formation

Biofilms are a major colonisation and virulence factor of many bacteria, and are an important aspect of the work described in this thesis. Bacterial biofilms are highly structured communities of behaviourally coordinated microbes which adhere to a surface and are enveloped inside an extracellular polymeric matrix (Donlan & Costerton 2002; Costerton *et al.* 1999). These may be single or multi-species structures (Shak *et al.* 2013b), and are vital for both colonisation and infection. The biofilm formation process is shown in Figure 1-5. After attachment to a surface, bacteria divide to form a microcolony and matrix production is initiated (Flemming & Wingender 2010). Other bacteria may then be recruited as the biofilm develops. The extracellular matrix is formed through the production of extracellular polymeric substances, and

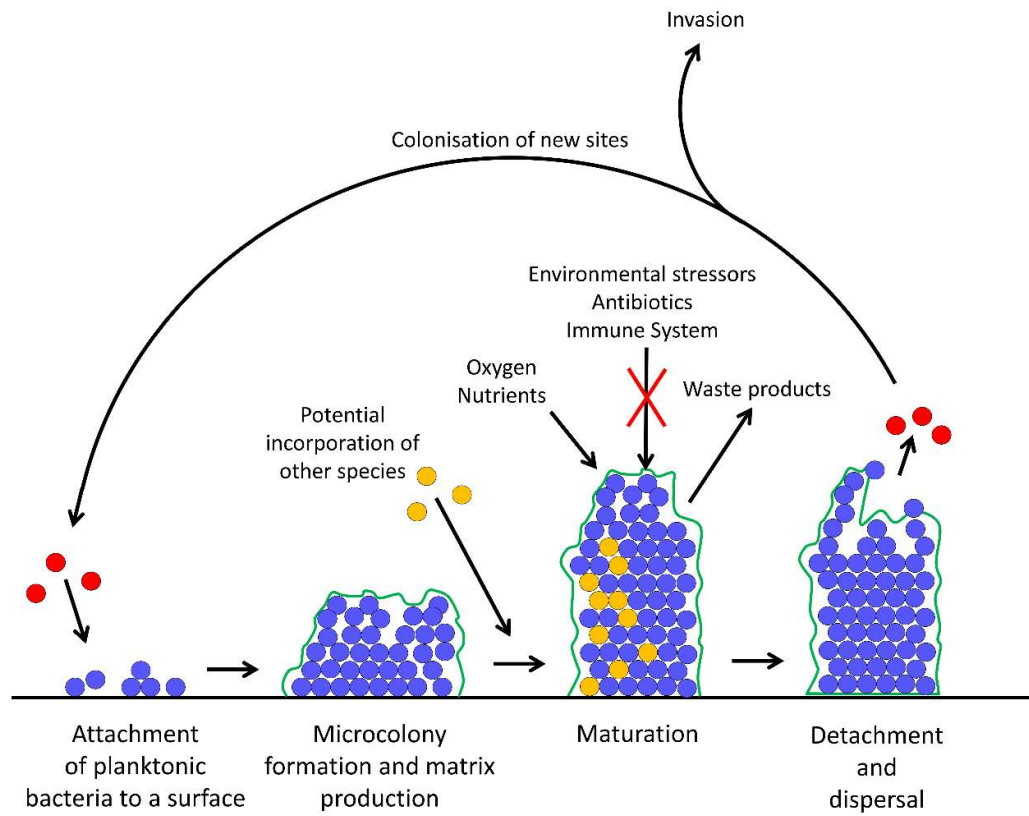


Figure 1-5. Stages of biofilm formation

provides a scaffold for biofilm architecture. The extracellular material produced is largely species-, strain-, and environment-dependent, with the main constituents being extracellular polysaccharides, proteins, and DNA (Foster *et al.* 2014; Domenech *et al.* 2012; Flemming & Wingender 2010; Rice *et al.* 2007; Cucarella *et al.* 2001; Cramton *et al.* 1999). In fact, the matrix can contribute over 90 % of the dry mass of biofilms (Flemming & Wingender 2010). Due to the close proximity of bacteria and the amount of extracellular DNA, biofilms also provide an environment for horizontal gene transfer (Chao *et al.* 2015; Savage *et al.* 2013; Domenech *et al.* 2012; Archer *et al.* 2011).

The major advantage of biofilm formation is an increased resistance to environmental stressors such as the host immune system and antibiotics, which allows bacteria to persist in hostile environments (Domenech *et al.* 2013; De la Fuente-Nunez *et al.* 2013; Marks *et al.* 2012a). This protection is achieved through the increased tolerance to stressors, rather than due to mutations or the acquisition of antibiotic resistance genes (Chao *et al.* 2015). The extracellular matrix acts as a barrier to antimicrobials, protecting bacteria within the biofilm (De la Fuente-Nunez *et al.* 2013; Archer *et al.* 2011; Kiedrowski & Horswill 2011; Flemming & Wingender 2010). Bacteria within biofilms are also a heterogeneous population, with a large proportion of bacteria existing in a sessile state, having a reduced metabolism and growth rate. These bacteria can therefore be less susceptible to antimicrobials which target replication machinery (Chao *et al.* 2015; De la Fuente-Nunez *et al.* 2013; Donlan & Costerton 2002; Costerton *et al.* 1999).

Mature biofilms can also act as a reservoir for infection, dispersing bacteria to infect other sites whilst evading eradication, therefore allowing infections to persist (Chao *et al.* 2015; Costerton *et al.* 1999; Fowler *et al.* 1997). The resistance of biofilms to antimicrobials impacts the effectiveness of infection treatment strategies, and the dispersion of bacteria to other sites allows the potential to seed infection and systemic disease. The role of biofilms in infectious disease, and the difficulty in their eradication, make biofilms particularly important in relation to public health (De la Fuente-Nunez *et al.* 2013; Donlan & Costerton 2002).

1.10.1. Pneumococcal biofilms

Biofilm formation is a key aspect of pneumococcal nasopharyngeal colonisation, which is a necessary step before pneumococcal disease (Gilley & Orihuela 2014; Blanchette-cain *et al.* 2013; Marks *et al.* 2012a; Domenech *et al.* 2012; Sanchez *et al.* 2011; Munoz-Elias *et al.* 2008). Pneumococci found in biofilms during colonisation are predisposed towards an avirulent and less invasive phenotype than their planktonic counterparts, for example through the downregulation of virulence genes including those for Ply production (Gilley & Orihuela 2014; Blanchette-cain *et al.* 2013; Qin *et al.* 2013; Sanchez *et al.* 2011; Trappetti *et al.* 2011). Due to biofilm formation, colonised nasopharyngeal pneumococci are far more difficult to eradicate than pneumococci in invasive disease (García-Rodríguez & Fresnadillo Martínez 2002; Varon *et al.* 2000; Cohen *et al.* 1999; Dagan *et al.* 1998; Dabernat *et al.* 1998; Cohen *et al.* 1997).

However, pneumococcal biofilms are able to disperse bacteria that may colonise new environments and potentially cause disease. Pneumococci dispersed from biofilms are a distinct population in comparison to both biofilm and planktonic bacteria. Dispersed pneumococci have been reported to display an increased transcription of genes associated with virulence, including those for the capsule, pneumolysin, the adhesin *pavA*, autolysin, and bacteriocin, but a reduction in the transcription of genes associated with competence and fratricide (Chao *et al.* 2015; Pettigrew *et al.* 2014; Marks *et al.* 2013). It has also been shown that planktonic, biofilm, and dispersed pneumococci are all able to colonise the mouse nasopharynx in an *in vivo* colonisation model, however dispersed pneumococci disseminate from the nasopharynx to the lungs and middle ear at a higher degree than planktonic and biofilm bacteria (Marks *et al.* 2013; Sanchez *et al.* 2010; Smith *et al.* 2002). Mice infected with dispersed pneumococci also show a greater inflammatory response than those infected with biofilm and planktonic bacteria, including more denudation of the nasal epithelium and larger inflammatory infiltrates in the middle ear and lungs (Blanchette-cain *et al.* 2013; Marks *et al.* 2013). Furthermore, biofilm bacteria aspirated into the lungs are cleared over time and do not penetrate into the bloodstream, whereas infection with dispersed pneumococci is associated with a greater bacterial burden in the lungs and bacteraemia (Marks *et al.* 2013). Therefore the

establishment of pneumococcal biofilms in the nasopharynx can provide protection from eradication while also seeding virulent bacteria to cause infection. In addition to this role in colonisation and the seeding of infection, pneumococcal biofilms have been directly associated with infections including chronic middle ear infections and chronic rhinosinusitis (Hoa *et al.* 2009; Reid *et al.* 2009; Hall-Stoodley *et al.* 2006; Sanderson *et al.* 2006).

DNaseI and proteinase K have been shown to inhibit pneumococcal biofilm formation and disperse pre-formed mature biofilms (Hall-Stoodley *et al.* 2008; Moscoso *et al.* 2006). This suggests that extracellular DNA (eDNA) and surface exposed and extracellular proteins are both required for pneumococcal biofilm formation, and are vital components of the mature biofilm extracellular matrix. Biofilms are also an important for genetic exchange, and competence genes are upregulated in biofilm pneumococci (Marks *et al.* 2013; Marks *et al.* 2012b; Domenech *et al.* 2012). Research with isogenic mutants has shown that pneumolysin, surface protein A, autolysin, glucosaminidase (LytB), lysozyme (LytC), choline binding protein A (CbpA), pneumococcal serine-rich repeat protein (PsrP), and pneumococcal choline-binding protein A (PcpA) are all required for biofilm formation to varying degrees (Blanchette-cain *et al.* 2013; Moscoso *et al.* 2006). The role of each of these factors has not yet been fully determined, however the role of pneumolysin has been partially elucidated, in that pneumolysin is known to be expressed early in biofilm development and its function appears to be independent of its haemolytic activity (Shak *et al.* 2013a). The role of polysaccharides in pneumococcal biofilms are not yet well defined (Chao *et al.* 2015; Domenech *et al.* 2012; Camilli *et al.* 2011; Moscoso *et al.* 2009). Interestingly, encapsulated pneumococci are poorer biofilm formers than their unencapsulated counterparts, which display greater adhesion and biofilm formation (Chao *et al.* 2015; Domenech *et al.* 2012; Moscoso *et al.* 2009). Furthermore, encapsulated pneumococci within biofilms decrease capsular polysaccharide production, thus exposing surface proteins for adhesion, and increase production of cell wall phosphorylcholine, which binds to platelet-activating factor receptor (PAFr) on host epithelial cells, enhancing bacterial adhesion (Gilley & Orihuela 2014; Shainheit *et al.* 2014; Sanchez *et al.* 2011). It is therefore clear that pneumococci form highly protective and complex biofilms in

the respiratory tract, and that these biofilms are key in both colonisation and infection, adding to the effectiveness of *S. pneumoniae* as an accomplished pathogen.

1.10.2. *S. aureus* biofilms

A variety of evidence suggests that *S. aureus* forms biofilms in the respiratory tract during colonisation (Iwase *et al.* 2010; Quinn *et al.* 2009; Sanderson *et al.* 2006). The ability of *S. aureus* strains to colonise the nasal epithelia has been shown to be associated with the ability to form biofilms *in vitro*, in that nasal colonised strains produced much larger biofilms than non-carrier strains (Quinn *et al.* 2009).

Furthermore, biofilms have been identified on the sinus mucosa of patients with chronic rhinosinusitis (Sanderson *et al.* 2006), however this may be a feature of the disease and not indicative of normal nasal colonisation. Interestingly, nasal colonisation of *Staphylococcus epidermidis* strains which secrete serine protease (Esp) has been shown to be negatively associated with *S. aureus* colonisation, and it is known that Esp inhibits biofilm formation and eliminates mature biofilms of *S. aureus in vitro* (Iwase *et al.* 2010). Furthermore, inoculation of both Esp producing *S. epidermidis* and pure Esp into the nasal cavities of people colonised with *S. aureus* eliminates *S. aureus* colonisation (Iwase *et al.* 2010).

The role of biofilms in diseases caused by *S. aureus* are better elucidated than for colonisation. Biofilms of *S. aureus* are associated with a variety of illnesses including endocarditis, osteomyelitis, periodontitis, chronic wound infection, ocular infections, and the infection of indwelling medical devices (Archer *et al.* 2011). *S. aureus* is one of the leading causes of contamination of indwelling medical devices, and is known to form biofilms on a huge variety of implants, including catheters, mechanical heart valves, aspirators, and pacemakers (Percival *et al.* 2015; Baldoni *et al.* 2009; Costerton *et al.* 2005). Of particular note is the contamination of central venous catheters and urinary catheters, which are often required to be implanted in patients for long-term use, and can become contaminated both internally and externally (Percival *et al.* 2015). It is therefore clear that biofilm formation may be an important predeterminant of the diseases caused by this bacterium and that biofilms of *S. aureus* represent a serious healthcare issue.

Attachment of *S. aureus* to a surface is partly mediated by microbial surface component recognizing adhesive matrix molecules (MSCRAMMs) (Foster *et al.* 2014). These are the largest class of cell wall-anchored proteins in *S. aureus* and have roles in adhesion to, and invasion of, host tissues, evasion of the immune response, and biofilm formation (Foster *et al.* 2014). Surface protein G (SasG), which binds to the extracellular matrix, and extracellular matrix protein-binding protein (Emp), which binds to host cells, are also both required for adhesion and aggregation (Zecconi & Scali 2013). In addition to these proteins, Polysaccharide Intercellular Adhesin (PIA) is also required for aggregation (Lister & Horswill 2014; O’Gara 2007), and PIA, SasG, Emp, and Extracellular adherence protein (Eap/Map) are all vital for the initial stages of biofilm formation (Zecconi & Scali 2013).

The extracellular matrix of *S. aureus* biofilms consists of polysaccharide, protein, and DNA. The contribution of each of these to the biofilm structure depends heavily on the strain and environmental conditions under which biofilms are formed (Abraham & Jefferson 2012; O’Gara 2007; Fitzpatrick *et al.* 2005). Furthermore, the effectiveness of mechanisms that may disperse biofilms depend on matrix composition (O’Neill *et al.* 2007; Chaignon *et al.* 2007). Similarly to *S. pneumoniae*, eDNA is important in biofilm formation by *S. aureus*, is a major component of the extracellular matrix, and allows genetic exchange between bacteria (Savage *et al.* 2013; Archer *et al.* 2011). Investigations into *S. aureus* nucleases demonstrate the importance of eDNA. Nucleases are downregulated during biofilm formation, increasing eDNA levels, whereas an increase in *nuc* expression reduces biofilm formation (Kiedrowski *et al.* 2011; Mann *et al.* 2009). There are two main biofilm formation pathways employed by *S. aureus*; the intracellular adhesion-dependent (*ica*-dependent) pathway and the *ica*-independent pathway, which produce either polysaccharide-based or protein-based biofilms, respectively (O’Gara 2007).

Ica-dependent biofilm formation involves the induction of the *ica* locus encoding *icaADBC* (O’Gara 2007; Cramton *et al.* 1999). The *ica* operon codes for products for the construction of polymeric N-acetylglucosamine (PNAG), which gives rise to Polysaccharide Intercellular Adhesin (PIA), and therefore this pathway results in polysaccharide-based biofilms (O’Gara 2007; Cramton *et al.* 1999). IcaR is arguably

the most important factor in regulation of the *icaADBC* operon, binding to the *icaADBC* promoter and repressing transcription (Cue *et al.* 2009; Jefferson *et al.* 2004). IcaR is involved in environmental regulation, being repressed during ethanol exposure (Cue *et al.* 2012; Conlon *et al.* 2002), and is in turn regulated by the protein regulator of biofilm formation (*rbf*) via SarX. Rbf upregulates expression of *sarX*, which in turn represses *icaR* transcription, thereby activating *icaADBC* expression and causing an increase in biofilm formation (Cue *et al.* 2013; Archer *et al.* 2011; Cue *et al.* 2009; Luong *et al.* 2009; Lim *et al.* 2004). Additional regulators of the *ica* locus also include staphylococcal accessory gene regulator SarA and sigma factor B (SigB) (Cue *et al.* 2013; Cerca *et al.* 2008; O’Gara 2007; Tormo *et al.* 2005).

Ica-dependent biofilm formation mechanisms tend to be favoured by MSSA strains (McCarthy *et al.* 2015; O’Gara 2007; O’Neill *et al.* 2007). Biofilm formation of MSSA strains is increased by exposure to NaCl, and correspondingly the *ica* operon is strongly induced by NaCl (and less so by glucose) (Agarwal & Jain 2013; O’Neill *et al.* 2007; Fitzpatrick *et al.* 2006; Lim *et al.* 2004). As the *ica*-dependent biofilm formation pathway forms polysaccharide-based biofilms, these are susceptible to treatment with sodium metaperiodate, which oxidises polysaccharide bonds, but are resistant to proteinase K degradation (O’Neill *et al.* 2007).

In contrast, *ica*-independent mechanisms of biofilm formation are characterised by biofilm associated protein (Bap), Staphylococcal Protein A (SpA), surface protein clumping factor B (ClfB), fibronectin binding proteins (FnBP), and autolysin (Atl) (Valle *et al.* 2012; Abraham & Jefferson 2012; Houston *et al.* 2011; Archer *et al.* 2011; O’Gara 2007; Cucarella *et al.* 2001). These biofilms are therefore protein-based (O’Gara 2007). Bap is a particularly important surface protein which promotes bacterial adherence and intercellular adhesion, and is positively regulated by SarA independently of the accessory gene regulator (Agr) system (Trotonda *et al.* 2005; Cucarella *et al.* 2001).

Ica-independent biofilm formation is favoured by MRSA strains, and is strongly induced by glucose (McCarthy *et al.* 2015; O’Gara 2007; O’Neill *et al.* 2007). Biofilms formed via this pathway are resistant to sodium metaperiodate degradation, but

susceptible to proteinase K (Nicholson *et al.* 2013; O'Neill *et al.* 2007; Kogan *et al.* 2006). Overall the formation of *S. aureus* biofilms is a complex, multifaceted process which depends on both strain and environmental factors, and it is clear that biofilms are vital in the array of diseases caused by *S. aureus*.

1.11. Effects of particulate matter on microbiota diversity

Alterations in the host microbiota have been strongly implicated in causing increased morbidity and mortality, however limited research exists examining the effect of PM on the diversity of any microbiota. To my knowledge, only one study has assessed the effects of PM on the respiratory tract microbiota. This study used culture-based methods to show that a mixture of SO₂, NO₂, CO, and PM₁₀ collected in Shenyang, China, altered the density of anaerobic bacteria in the oropharynx of rats (Xiao *et al.* 2013). However as this was culture-based, only culturable bacteria were examined. Furthermore, microbial diversity was not assessed and no data was presented to show which bacteria were recovered at any taxonomic level.

Inhaled PM may be cleared from the lungs via ciliary clearance and subsequently swallowed, or may deposit on foods and drink prior to ingestion, thereby entering the gastrointestinal tract (Lippmann 2014; Salim *et al.* 2013; Beamish *et al.* 2011). Therefore the effect of PM on the gastrointestinal microbiota has also been investigated. Mice exposed to ingested PM₁₀ for 35 days have been shown to have an altered gastrointestinal microbial diversity, in that the microbiota of control and PM-exposed mice clustered separately (Kish *et al.* 2013). Altered host gene expression, cytokine secretion, and gut permeability were identified in this study, but it was unclear whether the microbiota was altered due to these factors or due to direct effects of PM on the bacteria (Kish *et al.* 2013; Salim *et al.* 2013). Outside of the host, BC enters marine systems from the atmosphere and rivers, and has been found to change the diversity of marine microbial communities, which has the potential to impact marine ecosystems (Cattaneo *et al.* 2010).

1.12. Effects of particulate matter and other inhaled compounds on bacterial phenotypes

The mechanisms responsible for the PM-induced altered susceptibility to infection have been researched with focus on the effects on host cells and tissues (Section 1.5). However it is as yet unclear whether the altered resistance to infection is entirely due to alterations of the host, or whether PM also directly affects bacteria. Although research has investigated the response of bacteria to a PM-exposed host, there is extremely limited past research into the direct effect of PM on bacteria. One study has shown that urban PM₁₀ collected in Birmingham, UK, had no effect on the growth of *Haemophilus influenzae* or *S. pneumoniae* in Iso-sensitest broth (Adedeji *et al.* 2004). However this study did not characterise the composition of the PM collected, and assessed growth in only one medium (Adedeji *et al.* 2004).

Even though limited bacterial research has been conducted with PM, the effects of PM components, similar particles, and other inhaled compounds have been researched more extensively. One study has evaluated the effect of outdoor road dusts on bacterial growth and biofilm formation (Suraju *et al.* 2015). The reference material used was made to model outdoor dust, which may be considered a component of primary PM, though is not an ideal choice for PM investigations (Air Quality Expert Group 2012; Przyk *et al.* 2008). Outdoor dust reduced growth of *Enterococcus faecalis*, but not *Escherichia coli* or *P. aeruginosa*, and only had this effect at the highest concentration tested, 500 µg/ml (Suraju *et al.* 2015). 100 µg/ml outdoor dust also significantly increased biofilm formation of all three bacteria in both nutrient-rich and nutrient-poor growth conditions (Suraju *et al.* 2015).

Cigarette smoke contains a variety of harmful components including chemicals such as carbon monoxide and methane, aromatics, volatile organic compounds, and PM (You *et al.* 2015; B. Wang *et al.* 2012). In fact, cigarette smoke contributes to PM air pollution (De Marco *et al.* 2015; Invernizzi *et al.* 2004). However, there are a variety of sources of PM pollution as described in Section 1.1.3, and cigarette smoke is a minor contributor. The effect of brand on determining PM exposure has not been extensively researched, and as yet little is known about PM concentrations inhaled (Gerber *et al.*

2015). It is also worth noting that whereas all people are involuntarily exposed to background levels of PM, exposure to cigarette smoke is restricted to smokers and those exposed to second hand smoke, and the concentration and length of exposure differ from environmental PM (De Marco *et al.* 2015). Therefore although similarities can be identified between cigarette smoke and air pollution, there are key differences in both composition and personal exposure. Despite these differences, research into cigarette smoke can provide insight into potential mechanisms by which PM derived from air pollution may cause disease, and more is known about the effects of cigarette smoke on the host and on bacteria than for PM alone (McEachern *et al.* 2015; Feldman & Anderson 2013; Garmendia *et al.* 2012). Despite this, research into direct effects of cigarette smoke on bacteria is also still in its early stages.

Cigarette smoke has been shown to increase biofilm formation of *S. pneumoniae* (Feldman & Anderson 2013; Mutepe *et al.* 2013), *S. aureus* (Kulkarni *et al.* 2012), and a variety of other bacterial species (Huang *et al.* 2014; Antunes *et al.* 2012; Bagaitkar *et al.* 2011; Goldstein-Daruech *et al.* 2011). Biofilm formation of *S. pneumoniae* has been shown to be induced by cigarette smoke in a dose dependent manner (Feldman & Anderson 2013; Mutepe *et al.* 2013; Goldstein-Daruech *et al.* 2011). Interestingly, exposure to cigarette smoke has also been shown to upregulate two genes encoding two-component regulatory system 11 in *S. pneumoniae*, *hk11* and *rr11*, which code for a putative histidine kinase and its cognate response regulator, respectively (Feldman & Anderson 2013; Li *et al.* 2002). This system has been shown to be important in biofilm formation of *S. mutans*, as deletion of either *hk11* or *rr11* results in a decrease in biofilm formation, however it is not known what extracellular signals this system responds to (Li *et al.* 2002). It has therefore been proposed that this two-component system may also be an important aspect of pneumococcal biofilm formation in response to cigarette smoke (Feldman & Anderson 2013). Cigarette smoke condensate has also been found to attenuate the pore formation of Ply, reducing virulence and predisposing bacteria to a colonising, rather than infective phenotype (Mutepe *et al.* 2013). Interestingly, no effect has been observed on pneumococcal growth (Mutepe *et al.* 2013). *In vivo*, cigarette smoke exposure increases the pneumococcal bacterial burden

in mice upon subsequent infection, and is associated with increased morbidity (Phipps *et al.* 2010).

For *S. aureus*, cigarette smoke induces biofilm formation by increasing transcription of genes involved in biofilm formation (*sarA*, *rbf*) and decreasing transcription of genes involved in biofilm dispersion (*agr*) (Kulkarni *et al.* 2012). It is thought that this increase in biofilm formation is caused by the induction of oxidative stress, as increased transcription of oxidoreductases is also observed with cigarette smoke exposure (Kulkarni *et al.* 2012). Cigarette smoke also inhibits growth of MRSA in a dose-dependent manner (McEachern *et al.* 2015). Furthermore, prior exposure to cigarette smoke increases MRSA resistance to subsequent *in vitro* killing by macrophages, even though internalisation is not affected (McEachern *et al.* 2015). This may be due to the decrease in MRSA growth, as many antimicrobial killing mechanisms require active cell division (McEachern *et al.* 2015). In addition, MRSA exposed to cigarette smoke display a reduced susceptibility to cell lysis and antimicrobial peptide (AMP) binding due to upregulation of Multiple peptide resistance factor F (*mprF*), causing a modification of the surface charge of the bacterial cell wall (McEachern *et al.* 2015). Finally, cigarette smoke increases MRSA adherence and invasion of epithelial cells by increasing hydrophobicity (McEachern *et al.* 2015). *In vivo* this translates to an increased bacterial burden and greater mortality in mice associated with pneumonia from cigarette smoke exposed MRSA (McEachern *et al.* 2015).

1.13. Aims and Objectives

PM affects susceptibility to bacterial infection (Section 1.3.1), and evidence suggests that PM also alters the diversity of distinct microbiota (Section 1.11). Respiratory tract bacteria are exposed to inhaled PM in the respiratory tract, and can also be inhaled alongside PM (Section 1.6). These bacteria are directly responsible for the acute and chronic respiratory infections associated with PM exposure, and have a role in a variety of other respiratory tract illnesses such as COPD and asthma (Brugha & Grigg 2014; MacIntyre *et al.* 2014; Janssen *et al.* 2012; Erkan *et al.* 2008; Pelaia *et al.* 2006; Brunekreef & Forsberg 2005). However, the mechanisms of PM-induced morbidity and mortality have so far been evaluated with focus on the effects on host cells and tissues (Section 1.5), with extremely limited research into the effects on bacteria (Section 1.12). This chapter has therefore outlined the potential importance of the overlooked effect of PM on bacteria.

Two hypotheses were tested in this project. The first hypothesis was that BC alters the ability of respiratory tract bacteria to colonise or cause disease. To address this hypothesis, it was split into 2 questions. Firstly, does BC affect growth, the activity of extracellular virulence factors, or biofilm formation of *S. aureus* or *S. pneumoniae*? Secondly, does BC affect respiratory tract colonisation by *S. pneumoniae in vivo*?

The second hypothesis was that BC alters the diversity of the respiratory tract microbiota. As microbiota dysbiosis has been associated with respiratory disease, this was investigated in order to assess whether BC exposure may make the host more susceptible to opportunistic infections.

This study therefore investigated whether the respiratory infections associated with BC exposure may be, in part, due to the direct effects of BC on bacteria, as this is currently an unexplored aspect of the relationship between pollution and disease.

Chapter 2. Materials and Methods

All chemicals were supplied by Sigma-Aldrich (Dorset, UK) unless otherwise stated.

2.1. Bacterial strains and growth conditions

The bacterial strains used in this study are listed in Table 2-1. Bacterial frozen cultures were stored in either Tryptic Soy Broth (TSB) with 20 % (v/v) glycerol (*S. aureus*) or Brain Heart Infusion (BHI) with 10 % (v/v) glycerol (*S. pneumoniae*) at -80 °C.

Bacteria were routinely cultivated on either Luria-Bertani agar (LA) (*S. aureus*) or 5 % (v/v) Horse Blood Agar (*S. pneumoniae*) and incubated at 37 °C overnight. *S. pneumoniae* was incubated in a 5 % (v/v) CO₂ atmosphere whereas *S. aureus* was incubated in air. To prepare a bacterial inoculum for assays, an appropriate broth was inoculated with a single bacterial colony and incubated overnight in the same conditions. During liquid culture growth, *S. aureus* colonies were incubated shaking in air at 200 rpm.

2.2. Black Carbon

There is a current nomenclature debate relating to the use of terms to describe Black Carbon (BC), as there is no precise chemical definition. Briefly, BC is a collective term for a range of mostly pure carbon substances produced through incomplete combustion of fossil fuels and biomass, making it a form of primary PM, and is measured using light absorption techniques (Long *et al.* 2013; USEPA 2012; Air Quality Expert Group 2012). The composition of BC varies depending on its source, with particles associated with a variety of additional compounds related to the production process and containing varying levels of Elemental Carbon (EC) (Long *et al.* 2013). BC is also often referred to as EC or soot, though technically there are differences between these compounds (Long *et al.* 2013). EC refers to purely carbon particles released during primary combustion and measurements are based on chemical composition analysis or with thermal-optical methods (Long *et al.* 2013; Air Quality Expert Group 2012; USEPA 2012; Janssen *et al.* 2012). Soot refers to a complex mixture of mostly BC and Organic

Table 2-1. Bacterial strains used.

Strain	Strain Origin	Reference
<i>S. aureus</i>		
2.20	Environmental Hospital MSSA Isolate	Laboratory strain collection
Newman	Clinical wild-type MSSA isolate	(Duthie & Lorenz 1952)
PB3-32-1	Clinical MRSA isolate	University Hospitals Of Leicester. (Richards <i>et al.</i> 2015)
PB9	Clinical MSSA isolate	University Hospitals Of Leicester.
SH1000	8325-4 with <i>rsbU</i> mutation repaired. MSSA	(Horsburgh <i>et al.</i> 2002)
USA300	Clinical wound MRSA isolate FPR3757. NRS482.	Network on Antimicrobial Resistance in <i>S. aureus</i> (NARSA) Program. Supported under NIAID/ NIH Contract No. HHSN272200700055C.
<i>S. pneumoniae</i>		
D39	Serotype 2 wild-type lab strain	National Collection of Type Culture (NCTC) 7466, London, UK (Avery <i>et al.</i> 1944)
PR201	Unencapsulated derivative of D39	(Pearce <i>et al.</i> 2002)

Carbon (OC), and OC may be derived from both primary and secondary sources (Long *et al.* 2013; Air Quality Expert Group 2012; USEPA 2012).

The terms BC and Carbon Black (CB) are often also used interchangeably (Long *et al.* 2013). CB is a manufactured particle of almost pure EC with very low quantities of contaminating compounds, which is primarily used in rubber applications, therefore differs from BC which is an undesired by-product of combustion associated with a variety of contaminating compounds (Long *et al.* 2013). The confusion in nomenclature is partly due to the fact that epidemiological studies report the effects of BC, but because BC is not commercially available, CB is the normal proxy used to model BC in laboratory studies (Long *et al.* 2013). The carbon used in the work described in this thesis was CB, purchased from Sigma-Aldrich (UK) under product number 699632. However for the sake of simplicity, this will be referred to as BC. BC was provided as a powder with a size distribution of <500 nm, with <500 ppm trace metals, and a weight of 12.01 g/mol. For use in assays, a stock solution of BC was made by dispersing the powder in dH₂O which had been sterilised by autoclaving at 120 °C at 15 pSI for 15 minutes.

2.1. Growth media

Media was prepared using dH₂O and was routinely sterilised by autoclaving at 120 °C and 15 pSI for 15 minutes. Where necessary, filter sterilisation was also employed. Stericup filters (Millipore) with a 0.22 µm pore size were used for volumes over 50 ml, and 0.2 µm Acrodisc membranes (Pall) were used for smaller volumes.

2.1.1. Blood Agar

4 % (w/v) Blood Agar Base (Oxoid) was autoclaved and cooled to ~60 °C before adding either horse blood to a final concentration of 5 % (v/v), or rabbit blood to a final concentration of 6 % (v/v). For sheep blood agar, Blood Agar Base was replaced with Sheep Blood Agar Base (Oxoid), and sheep blood was added to a concentration of 6 % (v/v).

2.1.2. Brain Heart Infusion broth (BHI)

BHI broth was prepared with 3.7 % (w/v) Brain Heart Infusion broth powder (Oxoid) and autoclaved.

2.1.3. Brain Heart Infusion Serum Broth

Filtered foetal calf serum was added to cooled, autoclaved BHI broth to a final concentration of 20 % (v/v).

2.1.4. Chelexed RPMI (CRPMI)

CRPMI was prepared by mixing 6 % (w/v) chelex 100 (Sigma Ltd) in RPMI-1640 (Sigma Ltd) overnight at 4 °C. The chelex was removed by filtration and the pH was adjusted to pH 8.8. The medium was then filter sterilised and supplemented with an additional 10 % (v/v) RPMI-1640. CRPMI was stored at 4 °C.

2.1.5. DNase Agar

A solution of 4.2 % (w/v) DNase agar powder (Fluka BioChemika) was prepared and autoclaved.

2.1.6. Luria-Bertani (LB) Broth

LB broth was prepared with 1 % (w/v) tryptone (Oxoid), 0.5 % (w/v) yeast extract, 0.5 % (w/v) NaCl and the pH was adjusted to pH 7.5 and autoclaved.

2.1.7. Luria-Bertani Agar (LA)

LA was prepared as for LB with the addition of 1.5 % (w/v) Bioagar (BioGene Ltd).

2.1.8. Phosphate Buffered Saline (PBS)

Four PBS tablets (Oxoid, UK) were dissolved in 400 ml dH₂O and the solution was autoclaved.

2.1.9. Todd Hewitt Broth (THB)

A solution of 3.75 % (w/v) Todd Hewitt broth powder (Oxoid) was prepared and autoclaved.

2.1.10. Todd Hewitt Broth + Yeast Extract (THY)

THB was prepared with the addition of 0.5 % (w/v) yeast extract.

2.1.11. Tryptic Soy Broth (TSB)

A solution of 3 % (w/v) Tryptic Soy broth powder (BBL) was prepared and autoclaved. For *in vivo* work, 10 % (v/v) pre-autoclaved glycerol and 20 ng/ml of filter-sterilised heparin were added to autoclaved TSB immediately prior to use.

2.2. CFU growth analysis

10 ml cultures were set up in an appropriate growth medium (BHI, LB, or CRPMI), and incubated at 37 °C overnight. Generally, *S. pneumoniae* cultures were incubated in a 5 % (v/v) CO₂ atmosphere, and *S. aureus* cultures were incubated shaking in air at 200 rpm. However, *S. aureus* CRPMI cultures were also incubated in a 5 % (v/v) CO₂ atmosphere without agitation. After incubation, bacteria were sub-cultured into 10 ml fresh media to OD_{600nm} 0.05, or to OD_{600nm} 0.1 in CRPMI. Cultures were supplemented with 10, 50, or 100 µg/ml BC, and were then incubated statically at 37 °C in a 5 % (v/v) CO₂ atmosphere. Controls without supplementation were also included. At desired time points, usually every hour for the first 8 hours with a final reading at 24 hours, cultures were mixed and a sample was taken for serial dilution to determine CFU/ml using the Miles and Misra technique (Miles *et al.* 1938).

2.3. Exoprotein analysis

2.3.1. Haemolysis, DNase, and Lipase activity

A single bacterial colony of each strain was inoculated into 5 ml BHI, supplemented with 10, 50, or 100 µg/ml BC, and incubated overnight at 37 °C. *S. pneumoniae* was incubated in a 5 % (v/v) CO₂ atmosphere, and *S. aureus* was incubated shaking in air at

200 *rpm*. At 16 hours, cultures were normalised to account for growth differences with BC supplementation. Triplicate spots of 10 µl of each culture were then inoculated onto 6 % (v/v) sheep or rabbit blood agar plates, DNase agar, or Tributyrin Agar (Oxoid). Plates were incubated at 37 °C for 24 hours in a 5 % (v/v) CO₂ atmosphere. To measure nuclease activity, DNase plates were flooded with 1 N HCl to precipitate polymerised DNA, and the diameter of the zone of DNA hydrolysis around the colonies were measured. Zones of lysis on Tributyrin and blood plates could be measured directly. In all cases, bacteria free controls of BC alone were included.

2.3.2. Quantitative haemolysis activity assay

A single bacterial colony of each strain was inoculated into 10 ml BHI, supplemented with 10, 50, or 100 µg/ml BC, and incubated overnight at 37 °C. *S. pneumoniae* was incubated in a 5 % (v/v) CO₂ atmosphere, and *S. aureus* was incubated shaking in air at 200 *rpm*. At 16 hours, cultures were normalised to account for growth differences with BC supplementation. Cultures were then centrifuged at 3220 *x g*, 4 °C, for 5 minutes. To obtain secreted haemolysins, the supernatants were concentrated and sterilised with Amicon Ultra centrifugal concentrators (Millipore) at 3220 *x g* for 10 minutes. A 4 % (v/v) solution of either sheep or rabbit blood (Oxoid) was prepared by centrifuging 1 ml of blood at 2415 *x g* for 1 minute, and adding 400 µl of the pellet to 10 ml PBS. 50 µl of PBS was added to all wells of a 96-well round-bottomed plate (Nunc) apart from the first and third columns. 50 µl of each concentrated supernatant was then added to wells of the third and fourth columns. Wells of the fourth column were mixed thoroughly by pipetting and a log₂ serial dilution made in subsequent wells from left to right. For a positive control, 50 µl of 2 % (v/v) Triton X100 was added to all wells of the first column. 50 µl of the 4 % (v/v) sheep or rabbit blood solution was then added to all wells. Wells of the second column acted as negative controls of just PBS and blood. The plate was then incubated at 37 °C for 30 minutes. The highest dilution where complete haemolysis occurred was recorded for each sample.

2.4. Biofilm analysis

2.4.1. Staining method

A single bacterial colony of each strain was inoculated into 10 ml BHI or THB and incubated overnight at 37 °C. *S. pneumoniae* cultures were incubated in a 5 % (v/v) CO₂ atmosphere, and *S. aureus* cultures were incubated shaking in air at 200 rpm. Media choice for overnight growth was determined by the biofilm media to be used. After incubation, bacteria were sub-cultured into fresh biofilm media to an OD_{600nm} of 0.05, split into necessary aliquots, and supplemented with 0-100 µg/ml BC. *S. aureus* biofilms were formed in un-supplemented BHI, BHI + 4 % (w/v) NaCl, and BHI + 1 % (v/v) glucose. *S. pneumoniae* biofilm formation was assessed in TSB and BHI. Cultures were inoculated into quadruplicate wells of a 96-well flat-bottomed plate (Nunc), using 200 µl per well. Controls of media alone were included. Plates were then incubated at 37 °C in a 5 % (v/v) CO₂ atmosphere for 24 hours. OD_{600nm} readings were taken before incubation and at 24 hours using a BMG Labtech FLUOstar Omega plate reader. After incubation, wells were gently washed three times with PBS, then dried and heat fixed at 50 °C for 15 minutes in a Techne Hybridiser HB-1D Oven. Wells were stained with 200 µl of 1 % (v/v) safranin or 0.5-1 % (v/v) crystal violet for 30 minutes, washed twice with dH₂O, and dried at room temperature. The OD of each well was then measured, using OD_{490nm} for wells stained with safranin and OD_{570nm} for wells stained with crystal violet.

2.4.2. Quantification of biofilm viability

The protocol for biofilm assessment is exemplified in Figure 2-1. Bacteria were inoculated into 10 ml BHI or THB and incubated overnight at 37 °C. *S. pneumoniae* was incubated in a 5 % (v/v) CO₂ atmosphere, and *S. aureus* was incubated shaking in air at 200 rpm. Media choice for overnight growth was determined by the biofilm media to be used. After incubation, cultures were sub-cultured into fresh biofilm media to an OD_{600nm} of 0.05, split into necessary aliquots, and supplemented with 30, 50, or 100 µg/ml BC. Controls without supplementation were also included. *S. aureus* was assessed for its biofilm capabilities in un-supplemented BHI, BHI + 4 % (w/v) NaCl, and BHI + 1 % (v/v) glucose. *S. pneumoniae* biofilm formation was assessed in un-

supplemented TSB, THB, and BHI, and in these media supplemented with 1 % glucose, 0.5 % yeast extract, 0.5 % xylitol, 1-10 µg/ml sialic acid, and 1-10 µg/ml N-acetyl mannosamine. Pneumococcal media supplementation was tested with both single supplements and combinations of glucose and xylitol, glucose and sialic acid, and glucose and N-acetyl mannosamine. 3 ml of each culture was then seeded into triplicate wells of a 12-well plate for technological repeats, and incubated at 37 °C in a 5 % (v/v) CO₂ atmosphere for 24 hours. Alternatively, for adhesion assays, bacteria were incubated for just 2 hours. After incubation the supernatant, containing planktonic bacteria, was gently removed and set aside. Biofilms were then gently washed with 3 ml PBS, and this wash was removed and set aside. 1 ml pipette tips, which had been cut at the 500 µl mark to create a wider opening, were used to remove the supernatant and wash. This was done in order to reduce sheer stress in comparison to normal 1 ml tips. To recover biofilm bacteria, 1 ml PBS was added to each well and bacteria were removed from the surface of the plate using CellScrapers (VWR). To determine bacterial viability, the supernatant, wash, and biofilm samples were vortexed for 30 seconds to disperse biofilm clumps, and serial dilutions of these samples were plated out onto appropriate agar using the Miles and Misra technique (Miles *et al.* 1938). Results are given as total CFU per fraction, which refers to the total amount of viable biofilm, loosely adherent (wash), and planktonic (supernatant) bacteria recovered from each biofilm, therefore the sum of these fractions gives the total bacterial viability of the entire biofilm and surrounding medium.

2.4.3. DNaseI and proteinase K degradation of biofilms

In order to investigate the role of nucleic acid and protein in the extracellular biofilm matrix, mature biofilms were degraded with DNaseI (Nicholson *et al.* 2013; Hall-Stoodley *et al.* 2008) or proteinase K (Nicholson *et al.* 2013; Gilan & Sivan 2013; Kogan *et al.* 2006). After 24 hours biofilm development, the supernatant of each biofilm was removed and biofilms were washed as previously stated (Section 2.4.2). Next, 3 ml of 140 U/ml DNaseI or 100 µg/ml proteinase K was added to each well. DNaseI was prepared in 10 mM Tris supplemented with 2.5 mM MgCl₂, 0.5 mM CaCl₂, and 2.5 mM MnCl₂, and adjusted to pH 7.6, and proteinase K was prepared in 10 mM Tris-HCl adjusted to pH 7.5. Control wells containing buffer alone were also

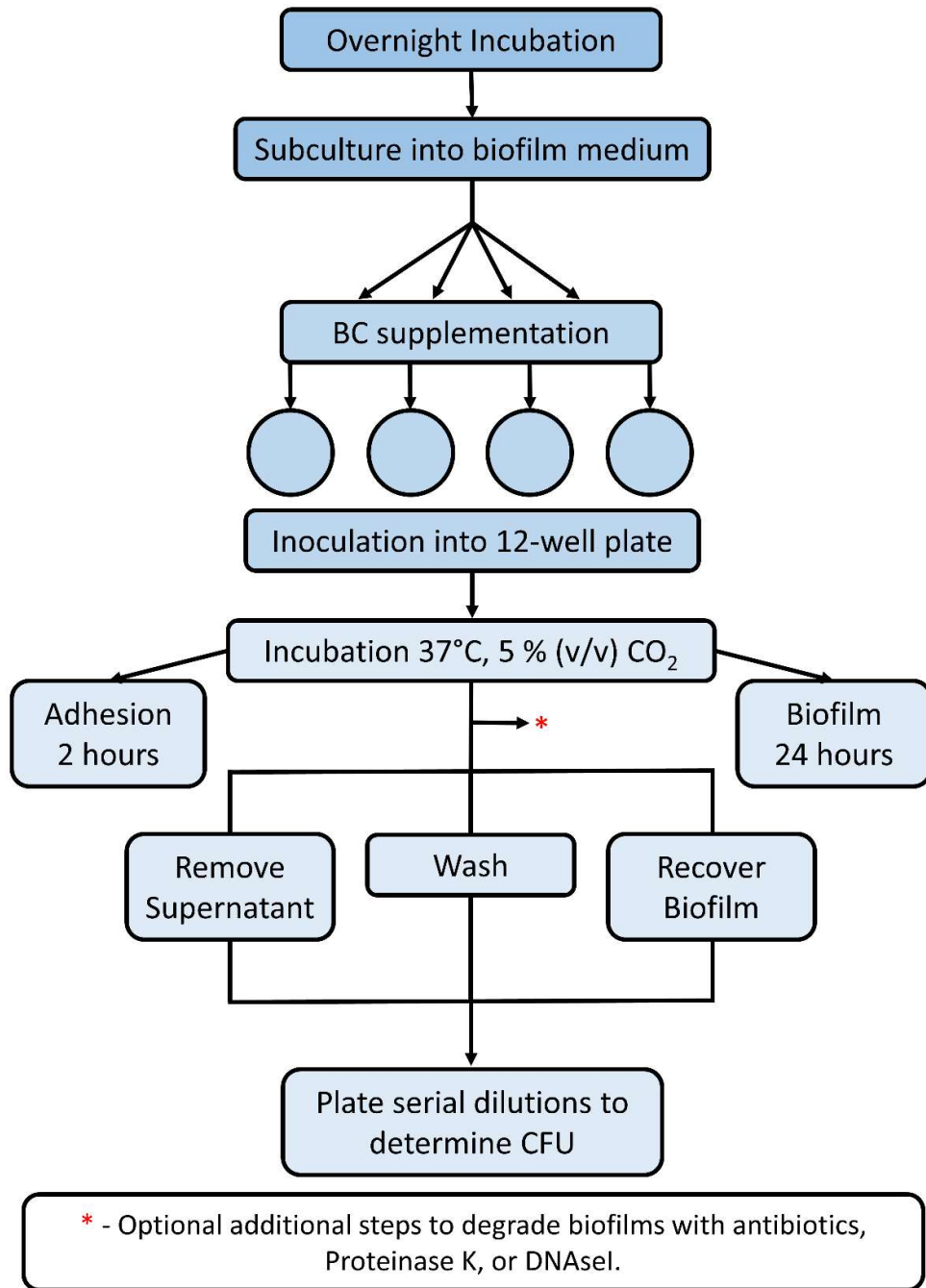


Figure 2-1. Protocol for the enumeration of bacterial viability of biofilms

included. Biofilms were then incubated at 37 °C in a 5 % (v/v) CO₂ atmosphere for 2 hours. After incubation, the supernatant was removed, biofilms were washed, and viable biofilm bacteria were quantified as previously described (Section 2.4.2).

2.4.4. Biofilm antibiotic tolerance

Methods were adjusted from Marks, *et al.* (2012a) to assess biofilm degradation by antibiotics (Chao *et al.* 2015; Marks *et al.* 2012a; Singh *et al.* 2010; Bartoszewicz *et al.* 2007; Abdi-Ali *et al.* 2006; Carmen *et al.* 2004). After 24 hours biofilm development, the supernatant of each biofilm was removed and biofilms were washed as previously stated (Section 2.4.2). Next, 3 ml of 500 µg/ml gentamicin was added to *S. pneumoniae* biofilms, and 50 mg/ml oxacillin was added to *S. aureus* biofilms. Concentrations of 0-1 mg/ml gentamicin and 0-50 mg/ml oxacillin were tested in assay development.

Antibiotics were prepared in PBS, and oxacillin was supplemented with 2 % (w/v) NaCl according to standard practice (CLSI 2015). Controls of PBS or PBS + 2 % (w/v) NaCl were also included. Plates were then incubated for 3 hours at 37 °C in a 5 % (v/v) CO₂ atmosphere. After incubation, supernatants were removed, biofilms were washed, and the viable biofilm bacteria were quantified as previously described (Section 2.4.2).

2.5. Microscopy

For examination by microscopy, biofilm cultures were prepared as previously described (Section 2.4.2), with one alteration. Cultures were inoculated into 12-well plates containing pre-sterilised 13 mm round glass coverslips. After incubation, coverslips were carefully removed and washed twice in 3 ml PBS for 5 minutes.

2.5.1. Scanning Electron Microscopy

To process biofilms for Scanning Electron Microscopy (SEM), biofilms were fixed in 2.5 % (v/v) glutaraldehyde in 0.1 Sörensen buffer, pH 7.4, for 2 hours at room temperature. After fixing, biofilms were washed in 0.1 M Sörensen buffer, pH 7.4, for 10 minutes. Following standard protocols (Dykstra & Reuss 2003), biofilms were washed twice in distilled de-ionised water for 5 minutes, and dehydrated through 30, 50, and 70 % (v/v) EtOH, incubating each at room temperature for 30 minutes. Slides

were then incubated at room temperature overnight in fresh 70 % (v/v) EtOH. The following day, samples were further dehydrated in 90 and 100 % (v/v) EtOH, followed by 100 % Analytical Grade Ethanol (x2), for 30 minutes each. Samples were then processed through 2:1 and 1:2 mixtures of EtOH and Hexamethyldisilazane (HMDS), into 100 % HMDS (x2), incubating each at room temperature for 30 minutes. Finally, the HMDS was removed and samples were allowed to air dry overnight. Dry samples were mounted onto SEM pin stubs and gold coated in a Polaron SC7640 sputter coater. Alternatively, to avoid degradation of the biofilms, an adapted protocol was also employed. For this method, coverslips were gold-coated directly after glutaraldehyde fixation and washing in Sørensen's buffer. All samples were viewed with a Hitachi S-3000H SEM. The entire surface of each coverslip was assessed and representative photos were taken at a variety of magnifications. The working distance, filament voltage, and other technical factors were adjusted as necessary.

2.5.2. Transmission Electron Microscopy and biofilm thickness

For Transmission Electron Microscopy (TEM), washed biofilms were infused with 10 % (v/v) Bovine Serum Albumin (BSA, Bio-Rad) in PBS for 30 minutes, then fixed in 2.5 % (v/v) glutaraldehyde in 0.1 M Sørensen's buffer, pH 7.4, overnight at 4 °C. The following day, samples were washed three times with 0.1 M Sørensen's buffer, pH 7.4, for 10 minutes, and a secondary fix was performed with 1 % (w/v) aqueous osmium tetroxide/1.5 % (w/v) potassium ferricyanide for 90 minutes. After fixation, biofilms were washed three times with distilled de-ionised water for 10 minutes, and dehydrated through 30, 50, and then 70 % (v/v) EtOH for 30 minutes each. Slides were then stored in fresh 70 % (v/v) EtOH overnight. The following day, samples were further dehydrated in 90 and 100 % (v/v) EtOH, followed by 100 % Analytical Grade Ethanol (x2), for 30 minutes each. Samples were then incubated at room temperature in propylene oxide for 10 minutes (x2), and processed through 3:1, 1:1, and 1:3 mixtures of propylene oxide and Spurr's Modified Resin for 90 minutes each, into 100 % Spurr's Modified Resin for 30 minutes. Samples were then transferred to fresh 100 % Spurr's Modified Resin for overnight incubation. The following day, Spurr's Modified Resin was changed twice, incubating for 90 minutes each time. Finally, coverslips were mounted into coffins which were submerged in fresh Spurr's Modified Resin and

polymerised at 60 °C for 16 hours overnight. Blocks were transferred to dry ice for ~30 seconds and the coverslips were removed, leaving biofilms in the resin. Biofilm cross-sections around 90 nm thick were cut from within each biofilm with a Reichert ultracut E ultramicrotome, and these sections were stained with 2 % (w/v) aqueous uranyl acetate and Reynold's lead citrate. Cross-sections were imaged on a JEOL JEM-1400 TEM and representative photos were taken (Glauert & Lewis 2014). For measurements of biofilm thickness, 18 cross-sections were taken and were measured blind at 12 equally spaced points with light microscopy.

2.6. Protein extraction and protein gels

2.6.1. Protein extraction

Biofilms were cultured as previously described (Section 2.4.2), and biofilm cells were recovered into 1 ml PBS. Cells were then centrifuged at 3220 x g and 4 °C for 5 minutes, and protein was extracted with a FastProtein Blue Matrix Kit (MP Bio). The manufacturer's instructions were followed with one alteration, extending the final centrifugation to 5 minutes. Samples were stored at -20 °C until use.

2.6.2. Standardisation of protein concentrations

To account for growth differences between BC-supplemented and un-supplemented cultures, each set of cultures for a strain were standardised to the same total protein concentration. To do this, the Bradford method of protein quantification was used. A series of standards of Bovine Serum Albumin (BSA) were made from 0.1-1.5 mg/ml protein. 100 μ l of each standard and each sample was then added, in triplicate, to 5 ml Bradford Dye (Bio-Rad), which had been diluted to the working concentration, and incubated at room temperature for 5 minutes. The OD_{595nm} of each sample was read, and the protein concentration of each was interpolated using the BSA standards. For samples from the same strain, protein concentrations were diluted to match at the highest possible concentration. Diluted samples were then rechecked by the same method to confirm accurate dilutions.

2.6.3. 1D SDS-PAGE

Proteins were separated by 1D SDS-PAGE using a 10 % (w/v) Separating Gel (12.27 ml Buffer A (45.4 g Tris, 1 g SDS in 500 ml dH₂O, pH 8.8), 8.32 ml acrylamide, 3.48 ml dH₂O, 864 µl 1 % (w/v) Ammonium Persulfate (APS), and 68.2 µl N,N,N',N' - tetramethylethylenediamine (Temed)) and a 5 % (w/v) Stacking Gel (3.5 ml Buffer B (15.1 g Tris, 1 g SDS in 500 ml dH₂O, pH 6.8), 1.16 ml acrylamide, 2.16 ml dH₂O, 175 µl 1 % (v/w) APS and 14 µl Temed). 40 µl of each standardised protein extraction was mixed with an equal volume of 2 x Laemmli Sample Loading Buffer (20 % (v/v) glycerol, 4 % (w/v) SDS, 100 mM Tris-HCl (pH 7.0), 200 mM Dithiothreitol (DTT), 0.2 % (w/v) Bromophenol Blue). Samples were then boiled for 3 minutes, briefly centrifuged to collect all liquid, and loaded into the gel alongside a lane loaded with 20 µl PageRuler Prestained Protein Ladder (Fermentas). Gels were run at 65 mA and 280 V in 1 x SDS-PAGE Running Buffer (0.32 % (w/v) Tris, 1.44 % (w/v) Glycine, 0.1 % (w/v) SDS in dH₂O). Bands were visualised by staining with Coomassie blue overnight (22.5 % (v/v) methanol, 10 % (v/v) glacial acetic acid, 0.25 % (w/v) Coomassie brilliant blue R250) followed by repeated washes in Destain (22.5 % (v/v) methanol, 10 % (v/v) glacial acetic acid).

2.7. Pneumococcal colonisation model

In vivo experiments were carried out with naïve 8-9 week old female outbred MF1 mice obtained from Charles River, Kent, UK. Upon arrival, mice were housed in groups of 2-5, depending on study requirements. Mice were allowed to acclimatise for one week in the Division of Biomedical Services, University of Leicester, on a 12 hour light-dark cycle and access to food and water *ad libitum*. All experiments were carried out in accordance with the Home Office Project Licence 60/4327 and adhered to the UK Animals (Scientific Procedures) Act (1986).

The amount of BC which could be tolerated by mice was determined by intranasally inoculating mice with 5 µg or 100 µg BC in 50 µl PBS. Inoculation with PBS alone was used as a control. Three mice were dosed per group. Mice were immediately culled and lungs were removed and used for histological analysis. Separately, the inoculating

dose of pneumococci required for use in the main colonisation experiment was determined. Four mice were inoculated with 5×10^5 CFU *S. pneumoniae* D39 in 15 μ l PBS, immediately culled, and nasal and bronchoalveolar lavages were performed to determine bacterial load.

The intranasal inoculation protocol and tissue sampling procedure for the main pneumococcal colonisation model are displayed in Figure 2-2, and were adapted from previous work (Richards *et al.* 2010). Mice were intranasally dosed with 15 μ l PBS containing either $\sim 5 \times 10^5$ CFU of *S. pneumoniae* D39, 7 mg/ml BC (equating to 105 μ g BC in the 15 μ l inoculum), a mixture D39 and BC at these concentrations, or PBS alone as a control. 14 mice were dosed per group (56 total). Before and immediately after inoculation, a viable count was performed to confirm the challenge dose was approximately 5×10^5 CFU of *S. pneumoniae* D39.

Mice reaching a severe (2+) lethargic state were culled to determine bacterial load before they became moribund. In the absence of disease, mice were culled at 7 and 14 days post-inoculation in order to determine bacterial load and for histological analysis, beginning at 10 am each day. Five mice per group were used to assess bacterial load in the nasopharynx, lungs, and blood, and two per group were used for histological analysis of the lungs, nares, cervical lymph nodes, and spleen. Allocation of mice to each inoculation group, the order in which groups were inoculated, and the order in which each cage was culled for sample recovery, was randomised at the beginning of the study. However after assignment, mice to be culled at each time-point was then fixed for the duration of the assay.

2.7.1. Preparation of pneumococci

S. pneumoniae D39 was streaked onto 5 % (v/v) horse blood agar plates and grown overnight at 37 °C in a 5 % (v/v) CO₂ atmosphere. The following day, a sweep of colonies was inoculated into 10 ml BHI and incubated with a loose lid overnight under the same conditions. After incubation the culture was centrifuged at 3220 \times g for 15 minutes and the supernatant was discarded. The pellet was resuspended in 1 ml BHI serum broth, and 700 μ l of this suspension was added to 15 ml fresh BHI serum broth

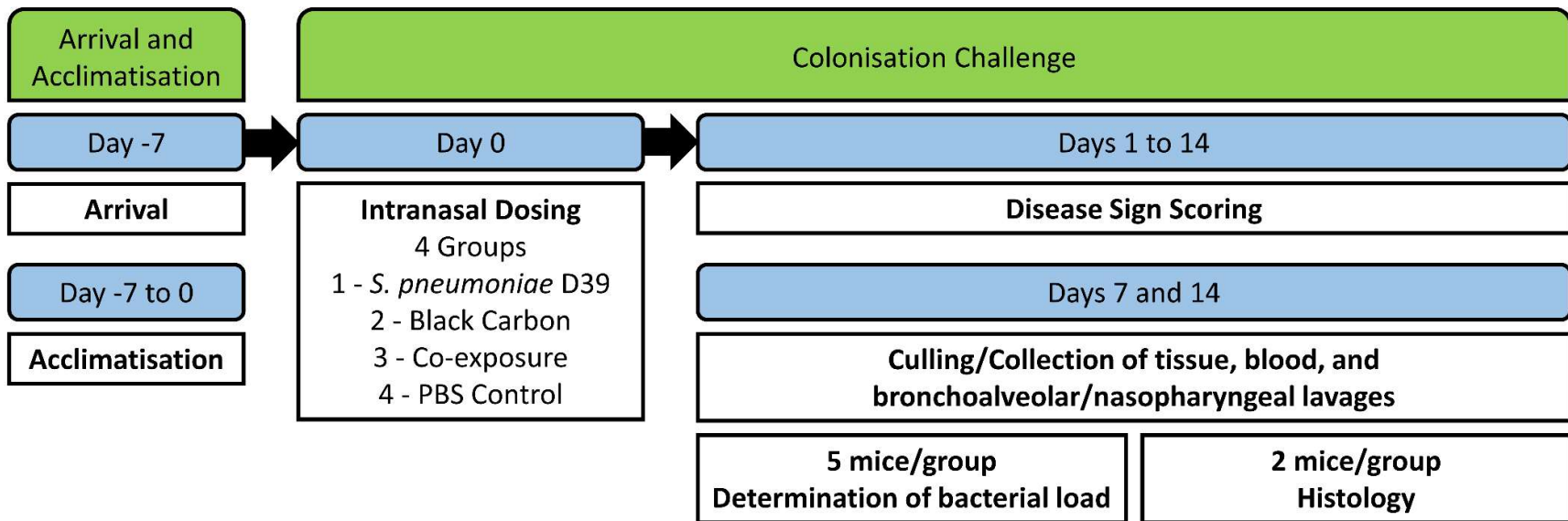


Figure 2-2. Protocol for assessing the impact of black carbon on pneumococcal colonisation of the MF1 mouse nasopharynx.

to achieve an OD_{500nm} of ~0.70. The culture was then incubated at 37 °C in a 5 % (v/v) CO₂ atmosphere for ~6 hours until an OD_{500nm} of 1.6 was reached. Finally, the culture was subdivided into 500 µl aliquots and stored at -80 °C (Canvin *et al.* 1995).

After storage at -80 °C for at least 24 hours, bacterial purity and viability was checked. Triplicate samples of bacteria were thawed, serially diluted in PBS, and plated onto 5 % (v/v) horse blood agar plates using the Miles and Misra technique (Miles *et al.* 1938). Plates were incubated overnight at 37 °C in a 5 % (v/v) CO₂ atmosphere, and viability per aliquot was calculated. Optichin (ethylhydrocupreine hydrochloride) sensitivity was confirmed by adding optochin discs (Oxoid) to plates at the initial site of streaking. The optochin sensitivity test is a routinely performed diagnostic test used to distinguish *S. pneumoniae* from other α-haemolytic Streptococcal species (Bowers & Jeffries 1955).

2.7.2. Intranasal dosing procedure

Mice were anaesthetised with 2.5 % (v/v) isoflurane at 1.6-1.8 litre O₂/min in an anaesthetic box (Kadioglu *et al.* 2000). Once fully anaesthetised, mice were scruffed and held in a horizontal position, and the required suspension was inoculated dropwise onto each of the nostrils for inhalation. Mice were then placed on their backs in their cages until recovery. After dosing, mice were monitored for one hour for any signs of distress as described in Section 2.7.3. Mice were maintained on regular drinking water and feed *ad libitum* throughout experiments, and checked for clinical signs of disease at least once daily. If any signs of distress or disease was observed, mice were reassessed every hour to monitor symptoms.

2.7.3. Disease sign scoring

Mice were scored for signs of disease by monitoring posture, piloerection, and lethargy as described in the Home Office Project Licence (60/4327) (Morton & Griffiths 1985). Table 2-2 describes this scoring protocol. In accordance with the Home Office Licence, animals that became 2+ lethargic were culled immediately.

Table 2-2. Scoring for disease severity in mice.

Score	Description
Normal	Normal behaviour, movement, and coat.
Hunched (+)	Back is slightly arched
Hunched (++)	Back is very arched
Starey (+)	Mild coat piloerection
Starey (++)	Pronounced coat piloerection
Lethargic (+)	Slow movement around the cage
Lethargic (++)	No movement around the cage
Moribund	No coat grooming, pronounced piloerection, severely lethargic, laboured breathing.

2.7.4. Culling mice

At pre-determined time-points, or if mice became 2+ lethargic, mice were culled. If mice were to be used to determine bacterial load they were deeply anaesthetised with 2.5 % (v/v) isoflurane at 1.6-1.8 litres O₂/min, and blood was collected by cardiac puncture using a 23 Gauge needle, in which the animal was exsanguinated under terminal anaesthesia. Death was confirmed by cervical dislocation. If mice were to be used for histopathological analysis, mice were deeply anaesthetised with 2.5 % (v/v) isoflurane at 1.6-1.8 litres O₂/min in an anaesthetic box, and culled by cervical dislocation. Death was confirmed by exsanguination. In both cases, anaesthesia was confirmed by non-responsiveness to a noxious stimulus (hind paw pinch) and decreased respiration rate.

2.7.5. Collection of blood, bronchoalveolar lavages, and nasal lavages to determine bacterial load and for microbiota investigations

At pre-determined time-points, or if mice became 2+ lethargic, mice were culled by exsanguination under terminal anaesthesia with 2.5 % (v/v) isoflurane at 1.6-1.8 litres O₂/min, and death was confirmed by cervical dislocation, as detailed in Section 2.7.4. From each cardiac puncture, 100 µl blood was immediately added to 900 µl TSB supplemented with 10 % (v/v) glycerol to preserve bacterial viability, and 20 ng/ml heparin to prevent clotting.

To perform bronchoalveolar lavages, the trachea of each culled mouse was exposed, a small incision was made, and a 3F Portex cannula was inserted and held in place with a suture. Five hundred microliters of TSB supplemented with 10 % (v/v) glycerol and 20 ng/ml heparin was rinsed into the lungs with a 1 ml syringe. The medium was recovered and used to repeat the wash a total of two times before being transferred into an eppendorf tube.

Nasal lavages were performed subsequent to bronchoalveolar lavages on culled, decapitated animals, by removing the head and lower jaw, inserting an 18 Gauge needle into the anterior of the nasal passages, and washing the nasal passages through with 500 µl TSB supplemented with 10 % (v/v) glycerol and 20 ng/ml heparin. The medium was

recovered and used to repeat the wash a total of three times before being transferred into an eppendorf tube. Washes and blood were immediately stored on dry ice and transferred to -80 °C within 1 hour.

2.7.6. Determination of bacterial load

After overnight storage at -80 °C, ten-fold serial dilutions of bloods and lavages were performed and plated out onto 5 % (v/v) horse blood agar plates using the Miles and Misra technique (Miles *et al.* 1938). As well as standard 5 % (v/v) horse blood agar plates, blood agar supplemented with 1 µg/ml gentamicin was used as a selective medium in the event of the presence of high numbers of non-pneumococci. Plates were incubated at 37 °C in a 5 % (v/v) CO₂ atmosphere and viable colonies were counted after 24 hours. Viable counts were converted to Log₁₀ CFU/ml for data analysis and presentation. Sample identity was written on plates but covered during CFU counting to avoid bias when assessing results.

2.7.7. Tissue collection for histopathology

At pre-determined time-points, mice were deeply anaesthetised with 2.5 % (v/v) isoflurane at 1.6-1.8 litres O₂/min in an anaesthetic box, culled by cervical dislocation, and death was confirmed by exsanguination as detailed in Section 2.7.4. Culled mice were dissected to expose the lungs, a small incision was made in the trachea, a 3FG Portex cannula was placed into the incision and held in place with a suture, and lungs were inflated with 800 µl 10 % (v/v) neutral buffered formalin. The lungs were then tied off and carefully removed from the thorax, and placed into 10 ml of 10 % (v/v) neutral buffered formalin. Cervical lymph nodes and the spleen were then excised without damaging the structures, and also transferred to 10 ml of 10 % (v/v) neutral buffered formalin. The lungs, cervical lymph nodes, and spleen samples were incubated at room temperature for 24 hours, then transferred to 70 % (v/v) industrial methylated spirits (IMS). Nasal tissue was collected by decapitating the mouse, removing the lower jaw, skin, and all outer tissue from the skull, and dissecting out the underlying nasal tissue. This tissue was transferred to 10 ml of 10 % (v/v) neutral buffered formalin for 48 hours, then to 10 % (v/v) formic acid for 36-48 hours for decalcification.

2.7.8. Tissue processing and analysis for histopathology

After fixation and decalcification (if required), samples were transferred to the Histology Facility, Core Biotechnology Services, University of Leicester, for processing using their standard protocols. Tissues were processed overnight with a Leica Tissue Processor (LEICA ASP3000 automated vacuum tissue processor). First, tissues were dehydrated through IMS and xylene and into paraffin wax, and then embedded into a paraffin wax block with a Leica EG 1160 paraffin embedding centre. 4 µm block sections were cut from each section with a rotary microtome. Lung tissues were sectioned at intervals of 300-400 µm, starting close to the main axial airway. Nasal tissue was mounted so that it was cut in longitudinal, rather than transverse, sections. Cut sections were then floated on a 45 °C water bath to remove creases and bubbles before being mounted on a microscope slide and dried overnight at 37 °C. For staining, slides were submerged in xylene (x3), an IMS gradient, dH₂O, Mayer's Haematoxylin (x3), dH₂O (x3), Eosin (x3), dH₂O, another IMS gradient, and finally xylene again (x3). Each slide was submerged for 90 seconds and then drained for 5 seconds before being submerged in the next reagent. Washing the slides in dH₂O after staining with Mayer's Haematoxylin allowed the haematoxylin to properly "blue". Coverslips were then mounted onto each slide with DPX medium (VWR). Slides were stored at room temperature. For analysis, slides were assigned codes to hide which exposure condition each mouse had been assigned to, and analysed blind by light microscopy with the assistance of an experienced pathologist.

2.8. Statistical analysis of *in vitro* and pneumococcal colonisation data

At least three biological repeats of each *in vitro* assay were performed on independent days (n=3). The specific number of repeats for each assay are indicated in each figure legend. GraphPad Prism version 6 was used to graph and analyse all *in vitro* data as well as bacterial burden data from the *in vivo* pneumococcal assay. T-tests were used to compare two groups, and ANOVA tests were used to compare three or more groups. A One-way ANOVA was performed when assessing multiple groups of a single variable.

A Two-way ANOVA was performed when assessing two variables. Details of the statistical test and post-tests (Dunnett, Tukey, and Sidak) used are given in each figure legend. Results were considered significant with a p value of less than 0.05.

2.9. Ion torrent sample preparation and analysis

A flow diagram for sample preparation for ion torrent analysis is shown in Figure 2-3. Briefly, DNA extractions were performed on nasal and bronchoalveolar lavages (Section 2.9.1), and a section of the 16S rRNA was amplified by PCR (Section 2.9.2). Samples were run on 2 % (w/v) agarose gels (Section 2.9.3) and the DNA concentration of each band was quantified using GeneTools (SynGene) based on the standards of the H1 Hyperladder (Bioline). Based on quantification, samples were pooled at 15 ng/sample, meaning that the volume of each sample added varied depending on DNA concentration. Pooled PCR reactions were purified using the Cycle Pure Kit (Omega, Bio-tek) according to the manufacturer's instructions, using the centrifugation protocol. This removed contaminating oligonucleotides and PCR constituents. DNA was eluted into 30 µl dH₂O, ran on a 2 % (w/v) agarose gel (Section 2.9.3), extracted and purified (Section 2.9.4), and eluted in a final volume of 30 µl dH₂O. Samples were sequenced on the ion torrent platform by the Genomics Service, University of Leicester. Ion torrent data was analysed using Qiime version 1.9.1 and R version 3.2.3, with the R packages Phyloseq and Vegan (Oksanen *et al.* 2016; R Core Team 2015; McMurdie & Holmes 2013). Scripts used for bioinformatics, analysis, and statistical testing are detailed in Appendices 3-10. Explanations of script workflows are given in Chapter 5 alongside results from microbiota analysis in the context of the data.

2.9.1. DNA extractions

DNA was extracted with the FastDNA Spin Kit (MP Bio). The following changes to the manufacturer's instructions were made. Sample homogenisation was performed for 60 seconds at a speed setting of 6.0, rather than 40 seconds. Next, samples were centrifuged at 14000 *x g* for 10 minutes to pellet debris. Additionally, a step was added before final elution of DNA; filters were air dried at room temperature for 5 minutes. Samples were stored at -20 °C until use.

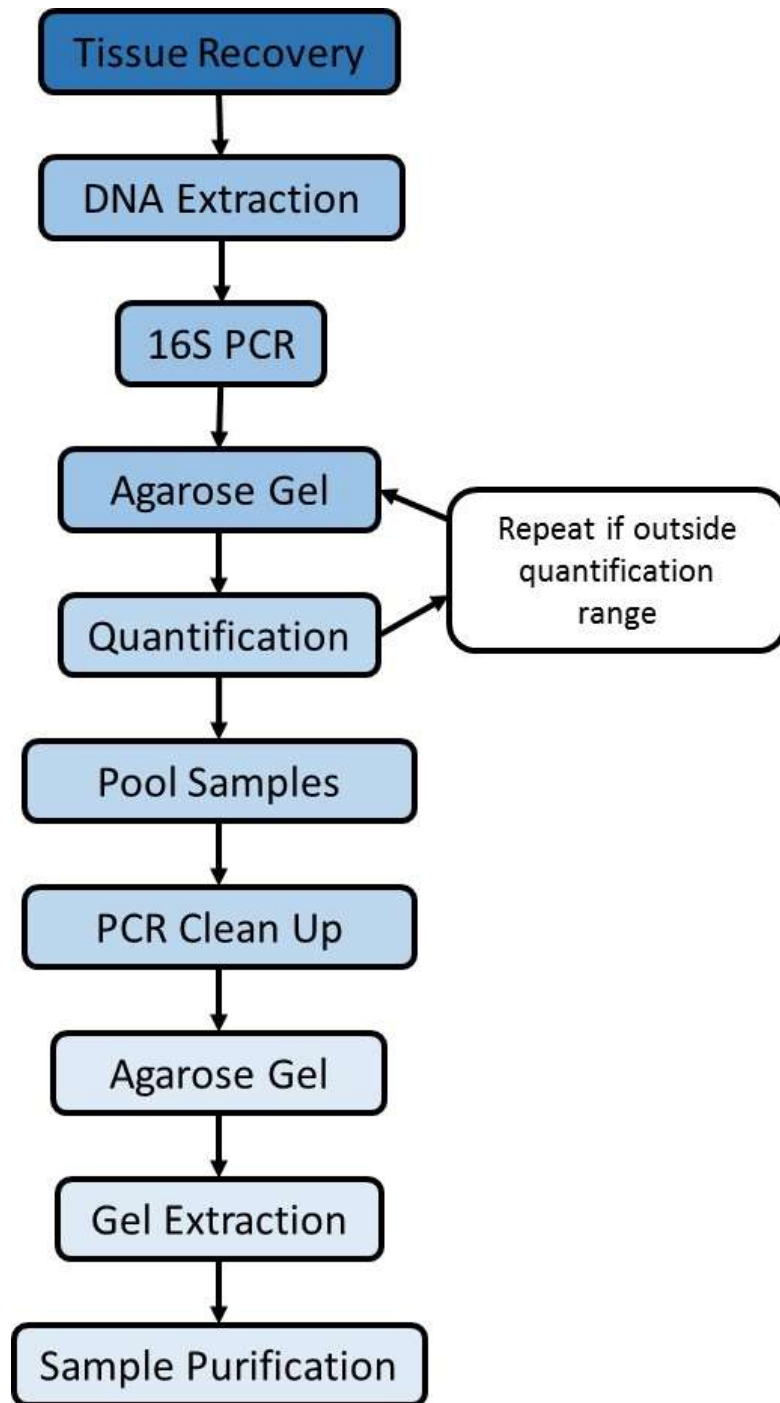


Figure 2-3. Flow diagram depicting sample preparation for analysis of the mouse respiratory tract microbiota nasopharynx.

2.9.2. Polymerase Chain Reaction (PCR)

Each 50 µl PCR reaction contained 10 µl 5x Q5 Buffer (NEB), 10 µl 5x Q5 GC Enhancer (NEB), 1 µl dNTP (10 mM), 0.5 µl Q5 High-Fidelity DNA Polymerase (NEB), 2.5 µl 334R Reverse Primer (10 µM), 2.5 µl 8F Forward Primer (10 µM), 13.5 µl dH₂O (UV treated at 700,000 uJ/cm² for 1 hour), and 10 µl template. Optimisation PCRs tested template dilutions of 1:2 to 1:100, the optimal dilution for lavages was 1:10. Modified 8F and 334R primers (Baker *et al.* 2003) were employed which included a linker primer sequence and unique barcode/MID (multiplex identifier). Each PCR reaction contained the same reverse primer but a forward primer with a unique barcode, which allowed the deconvolution of reads from pooled amplicon data. A full list of primers with barcodes is given in Appendix 11. These primers amplify across the V1 and V2 hypervariable sequences, and the binding locations of these primers are shown on Figure 2-4. All PCR reactions were carried out using the same batch of reagents to reduce variation (Polz & Cavanaugh 1998). Reactions were performed in a G-storm GS1 thermal cycler with the following protocol. An initial denaturation at 98 °C for 5 minutes, followed by 30 cycles of a 30 second denaturation step at 98 °C, a 30 second annealing step at 53 °C, and a 30 second extension step at 72 °C. A final extension step of 72 °C for 5 minutes finished the program. Cycle numbers of 23-35 were tested during optimisation.

2.9.3. Agarose gel electrophoresis

2 % (w/v) agarose (Lonza SeaKem) was dissolved in 1x Tris-Acetate-EDTA (TAE) by boiling. Once cooled to ~60 °C, 25 µg/ml ethidium bromide (EtBr) was added. Agarose was stored at 55 °C until required. The required volume of sample was mixed with 5x TAE loading buffer (12.5 % (w/v) Ficoll, 0.1 % (w/v) bromophenol blue) at a ratio of 1 µl loading buffer per 5 µl sample, prior to loading gels. H1 Hyperladder (Biolone) was run alongside samples to allow determination of sample DNA size and quantity. Gels were typically run at 100 V and bands were visualised using a UV transilluminator.

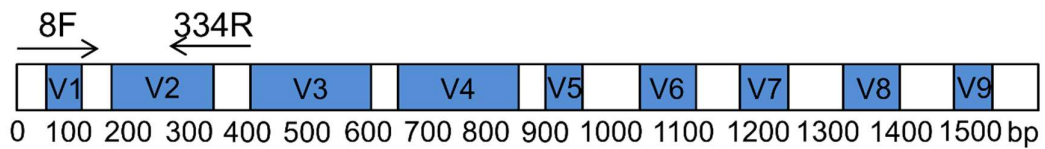


Figure 2-4. Overview of the 16S DNA sequence. Adapted from Lee, J. (2014) and Jumpstart Consortium Human Microbiome Project Data Generation Working Group (2012). Variable regions are shown in blue (V1-V8), and highly conserved regions are shown in white. Positions are based on *E. coli* strain ATCC 700926 reference sequence. Binding locations of the 8F and 334R primers are shown.

2.9.4. Gel extraction

PCR products were run on a 2 % (w/v) Agarose Gel as previously described (Section 2.9.3) and visualised on a Blue Light transilluminator. Excised bands were placed in tubes containing glass wool and centrifuged at 6708 x g for 2 minutes. The flow through was retained and the process repeated as many times as required. Each flow through from the same sample was then combined and purified with the Cycle Pure kit (Omega, Bio-Tek).

Chapter 3. The effect of BC on growth, virulence, and biofilm formation of *S. aureus* and *S. pneumoniae*

3.1. Introduction

The only previous investigation into the direct effect of PM on bacteria found that PM alone had no effect on growth of *H. influenzae* or *S. pneumoniae* (Adedeji *et al.* 2004). However, another study has found that road dusts differentially affected growth and biofilm formation of *E. faecalis*, *E. coli*, and *P. aeruginosa* (Suraju *et al.* 2015). Furthermore, cigarette smoke is also known to impact bacterial growth, production and secretion of virulence factors, and biofilm formation (McEachern *et al.* 2015; Mutepe *et al.* 2013; Feldman & Anderson 2013; Kulkarni *et al.* 2012; Goldstein-Daruech *et al.* 2011). Therefore this chapter will focus on the characterisation of the effect of BC on these phenotypes, addressing the first question this project aimed to address; Does BC affect growth, the activity of extracellular virulence factors, or biofilm formation of *S. aureus* or *S. pneumoniae*? This is the first investigation into the direct effects of BC on bacteria, the organisms responsible for the infections associated with PM exposure. This research may therefore reveal a previously overlooked impact of air pollution, providing a novel explanation for PM-associated disease.

3.1.1. Bacterial species and strains used in this research

The opportunistic pathogens *S. aureus* and *S. pneumoniae* were used as model organisms for this investigation. *S. aureus* strains SH1000 and Newman were used in the majority of investigations, however strains USA300, 2.20, PB3-32-1, and PB9 were also used in biofilm investigations. These additional strains were included to allow the assessment of MSSAs and MRSA, which employ different biofilm formation pathways as described in Section 1.10.2, and to include hospital, community, and environmental isolates, therefore covering a broad range of *S. aureus* strains. *S. pneumoniae* strains D39 and PR201 were chosen for investigation as these strains are widely used in research and there is a detailed biological knowledge associated with each of them. Furthermore, whereas D39 is an encapsulated strain, PR201 is an

unencapsulated derivative of D39, and therefore lacks a major pneumococcal virulence factor (Pearce *et al.* 2002). Unencapsulated pneumococci have been reported to have a greater biofilm formation capacity *in vitro* in comparison to their encapsulated counterparts (Domenech *et al.* 2012; Moscoso *et al.* 2006), therefore PR201 was included to complement D39 analysis.

3.2. The effect of BC on bacterial growth

To determine the effect of BC on bacterial growth, overnight cultures were diluted into fresh medium, mixed with 30, 50, or 100 µg/ml BC, and growth was assessed over the period of 1 to 8 hours, and at 24 hours (Section 2.2). Multiple BC concentrations were employed to determine whether any observed effects were concentration dependant. Control cultures without BC were also included for comparison. Viable counts were performed rather than optical density (OD) readings due to methodological restrictions, as BC interfered with the accuracy of OD readings in a non-consistent manner.

Three different media were used as the choice of growth medium has been shown to impact observed growth effects (Suraju *et al.* 2015; Adedeji *et al.* 2004), and because multiple media would be employed in various investigations throughout the project. The media selected were the nutrient rich and tissue-derived Brain-Heart Infusion (BHI) broth, the simpler yet also rich Luria-Bertani (LB) broth, and the nutrient restrictive tissue culture medium RPMI-1640 which had been chelexed to remove metal ions (CRPMI). Pneumococcal strains were unable to grow in the nutrient restrictive CRPMI medium, therefore only *S. aureus* strains were assessed under nutrient and metal-restricted conditions.

3.2.1. Effects of BC on growth of *S. aureus*

In the absence of BC, both Newman and SH1000 displayed comparable growth phenotypes to each other in both BHI and LB ($p > 0.05$, Figure 3-1 A-D). BC did not affect ($p > 0.05$) growth of SH1000 in BHI or LB over the period of 1 to 8 hours (Figure 3-1 A,C), however a significant ($p \leq 0.01$) BC-associated growth defect was observed in the minimal medium CRPMI (Figure 3-1 E). From 4 hours onwards, 50 and 100 µg/ml

BC significantly reduced viability (4 hours - $p \leq 0.01$, 5-8 hours - $p \leq 0.0001$) in comparison to control cultures. No effect ($p > 0.05$) was observed with exposure to 10 $\mu\text{g/ml}$ BC.

BC also reduced growth of *S. aureus* Newman, however this was only observed in BHI (Figure 3-1 B), and growth was unaffected ($p > 0.05$) in LB and CRPMI (Figure 3-1 D,F). 100 $\mu\text{g/ml}$ BC significantly reduced growth in BHI from 5 hours onwards (5 hours $p \leq 0.01$, 6-8 hours $p \leq 0.0001$), and 50 $\mu\text{g/ml}$ BC significantly reduced growth from 6 hours onwards (6/7 hours $p \leq 0.01$, 8 hours $p \leq 0.001$), in comparison to control cultures. No effect ($p > 0.05$) was observed with exposure to 10 $\mu\text{g/ml}$ BC. These results indicate a concentration dependent effect of BC on growth of both strains over the period of 1 to 8 hours.

Effects of BC on viability at 24 hours reflected growth effects identified over the period of 1 to 8 hours. That is to say, 50 and 100 $\mu\text{g/ml}$ BC significantly reduced SH1000 viability in CRPMI ($p \leq 0.05$ and $p \leq 0.001$, respectively. Figure 3-2 E), and 10, 50 and 100 $\mu\text{g/ml}$ BC significantly reduced viability of Newman in BHI ($p \leq 0.05$. Figure 3-2 B), in comparison to control cultures. It is interesting that a concentration dependent effect was observed with SH1000, but not Newman. Similarly to assessment over the period of 1 to 8 hours, no effect of BC was identified in LB for either strain at 24 hours (Figure 3-2 C,D), nor for SH1000 in BHI (Figure 3-2 A) or Newman in CPRMI (Figure 3-2 F). Since BC reduced growth of Newman and SH1000, but did so in two distinct media, these results indicate that BC may exert differential effects on closely related strains, which are growth condition dependent.

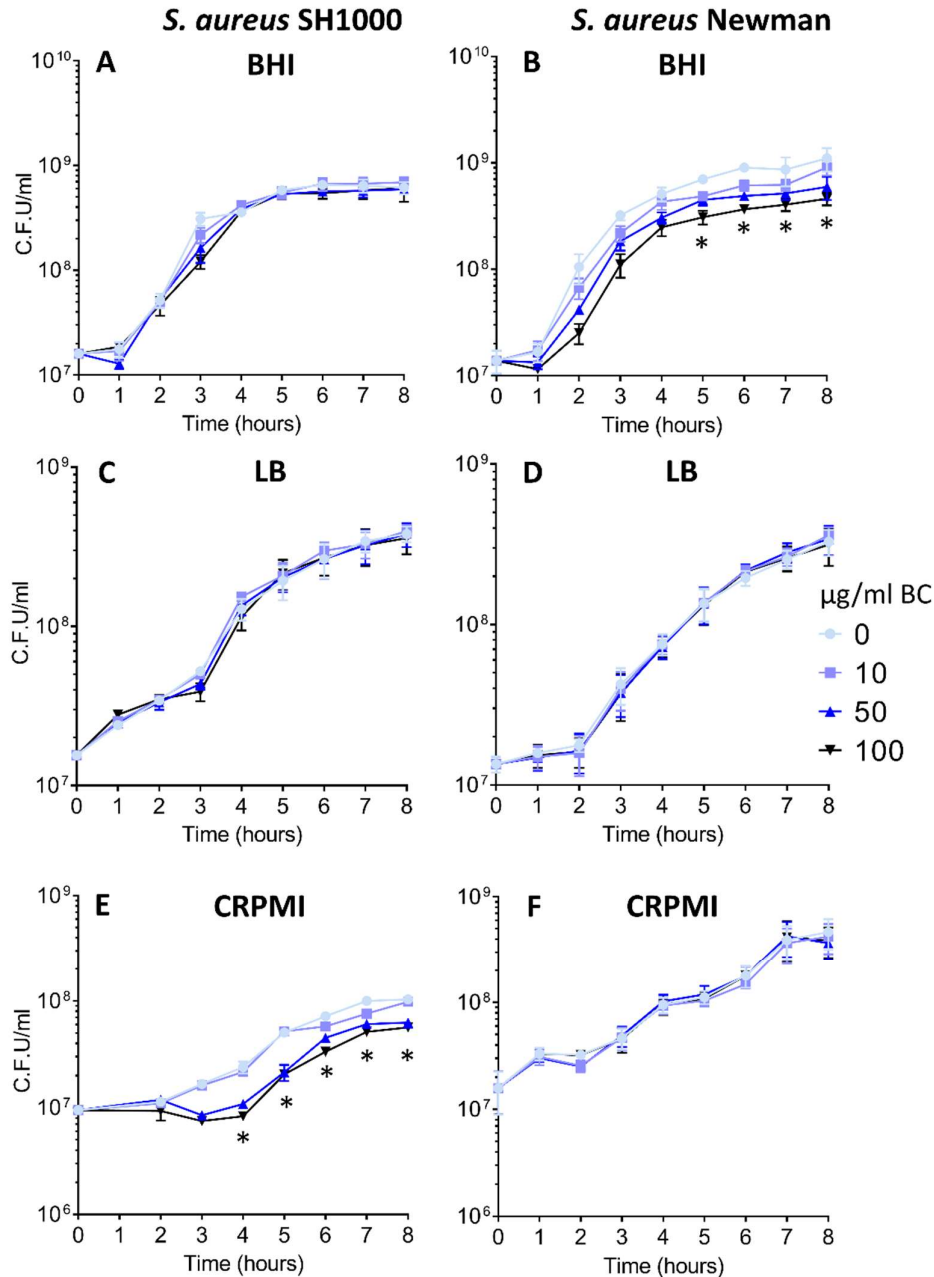


Figure 3-1. The effect of black carbon on growth of *S. aureus* over the period of 1 to 8 hours. Overnight bacterial cultures were diluted into fresh medium, mixed with 10, 50, or 100 µg/ml black carbon (BC), and incubated at 37°C in a 5 % CO₂ atmosphere. Serial dilutions of cultures were plated out each hour over the period of 1-8 hours to quantify bacterial growth. Growth of strains SH1000 (A, C, E) and Newman (B, D, F) was assessed in BHI (A, B), LB (C, D), and CRPMI (E, F). n=3. Error bars represent ± 1 SEM. Two-way ANOVA with Dunnett's multiple comparisons tests were performed to determine significance. * denotes significant results (p<0.05) in comparison to the control condition.

***S. aureus* SH1000 *S. aureus* Newman**

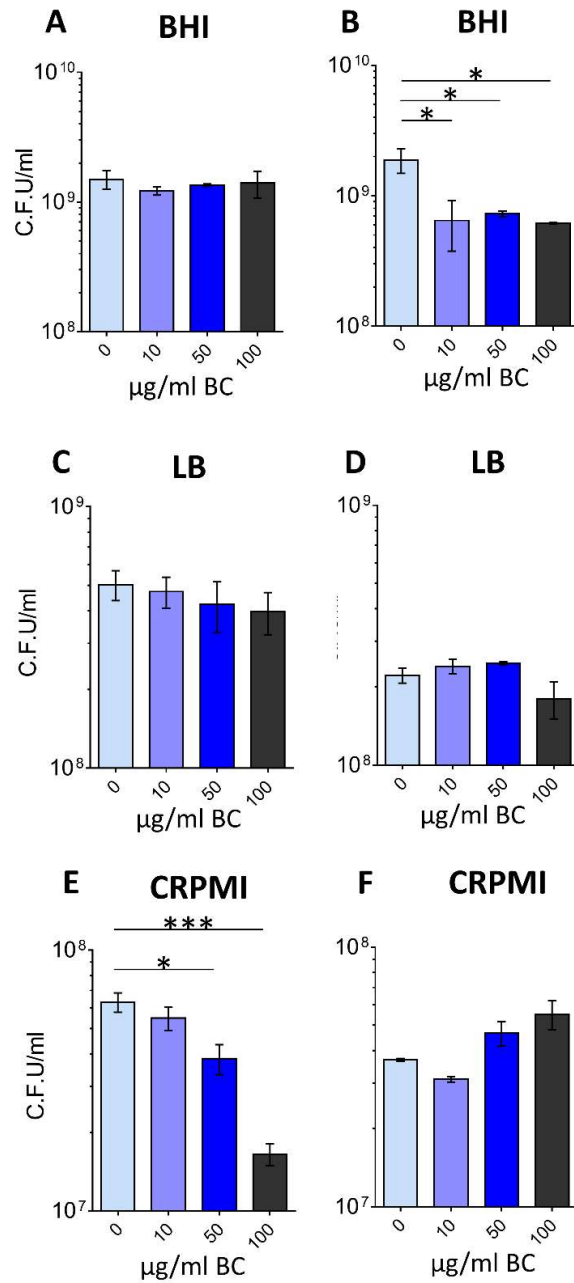


Figure 3-2. The effect of black carbon on viability of *S. aureus* after 24 hours co-incubation. Overnight bacterial cultures were diluted into fresh medium, mixed with 10, 50, or 100 $\mu\text{g/ml}$ black carbon (BC), and incubated at 37°C in a 5 % CO_2 atmosphere for 24 hours. Serial dilutions of cultures were plated out after incubation to quantify bacterial growth. Growth of SH1000 (A, C, E) and Newman (B, D, F) was assessed in BHI (A, B), LB (C, D), and CRPMI (E, F). $n=3$. Error bars represent ± 1 SEM. One-way ANOVA with Dunnett's multiple comparisons tests were performed to determine significance, significant results compared to the control are denoted with * ($p \leq 0.05$) or ** ($p \leq 0.01$).

3.2.2. Effects of BC on growth of *S. pneumoniae*

In the absence of BC, both D39 and PR201 reached a significantly ($p \leq 0.05$) greater bacterial density after 8 hours incubation in BHI (Figure 3-3 A,B) in comparison to incubation in LB (Figure 3-3 C,D). This was unsurprising as BHI is a richer medium than LB. BC was found to have no effect ($p > 0.05$) on growth of D39 or PR201 in BHI (Figure 3-3 A,B), or on growth of D39 in LB (Figure 3-3 C), over the period of 1 to 8 hours. In contrast, 100 $\mu\text{g/ml}$ BC significantly reduced growth of PR201 in LB from 5 hours onwards (5 hours $p \leq 0.01$, 6-8 hours $p \leq 0.0001$), and 50 $\mu\text{g/ml}$ BC significantly reduced growth from 6 hours onwards ($p \leq 0.0001$), in comparison to control cultures (Figure 3-3 D). No effect ($p > 0.05$) was observed with exposure to 10 $\mu\text{g/ml}$ BC. These results indicate a concentration dependent effect of BC in these conditions.

At 24 hours, both D39 and PR201 exhibited a large drop in viable cells in both media in comparison to 8 hours (Figures 3-3 and 3-4). Indeed, no viable D39 bacteria were recovered after 24 hours incubation in LB, regardless of BC exposure. *S. pneumoniae* is reported to exhibit an autolytic response during stationary phase, primarily induced by the autolysin LytA (Mellroth *et al.* 2012). Therefore this autolytic response is likely the cause of the reduction in viability observed.

BC had no effect ($p > 0.05$) on the viability of *S. pneumoniae* D39 at 24 hours in BHI (Figure 3-4 A), therefore BC was not found to affect D39 viability in either medium at any time-point assessed. Although BC was not observed to effect viability of PR201 in BHI over the period of 1 to 8 hours (Figure 3-3 B), at 24 hours BC caused a significant reduction in viability (50 $\mu\text{g/ml}$ $p \leq 0.05$, 100 $\mu\text{g/ml}$ $p \leq 0.0001$) in comparison to control cultures (Figure 3-4 B). Furthermore, results indicated that the effect of BC was concentration dependent. BC altered PR201 viability in LB at 24 hours, however a different effect was observed in comparison to over the period of 1 to 8 hours.

Although both 10 and 50 $\mu\text{g/ml}$ BC significantly ($p \leq 0.001$) decreased PR201 viability in comparison to control cultures, 100 $\mu\text{g/ml}$ BC significantly ($p \leq 0.001$) increased viability (Figure 3-4 C). These results were unexpected as 100 $\mu\text{g/ml}$ BC had been observed to decrease the growth of this strain over the period of 5 to 8 hours (5 hours $p \leq 0.01$, 6-8 hours $p \leq 0.0001$. Figure 3-3 D). The variation in the effects of BC between

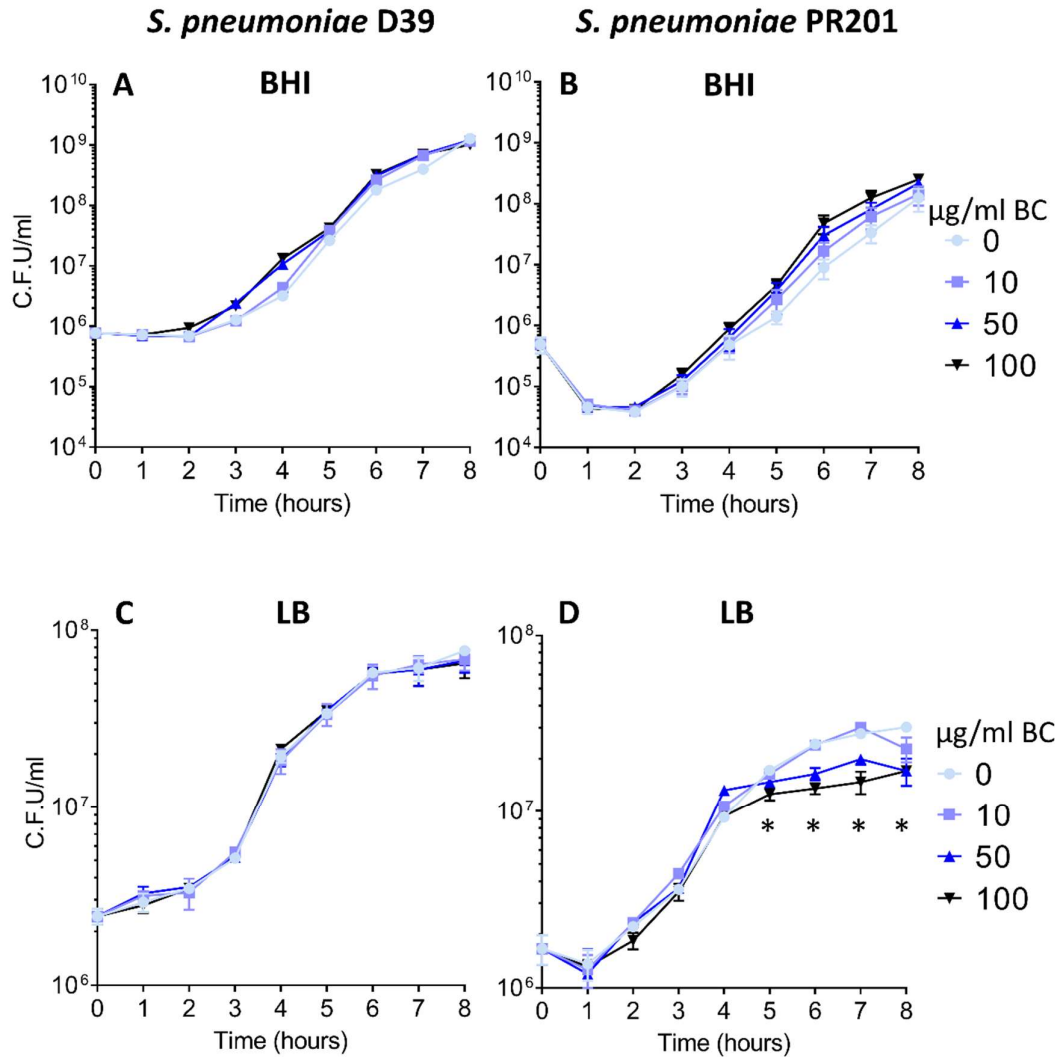


Figure 3-3. The effect of black carbon on growth of *S. pneumoniae* over the period of 1 to 8 hours. Overnight bacterial cultures were diluted into fresh medium, mixed with 10, 50, or 100 $\mu\text{g/ml}$ black carbon (BC), and incubated at 37°C in a 5 % CO_2 atmosphere. Serial dilutions of cultures were plated out each hour over the period of 1-8 hours to quantify bacterial growth. Growth of strains D39 (A, C), and PR201 (B, D) was assessed in BHI (A, B) and LB (C, D). $n=3$. Error bars represent ± 1 SEM. Two-way ANOVA with Dunnett's multiple comparisons tests were performed to determine significance. * denotes significant results ($p \leq 0.05$) in comparison to the control condition.

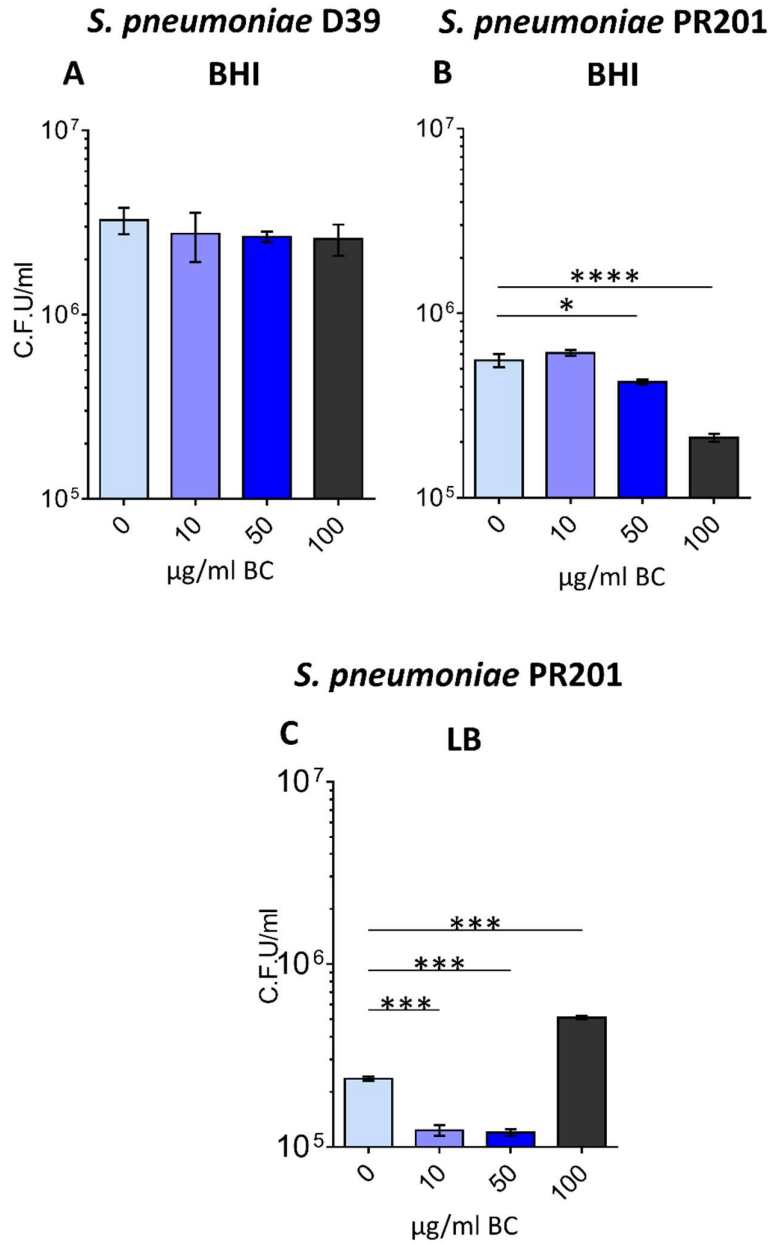


Figure 3-4. The effect of black carbon on viability of *S. pneumoniae* after 24 hours co-incubation. Overnight bacterial cultures were diluted into fresh medium, mixed with 10, 50, or 100 µg/ml black carbon (BC), and incubated at 37°C in a 5 % CO₂ atmosphere for 24 hours. Serial dilutions of cultures were plated out after incubation to quantify bacterial growth. Growth of D39 (A) and PR201 (B, C) was assessed in BHI (A, B) and LB (C). n=3. Error bars represent ± 1 SEM. One-way ANOVA with Dunnett's multiple comparisons tests were performed to determine significance, significant results compared to the control condition are denoted with * (p≤0.05) or *** (p≤0.001).

pneumococcal strains, growth conditions, concentrations, and growth phases, indicates a complex bacterial response to BC.

3.3. Effect of BC on virulence factors

3.3.1. BC has no effect on haemolysis

Two different *S. aureus* haemolysins were investigated (Section 2.3.1). α haemolysin is effective against rabbit erythrocytes, whereas β haemolysin is effective against sheep blood, so the activity of each can be differentiated using either rabbit or sheep blood agar (Dinges *et al.* 2000). Therefore *S. aureus* Newman and SH1000 were incubated with 10, 50, or 100 $\mu\text{g/ml}$ BC for 16 hours, then spotted onto rabbit and sheep blood agar plates. Plates were incubated for 24 hours and the zones of haemolysis around colonies were measured. Controls of BC alone had no effect on blood agar. No BC-induced differences were detected (Figure 3-5 A,B). Newman displayed a significantly greater haemolysis than SH1000 on rabbit blood agar ($p \leq 0.05$, Figure 3-5A), and a non-significant ($p > 0.05$) greater haemolysis on sheep blood agar (Figure 3-5 B).

In conjunction with the plate assay described, a quantitative analysis was performed with both *S. aureus* and *S. pneumoniae*. Following incubation with BC, supernatants were concentrated, serially diluted, and mixed with a 4 % (v/v) sheep or rabbit blood solution in PBS. Control cultures without BC were also used for comparison. Mixtures were incubated at 37 °C for 30 minutes to allow haemolysis to occur (Section 2.3.2). The highest dilution of each culture supernatant which caused complete haemolysis is shown in Figure 3-5 C-E. Controls of BC alone caused no haemolysis. Newman displayed significantly greater haemolysis than SH1000 in both 4 % (v/v) rabbit blood ($p \leq 0.0001$, Figure 3-5 C) and sheep blood ($p \leq 0.05$, Figure 3-5 D). Thus data from both the plate assay and the quantitative haemolysis assay show that Newman had a greater secretion of both α and β haemolysins than SH1000. In addition, both strains showed greater α haemolysis than β (Figure 3-5 C,D), however the only significant difference was between α and β haemolysis of Newman ($p \leq 0.0001$) in the quantitative assay. No differences were observed between D39 and PR201 ($p > 0.05$, Figure 3-5 E) and no differences in haemolysis were observed associated with BC exposure for any strain.

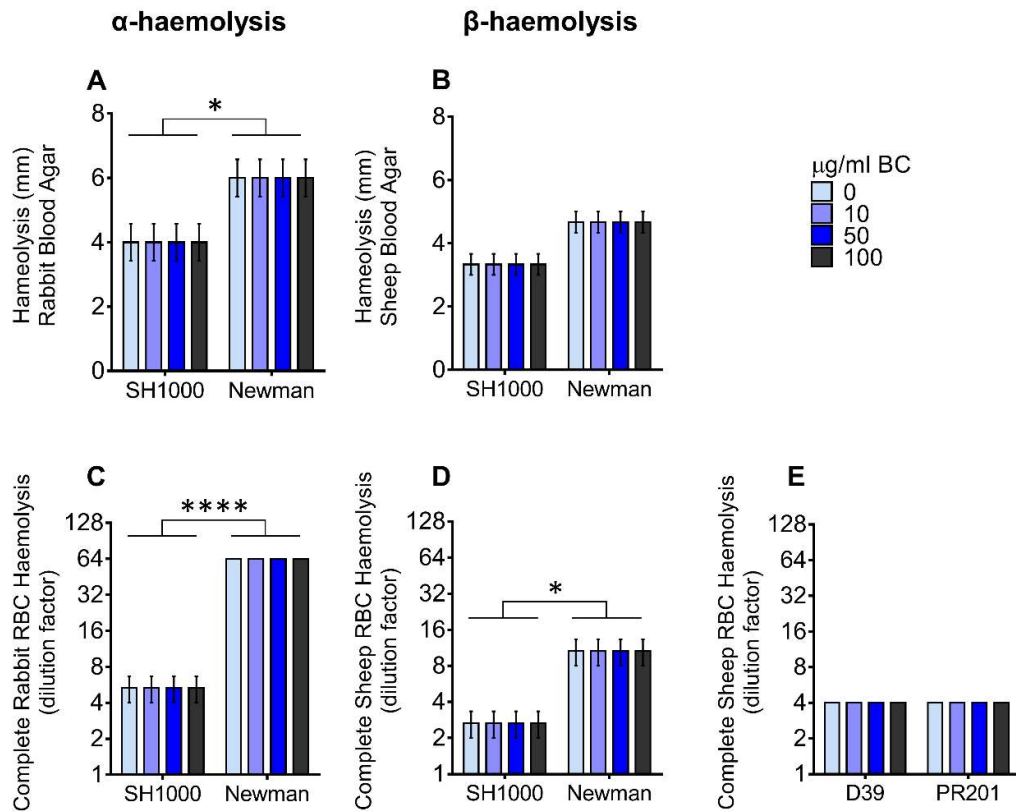


Figure 3-5. The effect of black carbon on haemolysis. Cultures of *S. aureus* Newman and SH1000 (A-D), and *S. pneumoniae* D39 and PR201 (E) were supplemented with 10, 50, or 100 µg/ml black carbon (BC) and incubated for 16 hours at 37°C in a 5 % CO₂ atmosphere. Cultures were then spotted onto agar plates supplemented with rabbit blood (A) or sheep blood (B) and incubated for 24 hours. The diameter of the zone of haemolysis after incubation is displayed in panels A and B. Alternatively, culture supernatants were concentrated and serially diluted, and added to either 4 % (v/v) rabbit (C) or sheep blood (D, E). The highest dilution of concentrated supernatant which caused complete haemolysis is displayed in panels C-E. n=3. Error bars represent ± 1 SEM. Two-way ANOVA with Dunnett's and Sidak's multiple comparisons tests were used to determine significance, significant results are denoted with * (p≤0.05) or **** (p≤0.0001). BC was found to have no effect (p>0.05) on haemolytic activity, but strain variation was identified.

3.3.2. BC has no effect on DNase or lipase secretion

To assess whether BC altered DNase or lipase secretion by *S. aureus*, strains Newman and SH1000 were incubated with 10, 50, or 100 µg/ml BC for 16 hours, then spotted onto DNase or Tributyrin (Oxoid) agar plates (Section 2.3.1). Plates were incubated for 24 hours and zones of DNA hydrolysis and lipolysis were measured (Figure 3-6 B). Controls of BC alone had no effect on either DNase or Tributyrin agar. Newman had a significantly ($p \leq 0.0001$) greater DNase activity than SH1000 (Figure 3-6 A), whereas SH1000 had a significantly ($p \leq 0.05$) greater lipase activity than Newman (Figure 3-6 B). However, BC exposure was found to have no effect ($p > 0.05$) on either DNase or lipase secretion of either strain.

3.4. Effect of BC on biofilm formation

Biofilm formation is required for pneumococcal nasopharyngeal colonisation (Gilley & Orihuela 2014; Blanchette-cain *et al.* 2013; Marks *et al.* 2012a; Domenech *et al.* 2012; Sanchez *et al.* 2011; Munoz-Elias *et al.* 2008), and is thought to be important in respiratory tract colonisation by *S. aureus* (Iwase *et al.* 2010; Quinn *et al.* 2009; Sanderson *et al.* 2006). Furthermore, biofilms are key in survival and pathogenicity (Chao *et al.* 2015; Domenech *et al.* 2013; Marks *et al.* 2012a; Domenech *et al.* 2012). Upon inhalation, BC is deposited on the surfaces of the airways where it comes into direct contact with bacteria (Kelly & Fussell 2012), therefore BC has the potential to alter biofilm formation in these sites.

3.4.1. Biofilm formation assay choice

For initial biofilm investigations, standard staining methodologies which have been used in a variety of studies were employed (Baker *et al.* 2010; Johnson *et al.* 2008; Cramton *et al.* 1999). Biofilms were formed in 96-well flat-bottomed plates with various concentrations of BC, and stained with either safranin or crystal violet. The OD of each biofilm-containing well was then measured (Section 2.4.1). However, biofilms assayed with this method were found to be highly variable between biological repeats of all strains tested, namely *S. pneumoniae* strains D39 and PR201, and

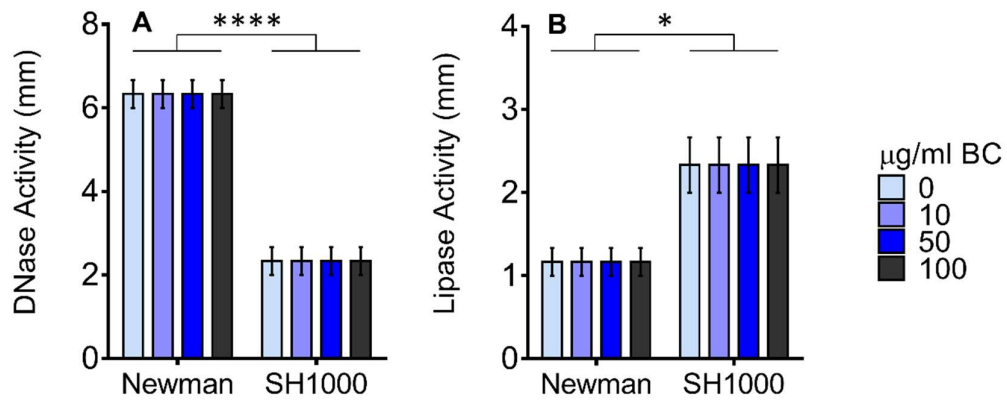
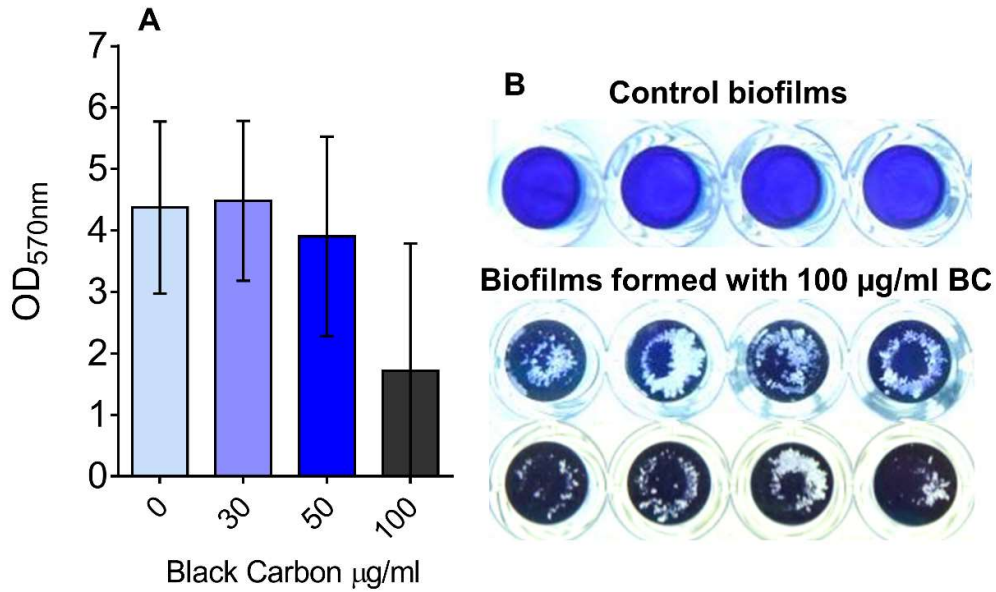


Figure 3-6. The effect of black carbon on DNase and lipase activity. *S. aureus* Newman and SH1000 cultures were supplemented with 10, 50, or 100 μg/ml black carbon (BC) and incubated for 16 hours at 37°C in a 5 % CO₂ atmosphere. Cultures were then spotted onto DNase (A) or Tributyrin (B) agar plates and incubated for 24 hours. Activity is given as the diameter of halos around colonies after incubation. n=3. Error bars represent ± 1 SEM. Two-way ANOVA with Dunnet's and Sidak's multiple comparisons tests were used to determine significance, significant results are denoted with * (p≤0.05) or **** (p≤0.0001). BC was found to have no effect (p>0.05) on haemolytic activity, but strain variation was identified.

S. aureus strains SH1000, Newman, 2.20, USA300, PB3-32-1, and PB9. Figure 3-7 A and C shows an example of this variability, with large error bars for biofilms of both *S. pneumoniae* PR201 and *S. aureus* SH1000 stained with 0.5 % (v/v) crystal violet. This method relies on making multiple OD readings across each biofilm-containing well, and calculating an average OD for each biofilm. It was therefore hypothesised that the variability observed is due to heterogeneity in biofilm thickness as visualised in Figure 3-7 B and D, with results dependent on the exact location of OD readings. It was also noted that this heterogeneity was exacerbated with BC-containing biofilms, as can be observed in images of BC-containing biofilms in Figure 3-7 B,D, and is reflected in the error bars of biofilms formed with 50 and 100 µg/ml BC (Figure 3-7 A,B). In addition to the issue of reproducibility, a second methodological limitation was encountered. Thicker biofilms were found to stain heavily with both safranin and crystal violet, exceeding the OD detection limit of equipment.

It was initially surprising that these limitations were encountered with this method, as it has been frequently used in multiple independent studies (Baker *et al.* 2010; Johnson *et al.* 2008; Cramton *et al.* 1999). However upon further investigation it became apparent that several research groups had used modified or alternative biofilm protocols (Bui *et al.* 2015; Huang *et al.* 2014; Bardiau *et al.* 2014; Kulkarni *et al.* 2012; Trappetti *et al.* 2011; Hall-Stoodley *et al.* 2008; Munoz-Elias *et al.* 2008). Consequently, a biofilm assay which quantified viable bacteria was developed based on previous research (Section 2.4.2) (Trappetti *et al.* 2011; Munoz-Elias *et al.* 2008; Hall-Stoodley *et al.* 2008). In brief, for this assay bacteria were seeded into 12-well plates, allowing the use of larger volumes. After 24 hours of incubation, planktonic bacteria were then removed and biofilms were washed to detach bacteria which were loosely adhered to the biofilm. Finally, biofilm bacteria were recovered by mechanical detachment. Numbers of viable bacteria in each of these three fractions were then determined by the Miles and Misra method (Miles *et al.* 1938). Figure 3-8 exemplifies each of these biofilm fractions in the biofilm (A), as well as how viable bacteria within each fraction are displayed graphically (B). Total CFU per fraction refers to the total amount of viable biofilm, loosely adherent, and planktonic bacteria recovered, therefore the sum of these fractions gives the total bacterial viability of the entire biofilm and surrounding medium.

S. pneumoniae PR201



S. aureus SH1000

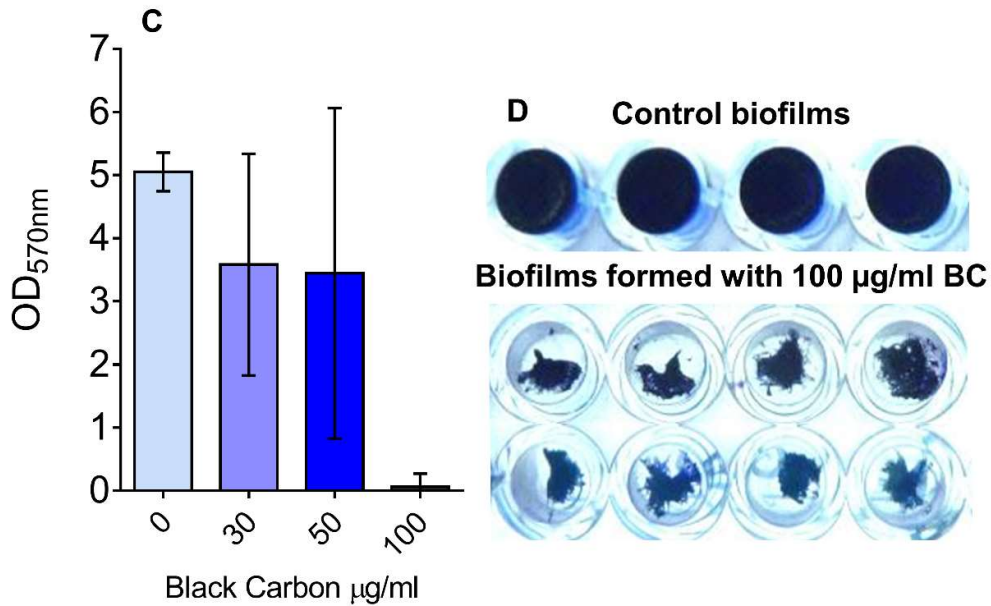


Figure 3-7. Biofilms stained with crystal violet. *S. pneumoniae* PR201 (A, B) and *S. aureus* SH1000 (C, D) were supplemented with 30, 50, or 100 $\mu\text{g/ml}$ Black Carbon (BC) and allowed to form biofilms in BHI or BHI + 4 % (w/v) NaCl, respectively. Biofilms were then washed and stained with 0.5 % (v/v) crystal violet, and OD_{570nm} measurements were taken. n=3. Error bars represent \pm 1 SEM. Representative images of stained biofilms are shown in panels B and D.

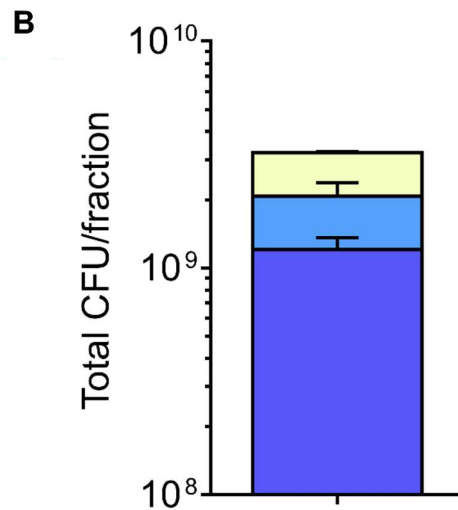
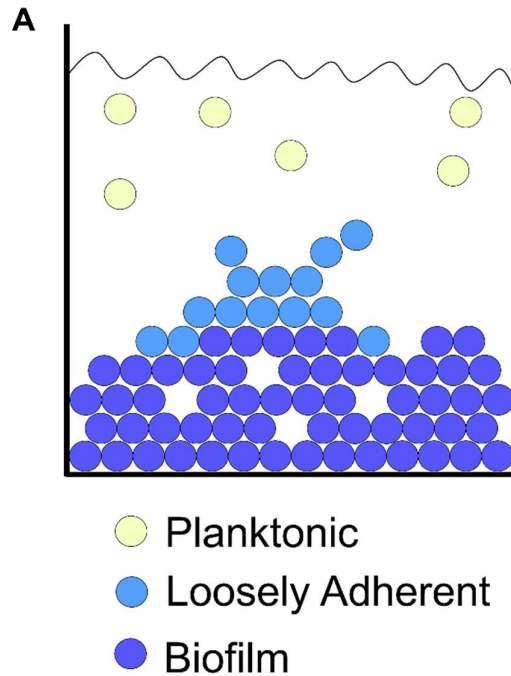


Figure 3-8. Biofilm structure. Panel A shows a diagrammatic representation of a biofilm in a well of a 12-well plate. Biofilm cells (purple) are those which are firmly attached to the substrate surface. Loosely adherent cells (blue) are those which are loosely attached to the biofilm structure. Planktonic cells (yellow) are those which have been released into the environment. Panel B shows these biofilm fractions displayed graphically. Total CFU/fraction refers to the total amount of viable biofilm, loosely adherent, and planktonic bacteria recovered from each biofilm and the surrounding growth medium.

Previous research has assessed biofilm formation by quantifying viable biofilm bacteria (Trappetti *et al.* 2011; Hall-Stoodley *et al.* 2008; Munoz-Elias *et al.* 2008), however the methodology developed for this thesis advanced on previous work by assessing viability of planktonic, loosely-adherent, and biofilm bacteria. This method allowed changes in total bacterial viability and the amount of bacteria in each fraction to be determined. It should be noted that the biofilm extracellular matrix is a major protective component of biofilms (Chao *et al.* 2015; De la Fuente-Nunez *et al.* 2013; Donlan & Costerton 2002). Therefore quantification of viable bacteria does not fully inform on all aspects of the biofilm, and this is expanded on in Section 4.7.

3.4.2. Variation in biofilm formation under different environmental conditions

To assess the effect of BC on biofilm formation, conditions which promoted maximal biofilm growth for each strain were first investigated. *S. aureus* forms biofilms through *ica*-dependent or *ica*-independent pathways, which are strongly induced by NaCl and glucose, respectively (O’Gara 2007). The biofilm formation of various *S. aureus* strains was therefore assessed in BHI supplemented with NaCl or glucose as described in Section 2.4.2. It was found that SH1000 and 2.20 formed biofilms most strongly in BHI supplemented with NaCl, Newman, USA300, and PB3-32-1 formed greatest biofilms in BHI supplemented with glucose, and PB9 formed biofilms most strongly in un-supplemented BHI (Figure 3-9). As each strain was assessed in un-supplemented BHI, BHI + glucose, and BHI + NaCl, it is impractical to show biofilm formation for all strains in all conditions in Figure 3-9. Therefore examples of biofilm formation in other media are given in Appendix 12 to allow comparison.

Biofilms of SH1000 had a significantly greater total cell viability than biofilms of 2.20 ($p \leq 0.05$), Newman ($p \leq 0.0001$), PB3-32-1 ($p \leq 0.01$), and PB9 ($p \leq 0.001$) (Figure 3-9). Therefore the only strain with a comparable ($p > 0.05$) total cell viability to SH1000 was USA300. Newman biofilms had the lowest total viability and were significantly lower than both 2.20 and USA300 ($p \leq 0.05$ and $p \leq 0.0001$, respectively), in addition to SH1000. The total viability of USA300 biofilms were also significantly ($p \leq 0.05$) greater than biofilms of PB9.

The method used has the advantage of clearly showing different biofilm structures and the variation between strains. Therefore in addition to quantifying and comparing total bacterial viability, the viability of each fraction can be assessed. Biofilms of all *S. aureus* strains had a lower proportion of planktonic cells and cells loosely adhered to the biofilm, in comparison to biofilm cells, which was significant ($p \leq 0.05$) for SH1000, 2.20, USA300 and PB3-32-1 (Table 3-1). No significant differences ($p > 0.05$) were observed between the amount of planktonic and loosely adherent cells for any strain (Table 3-1).

Although encapsulated pneumococci are known to be poor biofilm formers *in vitro* (Domenech *et al.* 2012; Moscoso *et al.* 2009), there has been some success in enhancing *in vitro* biofilm formation by supplementing biofilm media with glucose, yeast extract, xylitol, sialic acid, or N-acetyl mannosamine, or combinations of these (Domenech *et al.* 2012; Camilli *et al.* 2011; Kurola *et al.* 2011; Trappetti *et al.* 2009; Parker *et al.* 2009; Moscoso *et al.* 2006). Therefore, *S. pneumoniae* biofilm formation was assessed in three media (TSB, THB, and BHI), with combinations of the aforementioned supplements at a range of concentrations, as described in Section 2.4.2.

Of the media conditions and supplements tested, the encapsulated D39 strain was found to form greatest biofilms in THB supplemented with 0.5 % (w/v) yeast extract (THY), as shown in Figure 3-9. The unencapsulated strain PR201 was found to form greatest biofilms in BHI without supplementation (Figure 3-9). Biofilms of PR201 had a significantly greater ($p \leq 0.05$) total cell viability than biofilms of D39 (Figure 3-9). However there were no significant differences ($p > 0.05$) in the viability of the biofilm, planktonic, or loosely adherent fractions between the two strains (Table 3-1). As three media with different combinations and concentrations of supplements were investigated (Section 2.4.2), it is impractical to show biofilm formation in all conditions in Figure 3-9. Therefore examples of biofilm formation in other media are shown in Appendix 13 to allow comparison.

All *S. aureus* biofilms had a significantly ($p \leq 0.0001$) greater number of total viable bacteria, biofilm bacteria, planktonic bacteria, and loosely adherent bacteria than all pneumococcal biofilms. It should be noted that there was no obvious association

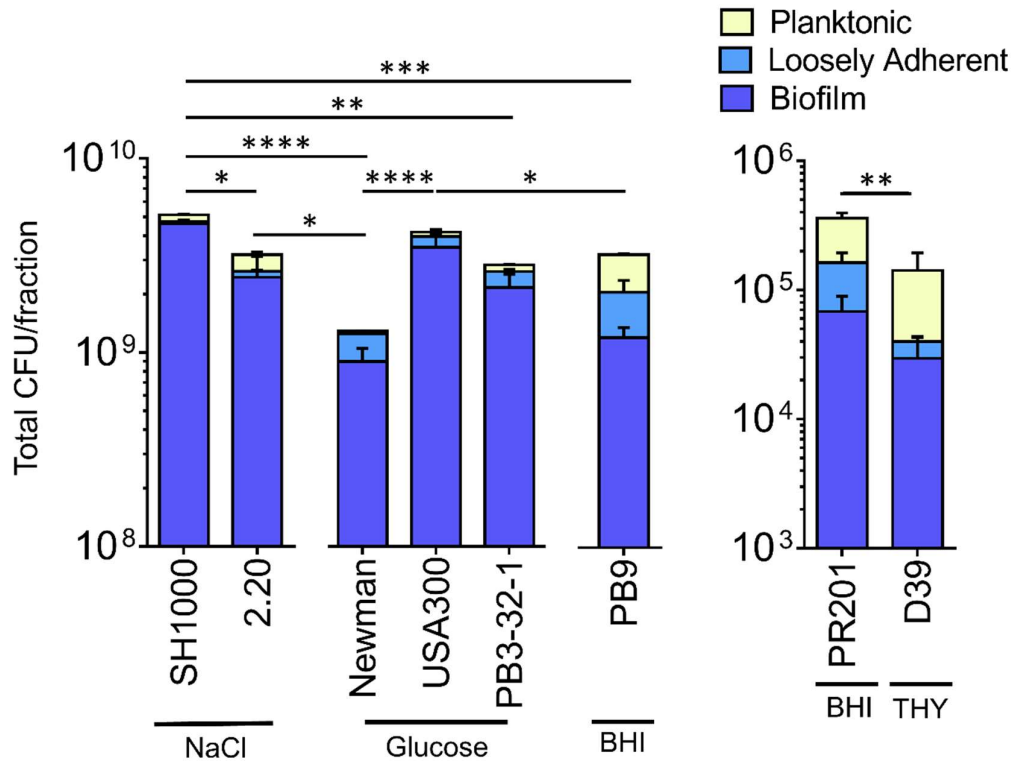


Figure 3-9. Biofilm formation of *S. aureus* and *S. pneumoniae* strains. Conditions which promoted greatest biofilm formation were determined for each strain; BHI+ 4 % (w/v) NaCl (SH1000, 2.20), BHI + 1 % (w/v) Glucose (Newman, PB3-32-1, USA300), BHI (PB9, PR201), or THY (D39). Viable bacterial cells were measured by sequential removal and quantification of planktonic, loosely- adhered, and biofilm bacteria. Total CFU/fraction refers to the total amount of viable biofilm, loosely adherent, and planktonic bacteria recovered from each biofilm and the surrounding growth medium. $n \geq 3$. Error bars represent +1 SEM. Two-way ANOVA with Sidak's multiple comparisons tests were performed to determine significance, significant differences in the total amount of bacteria are denoted with * ($p \leq 0.05$), ** ($p \leq 0.01$), *** ($p \leq 0.001$) or **** ($p \leq 0.0001$).

Table 3-1. Significant differences between biofilm, planktonic, and loosely adherent bacteria. Bacteria were induced to form biofilms in a variety of media; BHI+ 4 % (w/v) NaCl (SH1000, 2.20), BHI + 1 % (w/v) Glucose (Newman, PB3-32-1, USA300), BHI (PB9, PR201), or THY (D39). Viable bacterial cells were measured by sequential removal and quantification of planktonic, loosely- adhered, and biofilm bacteria. n≥3. 2-way ANOVA with Sidak’s multiple comparisons tests were used to determine significant differences between viable biofilm, planktonic, and loosely adherent bacteria, significant results are denoted with * (p≤0.05), ** (p≤0.01), *** (p≤0.001) or **** (p≤0.0001) and are in bold.

Bacterial Strain	Biofilm vs. Loosely Adherent		Biofilm vs. Planktonic		Planktonic vs. loosely adherent	
<i>S. aureus</i>						
SH1000	<0.0001	****	<0.0001	****	0.865	n/s
2.20	<0.0001	****	0.001	***	0.7149	n/s
Newman	0.4628	n/s	0.1248	n/s	0.8482	n/s
USA300	<0.0001	****	<0.0001	****	0.8968	n/s
PB3-32-1	0.0004	***	<0.0001	****	0.980	n/s
PB9	0.8569	n/s	0.9994	n/s	0.9063	n/s
<i>S. pneumoniae</i>						
D39	0.991	n/s	0.689	n/s	0.513	n/s
PR201	0.961	n/s	0.145	n/s	0.321	n/s

between biofilm formation conditions and total bacterial viability, or the ratio of biofilm bacteria to planktonic and loosely adherent bacteria. Instead, biofilm formation appeared to be entirely strain dependent.

3.4.3. BC alters biofilm formation in a strain dependent manner

After methodology and biofilm formation conditions had been established, the effect of BC on biofilm formation was evaluated. It is important to note that biofilm formation occurred in the presence of BC, rather than pre-formed biofilms being treated with BC. 100 µg/ml BC significantly decreased the total number of viable bacteria of both *S. aureus* SH1000 and Newman compared to control biofilms ($p \leq 0.05$, Figure 3-10 A,B). This indicates that BC inhibited growth during biofilm formation. However, this was not observed ($p > 0.05$) with 2.20, USA300, PB9, or PB3-32-1, indicating there is strain variation in this effect (Figure 3-10 C-F).

Furthermore, exposure to both 50 and 100 µg/ml BC caused a significant reduction in the number of viable biofilm bacteria for SH1000 ($p \leq 0.05$ and $p \leq 0.0001$, respectively, Figure 3-10 A). This reduction in biofilm cells was associated with a corresponding increase in loosely adherent bacteria in the 100 µg/ml BC condition ($p \leq 0.001$).

Newman had a similar response to BC exposure, although effects were also observed with 30 µg/ml BC. 30, 50, and 100 µg/ml BC all significantly reduced viable biofilm bacteria (30/50 µg/ml BC $p \leq 0.05$, 100 µg/ml BC $p \leq 0.0001$, Figure 3-10 B). However for this strain, the reduction in viable biofilm bacteria was not accompanied by a significant increase in loosely adherent bacteria. It is interesting that a concentration dependent effect was observed for both SH1000 and Newman. In contrast to these strains, BC had no effect ($p > 0.05$) on either *S. pneumoniae* D39 or PR201, in terms of total bacterial viability or in the amount of planktonic, loosely adherent, or biofilm bacteria (Figure 3-11).

To determine if the observed responses to BC were strain-specific or were affected by different environmental conditions, biofilm formation during BC exposure was re-examined with each strain, using biofilm media from earlier optimisation work (Section 3.4.2). For all strains, the effect of BC on biofilm formation was a consistent

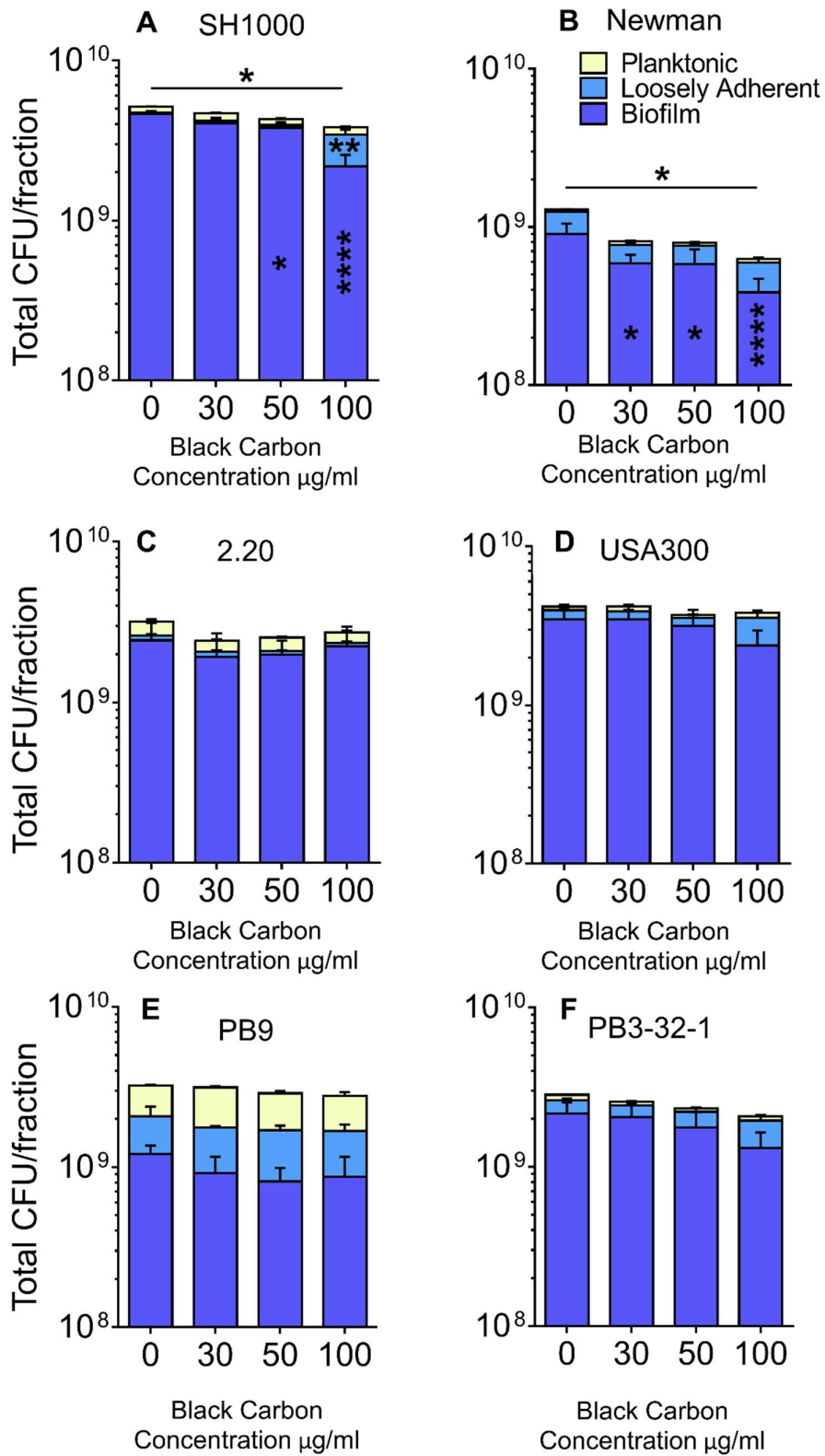


Figure 3-10. The effect of black carbon on *S. aureus* biofilms. Legend overleaf

Figure 3-10. The effect of black carbon on *S. aureus* biofilms. *S. aureus* SH1000 (A), Newman (B), 2.20 (C), USA300 (D), PB9 (E) and PB3-32-1 (F) were allowed to form biofilms in the presence or absence of 30-100 µg/ml black carbon (BC). Biofilms of strains SH1000 and 2.20 were formed in Brain-Heart Infusion (BHI) supplemented with 4 % (w/v) NaCl, biofilms of strains Newman, PB3-32-1, and USA300 were formed in BHI supplemented with 1 % (w/v) Glucose, and biofilms of PB9 were formed in unsupplemented BHI. Viable bacterial cells were then measured by sequential removal and quantification of planktonic, loosely- adhered, and biofilm bacteria. Total CFU/fraction refers to the total amount of viable biofilm, loosely adherent, and planktonic bacteria recovered from each biofilm and the surrounding growth medium. n=4. Error bars represent +1 SEM. Two-way ANOVA with Tukey's multiple comparisons tests were used to determine significance, significant results compared to the control condition are denoted with * ($p \leq 0.05$), ** ($p \leq 0.01$), or **** ($p \leq 0.0001$).

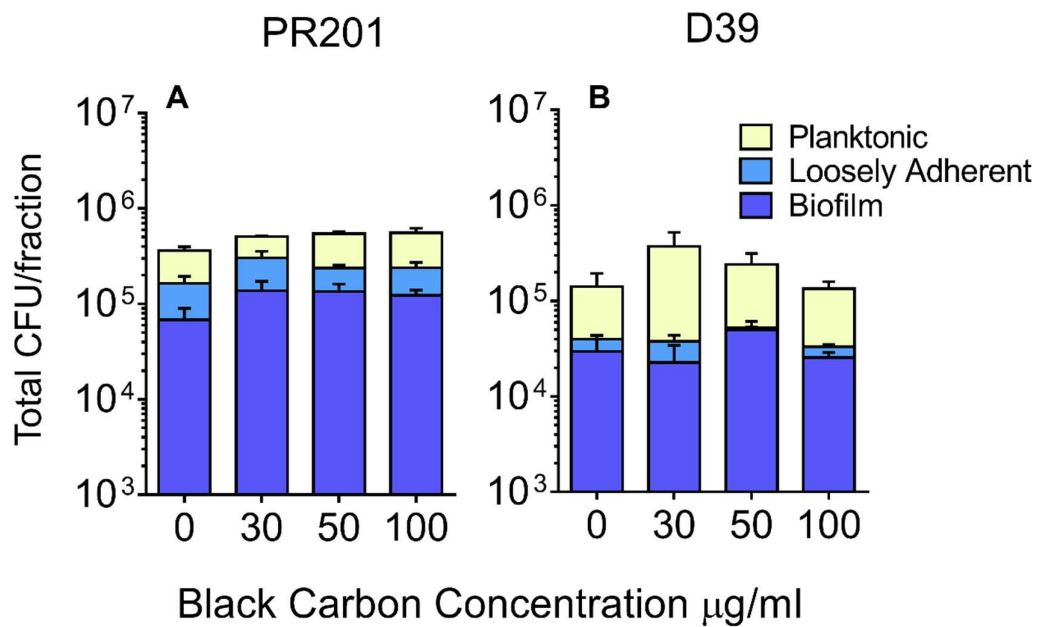


Figure 3-11. The effect of black carbon on *S. pneumoniae* biofilms. *S. pneumoniae* PR201 (A) and D39 (B) were allowed to form biofilms in the presence or absence of 30-100 $\mu\text{g/ml}$ black carbon (BC). Biofilms of PR201 were formed in Brain-Heart Infusion (BHI), whereas biofilms of D39 were formed in Todd Hewitt Broth supplemented with 0.5 % (w/v) Yeast Extract (THY). Viable bacterial cells were then measured by sequential removal and quantification of planktonic, loosely- adhered, and biofilm bacteria. Total CFU/fraction refers to the total amount of viable biofilm, loosely adherent, and planktonic bacteria recovered from each biofilm and the surrounding growth medium. $n \geq 3$. Error bars represent +1 SEM. Two-way ANOVA with Tukey's multiple comparisons tests were used to determine significance, no significant differences ($p > 0.05$) were identified in the effect of BC on biofilm formation of either strain.

strain-associated phenotype and did not alter in different environmental conditions. Examples of this consistency are shown in Appendix 14. Therefore BC was found to alter biofilm formation of *S. aureus* SH1000 and Newman, but of no other strains tested using this methodology, and these effects were consistent in different environmental conditions.

3.5. Discussion

The objective of this chapter was to determine whether BC affected the growth, the activity of extracellular virulence factors, or biofilm formation of *S. aureus* or *S. pneumoniae*. BC was observed to reduce growth and biofilm formation, showing that BC directly affects bacteria of the respiratory tract. These results also clearly demonstrated that BC has an intra- and inter-species differential impact.

3.5.1. BC alters bacterial growth and viability

The effect of BC on bacterial growth was investigated using a variety of media. It should be noted that there was no direct correlation between nutrient availability and BC-related growth effects. Instead, effects appeared to be dependent on the strain and environmental conditions employed. BC inhibited the growth of *S. aureus* Newman in BHI, and inhibited the growth of SH1000 in CRPMI, two distinctly different media. Growth effects in CRPMI may be more representative of the BC-bacterial interactions in the respiratory tract, as this minimal medium is more reflective of the restrictive environment *in vivo*, where freely available metal ions are sequestered and nutrient availability is kept low (Richards *et al.* 2015; Morrissey *et al.* 2002). Therefore these results may suggest that *in vivo*, growth of some strains would be affected by BC whereas others would not.

In contrast, BC was not observed to affect growth of *S. pneumoniae* D39 in the conditions employed in this research. Based on the effect of BC on growth of *S. aureus*, it may be useful to also assess the effect of BC on growth of *S. pneumoniae* in nutrient-restrictive conditions. Pneumococci are unable to grow in CRPMI, however supplementing CRPMI with 1 % (w/v) casamino acids makes the medium more

permissive to growth (Tarrant 2013; Baker 2009). Therefore future work could assess whether this modification allows pneumococcal growth and if so, the effect of BC could be reassessed in this medium.

BC also altered growth of *S. pneumoniae* strain PR201 in both BHI and LB, however this effect varied depending on BC concentration and time-points assessed. 50 and 100 µg/ml BC significantly reduced growth of this strain in LB over the period of 5 to 8 hours, however at 24 hours, 100 µg/ml BC actually significantly increased bacterial viability. Pneumococci are reported to undergo programmed cell death in stationary phase (Mellroth *et al.* 2012), therefore a reduction in the length of time spent in stationary phase before bacterial enumeration could result in the observed greater bacterial viability. I hypothesise that as 100 µg/ml BC significantly reduced growth of PR201 during exponential phase, these cultures entered stationary phase later than control cultures and those exposed to lower BC concentrations, resulting in less autolysis. This hypothesis could be tested by assessing pneumococcal growth every hour for 24 hours to construct a full growth curve. Unfortunately however, BC was found to affect OD readings of cultures in a non-reproducible manner, therefore viable counts were used in this project which is impractical for a 24 hour growth analysis.

Previous research has shown that ambient PM₁₀ collected in Birmingham, UK, had no effect on the growth of the encapsulated *S. pneumoniae* strain ATCC 49619 or *Haemophilus influenzae* strain NCTC 11931 (Adedeji *et al.* 2004). However, the investigation by Adedeji *et al.* (2004) does not necessarily contradict the data presented in this thesis. This is because only a single strain of each species was used in the investigation by Adedeji *et al.* (2004), in a single growth medium, and the research described in this chapter has identified that the effects of BC on bacterial growth were dependent on each strain and the specific environmental conditions tested. Furthermore, PM is heterogenous and varies in composition and concentration in both space and time (Kelly & Fussell 2012; Air Quality Expert Group 2012; Air Quality Expert Group 2005). Therefore as Adedeji *et al.* (2004) did not characterise the PM used, it is not known what proportion of the PM was comprised of BC and what other components were present.

BC exposure causes oxidative stress and the increased production of reactive oxygen species (ROS) in eukaryotic cells (Longhin *et al.* 2016; De Prins *et al.* 2014; Rosa *et al.* 2014; Zhao *et al.* 2012; Yang *et al.* 2009). The generation of ROS leads to DNA, RNA, protein, and lipid damage, resulting in cell damage and death (Rai *et al.* 2015; Zhao & Drlica 2014). Therefore I hypothesise that BC also causes oxidative stress in bacteria, and that exposure to high levels of BC may generate enough oxidative stress to be toxic to bacteria. This would explain the concentration dependent growth inhibition associated with BC exposure in this project. To investigate this hypothesis, future work could directly assess whether BC causes oxidative stress in bacteria through the use of fluorescence assays which detect and quantify ROS in real-time in live bacterial cells (Choi *et al.* 2015), or by measuring oxidative damage markers such as protein carbonylation and levels of 8-hydroxy 2'-deoxyguanosine, 8-hydroxyguanosine, and 8-hydroxyguanine (Belenky *et al.* 2015).

It is as yet unclear why the effects of BC on growth were not consistent for the species and strains investigated for this thesis. A transcriptomic investigation which could explore strain differences is discussed in Section 3.5.5. Alternatively, according to the presented oxidative stress hypothesis, the strain differences observed may be due to different stress response systems. Therefore if BC is found to generate oxidative stress in bacteria, oxidative stress mutants of the strains employed could be used to elucidate the mechanisms of resistance to BC toxicity.

A potential implication of the species- and strain- dependent effect of BC on growth may be the remodelling of the respiratory tract microbiota *in vivo*. It is established that cigarette smoke alters the respiratory tract microbiota diversity, decreasing prevalence of competitive anaerobic and aerobic commensals, and enhancing prevalence of pathogens, specifically *S. pneumoniae* and *S. aureus* (McEachern *et al.* 2015; Feldman & Anderson 2013; Morris *et al.* 2013; Garmendia *et al.* 2012; Brook 2011). BC-induced growth inhibition may have a similar effect in that BC may remodel the diversity of the respiratory tract microbiota by preventing growth of certain bacterial strains and therefore allowing other bacteria to outcompete their rivals. This is further explored in Chapter 5.

This research into the effects of BC on bacterial growth suggests that BC-growth effects are strain dependent and are influenced by nutrient availability. Importantly, these data have revealed a biologically relevant direct effect of BC on bacteria. What is not yet known is the mechanisms responsible for these effects.

3.5.2. BC has no effect on the virulence factors tested

BC exposure had no effect on the activity of the virulence factors investigated in this study. Haemolysins, nucleases, and lipases were chosen for investigation as they were simple to characterise, gave a rapid answer to whether BC potentially altered virulence, and are some of the major virulence factors of *S. aureus* and *S. pneumoniae*.

Extracellular release of virulence factors during planktonic growth was assessed in this project, however these virulence factors are also important in biofilm formation.

Pneumococcal pneumolysin and the α and β haemolysins of *S. aureus* are required for biofilm formation (Katayama *et al.* 2013; Shak *et al.* 2013a; Huseby *et al.* 2010; Caiazza & O'Toole 2003). Pneumolysin contributes towards early stage biofilm formation (Shak *et al.* 2013a), but the gene encoding Ply is downregulated within mature biofilms (Chao *et al.* 2015; Gilley & Orihuela 2014; Marks *et al.* 2013; Sanchez *et al.* 2011). Ply is highly immunogenic so it is likely that this downregulation in mature biofilms enhances survival (Cruse *et al.* 2010; Marriott *et al.* 2008; Ratner *et al.* 2006; van Rossum *et al.* 2005). Furthermore, *S. aureus* β -haemolysin is required for skin-colonisation, and β -haemolysin-deficient strains display a reduced colonisation capacity (Katayama *et al.* 2013). Similarly, *S. aureus* lipases are upregulated in biofilms as well as during deep-tissue infections (Hu *et al.* 2012).

Therefore as the virulence factors investigated are all important in biofilm formation, which is a key facet of nasopharyngeal colonisation (Gilley & Orihuela 2014; Blanchette-cain *et al.* 2013; Marks *et al.* 2012a), and BC has been shown to alter biofilm formation (Section 3.4.3), it may be interesting to repeat assessment of these virulence factors in biofilms. Biofilm assays could be carried out as described (Section 2.4.2), followed by assessment of these activity of these virulence factors (Section 2.3). Dispersed pneumococci are reported to be more virulent than biofilm or planktonic pneumococci, and display the increased transcription of genes associated with virulence

including pneumolysin (Chao *et al.* 2015; Pettigrew *et al.* 2014; Marks *et al.* 2013; Blanchette-cain *et al.* 2013; Sanchez *et al.* 2010; Smith *et al.* 2002). Therefore in addition to biofilm bacteria, pneumococci dispersed from biofilms could also be investigated.

It should be noted that only a few virulence factors were investigated in this study, and in limited conditions. Since this is a limited view, future work could continue this assessment with the other major virulence factors of *S. aureus* and *S. pneumoniae*. The most salient additional virulence factors of *S. aureus* to investigate would include fibronectin binding proteins and certain adhesins. Transcription of *fnbA* (encoding fibronectin binding protein A) has been shown to be increased by cigarette smoke exposure (Kulkarni *et al.* 2012), therefore BC may also affect production of Fnbps. Adhesins, including iron-regulated surface determinant protein (IsdA) and clumping factor B (ClfB), are vital for colonisation and biofilm formation (Edwards *et al.* 2012; Bien *et al.* 2011), therefore may be interesting to investigate in light of the effects of BC on biofilm formation. For *S. pneumoniae*, future work could investigate the neuraminidases (NanA, NanB, and NanC), capsular polysaccharide, surface protein A, and autolysin A (Kadioglu *et al.* 2008). NanA would be particularly interesting to investigate as it is responsible for cleaving N-acetylneuraminic acid from membrane glycoproteins, a function which may be used to expose attachment sites, and is vital in host colonisation and biofilm formation (Gualdi *et al.* 2012; Xu *et al.* 2011; Parker *et al.* 2009; Kadioglu *et al.* 2008; S. J. King *et al.* 2006). Furthermore, investigation of neuraminidase activity would be simple following standard protocols which use 2-O-(p-nitrophenyl)- α -d-N-acetylneuraminic acid (pNP-NANA) to assess neuraminidase activity (Manco *et al.* 2006).

It may also be interesting to investigate the effect of BC on virulence factor regulation and production, as it is possible that BC may upregulate the production of virulence factors which is not mirrored by increased secretion. To investigate this, quantitative reverse transcription PCR (qRT-PCR) could be employed to quantify RNA expression of the genes encoding the selected virulence factors described in this section (Casillas-Ituarte *et al.* 2012). Alternatively, rather than a targeted approach assessing the effect of

BC on production of certain virulence factors, a broader investigation using a transcriptomic approach could be employed. This is discussed in Section 3.5.5.

3.5.3. Variation in biofilm formation in the absence of BC

In the absence of BC, significant ($p \leq 0.05$) variation in biofilm formation was observed for strains of both *S. pneumoniae* and *S. aureus*. Strain variation is expected and has been identified in previous studies (Nicholson *et al.* 2013; Domenech *et al.* 2012), however it is difficult to compare the data obtained here to previous work due to the novel biofilm method used. Although biofilms of *S. pneumoniae* PR201 had a significantly greater ($p \leq 0.05$) total cell viability than biofilms of D39, this was not due to a significant increase in either biofilm, loosely adherent, or planktonic bacteria ($p > 0.05$). Instead, the amount of bacteria in each fraction was non-significantly ($p > 0.05$) greater in PR201 biofilms, resulting in a cumulative significant difference in total viability ($p \leq 0.05$). As loosely adherent bacteria are dislodged from the biofilms during the wash step, the large proportions of loosely adherent bacteria identified from biofilms of both D39 and PR201 suggests that these biofilms had a low structural integrity and were more susceptible to shear stress.

Biofilms of *S. aureus* strains SH1000, 2.20, USA300 and PB3-32-1 had significantly ($p \leq 0.05$) less loosely adherent bacteria than biofilm bacteria, indicating that very few cells were dislodged during the wash step. These data imply that these were strong biofilms highly resistant to shear stress. The environmental conditions which promoted greatest biofilm formation of *S. aureus* strains did not fully correlate with the conditions reported to be differentially associated with either MSSAs or MRSA, as has been previously suggested (McCarthy *et al.* 2015; O’Gara 2007; O’Neill *et al.* 2007). However, the specific response mechanisms which induce *S. aureus* biofilm production are yet to be fully defined (Bui *et al.* 2015), and in reality are more complex than the simple induction of either *ica*-dependent or *ica*-independent pathways (Agarwal & Jain 2013; O’Gara 2007). In fact, certain environmental conditions such as glucose are known to induce both pathways (Agarwal & Jain 2013; O’Gara 2007).

3.5.4. BC alters biofilm formation

BC significantly decreased the total number of viable bacteria ($p \leq 0.05$) and the number of bacteria in the biofilm fraction of both *S. aureus* SH1000 and Newman biofilms ($p \leq 0.05$ - $p \leq 0.0001$ depending on BC concentration). For SH1000, it is clear that BC reduced biofilm structural integrity and made biofilms more susceptible to sheer stress as this reduction in biofilm cells was associated with a corresponding significant (100 $\mu\text{g/ml}$ - $p \leq 0.001$) increase in loosely adherent bacteria. Therefore these data suggest that SH1000 biofilms formed in the presence of BC may disperse more bacteria than controls. Dispersal of biofilm bacteria is associated with the increased spread of bacteria to secondary sites and exacerbations of infections (Chao *et al.* 2015; Lister & Horswill 2014; Costerton *et al.* 1999; Fowler *et al.* 1997). Indeed, dispersed biofilm pneumococci are known to disseminate to the lungs at a higher degree than planktonic bacteria, and are more virulent (Marks *et al.* 2013; Blanchette-cain *et al.* 2013; Sanchez *et al.* 2010; Smith *et al.* 2002). If *S. aureus* bacteria dispersed from biofilms display a similar phenotype, which is currently unknown, these data would suggest that BC may increase the ability of SH1000 to disperse from colonised biofilms in the upper respiratory tract, and may spread to the lungs and cause infection. In contrast to SH1000, no significant increase ($p > 0.05$) in loosely adherent bacteria was identified with the significant decrease in biofilm bacteria for Newman. These results may therefore have been caused by the reduction in overall cell viability.

BC was not found to alter biofilm formation of pneumococcal strains D39 or PR201, or staphylococcal strains PB3, PB9, 2.20, or USA300. Previous work has shown that a single exposure to cigarette smoke had no effect on biofilm formation of *P. aeruginosa*, however two or three exposures caused an increase in biofilm mass (Antunes *et al.* 2012). Therefore future work could also characterise biofilm formation during repeated BC exposure following similar protocols. This is more similar to real PM exposure and would allow the determination of whether the BC-induced biofilm effects observed for SH1000 and Newman are exacerbated in these conditions, and whether the strains which were not affected in the current study would show a response.

It is interesting that the effects of BC again appeared to be strain specific and were not dependent on specific environmental conditions. Therefore these results indicate that strain differences may be what defines the response to BC, and that BC does not simply alter a specific biofilm formation pathway in certain environmental conditions. Chapter 4 expands on the characterisation of biofilms and this strain variation. The mechanisms responsible for the effects of BC on biofilm formation have not yet been elucidated and a transcriptomic approach to this investigation is discussed in Section 3.5.5.

Alternatively, previous research into the mechanisms by which cigarette smoke alters biofilm formation may provide targets for future research with BC. For *S. aureus*, cigarette smoke induces biofilm formation by increasing transcription of genes involved in biofilm formation (*sarA*, *ica*, *rbf*) and decreasing transcription of genes involved in biofilm dispersion (*agr*) (McEachern *et al.* 2015; Feldman & Anderson 2013; Kulkarni *et al.* 2012). Future work could employ qRT-PCR to quantify RNA expression of these genes and assess whether they are impacted by BC in biofilm formation. Furthermore, cigarette smoke increases transcription of oxidoreductases in *S. aureus*, therefore it is thought that the increase in biofilm formation is caused by the induction of oxidative stress (Kulkarni *et al.* 2012). In addition, oxidative stress alone has been shown to induce biofilm formation in *P. aeruginosa* (Antunes *et al.* 2012). Therefore these results suggest that the investigation of the effect of BC on oxidative stress resistance may also be useful to address in future work.

Previous research has identified that 100 µg/ml outdoor dust significantly ($p \leq 0.05$) enhanced biofilm formation of *E. faecalis*, *E. coli*, and *P. aeruginosa* in both nutrient-rich and nutrient-poor growth conditions (Suraju *et al.* 2015). Furthermore, cigarette smoke also increases biofilm formation of *S. pneumoniae* and *S. aureus* (Feldman & Anderson 2013; Mutepe *et al.* 2013; Kulkarni *et al.* 2012). Inhalation of cigarette smoke is associated with increases in morbidity and mortality, including increases in a variety of respiratory tract infections. In fact, cigarette smoke is a major risk factor for the development of pneumococcal pneumonia (Feldman & Anderson 2011). It is therefore interesting that past research has identified biofilm increases caused by outdoor dust and cigarette smoke exposure, whereas only biofilm decreases were observed in the research for this thesis. Thus, these data indicate that the mechanisms

by which BC causes disease may be notably different from those responsible for disease caused by dusts and cigarette smoke. It is therefore clear that the effects of BC on bacteria warrant further investigation.

3.5.5. Future investigations into the mechanisms of BC effects

The mechanisms responsible for the effects of BC on growth and biofilm formation were not elucidated in the current investigation. Furthermore, although BC was not observed to affect extracellular release of the virulence factors investigated, few were investigated and in limited conditions. To further investigate the effect of BC on bacteria, assess whether BC alters production of any virulence factors, and determine the mechanisms of growth and biofilm effects, a transcriptomics approach could be used. Future work could culture bacteria in the presence of BC in planktonic conditions, or form biofilms in the presence of BC as described (Section 2.4.2), and assess the transcriptome using RNA-Seq (Croucher & Thomson 2010). This technique would allow the characterisation of the effect of BC on bacteria without the requirement for targeted investigation of particular genes, such as in qRT-PCR (Casillas-Ituarte *et al.* 2012). Furthermore, this technique may provide information on why the effect of BC varied between species and strains.

3.5.6. Conclusions

BC was found to alter bacterial growth and biofilm formation in a species dependent manner. However, BC was not identified to affect the activity of key virulence factors. Investigations into these factors were completed in parallel to each other and it was decided to focus on the effect of BC on biofilm formation, which is further explored in Chapter 4. This work has clearly shown intra- and inter-species variation in the response to BC. Therefore it is highly likely that BC will also affect other bacteria in a strain-specific manner. In regards to human health, this could have important implications in remodelling the respiratory tract microbiota, the diversity and functioning of which is vital for protection against pathogens and maintaining the health of hosts. This is expanded upon in Chapter 5. Importantly, this is the first research to show that BC directly affects bacteria.

Chapter 4. Further investigations into BC-induced biofilm alterations

4.1. Introduction

Chapter 3 explored the effect of BC on growth, virulence, and biofilm formation of *S. aureus* and *S. pneumoniae*. BC was found to significantly alter biofilm formation in a strain dependent manner, therefore it was decided to further assess the effects of BC on biofilms. To address this aim, biofilm architecture and structure, potential mechanisms of BC induced effects, the biofilm extracellular matrix, and biofilm functioning were investigated. The importance of biofilm formation is described before in Section 1.10.

It has been reported that unencapsulated pneumococci have a greater biofilm formation capacity *in vitro* in comparison to encapsulated strains (Domenech *et al.* 2012; Moscoso *et al.* 2006). Indeed, the unencapsulated PR201 strain was identified to form significantly greater biofilms than the encapsulated D39 strain in Chapter 3. Additionally, it was found that D39 did not survive processing for some investigations described in this chapter, and so only data for the PR201 strain is presented for electron microscopy analysis (Sections 4.2 and 4.3) and degradation of biofilms with proteinase K and DNaseI (Section 4.7). *S. aureus* strains Newman and SH1000 were investigated as biofilms of these strains had been observed to be significantly altered by BC in Chapter 3. In certain assays however, additional *S. aureus* strains such as USA300 were also included to allow additional comparison with a strain which had not previously been observed to be affected by BC.

The choice of media used for the biofilm assays described in this chapter was determined by the biofilm conditions tested in Chapter 3 (Section 3.4.2). The environmental conditions which were found to promote greatest biofilm formation in Chapter 3 were employed. Briefly, biofilms of *S. aureus* strains SH1000 and 2.20 were formed in BHI supplemented with 4 % (w/v) NaCl, whereas biofilms of strains Newman, PB3-32-1, and USA300 were formed in BHI supplemented with 1 % (w/v) Glucose. Biofilms of *S. aureus* PB9 and *S. pneumoniae* PR201 were both formed in unsupplemented BHI, and biofilms of *S. pneumoniae* D39 were formed in THY.

4.2. BC alters biofilm architecture

The objective of this section was to determine whether the observed BC-induced changes in biofilm viability (Chapter 3) were paralleled by changes in biofilm structure. Furthermore, biofilms of strains which appeared unaffected by BC in Chapter 3 were assessed to see if there was a modulation of architecture that was not accompanied by changes in bacterial viability. To investigate biofilm architecture, biofilms were analysed by Scanning Electron Microscopy (SEM). BC was also imaged by SEM to permit the identification of BC within bacterial biofilms. Figure 4-1 shows the appearance of dry BC powder without processing at two magnifications. Dry BC powder was imaged as BC did not bind to the 12-well plates used for bacterial biofilm formation assays (Section 2.4.2). This meant that the BC could not be imaged once it had been suspended in a biofilm formation media, as it was washed out of the wells during processing for SEM.

Biofilms were grown in the presence of 30, 50, and 100 µg/ml BC on round glass coverslips, then processed for visualisation with SEM as described (Section 2.5.1) (Dykstra & Reuss 2003). Imaging with this method revealed striking biofilm structural modifications in the presence of BC. Figure 4-2 shows examples of the alterations in biofilm architecture observed. Biofilms of *S. pneumoniae* PR201 formed in the presence of BC displayed large BC-associated structures with channels running throughout the biofilm (Figure 4-2 B), in contrast to the flat structures of biofilms formed without BC (Figure 4-2 A). BC-formed biofilms of *S. aureus* SH1000 showed more irregularities in the surface in comparison to controls (Figure 4-2 C), with BC-associated protrusions evident (Figure 4-2 D). Unfortunately the standard techniques used for SEM preparation involved processing through an ethanol gradient (Section 2.5.1), which destroyed biofilm samples for certain strains, and particularly for biofilms formed under high BC concentrations. For example, Figure 4-2 shows biofilms of SH1000 formed in the presence of 50 µg/ml BC as those formed in the presence of 100 µg/ml BC were destroyed during processing.

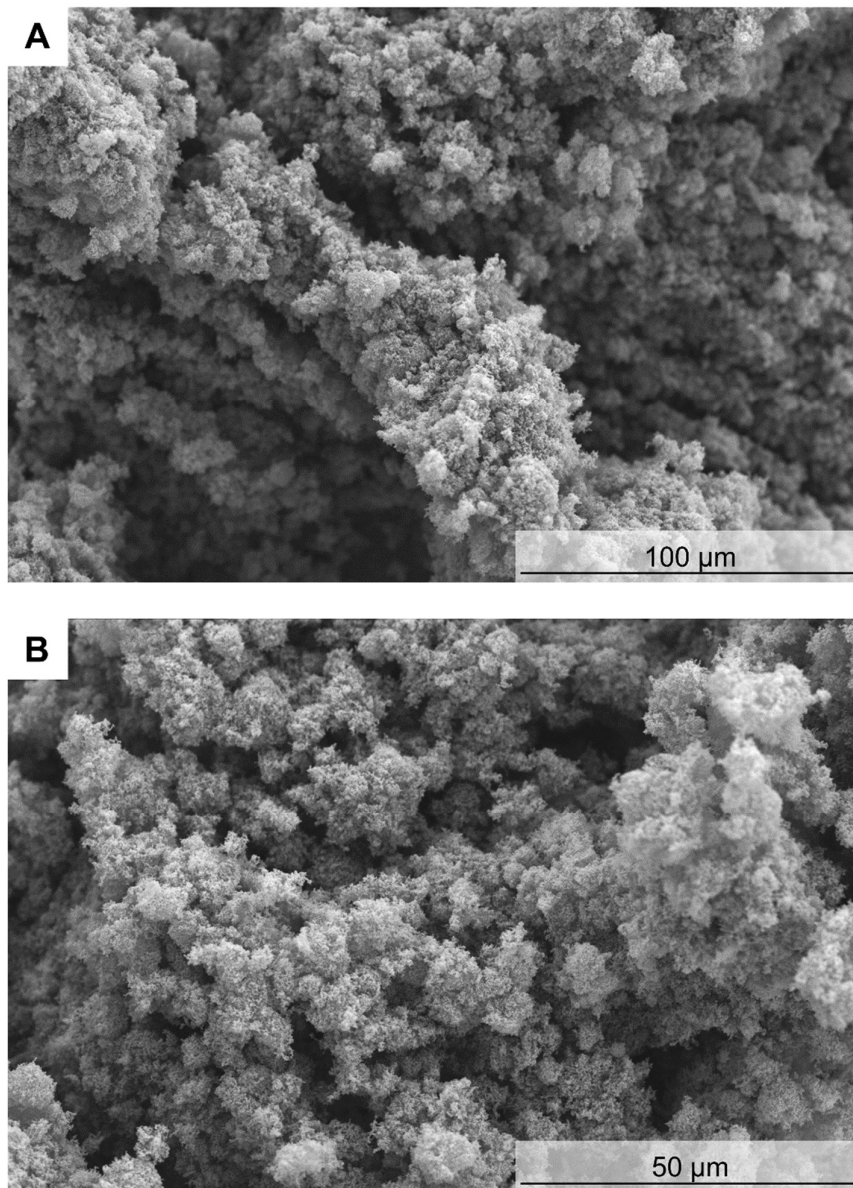


Figure 4-1. Black Carbon imaged by Scanning Electron Microscopy (SEM) at two magnifications (A+B). Dry Black Carbon (BC) power was imaged as BC alone did not bind to the 12-well plates used for the formation of bacterial biofilms. This meant that BC suspended in biofilm formation media could not be imaged by SEM, as it was washed away during processing.

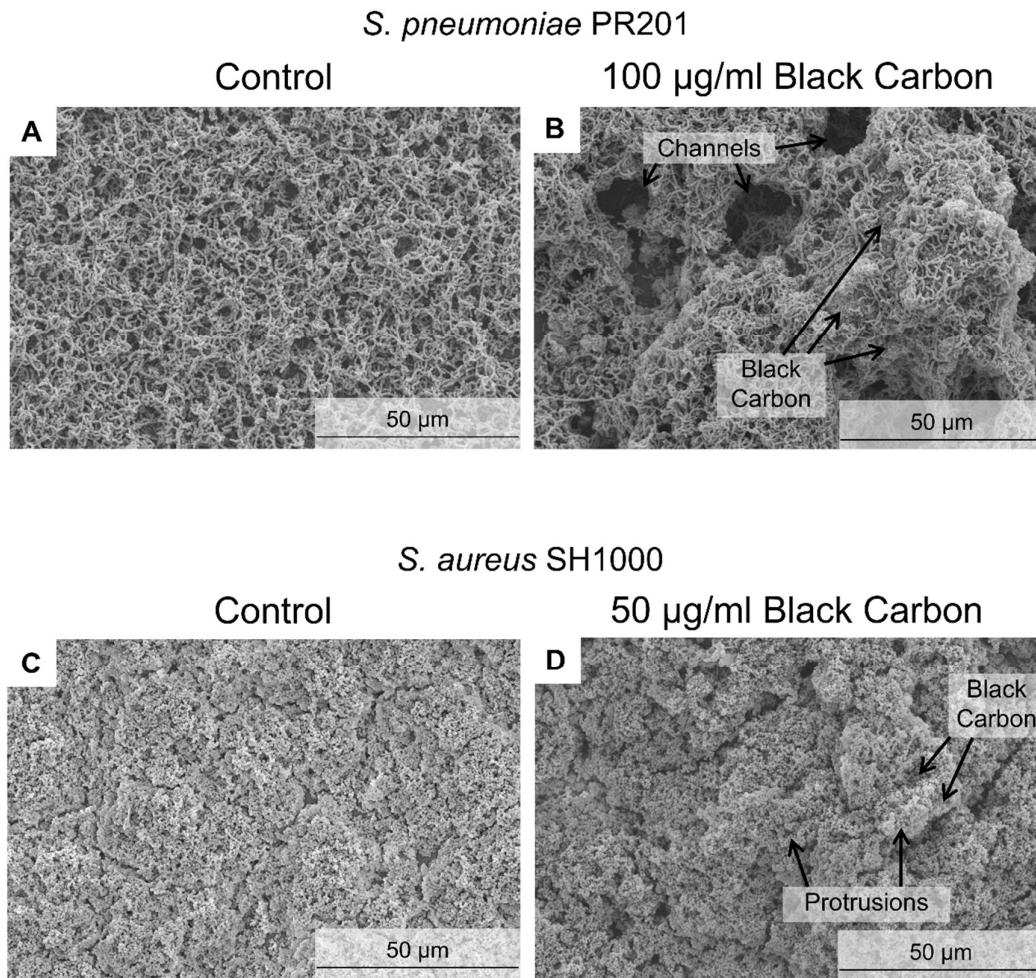


Figure 4-2. The effect of black carbon on bacterial biofilm architecture. *S. pneumoniae* PR201 (A, B) and *S. aureus* SH1000 (C, D) were allowed to form biofilms with (B+D) and without (A+C) black carbon, and imaged by Scanning Electron Microscopy. Biofilms of *S. pneumoniae* PR201 were formed in Brain-Heart Infusion (BHI), whereas biofilms of *S. aureus* SH1000 were formed in BHI supplemented with 4 % (w/v) NaCl. Images are representative of the entire biofilm structure. $n \geq 3$ biological repeats of each biofilm, processed for SEM separately.

From these findings, methodology was adapted to better preserve biofilms during processing. This modified method was based on the standard techniques already employed, but avoided dehydration of biofilm structures by directly imaging biofilms after washing and gold-coating (Section 2.5.1). This method appeared to better preserve both control and BC-formed biofilm structures, and the BC-induced modifications observed using standard SEM preparation methodologies were more evident when visualised with the adapted technique. Using this method, control biofilms of PR201 were observed to be flat structures (Figure 4-3 A,C,E). It is likely that this structure would limit environmental contact and therefore potential exposure to stressors. In contrast, BC caused a dramatic alteration in biofilm architecture, resulting in a complex honeycomb structure with large channels (Figure 4-3 B,D,F). Despite the alterations made to SEM preparation methodologies in order to preserve biofilm structures for visualisation, D39 biofilms were still degraded by processing and so could not be investigated.

Similarly to biofilms of PR201, control biofilms of *S. aureus* SH1000, Newman, and USA300 were flat structures limiting environmental contact (Figures 4-4 A,C,E, 4-5 A,C,E, and 4-6 A,C,E). BC was found to alter the biofilm structure of all *S. aureus* strains investigated, however a different affect was observed in comparison to the effect on *S. pneumoniae*. BC induced the development of BC-associated biofilm protrusions from the otherwise smooth surface of SH1000 (Figure 4-4 B,D,F), USA300 (Figure 4-5 B,D,F) and Newman (Figure 4-6 D,D,F) biofilms. However, these protrusions were more numerous and more evident in biofilms of SH1000 and USA300 in comparison to Newman biofilms. Therefore BC was found to have a striking and differential impact on biofilm architectures of all strains of *S. pneumoniae* and *S. aureus* tested. It is interesting that BC altered biofilm architecture of both *S. pneumoniae* PR201 and *S. aureus* USA300, as no effect on viability was observed in earlier assays using these strains (Section 3.4.3). It is worth noting that BC was observed to be incorporated into biofilms of all *S. pneumoniae* (Figure 4-3 B,D,F) and *S. aureus* (Figures 4-4, 4-5, and 4-6 B,D,F) strains assessed, but BC alone did not bind to the 12-well plates used for biofilm formatin assays. This indicated that the BC must have been incorporated into biofilms by these bacteria.

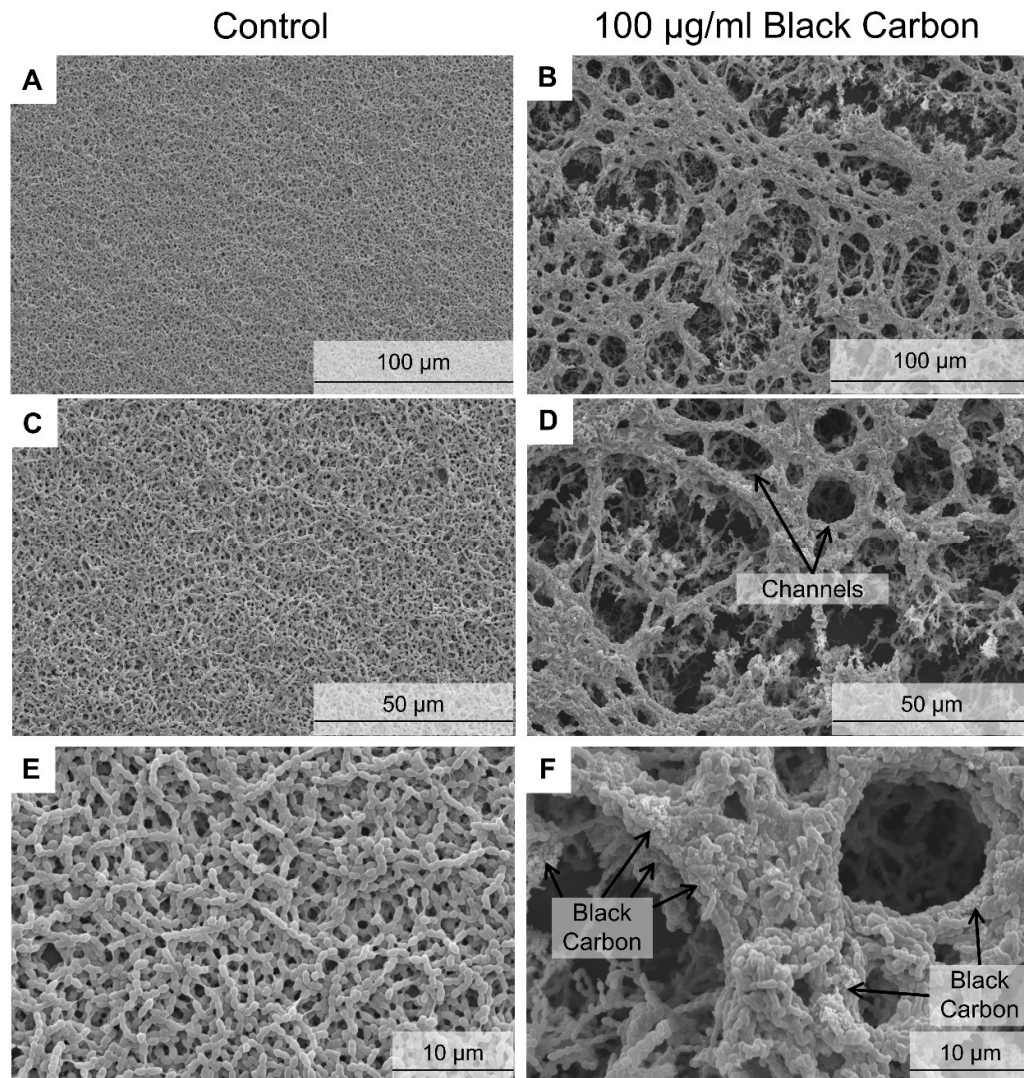


Figure 4-3. The effect of black carbon on *S. pneumoniae* PR201 biofilm architecture. *S. pneumoniae* PR201 was allowed to form biofilms with (B, D, F) and without (A, C, E) 100 µg/ml black carbon in Brain-Heart Infusion (BHI), and imaged by Scanning Electron Microscopy (SEM) at increasing magnifications (A+B, C+D, E+F). Images are representative of the entire biofilm structure. $n \geq 3$ biological repeats of each biofilm, processed for SEM separately.

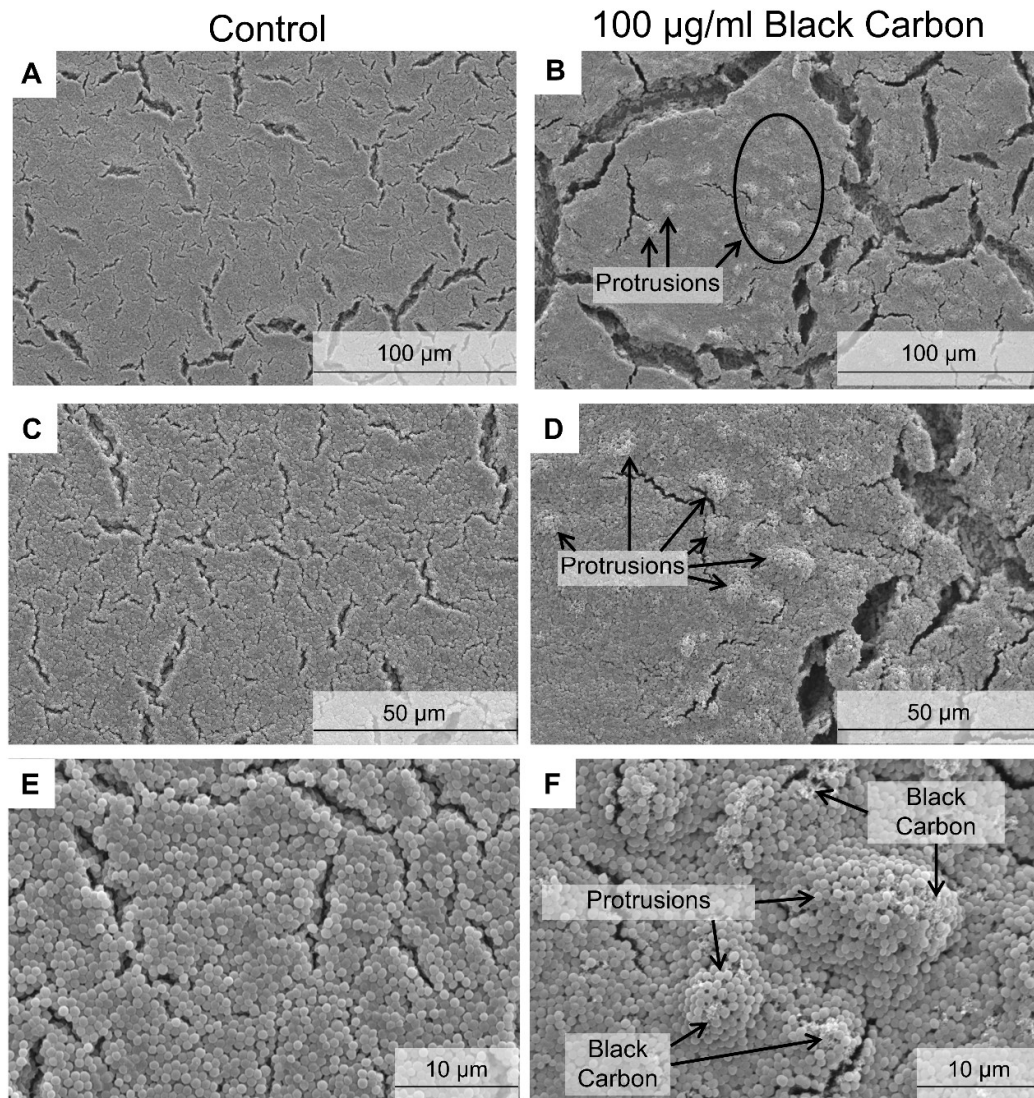


Figure 4-4. The effect of black carbon on *S. aureus* SH1000 biofilm architecture. *S. aureus* SH1000 was allowed to form biofilms with (B, D, F) and without (A, C, E) 100 µg/ml black carbon in Brain-Heart Infusion (BHI) supplemented with 4 % (w/v) NaCl, and imaged by scanning electron microscopy (SEM) at increasing magnifications (A+B, C+D, E+F). Images are representative of the entire biofilm structure. $n \geq 3$ biological repeats of each biofilm, processed for SEM separately.

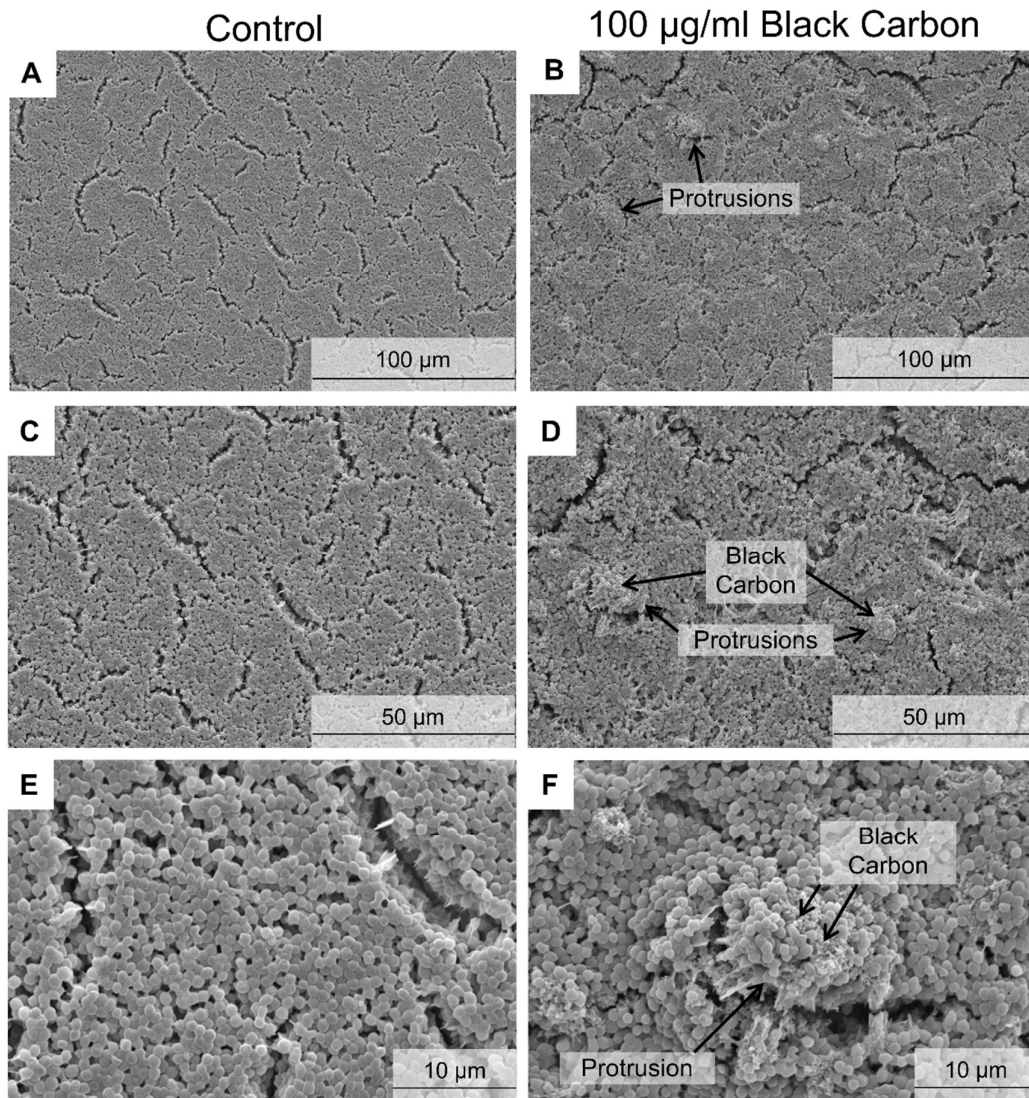


Figure 4-5. The effect of black carbon on *S. aureus* USA300 biofilm architecture. *S. aureus* USA300 was allowed to form biofilms with (B, D, E) and without (A, C, E) 100 µg/ml black carbon in Brain-Heart Infusion (BHI) supplemented with 1 % (w/v) glucose, and imaged by scanning electron microscopy (SEM) at increasing magnifications (A+B, C+D, E+F). Images are representative of the entire biofilm structure. $n \geq 3$ biological repeats of each biofilm, processed for SEM separately.

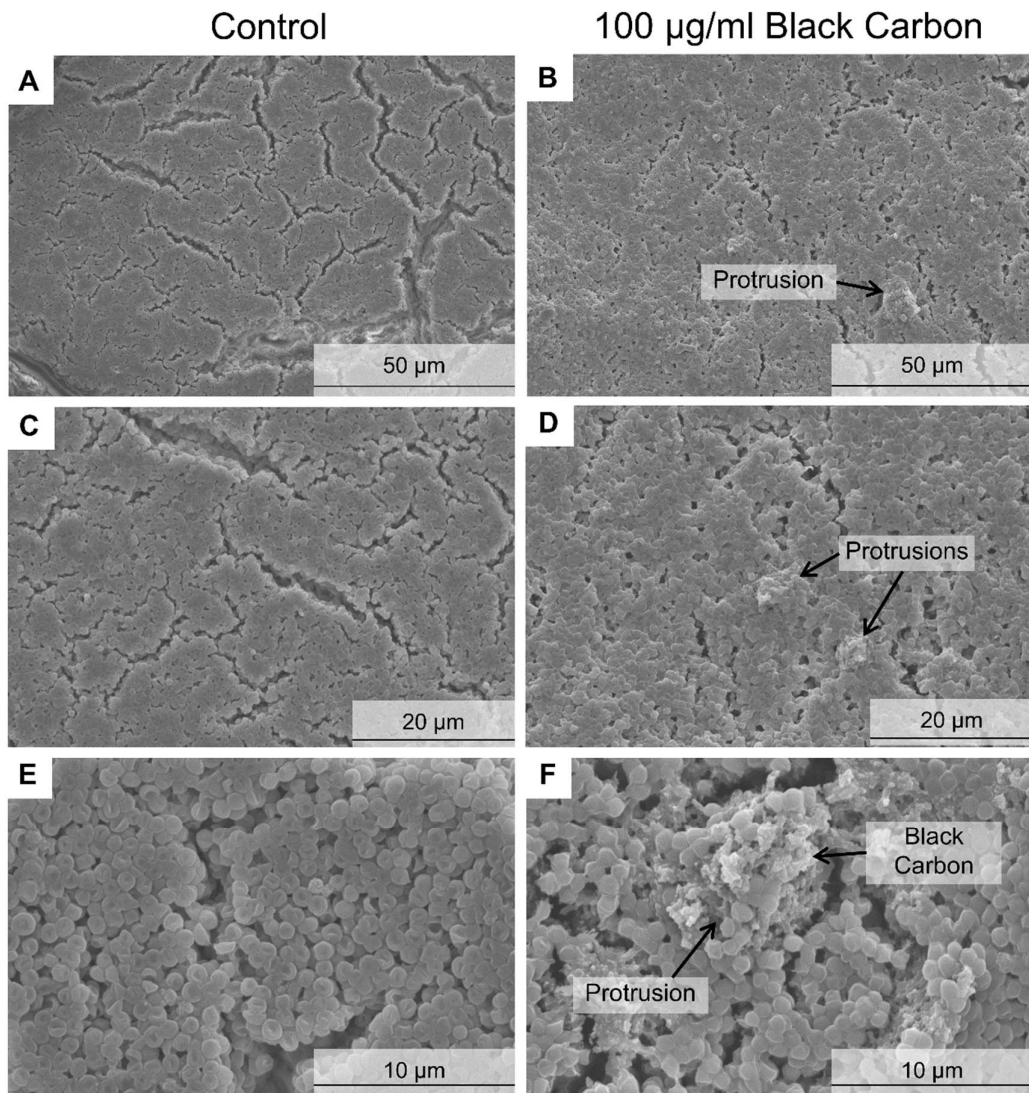


Figure 4-6. The effect of black carbon on *S. aureus* Newman biofilm architecture. *S. aureus* Newman was allowed to form biofilms with (B, D, F) and without (A, C, E) 100 µg/ml black carbon in Brain-Heart Infusion (BHI) supplemented with 1 % (w/v) glucose, and imaged by scanning electron microscopy (SEM) at increasing magnifications (A+B, C+D, E+F). Images are representative of the entire biofilm structure. $n \geq 3$ biological repeats of each biofilm, processed for SEM separately.

4.3. Further analysis of biofilm structural modifications

To further investigate BC induced changes in biofilm architecture, biofilm thickness was assessed and biofilms were visualised with Transmission Electron Microscopy (TEM). Both of these investigations required biofilms to be processed through fixative and ethanol into resin, polymerisation, and the cutting and staining of cross-sections (Section 2.5.2). These methods are extremely lengthy and time consuming, require the experimenter to be trained on specific machinery, and few samples can be processed at one time. Furthermore, accurate assessment of biofilm thickness by light microscopy is also a time consuming analysis. Unfortunately this meant that few strains could be assessed using these methods, and therefore strains PR201, SH1000, and Newman were chosen based on the previous observations of notable BC induced biofilm modifications.

4.3.1. BC increases biofilm thickness

To assess biofilm thickness, biofilms were grown on glass coverslips as for SEM, processed, and biofilm cross-sections were cut, stained, and imaged with light microscopy as described in Section 2.5.2. Control biofilms of PR201 (Figure 4-7 A), SH1000 (Figure 4-7 C), and Newman (Figure 4-7 E) were flat structures as observed in SEM analysis (Section 4.2). Interestingly, control biofilms of PR201 and Newman were observed to be a similar thickness. PR201 biofilms were $89 \pm 8.5 \mu\text{m}$ thick (Figure 4-7 G), and Newman biofilms were $92 \pm 11.8 \mu\text{m}$ thick (Figure 4-7 I). Surprisingly however, SH1000 control biofilms were much thinner, only $53 \pm 5.8 \mu\text{m}$ thick (Figure 4-7 H). Biofilms formed in the presence of BC were significantly (PR201 $p \leq 0.01$, Newman/SH1000 $p \leq 0.001$) thicker than their control counterparts for all strains assessed (Figure 4-7 B,D,F,G-I). PR201 biofilms increased in thickness by $25 \mu\text{m}$ to $114 \pm 35.7 \mu\text{m}$. BC altered Newman biofilm thickness to the greatest extent, increasing biofilms by $51 \mu\text{m}$ to $143 \pm 47.4 \mu\text{m}$ thick. SH1000 biofilm thickness was also increased by BC, but to a far lesser extent than Newman, by $8 \mu\text{m}$ to $61 \pm 5.9 \mu\text{m}$.

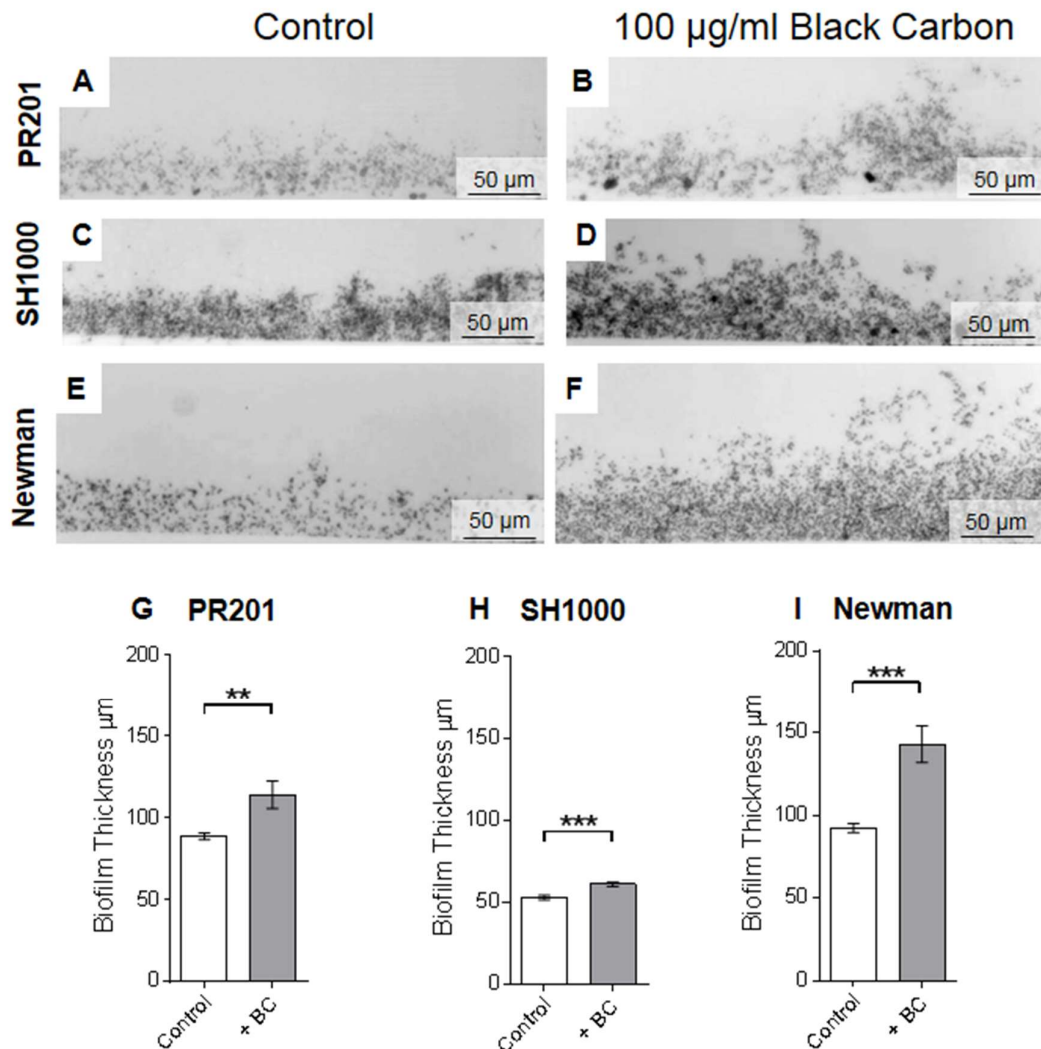


Figure 4-7. The effect of black carbon on biofilm thickness. *S. pneumoniae* PR201 (A, B, G), *S. aureus* SH1000 (C, D, H) and *S. aureus* Newman (E, F, I) were allowed to form biofilms with (B, D, F) and without (A, C, E) 100 µg/ml black carbon (BC). Biofilms were formed in Brain-Heart Infusion (BHI – PR201), BHI + 4 % (w/v) NaCl (SH1000), or BHI + 1 % (w/v) glucose (Newman). Biofilm cross-sections were then examined under light microscopy. Images are representative of the entire biofilm structure. $n \geq 3$ biological repeats of each biofilm were assessed. For measurements of biofilm thickness (G, H, I), 18 cross-sections were taken from each biofilm and were measured at 12 equally spaced points with light microscopy, $n=216$ measurements per sample. Measurements were performed blind so that the strain and whether biofilms were formed with or without BC was unknown. Error bars represent ± 1 SEM. T-tests were performed to determine significance, significant values are denoted with ** ($p \leq 0.01$) or *** ($p \leq 0.001$).

4.3.2. Association of bacteria with BC in biofilms

Due to the BC induced alterations in biofilm composition and architecture observed so far, the physical interactions between BC and biofilm cells were investigated by TEM as described in Section 2.5.2 (Glauert & Lewis 2014). Pneumococci were observed to be closely associated with BC particles in BC-formed biofilms (Figure 4-8 B), as was also observed in SEM analysis (Section 4.2). In contrast, *S. aureus* SH1000 and Newman bacteria displayed no association with, or clumping around, BC (Figure 4-8 D,F) TEM analysis also showed that BC had no impact on bacterial cell wall thickness. Therefore it appeared that BC closely associated with pneumococci in biofilms, but not with *S. aureus* bacteria.

4.4. Biofilm architectural modifications are not just due to the physical presence of BC particles

To assess whether observed effects of BC on biofilm formation were due to a biological response to BC, or simply due to the presence of exogenous particles acting as a scaffold, biofilm formation was investigated using an inert particle. For this investigation, quartz reference particles (DistriLab) with a similar size distribution (3500-350 nm) to BC were employed. Quartz is chemically stable and therefore does not react with most substances even at high temperatures. This made quartz a good proxy for BC as it is physically similar but chemically inert. Prior to this investigation, quartz was imaged by SEM to allow the identification of quartz within bacterial biofilms, and to demonstrate the structural similarities between quartz and BC. Figure 4-9 shows the appearance of quartz at increasing magnifications, which can be compared to BC imaged by SEM as displayed earlier in Figure 4-1. Dry quartz powder was imaged without processing, as quartz alone did not adhere to the 12-well plates used for biofilm formation assays (Section 2.4.2)

To investigate the effect of quartz on biofilm architecture, biofilms were investigated by SEM, with the substitution of quartz for BC. Pneumococcal strain PR201, and *S. aureus* strains SH1000, Newman, and USA300 were investigated. Biofilms formed

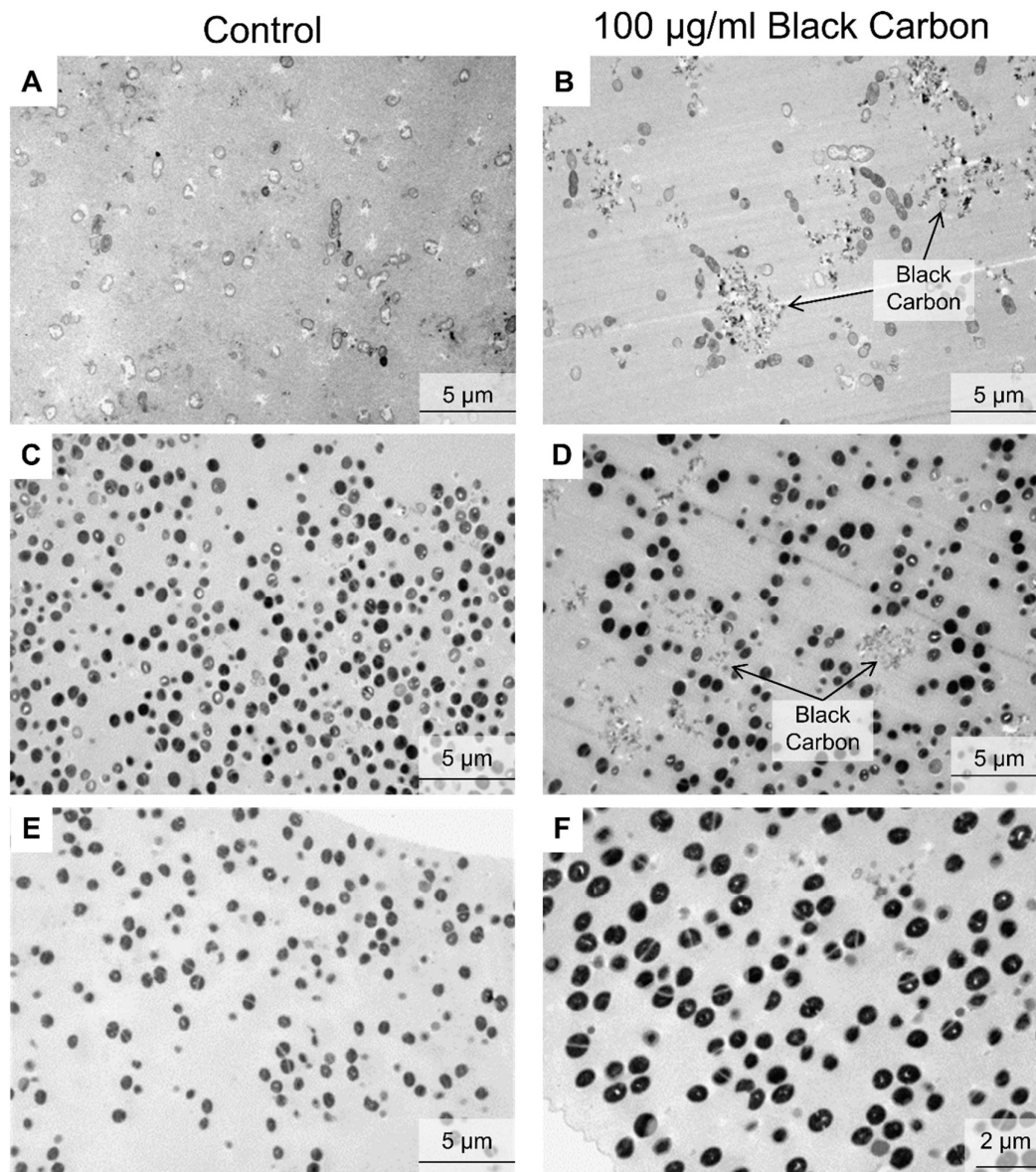


Figure 4-8. The association between black carbon and bacteria in biofilms. *S. pneumoniae* PR201 (A+B), *S. aureus* SH1000 (C+D) and Newman (E+F) were allowed to form biofilms with (B, D, F) or without (A, C, E) 100 µg/ml black carbon, and imaged by transmission electron microscopy (TEM). Biofilms were formed in Brain-Heart Infusion (BHI – PR201), BHI + 4 % (w/v) NaCl (SH1000), or BHI + 1 % (w/v) glucose (Newman). Images are representative of the entire biofilm structure. $n \geq 3$ biological repeats of each biofilm were assessed.

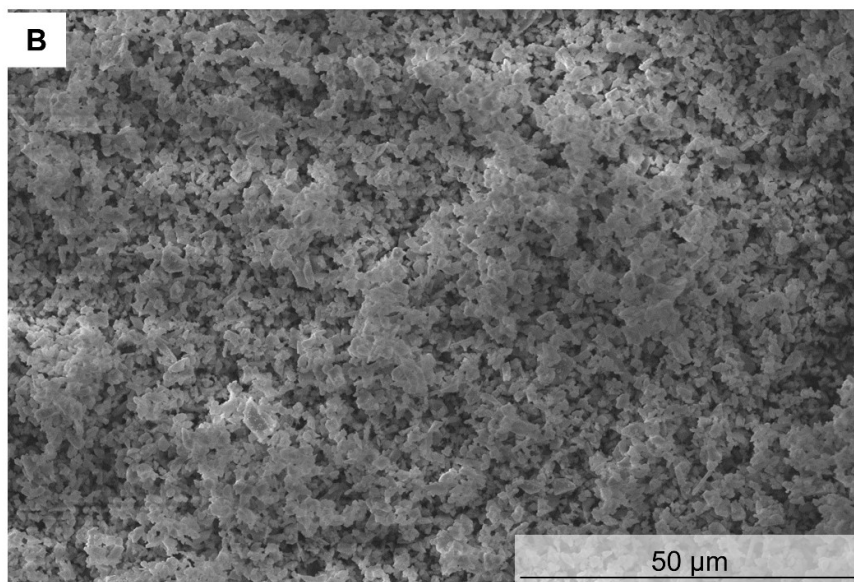
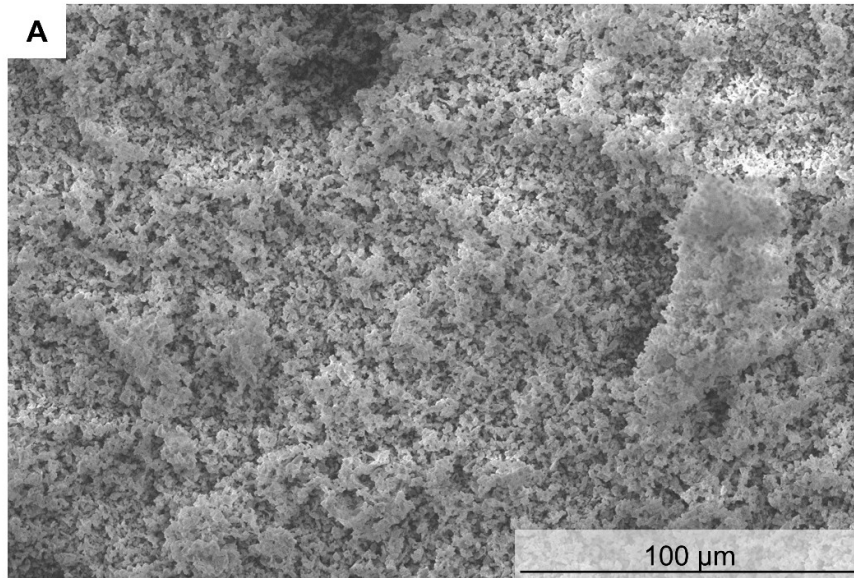


Figure 4-9. Quartz imaged by Scanning Electron Microscopy at two magnifications (A+B)

with quartz were found to be identical in their architecture to their control counterparts. All BC-induced structural modifications, such as protrusions and channels, were absent for all strains of *S. pneumoniae* and *S. aureus* tested. These results are exemplified in Figure 4-10 with *S. aureus* SH1000 and *S. pneumoniae* PR201. This figure shows biofilms formed in the presence quartz (Figure 4-10 C,D) compared to control biofilms (Figure 4-10 A,B), and biofilms formed in the presence of BC (Figure 4-10 E,F). Biofilms formed with 30 µg/ml quartz are shown as during SEM analysis of biofilms formed with higher quartz concentrations, excessive accumulation of electric charging occurred, interfering with imaging. Biofilms formed with the same concentration of BC show that BC-induced architectural modifications were observed at this particle concentration. Both control biofilms (Figure 4-10 A,B) and biofilms formed with quartz (Figure 4-10 C,D) appear identical for both strains, both are flat structures with no protrusions or channels present. In the BC biofilms, a honeycomb architecture with channels is evident for *S. pneumoniae* PR201 (Figure 4-10 E), and BC-associated protrusions are visible for *S. aureus* SH1000 (Figure 4-10 F). These results indicate that the effects of BC on biofilm architecture were not simply due to the presence of particles, but are a biological response to BC.

4.5. Biofilm alterations are observed within two hours of attachment

It was decided to investigate if the effects of BC on biofilm formation were observed within the first two hours of attachment, or solely with mature biofilms. Biofilms were formed in the presence of BC as previously described (Section 2.4.2), and bacterial viability was assessed after 2 hours incubation rather than 24 hours. Control biofilms without BC were also included. In Figure 4-11, total CFU per fraction refers to the total amount of viable attached, loosely adherent, and planktonic bacteria recovered from each well, therefore the sum of these fractions gives the total bacterial viability of the entire well.

Pneumococcal strains D39 and PR201 were chosen for this investigation as although BC was not found to alter biofilm viability of these strains at 24 hours (Section 3.4.3),

BC-formed biofilms of PR201 displayed the most prominent architectural features (Section 4.2). In addition, *S. aureus* SH1000 and Newman were included as BC exposure induced alterations in biofilm structure (Section 4.2) and mature biofilm viability (Section 3.4.3) for these strains, and USA300 was used for comparative purposes as BC had been found to induce architectural changes (Section 4.2) but not affect mature biofilm viability of this strain (Section 3.4.3).

BC had no effect on total bacterial viability or the amount of attached bacteria of *S. pneumoniae* strains PR201 or D39 after 2 hours (Figure 4-11 A,B). These data agree with mature biofilms, which were also unaffected by BC at 24 hours (Section 3.4.3). In contrast, BC significantly reduced the amount of attached bacteria of *S. aureus* strains SH1000 (50/100 $\mu\text{g/ml}$ BC - $p \leq 0.01$) and Newman (30/50/100 $\mu\text{g/ml}$ BC - $p \leq 0.0001$, Figure 4-11 C,D). These results correlate with the effect of BC on the development of mature biofilms, as these were the only strains which displayed a significant reduction in viability of biofilm bacteria at 24 hours (Section 3.4.3. $p \leq 0.05$). Furthermore, BC exposure was associated with a significant reduction in total bacterial viability of *S. aureus* strain Newman (30/50/100 $\mu\text{g/ml}$ BC - $p \leq 0.0001$) in comparison to control biofilms (Figure 4-11 D). Interestingly, Newman also displayed a significant reduction in total bacterial viability at 24 hours (Section 3.4.3. 100 $\mu\text{g/ml}$ BC - $p \leq 0.05$). These results therefore indicate that effects of BC on biofilm development are observed after just 2 hours. However there is some variation as SH1000 also showed a significant reduction in total viability with BC exposure at 24 hours (Section 3.4.3. $p \leq 0.05$), but not after 2 hours (Figure 4-11 C). No BC-related effect was observed with *S. aureus* USA300 (Figure 4-11 E), and similarly no significant effect had been observed at 24 hours (Section 3.4.3). These results reinforce the conclusion that the effects of BC on biofilm formation are strain specific, and reveal that the BC induced alterations in biofilm formation are initiated within the first 2 hours of attachment.

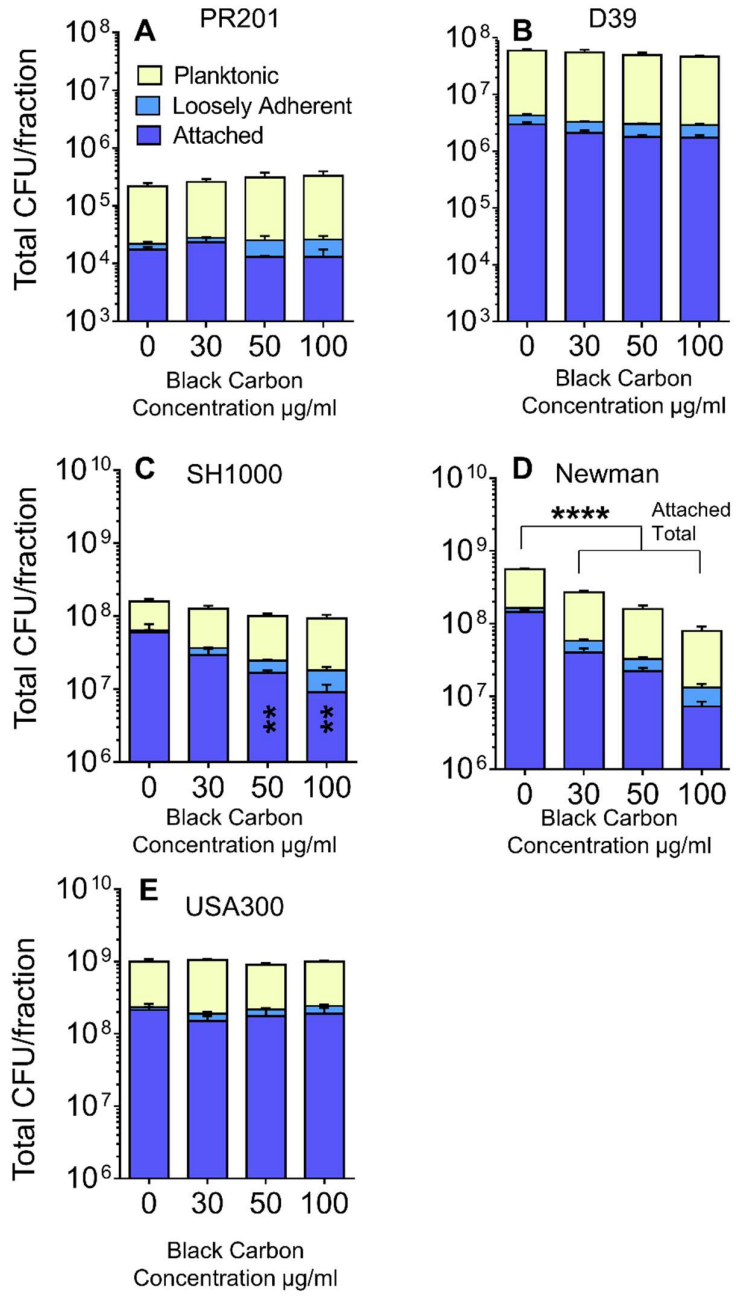


Figure 4-11. The effect of BC on bacterial attachment to a surface. *S. pneumoniae* PR201 (A) and D39 (B), and *S. aureus* SH1000 (C), Newman (D), and USA300 (E) were cultured with or without 30-100 µg/ml black carbon under biofilm formation conditions for 2 hours. Viable bacterial cells were then measured by sequential removal and quantification of planktonic, loosely- adhered, and biofilm bacteria. Total CFU/fraction refers to the total amount of viable biofilm, loosely adherent, and planktonic bacteria recovered from each biofilm and the surrounding growth medium. n=4. Error bars represent +1 SEM. Two-way ANOVA with Tukey’s multiple comparisons test were used to determine significance, significant results compared to the control condition are denoted with ** (p≤0.01) or **** (p≤0.0001)

4.6. BC does not alter the protein expression profile of biofilm cells

To identify if the BC-induced biofilm alterations observed were associated with any substantial protein changes, the protein profile of biofilm cells was assessed. Biofilms were formed in the presence of BC, then planktonic and loosely adherent cells were discarded, and protein extractions were performed on biofilm cells (Section 2.6). Control biofilms without BC were also included. The protein profile of control vs BC-formed biofilms was then visualised using 1D SDS-PAGE. Unfortunately, protein extraction protocols which separately assess secreted proteins, non-covalently bound proteins, cell wall proteins, and membrane and cytoplasmic proteins could not be used as BC was found to persist in samples throughout processing causing problems in running SDS-PAGE gels. Therefore total protein extracts were performed using FastProtein Blue Matrix Kits. All *S. aureus* strains used in biofilm assays were investigated (SH1000, Newman, USA300, PB3-32-1, 2.20, and PB9) as well as *S. pneumoniae* strain PR201. No identifiable differences were observed in the protein profiles of biofilms formed under control conditions and biofilms formed in the presence of BC (Figure 4-12) for any strain.

4.7. The biofilm extracellular matrix

BC has been found to significantly alter biofilm formation and architecture of *S. pneumoniae* and *S. aureus*. This section aimed to determine whether these phenotypes were also associated with alterations in the biofilm extracellular matrix. A variety of different factors are involved in the production of the extracellular matrix, which is largely species-, strain-, and environment-dependent, and may be comprised of protein, polysaccharide, and DNA (Foster *et al.* 2014; Domenech *et al.* 2012; Flemming & Wingender 2010; Rice *et al.* 2007; Cucarella *et al.* 2001; Cramton *et al.* 1999). For this investigation, two major extracellular components, DNA and protein, were assessed. Initial investigations also attempted to elucidate the contribution of polysaccharide to the matrix, however these were unsuccessful and are discussed in regard to future work (Section 4.9.5). For these investigations, biofilms were formed in the presence of

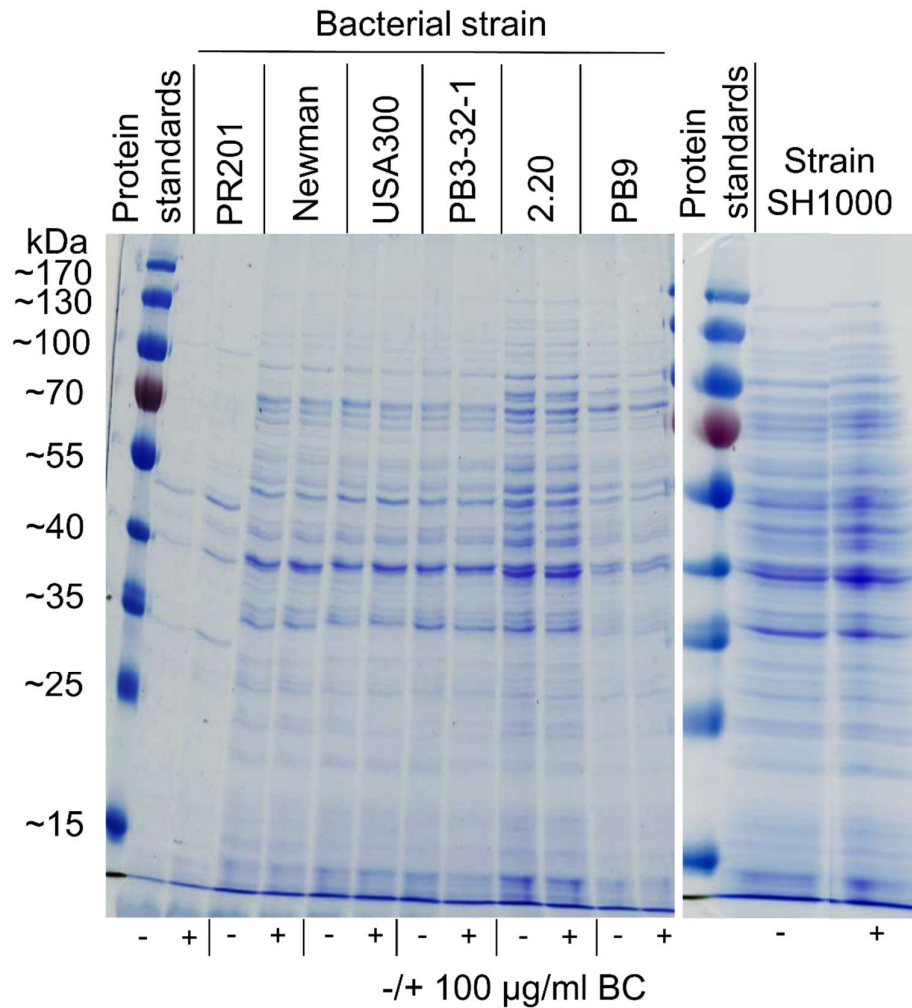


Figure 4-12. BC had no detectable effect on the protein profile of biofilm bacteria. 1D SDS-PAGE of whole cell protein extracts of biofilms formed in the presence or absence of 100 µg/ml black carbon (BC) at 37 °C in 5 % (v/v) CO₂. The PageRuler Prestained Protein Ladder (Fermentas) was used to provide protein standards, displayed alongside the gels. *S. pneumoniae* strain PR201, and *S. aureus* strains Newman, USA300, PB3-32-1, 2.20, PB9, and SH1000 were investigated.

100 µg/ml BC, planktonic and loosely adherent bacteria were removed, and biofilms were incubated with either DNaseI (Nicholson *et al.* 2013; Hall-Stoodley *et al.* 2008) or proteinase K (Nicholson *et al.* 2013; Gilan & Sivan 2013; Kogan *et al.* 2006) in order to degrade the DNA or protein components of matrices, respectively (Section 2.4.3). These degradation assays are commonly used to assess the contribution of DNA and protein to the biofilm matrix (Nicholson *et al.* 2013; Kulkarni *et al.* 2012; Hall-Stoodley *et al.* 2008; Kogan *et al.* 2006; Moscoso *et al.* 2006). After incubation, planktonic and loosely adherent bacteria were again removed and discarded, and the remaining biofilm bacteria were quantified to determine the level of biofilm degradation. Control biofilms without BC were also included. D39 biofilms did not survive processing for this method, so data are not available for this strain.

4.7.1. BC does not alter biofilm degradation by DNaseI

eDNA is reported to be a major component of the pneumococcal biofilm matrix (Domenech *et al.* 2012; Carrolo *et al.* 2010; Moscoso *et al.* 2009; Hall-Stoodley *et al.* 2008; Moscoso *et al.* 2006). Therefore it was surprising that control biofilms of *S. pneumoniae* PR201 were not significantly ($p>0.05$) affected by incubation with DNaseI (Figure 4-13 A). Similarly, DNaseI had no effect ($p>0.05$) on PR201 biofilms formed in the presence of BC (Figure 4-13 A). eDNA is also reported to be important in the formation of staphylococcal biofilms (Savage *et al.* 2013; Archer *et al.* 2011) and accordingly, SH1000 biofilms were significantly degraded by DNaseI in both the control and BC-formed conditions (Figure 4-13 B, $p\leq 0.05$). These results indicate that DNA is a major component of the extracellular matrix of this strain. However, there was no significant difference ($p>0.05$) between DNaseI degradation of control and BC-biofilms (Appendix 15), indicating that BC does not alter the contribution of eDNA to the matrix. In contrast, DNaseI was found to have no significant effect ($p>0.05$) on the control or BC-biofilms of *S. aureus* strains Newman (Figure 4-13 C) or USA300 (Figure 4-13 D). These results show that there was no difference in the degradation of biofilms formed with or without BC by DNaseI.

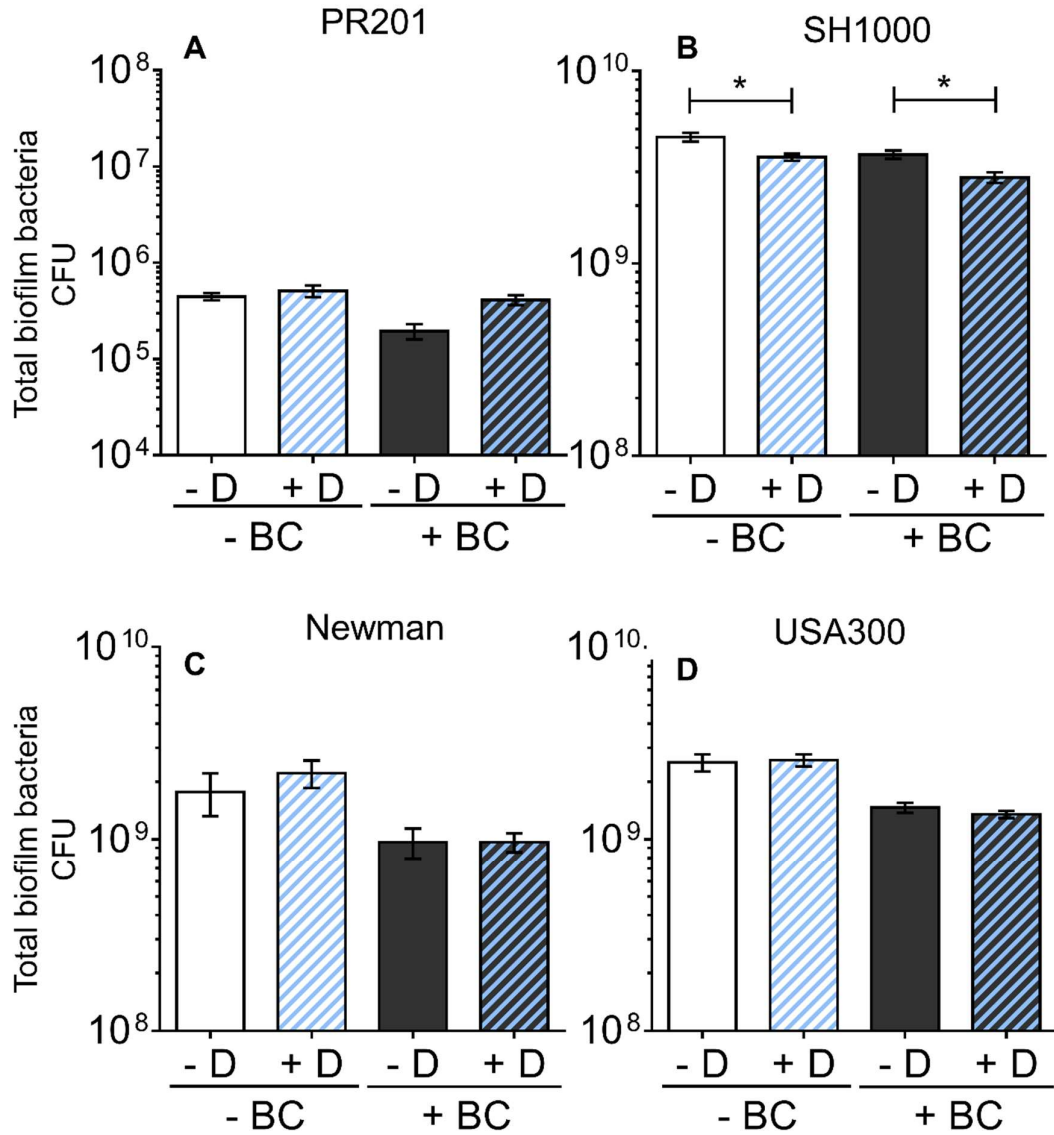


Figure 4-13. The effect of black carbon on biofilm matrix DNA. *S. pneumoniae* PR201 (A), *S. aureus* SH1000 (B), Newman (C), and USA300 (D) were allowed to form biofilms in the presence (black) or absence (white) of 100 $\mu\text{g/ml}$ black carbon (BC) for 24 hours. Biofilms were formed in Brain-Heart Infusion (BHI – PR201), BHI + 4 % (w/v) NaCl (SH1000), or BHI + 1 % (w/v) glucose (Newman and USA300). Planktonic and loosely-adherent bacteria were then removed, and biofilms were exposed to 140 U/ml DNaseI (D) for 2 hours (blue stripes). Separate biofilms were incubated in the same base solution but without DNaseI for comparison (no stripes). After incubation, planktonic and loosely adherent bacteria were removed and discarded, and the remaining biofilm bacteria were quantified. Total biofilm bacteria (CFU) refers to the total amount of biofilm bacteria recovered. n=3. Error bars represent ± 1 SEM. T-tests were used to determine significance, significant results are denoted with * (p ≤ 0.05).

4.7.2. BC alters biofilm degradation by proteinase K

Although protein is reported to be a major component of the pneumococcal biofilm matrix (Domenech *et al.* 2012; Carolo *et al.* 2010; Moscoso *et al.* 2009; Hall-Stoodley *et al.* 2008; Moscoso *et al.* 2006), control biofilms of *S. pneumoniae* PR201 were not significantly ($p>0.05$) affected by incubation with proteinase K (Figure 4-14 A).

Interestingly however, biofilms formed in the presence of 100 $\mu\text{g/ml}$ BC were significantly disrupted by proteinase K (Figure 4-14 A, $p\leq 0.01$). These results suggest that BC induces changes in the construction of the extracellular matrix of PR201, resulting in a more proteinaceous structure. Similarly, *S. aureus* strain SH1000 control biofilms were not significantly degraded ($p>0.05$) by proteinase K (Figure 4-14 B), but SH1000 BC-biofilms were significantly degraded ($p\leq 0.01$). In contrast, control biofilms of *S. aureus* Newman and USA300 biofilms were significantly disrupted by the addition of proteinase K (Figure 4-14 C,D; $p\leq 0.01$) indicating a major role of protein in the extracellular matrices of these strains, but proteinase K no longer had a significant effect on biofilms of either strain formed in the presence of BC ($p>0.05$, Figure 4-14 C,D). These results show that biofilms formed in the presence of BC had an altered resistance to proteinase K degradation, implying that BC altered the protein content of the biofilm matrix.

4.8. Biofilms formed in the presence of BC display an altered tolerance to antibiotics

A major advantage of biofilm formation is the increased protection provided against stressors such as antibiotics, as discussed before in Section 1.10 (Chao *et al.* 2015; De la Fuente-Nunez *et al.* 2013; Lewis 2008; Donlan & Costerton 2002; Costerton *et al.* 1999). Therefore this section investigated whether BC-induced biofilm changes were paralleled by alterations in antibiotic tolerance. Biofilms were formed in the presence of 100 $\mu\text{g/ml}$ BC, and planktonic and loosely adherent bacteria were removed. Biofilms were then incubated with an appropriate antibiotic for 3 hours. After incubation, planktonic and loosely adherent bacteria were removed and discarded, and remaining viable biofilm bacteria were quantified to determine bacterial survival (Section 2.4.4).

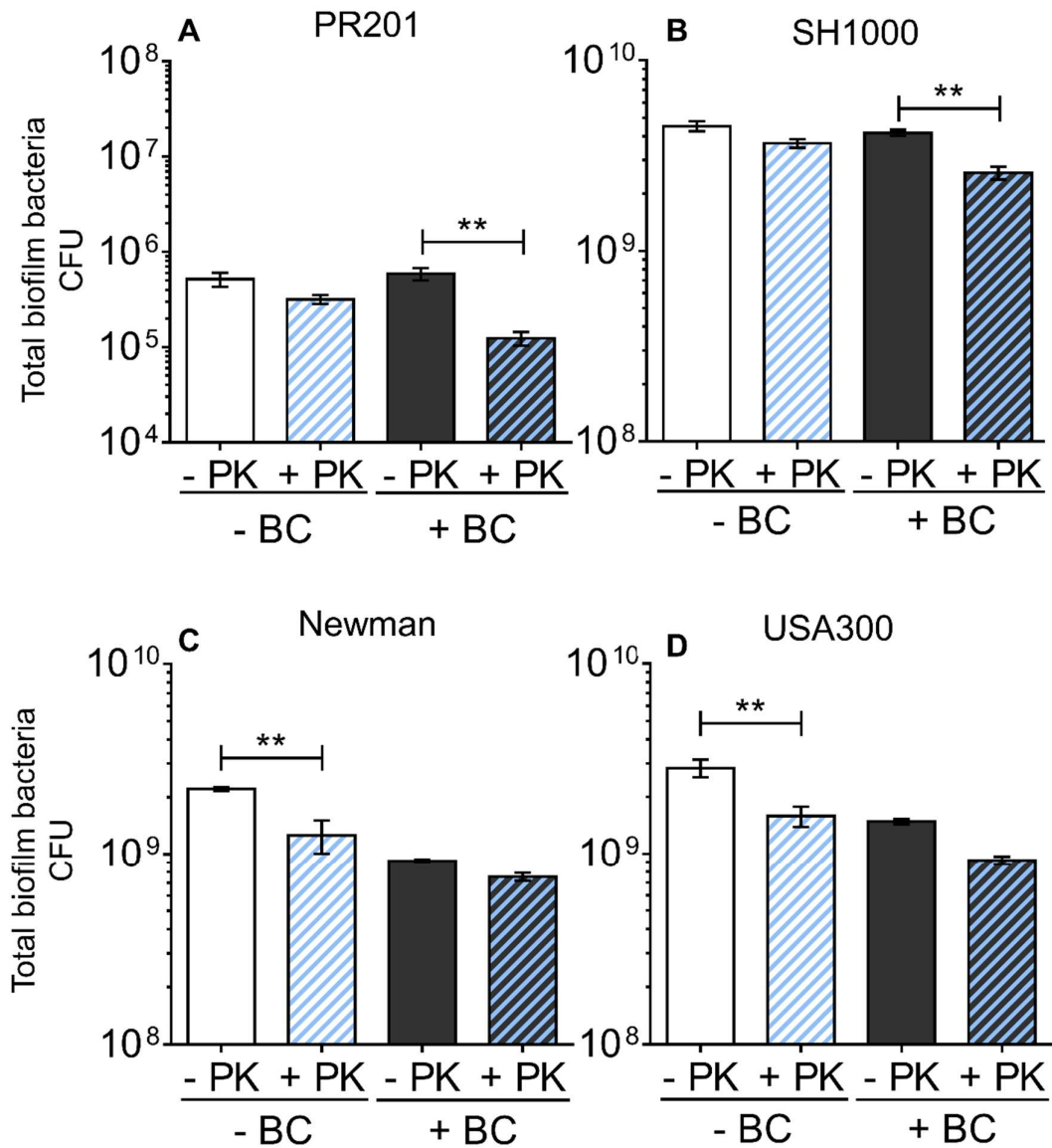


Figure 4-14. The effect of black carbon on biofilm matrix protein. *S. pneumoniae* PR201 (A), *S. aureus* SH1000 (B), Newman (C), and USA300 (D) were allowed to form biofilms in the presence (black) or absence (white) of 100 $\mu\text{g/ml}$ black carbon (BC) for 24 hours. Biofilms were formed in Brain-Heart Infusion (BHI – PR201), BHI + 4 % (w/v) NaCl (SH1000), or BHI + 1 % (w/v) glucose (Newman and USA300). Planktonic and loosely-adherent bacteria were then removed, and biofilms were exposed to 100 $\mu\text{g/ml}$ proteinase K (PK) for 2 hours (blue stripes). Separate biofilms were incubated in the same base solution but without proteinase K for comparison (no stripes). After incubation, planktonic and loosely adherent bacteria were removed and discarded, and the remaining biofilm bacteria were quantified. Total biofilm bacteria (CFU) refers to the total amount of biofilm bacteria recovered. $n=3$. Error bars represent ± 1 SEM. T-tests were used to determine significance, significant results are denoted with ** ($p \leq 0.01$).

Control biofilms without BC were also included. Gentamicin was the antibiotic used against pneumococci as gentamicin is effective against planktonic pneumococci, but does not effectively penetrate into pneumococcal biofilms (Chao *et al.* 2015; Marks *et al.* 2012a; Bartoszewicz *et al.* 2007; Abdi-Ali *et al.* 2006; Carmen *et al.* 2004).

Oxacillin was used as the antibiotic against *S. aureus* as it is a clinically relevant antibiotic but poorly penetrates biofilms of *S. aureus* (Singh *et al.* 2010). Due to their poor biofilm penetration, these antibiotics are therefore useful discriminators of biofilm organisation.

For this investigation, *S. pneumoniae* D39 and *S. aureus* strains SH1000, Newman, and USA300 were used. The architecture of pneumococcal strain PR201 was strongly altered by BC (Section 4.2), and so penetration of antibiotics may have been affected. However during optimisation to determine the gentamicin concentration to use in this experiment, all concentrations tested (5 µg/ml - 1 mg/ml) resulted in complete destruction of PR201 biofilms and no viable bacteria survived (data not shown). Therefore D39 was substituted. SH1000, Newman, and USA300 were included as being the strains most affected by BC, and for comparison between these strains.

Interestingly, all BC-formed biofilms showed a different antibiotic tolerance to their control counterparts. Control biofilms of D39 were significantly susceptible to gentamicin treatment, however biofilms formed in the presence of BC were not (Figure 4-15A). Similarly, control biofilms of SH1000 were more degraded by oxacillin than BC-biofilms (Figure 4-15 B). The opposite effect was observed for *S. aureus* strains Newman and USA300, in that BC-formed biofilms of these strains were more susceptible to oxacillin than control biofilms (Figure 4-15 C and D). In fact, Newman BC-biofilms were totally eradicated by antibiotic treatment. Appendix 16 displays the percentage survival of biofilms so that direct comparisons can be made between the effectiveness of antibiotic treatment of control and BC biofilms. This data shows that there was no significant difference ($p > 0.05$) between survival of D39 bacteria in control and BC-biofilms after antibiotic treatment. Interestingly however, BC-biofilms of SH1000 were significantly ($p \leq 0.01$) more tolerant of oxacillin than controls, and BC-biofilms of Newman and USA300 were significantly more susceptible to oxacillin than controls (Newman $p \leq 0.01$, USA300 - $p \leq 0.05$).

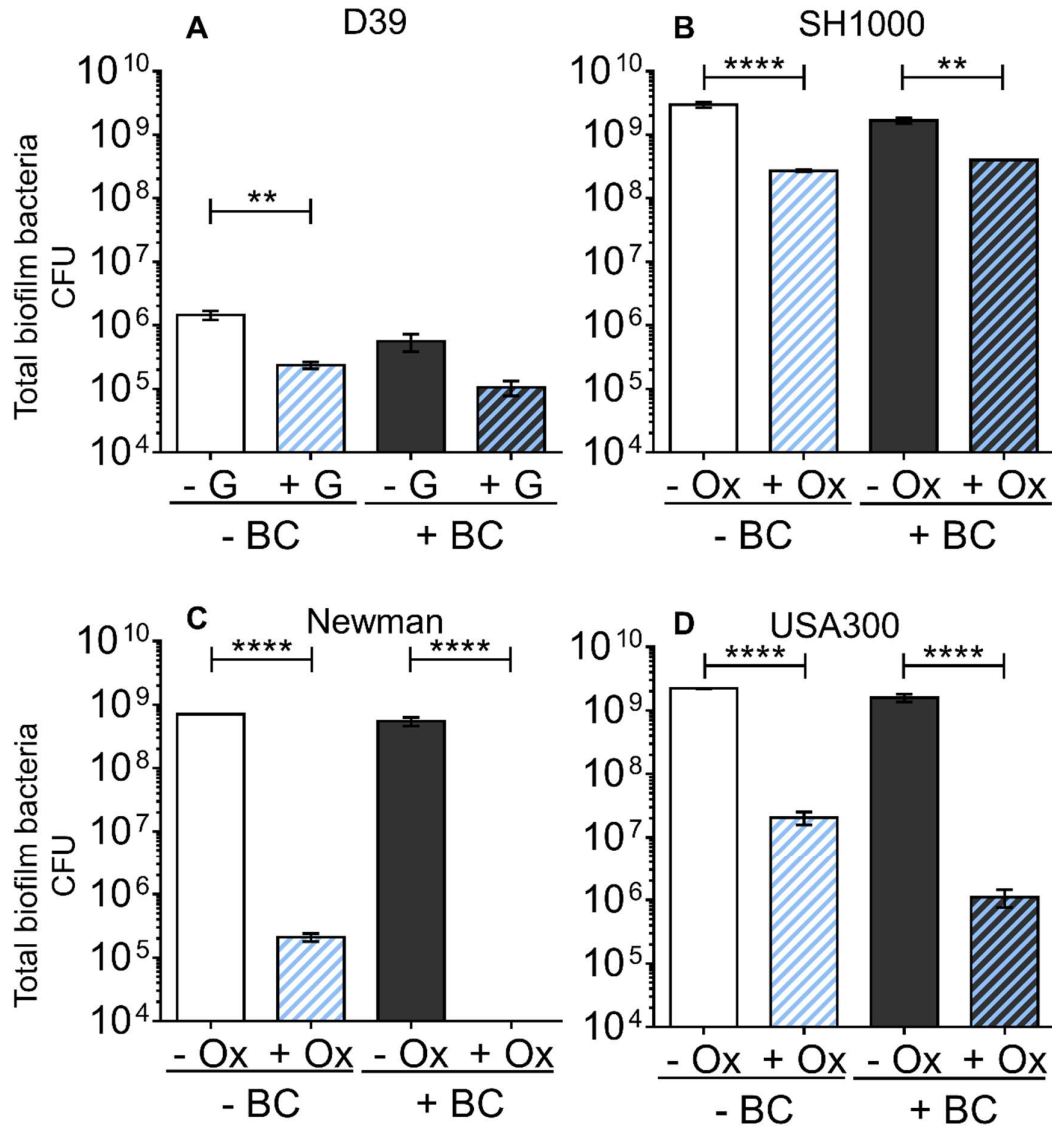


Figure 4-15. Antibiotic tolerance of control and BC-formed biofilms. *S. pneumoniae* D39 (A) and *S. aureus* SH1000 (B), Newman (C) and USA300 (D) were allowed to form biofilms in the presence (black) or absence (white) of 100 μ g/ml BC for 24 hours. Biofilms were formed in Todd-Hewitt Broth supplemented with 0.5 % (w/v) yeast extract (THY – D39), Brain-Heart Infusion (BHI) + 4 % (w/v) NaCl (SH1000), or BHI + 1 % (w/v) glucose (Newman and USA300). Planktonic and loosely-adherent bacteria were then removed, and biofilms were exposed to either 50 mg/ml oxacillin (Ox) in 2 % (w/v) NaCl or 500 μ g/ml gentamicin (G) for 3 hours (blue stripes). Separate biofilms were incubated with the same medium but without antibiotics for comparison. After incubation, planktonic and loosely adherent bacteria were removed and discarded, and the remaining biofilm bacteria were quantified. Total biofilm bacteria (CFU) refers to the total amount of biofilm bacteria recovered. n=3. Error bars represent \pm 1 SEM. T-tests were used to determine significance; significant results are denoted with ** ($p \leq 0.01$) or **** ($p \leq 0.0001$).

4.9. Discussion

This chapter reports further investigations into the effect of BC on biofilms by assessing biofilm architecture and structure, potential mechanisms of BC-induced effects, matrix composition, and biofilm functioning. All strains of *S. pneumoniae* and *S. aureus* evaluated displayed clear signs of biofilm modulation in response to BC.

4.9.1. BC alters pneumococcal biofilm structures

To visualise biofilms by electron microscopy in this project, biofilms were formed on glass coverslips (Section 2.5.1). Past research has reported that pneumococci form poor biofilms on glass substrates, which has been suggested to be due to glass providing a less ample support for biofilm formation in comparison to biotic surfaces (Chao *et al.* 2015; Marks *et al.* 2012a; Sanchez *et al.* 2011). Interestingly however, control biofilms of PR201 were thick flat structures, showing larger and more complex biofilms than reported in these past investigations (Chao *et al.* 2015; Marks *et al.* 2012a). It is possible that the enhanced biofilm formation observed in this project is due to the adapted preparation methodology employed to avoid dehydration of biofilm structures (Section 2.5.1). Alternatively, this may be due to the use of unencapsulated pneumococci, which are known to be better than encapsulated strains at forming biofilms *in vitro* (Chao *et al.* 2015; Domenech *et al.* 2012; Moscoso *et al.* 2009).

The most dramatic difference between control PR201 biofilms and those formed in the presence of BC was the development of a honeycomb structure with water channels, which is an architecture associated with *in vivo* biofilms formed during nasopharyngeal colonisation (Marks *et al.* 2012a). In fact, this structure has only ever been previously reported to be reproduced *in vitro* on surfaces coated with epithelial cells (Marks *et al.* 2012a). These data are the first to show the development of pneumococcal biofilm honeycomb structures on an abiotic surface. Therefore in this project, BC appeared to cause a drastic modulation of PR201 biofilm formation, causing abiotic *in vitro* biofilms to emulate the structure of nasopharyngeal biofilms. Interestingly, pneumococci were observed to tightly associate with BC particles, which appeared to be incorporated into this honeycomb structure.

Furthermore, PR201 biofilms formed in the presence of BC were significantly ($p \leq 0.01$) thicker than their control counterparts. This was surprising as the total number of bacteria within control and BC-biofilms were not found to be significantly different in Chapter 3. These results therefore indicate that the increase in biofilm thickness was not caused by an increase in viable bacteria, but instead may be due to the presence of more non-viable bacteria, an increase in matrix production, and/or due to the induction of the honeycomb architecture observed. Additionally, no variation in the amount of viable biofilm or loosely adherent bacteria was identified in Chapter 3 (Section 3.4.3), indicating that the structural stability of the PR201 biofilms were not compromised by the increased thickness in these conditions.

Biofilms are vital for pneumococcal colonisation of the respiratory tract, and colonisation is a necessary step before disease may occur (Gilley & Orihuela 2014; Blanchette-cain *et al.* 2013; Marks *et al.* 2012a; Domenech *et al.* 2012; Sanchez *et al.* 2011; Munoz-Elias *et al.* 2008). Biofilms are also key in infection as they provide protection from the immune system and may act as a bacterial reservoir, dispersing bacteria which can infect other sites (Chao *et al.* 2015; Pettigrew *et al.* 2014; Marks *et al.* 2013; Sanchez *et al.* 2011). I hypothesise that as BC caused *in vitro* biofilms to mimic the structure of nasopharyngeal biofilms *in vivo*, this effect may be exaggerated *in vivo* whereby BC may further enhance nasopharyngeal colonisation. Enhanced colonisation could provide a mechanism to explain the increase in pneumococcal pneumonia in people exposed to high levels of PM (Brugha & Grigg 2014; MacIntyre *et al.* 2014; Qiu *et al.* 2014; Darrow *et al.* 2014; Gittins *et al.* 2013; Janssen *et al.* 2012; Brunekreef & Forsberg 2005).

To test this hypothesis, future work could assess pneumococcal colonisation of the murine respiratory tract in the presence and absence of BC, and image the resulting nasopharyngeal biofilms using the method described by Marks *et al.* (2012a).

Alternatively, additional *in vitro* methods could be employed. Biofilm formation on biotic surfaces has been reported to better correlate with *in vivo* biofilm structure and antibiotic sensitivities than biofilms formed on abiotic surfaces (Marks *et al.* 2012a). Therefore the microscopy and antibiotic sensitivity assays presented in this thesis could be repeated with pneumococcal biofilms grown on epithelial cell lines as described in

Marks *et al.* (2012a). This would allow the determination of whether the observed BC-associated structural phenotypes are exaggerated in these conditions, and would inform on potential *in vivo* alterations while fitting with the Home Office 3R's. The 3R's detail Home Office guidelines to reduce the number of animals used, refine techniques, and, where possible, replace the experiment with a non-animal method.

Although this work revealed that BC induces interesting structural modifications in *S. pneumoniae* PR201, only this strain was investigated. These investigations could therefore be repeated with additional strains of *S. pneumoniae* in order to determine whether the observed effects are strain specific or occur with all pneumococci. In particular, it may be advantageous to compare encapsulated and unencapsulated pneumococci. Initial attempts to investigate biofilms of the encapsulated D39 strain by electron microscopy were unsuccessful and these biofilms were degraded during processing. The greatest disruption to biofilm structure occurred during the dehydration steps of processing, therefore methodologies were modified to eliminate the dehydration steps in an effort to overcome these issues (Section 2.5.1). Unfortunately these modifications were not sufficient to allow assessment of D39, and biofilms were still degraded.

It should be noted that the issue of biofilm degradation during processing for electron microscopy was most prevalent with D39 biofilms, however was not restricted to D39 alone. Biofilms of some *S. aureus* strains, including SH1000, which had been formed in the presence of 100 µg/ml BC, were also degraded during processing using the standard protocols described (Section 2.5.1). In contrast however, the modified protocol employed was sufficient to preserve and prepare these biofilms for microscopy. It is unclear why these adapted methodologies were sufficient to allow the examination of all *S. aureus* strains but not *S. pneumoniae* D39. A potential explanation may be that the pneumococcal matrix is highly hydrated and this is known to cause issues when processing of biofilms for electron microscopy (Hammerschmidt *et al.* 2005).

Future work could prepare biofilms of other encapsulated strains for visualisation by electron microscopy, such as the clinically relevant TIGR4 strain (Tettelin *et al.* 2001), in order to determine whether these issues are specific to D39 or occur with all

encapsulated pneumococci. Previous work has identified that conventional electron microscopy preparation results in the loss of capsular polysaccharide (Hammerschmidt *et al.* 2005), therefore I expect that the issues encountered with D39 will be present for all encapsulated strains. If this is the case, alternative processing steps could be employed. A lysine-acetate-based formaldehyde-glutaraldehyde ruthenium red-osmium (LRR) fixation procedure could be attempted as this has been shown to better preserve biofilm structures of encapsulated pneumococci in comparison to conventional techniques using aldehyde fixation, osmification, and dehydration (Marks *et al.* 2012a; Hammerschmidt *et al.* 2005). This was not attempted during the work detailed in this thesis because it was decided that the adaptations of standard techniques described would likely allow visualisation of D39 biofilms. Unfortunately time restrictions meant that the LRR fixation methodology could then not be attempted once it was realised that the adapted methods employed were not sufficient to allow analysis of this strain.

4.9.2. BC alters *S. aureus* biofilm structures

In the absence of BC, biofilms of *S. aureus* were flat structures as have been previously observed (Smith *et al.* 2008; Marques *et al.* 2007). Similarly to *S. pneumoniae*, BC also impacted the biofilm structure of *S. aureus*, although there was a slightly different effect. When formed in the presence of BC, *S. aureus* biofilms were thicker than control biofilms and displayed BC-associated protrusions. BC was found to increase the amount of loosely adherent SH1000 bacteria in comparison to controls in Chapter 3 (Section 3.4.3). Therefore I hypothesise that these biofilm protrusions are the source of the decreased structural integrity observed, in that these protrusions are more able to detach from the biofilm surface.

A potential confounding factor for this hypothesis is that biofilm protrusions were also identified with Newman and USA300, which did not exhibit an increase in loosely adherent bacteria associated with BC exposure (Section 3.4.3). Protrusions from biofilms of Newman and USA300 were less numerous than those for SH1000, therefore it is possible that these protrusions did not reach a required density to significantly affect overall integrity in the *in vitro* assays. Indeed, USA300 is known to form more robust biofilms than SH1000 (Nicholson *et al.* 2013). To investigate this, future work

could assess biofilm formation of Newman and USA300 with higher BC concentrations than presented in this thesis, and identify whether the protrusion phenotype is enhanced for these strains in these conditions. If so, this work could then identify whether this corresponds with an increase in loosely-adherent bacteria using the biofilm viability assay described in Chapter 3. Biofilms of *S. pneumoniae* and *P. aeruginosa* have been shown to have an increased mass when formed in the presence of cigarette smoke, however effects are dose dependent and become more pronounced after repeated exposure, providing a basis for this future work (Feldman & Anderson 2013; Mutepe *et al.* 2013; Antunes *et al.* 2012). In addition, it may be advisable to assess BC-induced biofilm structural modifications with additional *S. aureus* strains to the ones characterised in this chapter, such as those investigated in Chapter 3. This would allow the determination of whether protrusions are found universally and how these correlate with alterations in the structural integrity.

In conclusion, it appears that BC induces the production of biofilm protrusions in *S. aureus*, which may be the source of the reduced structural stability of BC-biofilms observed in Section 3.4.3, and may enhance bacterial dispersion *in vivo*. One limitation of this work is that although protrusions were observed in BC-biofilms of *S. aureus*, these were not quantified. It would have been useful for the amount of protrusions to be quantified across biofilms of each strain and each biological repeat, in order to determine if the BC-biofilms of strain SH1000 had significantly more protrusions than Newman or USA300. If a significant difference were identified, this would bolster the hypothesis that these protrusions may be the source of the reduced stability of SH1000 biofilms. For this assessment, either random areas of the biofilm could have been assessed to ensure measurements are not influenced by experimenter bias, or the entire biofilm surface could have been imaged and assessed. The first of these may have been advisable, as due to the magnification of SEM, assessment of the entire biofilm surface for each strain and repeat would have been extremely time consuming.

4.9.3. Mechanisms of biofilm induced modifications

The biofilm modifications reported in this thesis do not appear to be simply due to BC particles acting as a mechanical scaffold for biofilm formation, as quartz had no effect

on biofilm structure of *S. pneumoniae* or *S. aureus*. Therefore the work described in this thesis suggests that the effects of BC on biofilm formation were biological, however it is not yet known what the mechanisms behind these effects were and it is clear that further work is required. The protein expression profiles of control and BC-formed biofilms were investigated in an attempt to identify potential explanations for differences in biofilm formation, however no differences were identified. To better visualise differences, 2D SDS-PAGE gels could be employed in future work to separate proteins in two dimensions by their isoelectric point and mass, allowing the visualisation of individual protein spots (Melo *et al.* 2013). Alternatively, to investigate the proteome of bacteria in control and BC-biofilms in more detail, mass spectrometric-based approaches could be used, such as iTRAQ LC-MS (Isobaric tag for relative and absolute quantitation, liquid chromatography–mass spectrometry) (Wiese *et al.* 2007) or GeLC–MS (Moche *et al.* 2015; Dzieciatkowska *et al.* 2014). iTRAQ LC-MS involves performing protein extractions, tagging peptides, and analysing the sample with MS. In contrast, GeLC-MS involves separating proteins by SDS-PAGE followed by gel digestion and LC-MS, and is reported to identify low level proteins better than peptide-level fractionation (Dzieciatkowska *et al.* 2014). These techniques would potentially provide more information on altered protein production during BC-biofilm formation in comparison to controls.

4.9.4. Biofilm alterations are also observed after 2 hours attachment

It was determined that the effects of BC on biofilm formation appeared to be initiated within the first 2 hours of attachment. Strains which showed a significant reduction in biofilm bacteria at 24 hours when formed in the presence of BC, generally also showed a significant reduction in bacterial attachment after 2 hours. These results suggest that the cause of biofilm modifications with BC exposure are initiated during or within the first 2 hours of attachment, and may be due to altered bacterial adhesion or the induction of factors which alter biofilm formation. Attachment of *S. aureus* bacteria to a surface is mediated by microbial surface component recognizing adhesive matrix molecules (MSCRAMMs), surface protein G (SasG), extracellular matrix protein-binding protein (Emp), Extracellular adherence protein (Eap/Map), and Polysaccharide

Intercellular Adhesin (PIA) (Lister & Horswill 2014; Foster *et al.* 2014; Zecconi & Scali 2013; O’Gara 2007). Therefore to test this hypothesis, future work could assess whether BC alters the expression of the genes encoding these factors during attachment using qRT-PCR (Casillas-Ituarte *et al.* 2012). In conclusion, BC was found to drastically alter biofilm structures of all *S. pneumoniae* and *S. aureus* strains tested, and these effects may be initiated during bacterial attachment.

4.9.5. BC alters biofilm matrix composition

Extracellular DNA, protein, and polysaccharides are reported to be major components of pneumococcal and *S. aureus* biofilms, as described in Section 1.10 (Domenech *et al.* 2012; O’Gara 2007). Matrix composition thereby alters the effectiveness of dispersal mechanisms (O’Neill *et al.* 2007; Chaignon *et al.* 2007). *S. pneumoniae* PR201 biofilms formed in the absence of BC were not significantly degraded by DNaseI or proteinase K ($p>0.05$). These results were surprising as both protein and DNA are major components of pneumococcal biofilms (Blanchette-cain *et al.* 2013; Shak *et al.* 2013a; Domenech *et al.* 2012; Hall-Stoodley *et al.* 2008; Moscoso *et al.* 2006). Past research has found both DNaseI and proteinase K can significantly reduce pneumococcal biofilm biomass using similar methodologies, however this is strain dependent (Hall-Stoodley *et al.* 2008; Moscoso *et al.* 2006). Previous investigations have assessed biofilm degradation of the encapsulated clinical isolates BS68, BS69, BS71, BS72, BS73, BS75 (Hall-Stoodley *et al.* 2008), and the unencapsulated strain R6 (Moscoso *et al.* 2006). However to my knowledge, this is the first time that dispersion of biofilms of the unencapsulated strain PR201 has been assessed using proteinase K and DNaseI.

In the research described in this thesis, only *S. aureus* SH1000 biofilms were significantly degraded by DNaseI ($p\leq 0.01$), whilst biofilms of Newman and USA300 were unaffected ($p>0.05$). Directly contrasting DNaseI degradation, control biofilms of Newman and USA300 were significantly ($p\leq 0.01$) degraded by proteinase K, whereas SH1000 control biofilms were not ($p>0.05$). Biofilms of Newman and USA300 were formed in a glucose enriched environment, which is reported to induce the production of proteinaceous biofilm matrices susceptible to proteinase K degradation (Nicholson *et*

al. 2013; Archer *et al.* 2011; O'Neill *et al.* 2007; O'Gara 2007; Kogan *et al.* 2006). Therefore the proteinase K degradation results were expected for these strains.

These results differ from some past research, although there is variation in the reported effects of proteinase K and DNaseI on biofilms of these strains within the literature (Nicholson *et al.* 2013; Kulkarni *et al.* 2012). Previous research has found that proteinase K and DNaseI are unable to disperse mature biofilms of SH1000 or USA300 (Nicholson *et al.* 2013). Furthermore, proteinase K and DNaseI have been both reported to both cause dispersal of Newman biofilms (Nicholson *et al.* 2013), and have no effect on Newman biofilms (Kulkarni *et al.* 2012). The same protocols for dispersal of biofilms with proteinase K and DNaseI have been used in the research detailed in this thesis and in the past research described (Nicholson *et al.* 2013; Kulkarni *et al.* 2012), therefore this is not likely to be the cause of the strain differences identified. Instead the variation may be due to the biofilm formation and quantification methods used, as in the previous work described, staining methodologies were employed to assess biofilm formation (Nicholson *et al.* 2013; Kulkarni *et al.* 2012).

Interestingly, BC altered biofilm degradation by proteinase K for all *S. pneumoniae* and *S. aureus* strains investigated, but had no effect on biofilm degradation by DNaseI. The degradation assays employed are commonly used to assess the contribution of protein and DNA to the mature biofilm matrix (Nicholson *et al.* 2013; Kulkarni *et al.* 2012; Hall-Stoodley *et al.* 2008; Kogan *et al.* 2006; Moscoso *et al.* 2006). Therefore these results suggest that the matrices of *S. pneumoniae* PR201 and *S. aureus* SH1000 had been made more proteinaceous by BC, but the protein based matrix of Newman and USA300 had been made less proteinaceous. Alternatively, it is possible that these results could suggest that BC altered the sensitivity of biofilms to degradation by proteinase K rather than the protein content, making PR201 and SH1000 biofilms more sensitive and Newman and USA300 biofilms more resistant to enzymatic treatment. This may be due to the altered biofilm architectures, making the biofilms more accessible to degradation. If so, it is unclear why BC would alter biofilm resistance to proteinase K but not DNaseI.

Two of the major biofilm matrix components, protein and nucleic acid, have been discussed, however a third component, polysaccharide, has so far been ignored (Flemming & Wingender 2010). The role of polysaccharides in pneumococcal biofilms are not yet well defined, however it is recognised that encapsulated pneumococci are poorer biofilm formers than their unencapsulated counterparts (Chao *et al.* 2015; Domenech *et al.* 2012; Camilli *et al.* 2011; Moscoso *et al.* 2009). Furthermore, encapsulated pneumococci are reported to reduce capsule production during biofilm formation to enhance bacterial adhesion (Gilley & Orihuela 2014; Shainheit *et al.* 2014; Sanchez *et al.* 2011). Therefore polysaccharide may not be a vital component of pneumococcal biofilms.

In contrast it is well established that *S. aureus* biofilms are primarily either protein- or polysaccharide-based (Archer *et al.* 2011; O’Gara 2007). In the research described in this thesis, SH1000 biofilms were formed in a medium supplemented with NaCl, which is reported to produce polysaccharide based structures (O’Gara 2007). The importance of polysaccharide in the biofilm matrix was therefore assessed alongside proteinase K and DNaseI degradation assays, by degrading control and BC-formed biofilms with sodium metaperiodate (Qin *et al.* 2007; O’Neill *et al.* 2007; Kogan *et al.* 2006). Unfortunately, exposure to sodium metaperiodate resulted in total bacterial death of all strains regardless of concentration used (1-10 mM in 50 mM sodium acetate buffer, pH 4.5).

Biofilm degradation by sodium metaperiodate has been assessed in previous research, however to my knowledge, only in conjunction with methods that quantify biofilm formation by staining (Qin *et al.* 2007; O’Neill *et al.* 2007; Kogan *et al.* 2006).

Therefore any effect of sodium metaperiodate on bacterial viability may not have altered staining, and it may have been possible to observe biofilm degradation.

However since quantification of viable bacteria was used in this thesis, these methods was found to be unsuitable for assessment. Future work could therefore reattempt the examination of the role of polysaccharide in biofilms, and whether BC alters this contribution, using the glycoside hydrolase dispersin B (DspB) (Nicholson *et al.* 2013; Kaplan *et al.* 2003). Alternatively, it would be possible to concurrently investigate the roles of nucleic acid, protein, and polysaccharide in control and BC-biofilms through

staining and confocal microscopy. Potential dyes which could be used together include as DAPI (4',6-diamidino-2-phenylindole), which binds to A-T rich DNA and stains blue, Sypro Red, which stains proteins red, and Alexa Fluor 647, which is a far-red dye for polysaccharides. However initial investigations into confocal microscopy would be required to optimise staining and accurate signal detection.

4.9.6. BC alters antibiotic tolerance of biofilms

Method optimisation determined the amount of oxacillin and gentamicin required to significantly reduce viability of control *S. aureus* and *S. pneumoniae* biofilms. The minimum bactericidal concentration of planktonic cultures is ~32 µg/ml gentamicin for *S. pneumoniae*, ~2 µg/ml oxacillin for MSSAs, and ~256 µg/ml for MRSA (EUCAST 2015; Marks *et al.* 2012a; Gould *et al.* 2012). However, to achieve a significant ($p \leq 0.05$) reduction in the viability of control biofilms, a minimum of 500 µg/ml gentamicin and 50 mg/ml oxacillin was required for *S. pneumoniae* and *S. aureus*, respectively (Appendix 16). Even at these high doses, neither concentration was sufficient to cause total bacterial eradication. These results therefore highlight the importance and effectiveness of a biofilm mode of growth in protecting bacteria from antibiotics. It is also known that colonised nasopharyngeal pneumococci in biofilms are far more difficult to eradicate than pneumococci in invasive disease, which fits with these results (García-Rodríguez & Fresnadillo Martínez 2002; Varon *et al.* 2000; Cohen *et al.* 1999; Dagan *et al.* 1998; Dabernat *et al.* 1998; Cohen *et al.* 1997). It is also therefore no surprise that biofilms are a particular problem in public health due to the difficulty in their eradication (De la Fuente-Nunez *et al.* 2013; Donlan & Costerton 2002).

Similarly to the results described in this thesis, past research has found that 250-500 µg/ml of gentamicin is required to cause a significant reduction in pneumococcal biofilm viability (Marks *et al.* 2012a; Bartoszewicz *et al.* 2007). For *S. aureus*, exposure to 20 mg/ml of oxacillin in BHI overnight has been found to be inadequate to achieve a sufficient reduction in viability of dispersed biofilm clumps to be able to define this as a minimal bactericidal concentration (Fux *et al.* 2004). Furthermore, these clumps were more tolerant to oxacillin than planktonic bacteria. Therefore the tolerance

of *S. aureus* and pneumococcal biofilms to oxacillin and gentamicin identified in this work agree with previous research.

Oxacillin is a clinically relevant antibiotic which is highly effective against planktonic bacteria but poorly penetrates well organised biofilms, which makes this antibiotic a good discriminator of biofilm organisation (Singh *et al.* 2010). Newman and USA300 biofilms formed in the presence of BC were significantly more sensitive to oxacillin than control biofilms, whereas SH1000 biofilms formed in the presence of BC were more tolerant of oxacillin. Oxacillin is one of the first-line antibiotics used to treat *S. aureus* infections. Therefore, the increase in tolerance of SH1000, a methicillin sensitive *S. aureus*, to a penicillin based antibiotic after exposure to BC, has implications for the treatment of respiratory infections. It is possible that these strain differences in tolerance of biofilms to oxacillin may alter strain distribution *in vivo* during antibiotic treatment and impact the outcome of infection.

It is interesting that the effect of BC on biofilm antibiotic tolerance did not correspond with the effect of BC on biofilm viability (Section 3.4.3) or with the observed alterations in biofilm architecture (Section 4.2). In fact, for *S. aureus*, antibiotic tolerance results correlated most strongly with biofilm degradation by proteinase K. Biofilms formed in the presence of BC appeared to be inversely affected by proteinase K and oxacillin degradation. To clarify this point, BC-biofilms of Newman and USA300 were not significantly altered by proteinase K, but were more sensitive to oxacillin than control biofilms. In contrast, SH1000 BC-biofilms were significantly degraded by proteinase K, but were more tolerant of oxacillin than control biofilms. The resistance of biofilms to environmental stressors, including antibiotics, is known to be partially due to the extracellular matrix, which acts as a barrier to antimicrobials (Chao *et al.* 2015; De la Fuente-Nunez *et al.* 2013; Archer *et al.* 2011; Kiedrowski & Horswill 2011; Flemming & Wingender 2010). These data suggest that BC exposure caused in changes in biofilm composition that directly altered tolerance to antibiotics. A BC-induced decrease in the contribution of protein to the extracellular matrix seemed to be correlated with increased tolerance of oxacillin, whereas an increase protein was correlated with decreased tolerance of oxacillin. Future work could repeat this investigation with a larger strain set and additional antibiotics to determine whether

proteinase and antibiotic BC-biofilm degradation consistently show an inverse relationship.

Gentamicin is also an excellent discriminator of biofilm organisation (Chao *et al.* 2015; Marks *et al.* 2012a; Bartoszewicz *et al.* 2007; Abdi-Ali *et al.* 2006; Carmen *et al.* 2004). Although biofilms of *S. pneumoniae* strain D39 formed in the presence of BC were more resistant to gentamicin treatment than controls, this was not a significant difference ($p > 0.05$). Future work could reattempt this investigation with antibiotics used against clinical pneumococcal infections, such as penicillin, to further investigate the clinical relevance of biofilm modifications. Unfortunately, biofilm tolerance to gentamicin cannot be compared to proteinase degradation data as D39 was used for antibiotic assays and PR201 was used for proteinase K assays as described before (Section 4.7.2 and 4.8). Future work could therefore attempt to repeat this investigation with a wider pneumococcal strain set and directly compare results for proteinase degradation and antibiotic tolerance within a single strain.

4.9.7. Conclusions

BC was observed to alter biofilm formation, resulting in altered structures, matrices, and functioning. It is as yet unclear what the mechanisms behind the observed biofilm modifications are, and further research is required to elucidate why such distinct strain differences are observed. The intra- and inter-species variation in the impact of BC implies that colonisation and the composition of the respiratory tract microbiota may be altered, which may have a role in the health effects of pollution by causing microbiota dysbiosis, or affecting the *in vivo* success of particular bacterial strains.

Chapter 5. Effects of BC on pneumococcal colonisation and the respiratory tract microbiota

5.1. Introduction

The link between BC exposure and disease has classically been assessed from a host-centric viewpoint (Provost *et al.* 2016; Longhin *et al.* 2016; Aztatzi-Aguilar *et al.* 2015; Mannucci *et al.* 2015; Kumar *et al.* 2015; Zhao *et al.* 2014; Janssen *et al.* 2012; Patel *et al.* 2011). I suggest that BC may also affect *in vivo* colonisation and/or the diversity of the microbiota, and that alterations in colonisation or the host-microbiota relationship may contribute towards BC-associated disease. Therefore the objectives of the work described in this chapter were two-fold; firstly, to identify whether BC exposure altered respiratory tract colonisation of *S. pneumoniae* in a murine model, and secondly, to determine the effects of BC exposure, pneumococcal colonisation, and BC-pneumococcal co-inhalation on the respiratory tract microbiota. This chapter will describe the optimisation and delivery of this work.

S. pneumoniae primarily colonises the human nasopharynx and it is estimated that 30-88 % of children are colonised, but carriage declines to 5-20 % in adults (Wyllie *et al.* 2014; Shak *et al.* 2013b; Mook-kanamori *et al.* 2011; Lanie *et al.* 2007; Hussain *et al.* 2005; Bogaert *et al.* 2004). Nasopharyngeal colonisation is a vital step before infection can occur, and is therefore a major risk factor for the development of pneumococcal disease (Simell *et al.* 2012; Weiser 2010). However, the mechanisms which promote dissemination of *S. pneumoniae* from the nasopharynx to the lower respiratory tract (LRT) are not fully understood. Multiple murine colonisation and infection models exist for *S. pneumoniae*, the outcome of which are dependent on many factors, including the dosing procedure, bacterial concentration, bacterial strain, and mouse strain (Haste *et al.* 2014; Richards *et al.* 2010; Kadioglu & Andrew 2005). A stable model of nasopharyngeal colonisation of MF1 mice has been established in which pneumococcal serotype 2 strain D39 persists in the nasopharynx, but does not enter the LRT (Richards *et al.* 2010). This model was used in the research described in this

chapter. An additional advantage of this model is that the use of outbred MF1 mice mimics the genetic variation in human populations exposed to air pollution.

5.2. Establishing lung pathology of BC

In order to determine the concentration and total amount of inhaled BC mice could tolerate without visible ill effects, MF1 mice were intranasally inoculated with either 5 µg (low-dose) or 100 µg (high-dose) of BC in 50 µl PBS, equating to 100 µg/ml and 2 mg/ml, respectively. Six mice were used for each group, and an additional six were dosed with PBS as a control. To establish penetration of BC into the LRT and the induction of pathological effects, lung histopathological analyses were performed immediately after, and then 7 days after, intranasal dosing (n=3 mice per group, per time-point). The lungs of control mice all appeared normal and were without signs of pathological significance at both time-points (Figures 5-1 A, 5-2 A, and 5-3 A).

When assessed immediately after inoculation, BC aggregates can be seen in the bronchioles, but not the alveoli, of mice inoculated with the low BC dose (Figures 5-1 B and 5-2 B). Interestingly, BC aggregates were additionally visible in the alveoli of mice inoculated with the high BC dose (Figures 5-1 C and 5-2 C). Therefore the concentration of BC used had a significant effect in the depth of penetration of BC. The presence of BC at this time-point was not associated with any overt signs of inflammation or pathology, possibly due to the short time between inoculation and tissue recovery.

At 7 days post-inoculation, the bulk of BC in the low-dose group had been cleared from the lungs, though occasional small aggregates were still evident (Figures 5-3 B and 5-4 A). For the high-dose group, the BC had not been fully cleared from the lungs and there were clear signs of pathological significance, as there were a number of BC-loaded alveolar macrophages (Figures 5-3 C and 5-4 B). However, all mice were without signs of disease for the duration of the experiment.

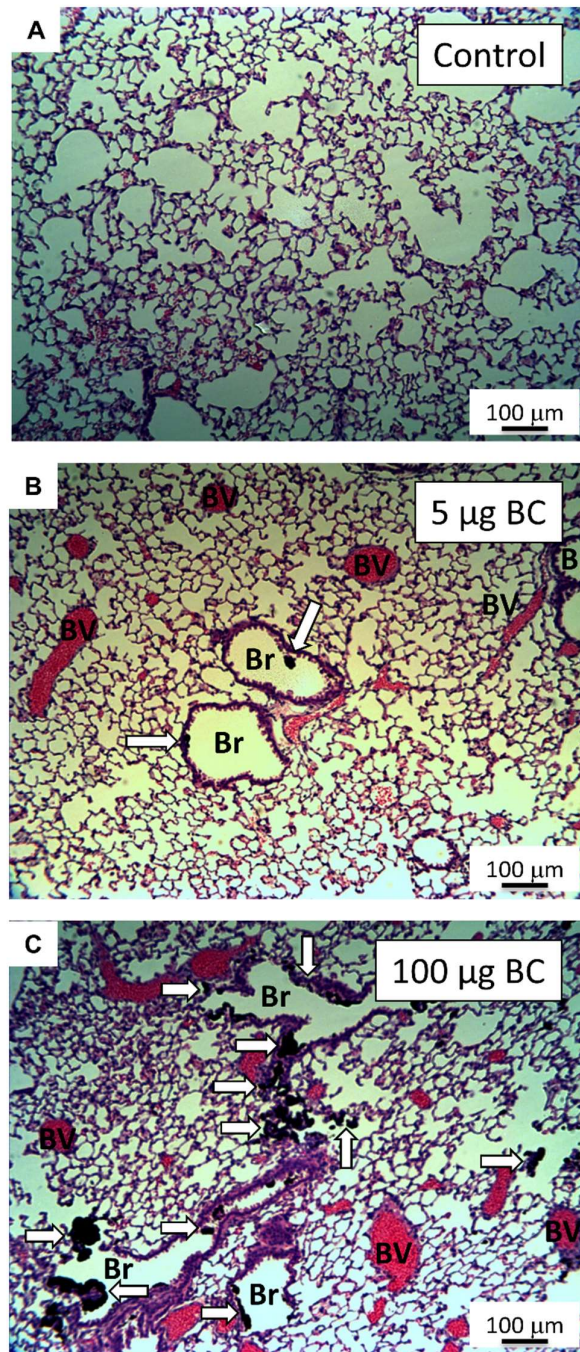


Figure 5-1. Penetration of black carbon into the lungs immediately after intranasal inoculation. Mice were intranasally dosed with 50 µl PBS as a control (A), 5 µg black carbon (BC) in 50 µl PBS (B), or 100 µg BC in 50 µl PBS (C). n=3 mice per group. Mice were then immediately culled and lungs were removed for histological analysis. Panels show representative formalin fixed, paraffin embedded lung sections stained with haematoxylin and eosin (H+E). Sections were imaged using light microscopy. Areas containing BC deposits are indicated with arrows. BV - Blood Vessel. Br - Bronchioles

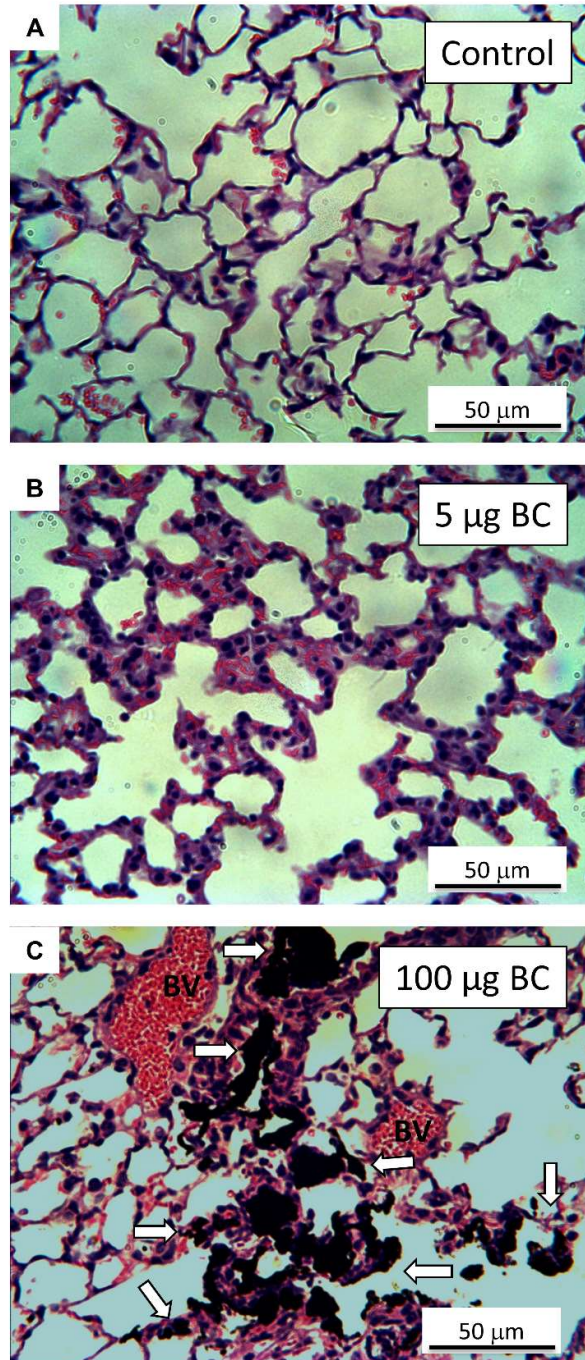


Figure 5-2. Penetration of black carbon into alveoli immediately after intranasal inoculation. Mice were intranasally dosed with 50 µl PBS as a control (A), 5 µg black carbon (BC) in 50 µl PBS (B), or 100 µg BC in 50 µl PBS (C). n=3 mice per group. Mice were then immediately culled and lungs were removed for histological analysis. Panels show representative formalin fixed, paraffin embedded lung sections stained with haematoxylin and eosin (H+E). Sections were imaged using light microscopy. Areas containing BC deposits are indicated with arrows. BV - Blood Vessel.

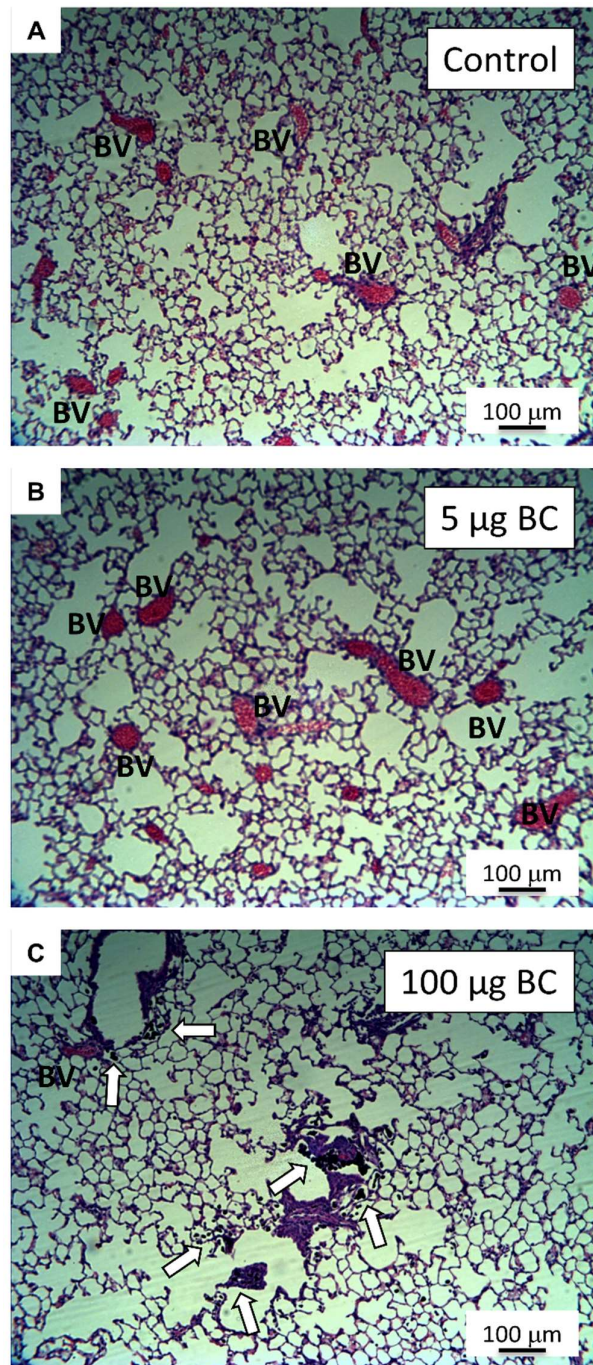


Figure 5-3. Persistence of black carbon in the lungs at 7 days post-inoculation. Mice were intranasally dosed with 50 µl PBS as a control (A), 5 µg black carbon (BC) in 50 µl PBS (B), or 100 µg BC in 50 µl PBS (C). n=3 mice per group. At 7 days post-inoculation mice were culled and lungs were removed for histological analysis. Panels show representative formalin fixed, paraffin embedded lung sections stained with haematoxylin and eosin (H+E). Sections were imaged using light microscopy. Areas containing BC-loaded macrophages are indicated with arrows. BV - Blood Vessel.

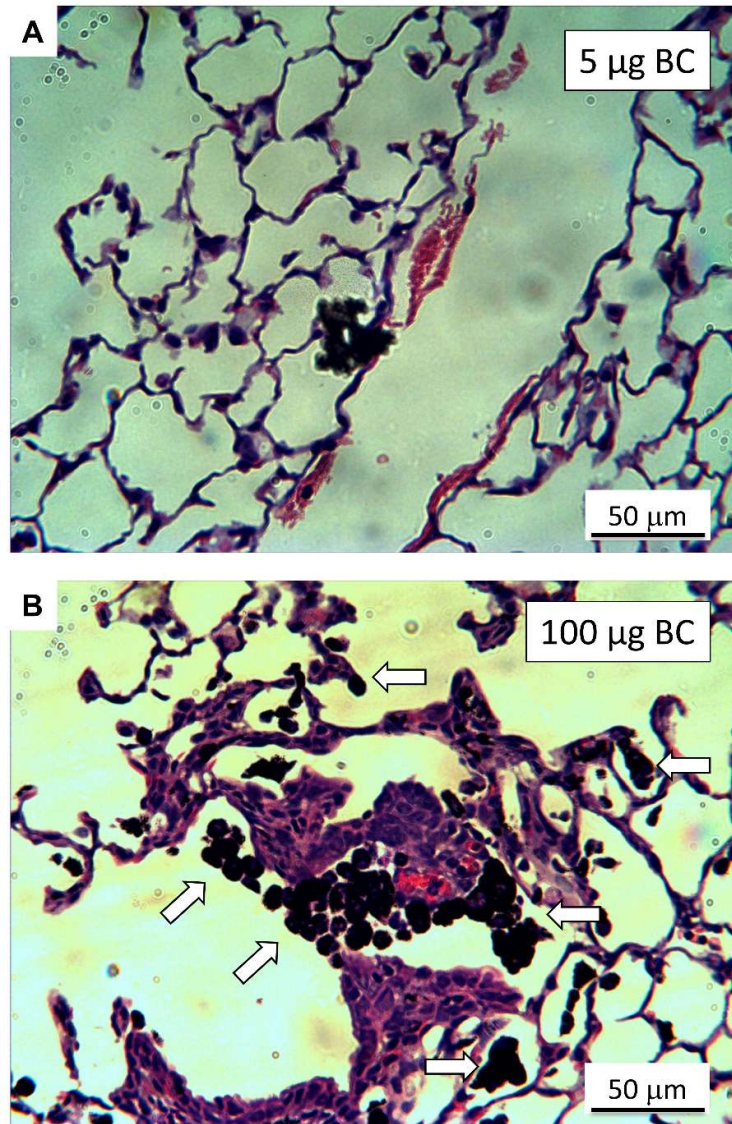


Figure 5-4. Comparison of black carbon persistence in the lungs at 7 days post-inoculation. Mice were intranasally dosed with either 5 µg black carbon (BC) in 50 µl PBS (A) or 100 µg BC in 50 µl PBS (B). n=3 mice per group. At 7 days post-inoculation mice were culled and lungs were removed for histological analysis. Panels show representative formalin fixed, paraffin embedded lung sections stained with haematoxylin and eosin (H+E). Sections were imaged using light microscopy. Areas containing BC-loaded macrophages are indicated with arrows.

5.3. Optimising inoculation volume for pneumococci and BC

In the host, pneumococci first colonise the nasopharynx and may later spread to the LRT (Shak *et al.* 2013b; Simell *et al.* 2012; Hogberg *et al.* 2007). Therefore inoculation procedures were required to restrict inoculation of pneumococci to the upper respiratory tract (URT) as far as possible, in order to promote nasopharyngeal colonisation. To assess whether the inoculation volume chosen was suitable, four MF1 mice were intranasally inoculated with 15 μ l of 5×10^5 CFU *S. pneumoniae* D39 whilst held in a horizontal position. Mice were culled immediately after inoculation and nasal and bronchoalveolar lavages were performed to determine bacterial load and assess whether this volume was restricted to the URT. ~ 4.82 log CFU/ml of pneumococci were detected in the nasal lavage fluid of all four mice, showing high reproducibility, but no pneumococci were detected in the bronchoalveolar lavage fluid (Figure 5-5). It was therefore decided that this inoculation volume was appropriate for use. The maximal amount of BC which could be suspended in this volume with the desired concentration of pneumococci was 105 μ g.

5.4. Murine colonisation model

After dosing procedures had been established, mice were intranasally inoculated with 15 μ l PBS containing (i) 105 μ g BC, (ii) 5×10^5 *S. pneumoniae* D39, (iii) a mixture of D39 and BC, or (iv) PBS alone as a control, as described in Section 2.7. Mice were assessed for an hour after inoculation and all mice tolerated dosing with no signs of distress. Both before and immediately after inoculation, a viable count was performed to confirm the challenge dose was $\sim 5 \times 10^5$ CFU. At pre-determined time-points, blood was taken and nasal and bronchoalveolar lavages were performed to determine bacterial load. Pneumococci were identified through analysis of colony morphology, growth on 5 % (v/v) horse blood agar plates supplemented with 1 μ g/ml gentamicin, Gram staining, and optochin sensitivity. The lungs, spleen, cervical lymph nodes, and nasal tissue were taken for histological analysis from mice distinct from those used to determine bacterial load.

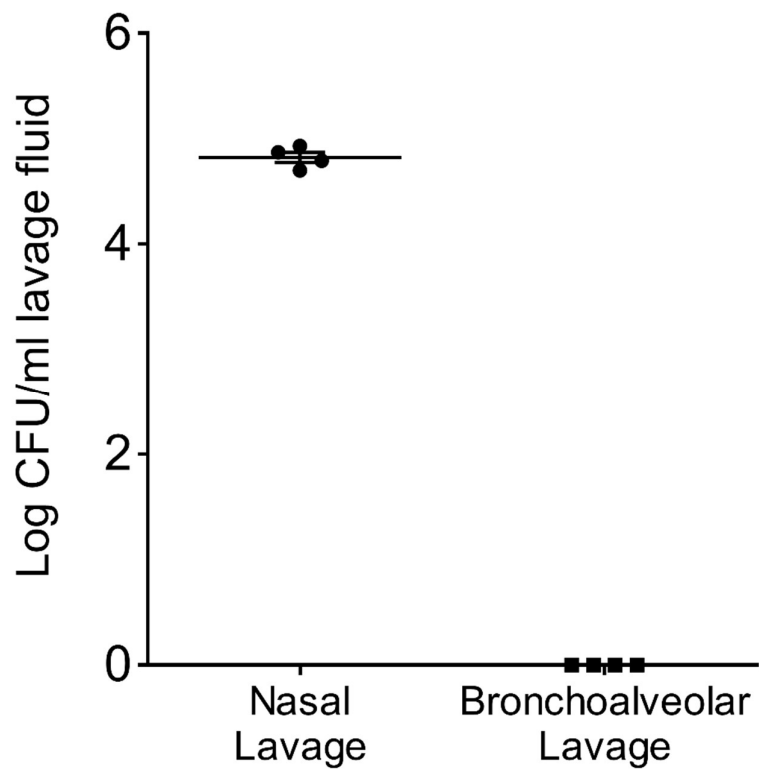


Figure 5-5. Bacterial load recovered after intranasal inoculation with *S. pneumoniae* D39. MF1 mice received an intranasal inoculation of 15 ul PBS containing 5×10^5 CFU *S. pneumoniae* D39. Mice were then immediately culled and nasal and bronchoalveolar lavages were performed to determine bacterial load. Detectable numbers of pneumococci are displayed. n=4. Error bars represent ± 1 SEM.

5.4.1. Pneumococcal colonisation of the murine respiratory tract

The major result of this work is that co-inoculation of BC and pneumococci promotes the spread of *S. pneumoniae* from the URT to the LRT (Figure 5-6). At 7 days post-inoculation, similar ($p>0.05$) quantities of pneumococci were recovered from the URT of mice co-exposed to *S. pneumoniae* and BC, and those inoculated with *S. pneumoniae* alone (Figure 5-6 A). In contrast, pneumococci were only detected in the LRT when the mice had been inoculated with *S. pneumoniae* and BC (Figure 5-6 B; $p\leq 0.01$ in comparison to all other groups). $3.55\text{-}3.9$ Log₁₀ CFU/ml pneumococci were recovered from the LRT of four of the five mice in this group. The fact that *S. pneumoniae* was only detected in the LRT of mice inoculated with BC and pneumococci shows that inoculation in the presence of BC promotes the dissemination of *S. pneumoniae*. This study did not investigate how BC caused the spread of pneumococci to the lungs at 7 days post-inoculation, however I present 2 major hypotheses for this observation in Section 5.6.3. Briefly, I propose that either BC altered the ability of *S. pneumoniae* D39 to colonise the mouse nasopharynx, resulting in a greater dispersion of bacteria to the LRT, or that BC and D39 were co-inoculated into the LRT at a level below the detection threshold, and that BC enhanced survival in the LRT in these conditions.

At 14 days post-inoculation, similar levels of pneumococci were found in the URT of mice in the D39 alone and D39+BC groups ($p>0.05$, Figure 5-6 C), however there was a slight decrease in colonisation levels from 7 days, which corresponds with previous research (Richards *et al.* 2010). Interestingly, the presence of pneumococci in the LRT observed at 7 days post-inoculation in the D39+BC group was not evident, and all pneumococci had been cleared (Figure 5-6 D). Similarly, no pneumococci were found in the LRT of mice in the D39 alone group (Figure 5-6 D). No pneumococci were found in the blood at either time-point. Furthermore, mice in the PBS and BC control groups had no pneumococci detected in any site throughout the experiment (Figure 5-6). Therefore in this colonisation assay, BC induced the spread of pneumococci from the URT to the LRT, but in these conditions this was a transient effect.

No mice showed clinical signs of disease, and all survived throughout the experiment, apart from one in the *S. pneumoniae* D39 group. After 2 days of no signs of adverse

effects, the health of this mouse declined to 2++ lethargic on day 3. This mouse was immediately culled, blood was taken, and nasal and bronchoalveolar lavages were performed to determine bacterial load. Surprisingly these results showed 3×10^4 total CFU *S. pneumoniae* D39 in the URT, 1×10^4 total CFU in the LRT, and 1.75×10^4 total CFU in the blood. It is therefore clear that pneumococci had caused bacteraemia, however it is unknown why this occurred. All mice from this group were inoculated with the same stock dose, no others had detectable pneumococci in the LRT or blood at any time-point, and all scored as normal for disease severity throughout the assay.

5.4.2. Pathological effects of pneumococcal colonisation and BC inhalation

The analysis of hematoxylin and eosin stained tissue samples was completed with assistance from Dr. Sarah Bolton, an independent consultant pathologist. Both BC inhalation and invasive pneumococcal disease cause inflammation (Xie *et al.* 2010; Tellabati *et al.* 2010; Folkmann *et al.* 2009; Yang *et al.* 2009; Kadioglu *et al.* 2008; Renwick 2004; Gallagher *et al.* 2003). Therefore the pathological effects of BC and pneumococcal exposure was investigated. Histological analysis of the lungs, nares, cervical lymph nodes, and spleens revealed no overt signs of pathology in any of the four groups; PBS, BC, D39, or D39+BC (Figures 5-7 and 5-8). Occasional low grade inflammation was identified in the perivascular, peribronchiolar, or alveolar compartments, but this was found in mice from all groups (Figures 5-7 A-D and 5-8 A-D). Nasal tissue histology samples show turbinates, multi-layered tissue lined externally with epithelial cells and sat on a substrate of glandular tissue, matrix, blood vessels (Figures 5-7 E-H and 5-8 E-H). However no sites of irritation are visible in nasal tissue samples. Physical features of note are identified in the lymph nodes and spleen (Figures 5-7 I-P and 5-8 I-P). Again, no differences were identified between groups. Furthermore, no BC particles were detected in any of the sites in either the BC or D39+BC groups (Figures 5-7 and 5-8). This indicated that BC had been cleared from the nasal passages by 7 days post-inoculation. Therefore although BC induced the spread of pneumococci to the lungs at 7 days post-inoculation, this was not associated with any overt signs of pathology.

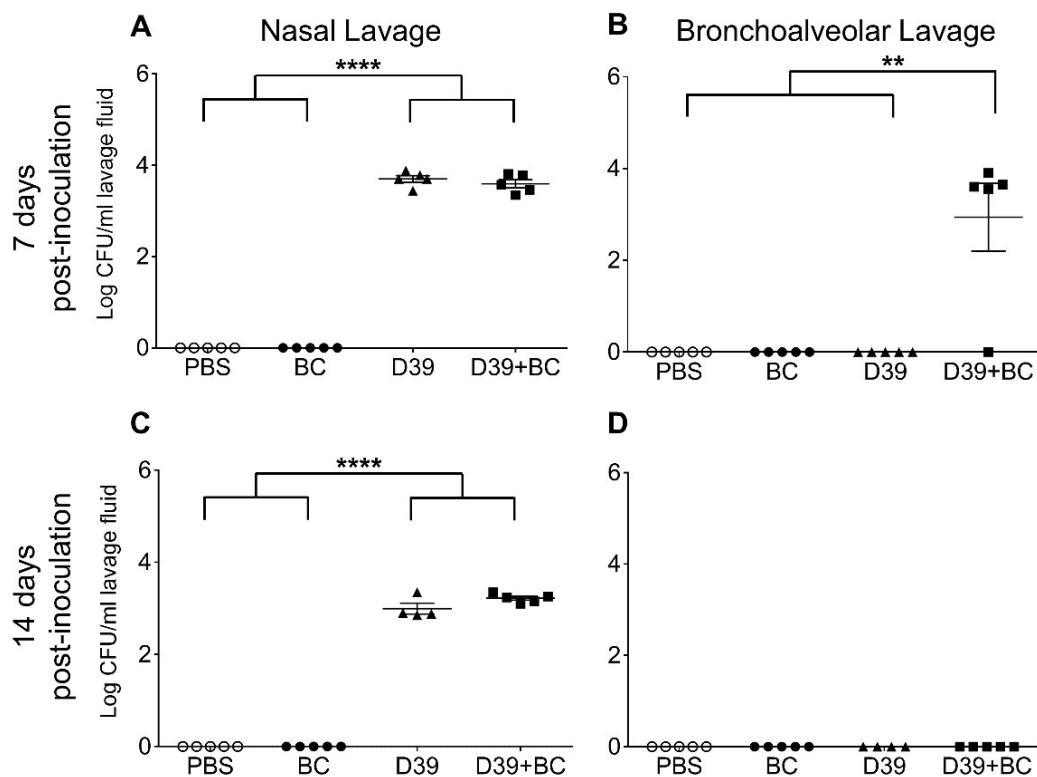
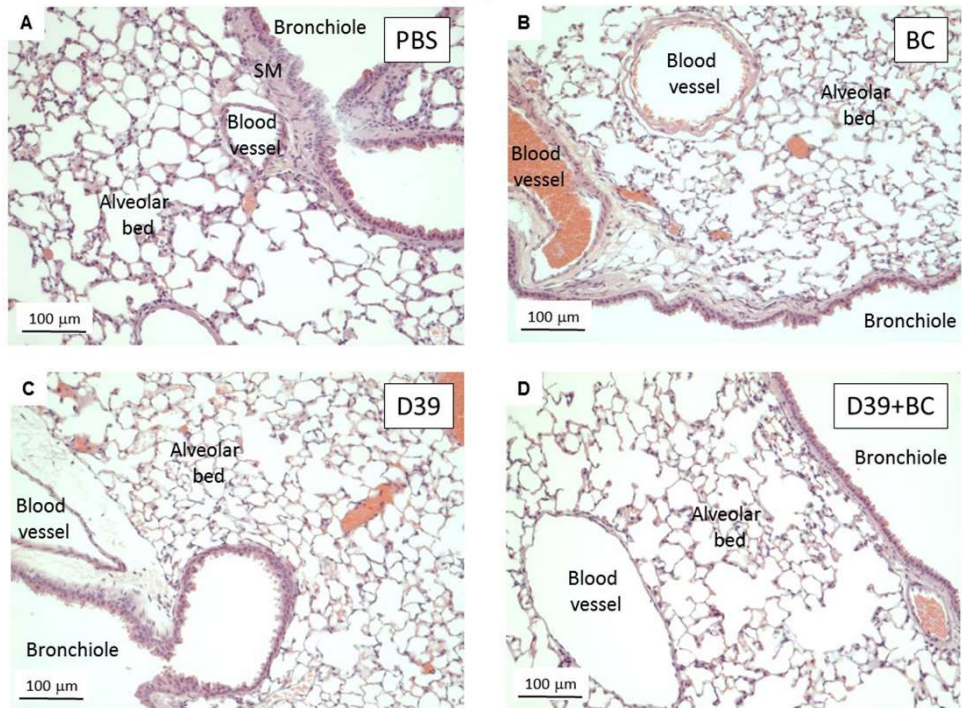


Figure 5-6. The effect of black carbon on pneumococcal colonisation of the respiratory tract of MF1 mice. Female MF1 mice were intranasally inoculated with 15 μ l of PBS, 7 mg/ml black carbon (BC), 6.45×10^5 CFU of *S. pneumoniae* D39 (D39), or a combination of BC and *S. pneumoniae* D39 (D39+BC). 7 mg/ml BC was chosen as this equated to a total of 105 μ g BC in the inoculum. At 7 and 14 days, nasal and bronchoalveolar lavages were performed and serial dilutions were plated out to determine bacterial load. No mice showed clinical signs of morbidity. n=5 mice per group and per time-point, except for the D39 group at 14 days post-inoculation, where n=4. Error bars represent \pm 1 SEM. Groups were compared with individual t-tests. All mice were used in analysis. Significant results are denoted with ** $p \leq 0.01$ and **** $p \leq 0.0001$.

LUNGS - 7 days post-inoculation



NARES - 7 days post-inoculation

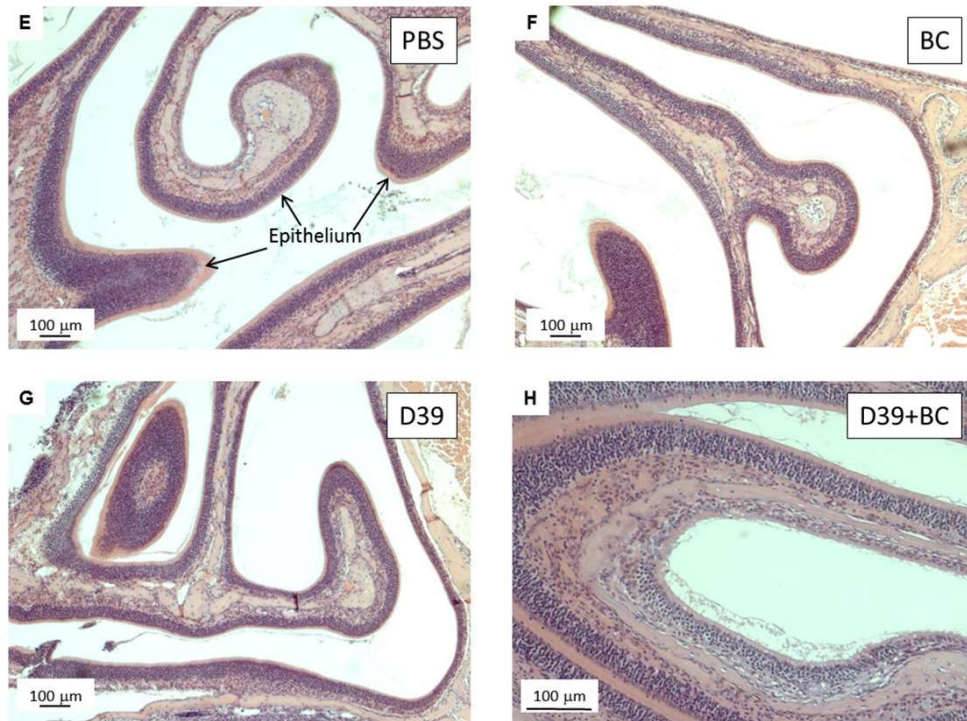
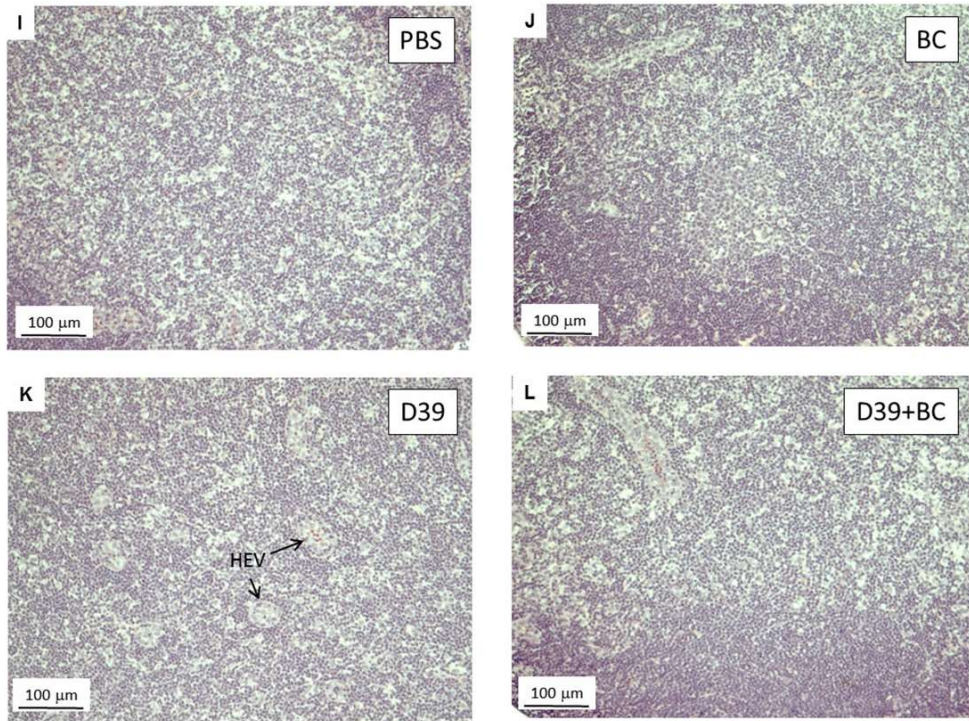


Figure 5-7. Histological analysis of lungs, nares, cervical lymph nodes, and spleen at 7 days post-inoculation. Continued overleaf.

CERVICAL LYMPH NODES - 7 days post-inoculation



SPLEEN - 7 days post-inoculation

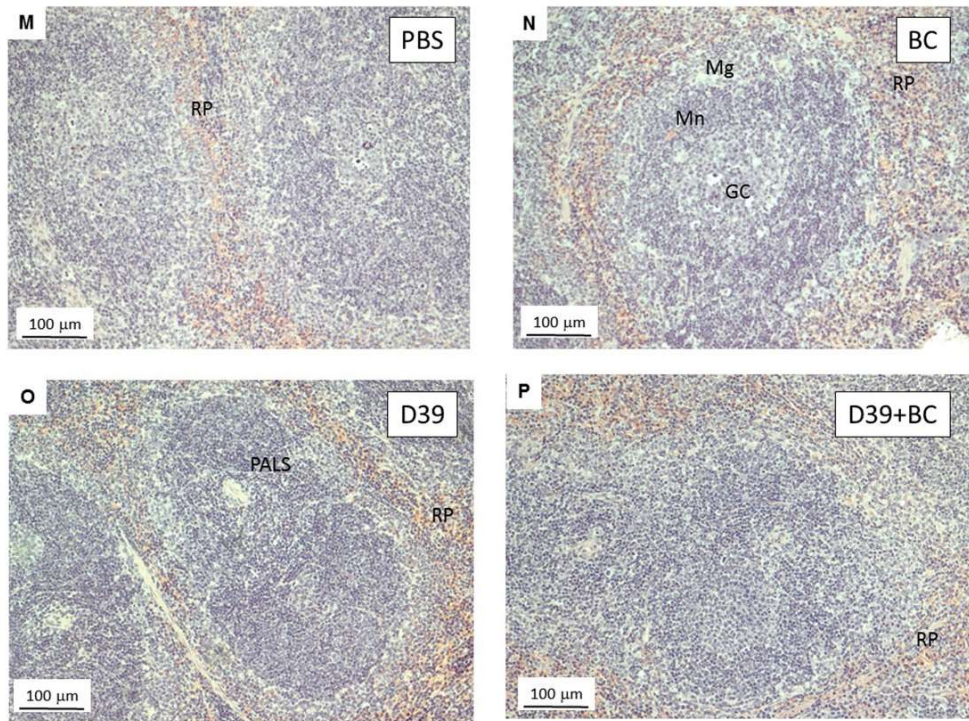
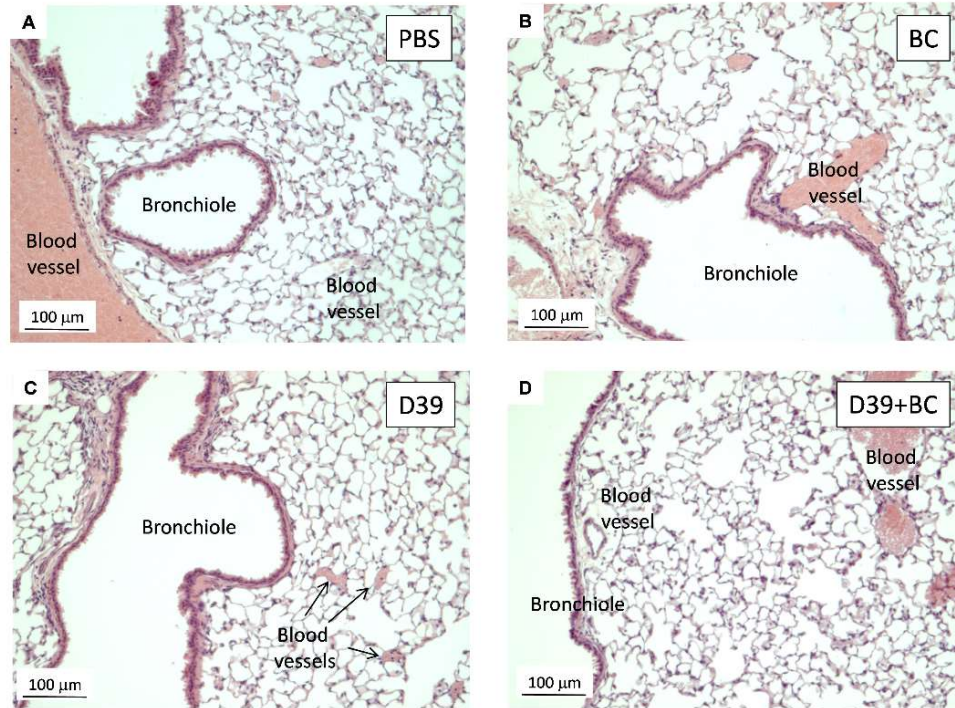


Figure 5-7 continued. Histological analysis of lungs, nares, cervical lymph nodes, and spleen at 7 days post-inoculation. Legend overleaf

Figure 5-7. Histological analysis of lungs, nares, cervical lymph nodes, and spleen at 7 days post-inoculation. Female MF1 mice were intranasally dosed with 15 μ l PBS (A, E, I, M), black carbon (BC-B, F, J, N), *S. pneumoniae* D39 (D39-C, G, K, O), or D39+BC together (D39+BC-D, H, L, P), and culled 7 days post-inoculation. Formalin fixed, paraffin embedded tissue sections of lungs (A-D), nares (E-H), cervical lymph nodes (I-L), and spleen (M-P) were stained with haematoxylin and eosin (H+E). Sections were imaged using light microscopy using 5x or 10x magnification. Physical features of notes are labelled for identification. Lymph nodes: High Endothelial Venules (HEV) are the entry point for lymphocytes. Spleen: Follicles comprised of a germinal centre (GC), a mantle (Mn) zone, and a marginal (Mg) zone. White pulp comprises the Peripheral Arteriolar Lymphoid Sheath (PALS), follicles, and lymphoid cells, surrounded by Red Pulp (RP).

LUNGS - 14 days post-inoculation



NARES - 14 days post-inoculation

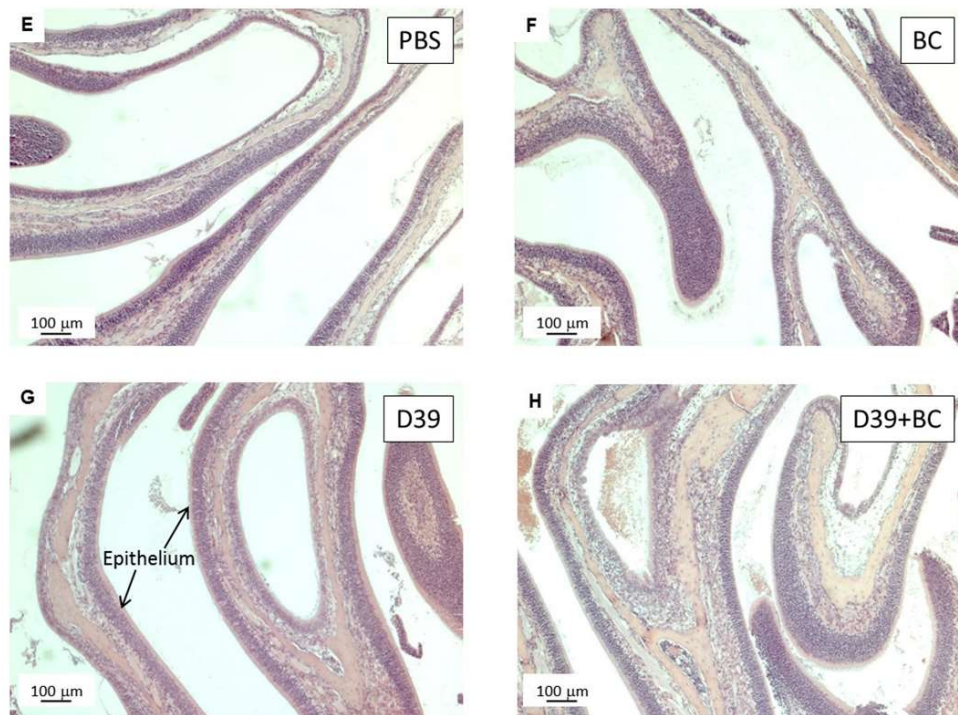
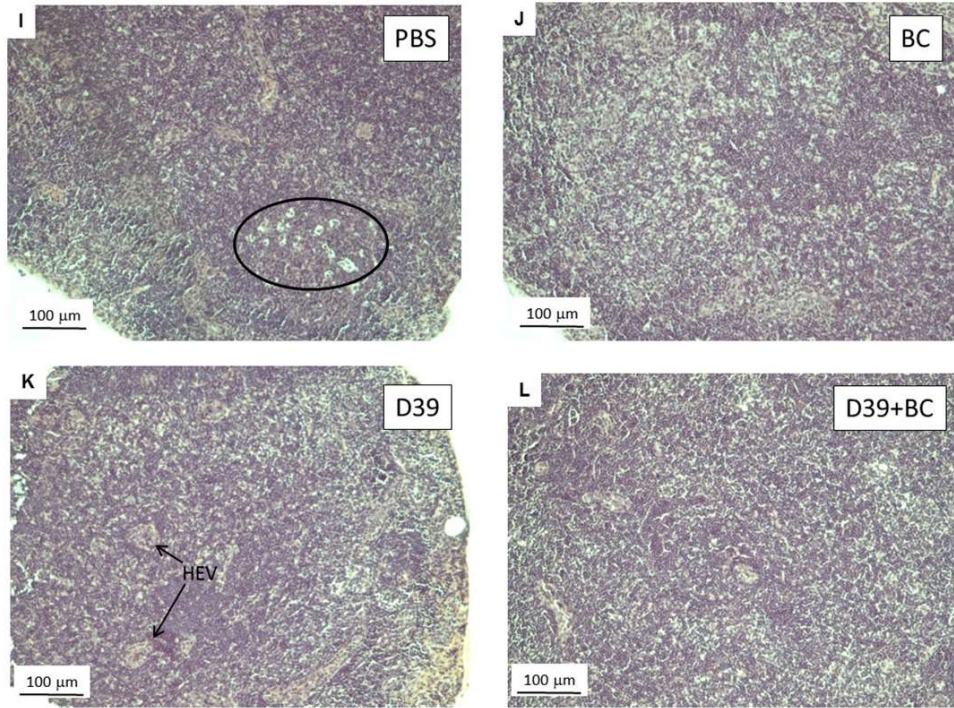


Figure 5-8. Histological analysis of lungs, nares, cervical lymph nodes, and spleen at 14 days post-inoculation. Continued overleaf.

CERVICAL LYMPH NODES - 14 days post-inoculation



SPLEEN - 14 days post-inoculation

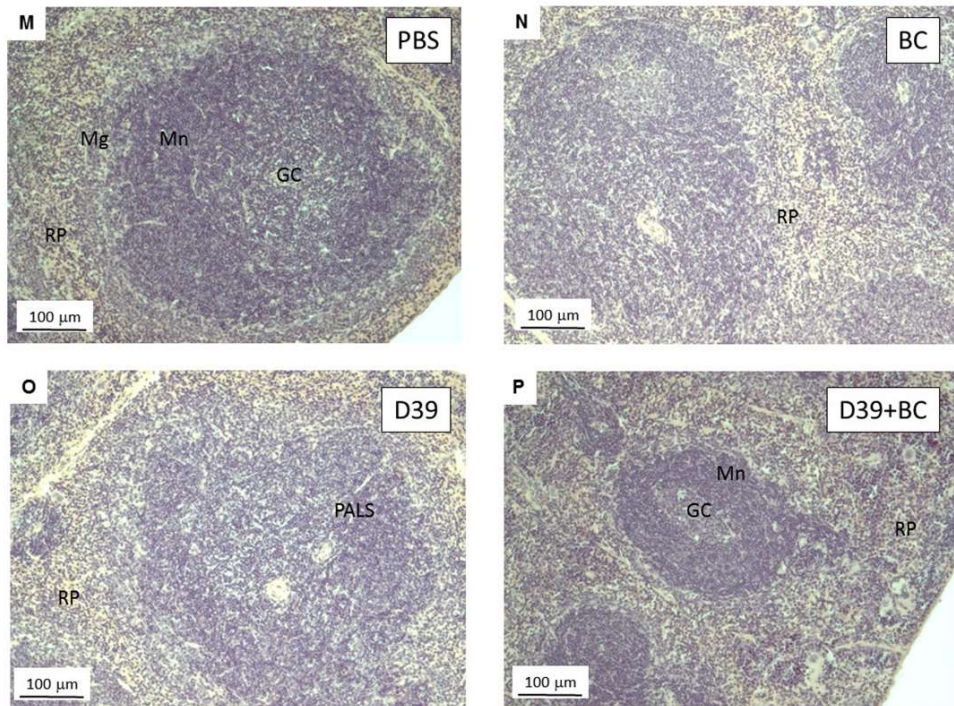


Figure 5-8. Histological analysis of lungs, nares, cervical lymph nodes, and spleen at 14 days post-inoculation. Legend overleaf.

Figure 5-8. Histological analysis of lungs, nares, cervical lymph nodes, and spleen at 14 days post-inoculation. Female MF1 mice were intranasally dosed with 15 μ l PBS (A, E, I, M), black carbon (BC-B, F, J, N), *S. pneumoniae* D39 (D39-C, G, K, O), or D39+BC together (D39+BC-D, H, L, P), and culled 14 days post-inoculation. Formalin fixed, paraffin embedded tissue sections of lungs (A-D), nares (E-H), cervical lymph nodes (I-L), and spleen (M-P) were stained with haematoxylin and eosin (H+E). Sections were imaged using light microscopy using 5x or 10x magnification. Physical features of notes are labelled for identification. Lymph nodes: High Endothelial Venules (HEV) are the entry point for lymphocytes. Occasional foci of apoptotic nuclei were seen (circled). Spleen: Follicles comprised of a germinal centre (GC), a mantle (Mn) zone, and a marginal (Mg) zone. White pulp comprises Peripheral Arteriolar Lymphoid Sheath (PALS), follicles, and lymphoid cells, surrounded by Red Pulp (RP).

5.5. Microbiota investigations

The URT is a main site of entry for colonising microbes, and harbours a microbiota which substantially varies from person to person (Bogaert *et al.* 2011; Frank *et al.* 2010). The microbiota diversity is homogenous throughout the respiratory tract, but progressively decreases in density from the upper airways down to the LRT (Dickson & Huffnagle 2015; Dickson *et al.* 2014; Morris *et al.* 2013; Charlson *et al.* 2011). The objective of this section was to determine the effect of BC exposure and pneumococcal colonisation on the respiratory tract microbiota.

5.5.1. DNA extraction protocol choice

For microbiota analysis, a DNA extraction technique was desired which allowed a high throughput of samples, unbiased extraction of DNA from different bacteria, and limited the possibility of human error. It was decided that DNA extraction kits were suitable for this work, however many commonly used DNA extraction kits have been found to be contaminated with microbial DNA, which is a particular problem when attempting to sequence DNA from low bacterial content samples such as the respiratory tract (Salter *et al.* 2014; Mohammadi *et al.* 2005). To assess this issue of contamination, Salter *et al.* (2014) carried out a 16S rRNA quantitative PCR analysis on cultures of *Salmonella bongori* extracted with a variety of commercial DNA extraction kits. DNA extraction of 10^5 CFU of *S. bongori* with a FastDNA Spin Kit for Soil, followed by 16S rRNA sequencing, revealed that ~90 % of sequences were *S. bongori*, and only ~10 % were contaminants. In contrast, extraction of the same *S. bongori* culture with the UltraClean Microbial DNA Isolation Kit and the QIAmp DNA Stool Mini Kit resulted in over 50 % and over 80 % of sequences being contaminants, respectively.

Distinct contaminant profiles have also been described within each brand of kits. Salter *et al.* (2014) reported a lower diversity of contamination within FastDNA Spin Kits in comparison to QIAmp DNA Stool Mini Kits. Furthermore, contamination within the FastDNA Spin Kits are characterised by *Burkholderiaceae*, which are not usually associated with the respiratory tract but tend to be isolated from soils, water, and plants (Coenye 2014; Brenner *et al.* 2005). Therefore, due to the apparent lower level of

contamination than competitors and that few of these contaminants are found in the respiratory tract (and so can be excluded from the data set if encountered), FastDNA Spin Kits were chosen for the work described in this thesis. In addition to the intrinsic contamination between types of kits used, batch specific variation has also been observed (Salter *et al.* 2014). Therefore, all DNA extracts were performed with a single kit to eliminate this variation and allow any contaminants to be identified in controls and subtracted from samples if required.

5.5.2. Initial tests for diversity showed potential contamination issues

An initial microbiota investigation using two naïve MF1 mice was carried out. DNA was extracted from nasopharyngeal and bronchoalveolar lavages, and a fragment of the 16S rRNA was amplified to assess the microbiota in the URT and LRT, respectively. Sequencing was then performed using the Ion Torrent platform, as described in Section 2.9. Analysis of sequencing data was performed with assistance from Dr. Adam Berg, Department of Genetics, University of Leicester, who developed the analysis pipeline and provided scripts, displayed in Appendix 10. Figure 5-9 shows the relative abundance of the families identified. The major 19 families are shown, but due to the low abundance of the remaining families it is impractical to display them separately, so these are grouped into “Other”. *Oxalobacteraceae* was the dominating family in both the URT and LRT, on average accounting for 64 % and 66 % of total sequences, respectively. This was mostly due to the high abundance of the genus *Ralstonia*, which accounted for 62 % of total URT sequences and 64 % of total LRT sequences. Although there is some evidence that *Ralstonia* may be a major constituent of the murine and human respiratory tract (Yun *et al.* 2014; Morris *et al.* 2013), it is generally accepted that this genus is a common contaminant encountered in microbiota sequencing, particularly for low bacterial content samples. Contamination may have been introduced by the method of DNA extraction as described previously, or may have been introduced by handling samples in the laboratory. Control measures were implemented in sequencing to attempt to overcome these contamination issues, described in Section 5.5.3.

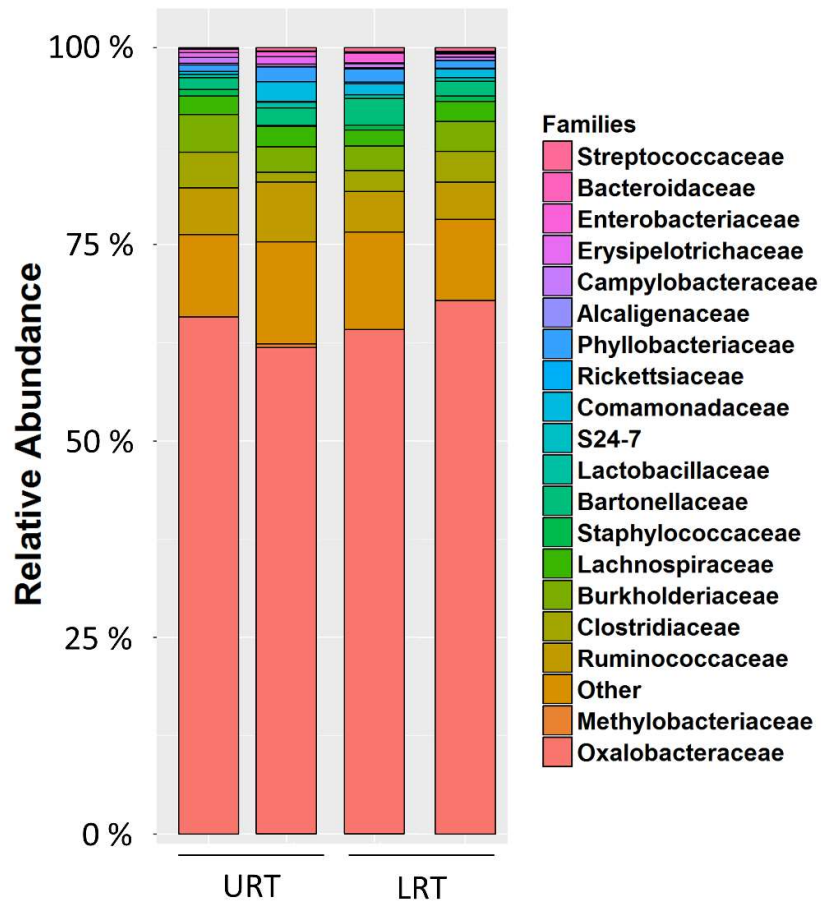


Figure 5-9. Microbiota profiles of the upper and lower respiratory tracts of naïve MF1 mice. Nasal and bronchoalveolar lavages were performed on two naïve MF1 mice to determine the microbiota composition of the upper (URT) and lower (LRT) respiratory tracts, respectively. The relative abundance of the 19 most abundant families are displayed, with all remaining families grouped into “Other”. S24-7 is a family within the order Bacteroidales.

5.5.3. Amplification of microbial DNA

Various control measures were implemented in order to overcome the issues encountered during initial microbiota investigations (Section 5.5.2). DNA extractions and the set-up of PCR reactions were performed in a Cat II microbiological cabinet with filter tips, all consumables were UV treated at 700,000 uJ/cm² for 1 hour prior to use, and the cabinet was thoroughly cleaned with bleach and IMS to reduce the possibility of further DNA contamination. Furthermore, as well as test samples, controls were included. DNA extractions were performed on dH₂O to test for contamination arising from the extraction kits and handling samples in the laboratory. DNA extracts were also performed on the medium used for nasal and bronchoalveolar lavages to control for any additional DNA contamination introduced from the lavage medium. These controls are generally referred to as negative extraction controls, being DNA extractions of medium rather than test samples.

In brief, DNA was extracted from nasal and bronchoalveolar lavages from the murine colonisation model (Section 5.4). Five nasal lavages and five bronchoalveolar lavages, one per mouse, were performed for each exposure group (PBS, BC, D39, D39+BC) at both time-points, totalling 80 samples. A fragment of the 16S rRNA gene was then amplified by PCR and PCR products were visualised on agarose gels (Section 2.9). Two example gels, showing PCR products of nasal lavages performed at 7 days post-inoculation, are given in Figure 5-10. All samples have strong and well defined bands at ~400 bp. Each set of PCRs included duplicates of negative extraction controls and negative PCR controls, which consistently showed no products. Negative PCR controls refer to PCR reactions set up with dH₂O instead of template. These results suggested that contamination did not appear to be an issue.

The DNA concentration of each band was quantified using GeneTools (SynGene), samples were pooled at 15 ng/sample, and the pooled DNA was purified (Section 2.9). For the controls, which did not produce a PCR product and therefore could not be quantified, samples were pooled at 1.5 times the largest volume added for a sample. This larger volume was used so that any contaminating sequences in these samples could be identified in sequencing, even if the contamination was at too low a level to

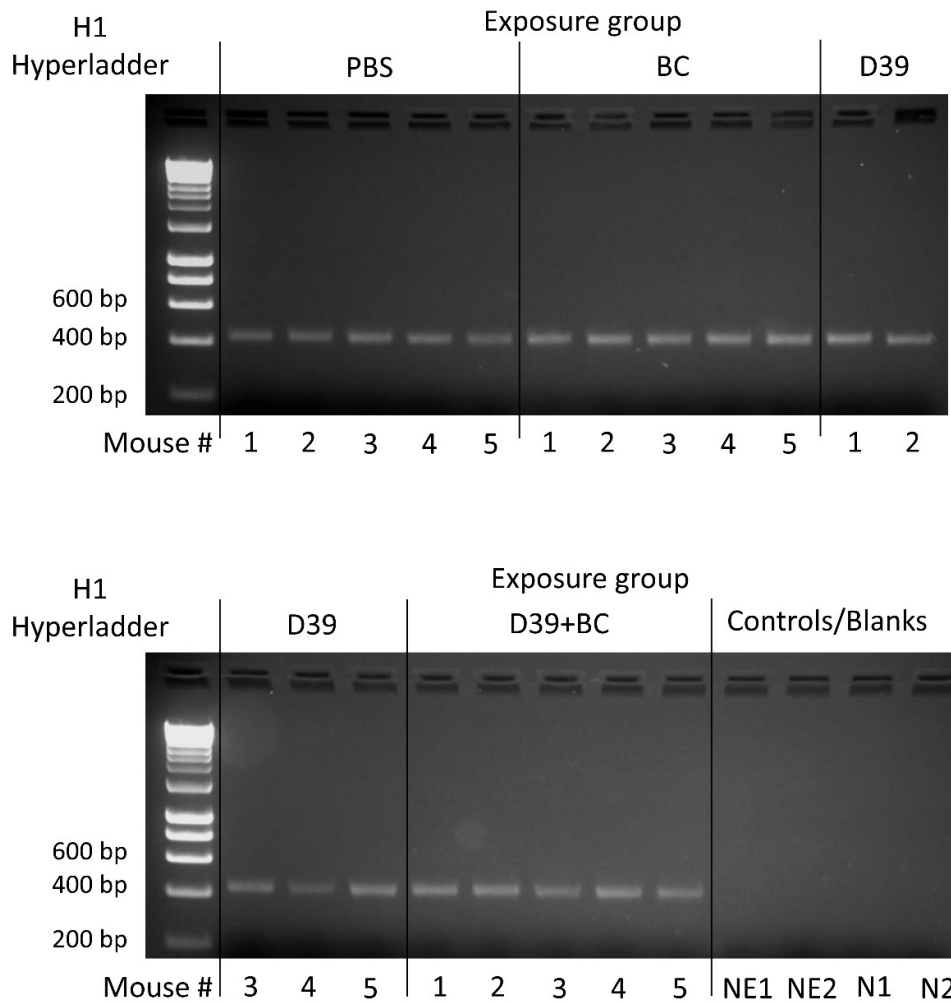


Figure 5-10. Example agarose gel of PCR amplifying microbial 16S DNA from mouse nasal lavages. Female MF1 mice were intranasally inoculated with 15 μ l of PBS (PBS), 100 μ g/ml black carbon (BC), 5×10^5 *S. pneumoniae* D39 (D39), or a mixture of D39 and BC (D39+BC). At 7 days post-inoculation mice were culled and nasal lavages were performed. DNA extractions were performed on lavage fluid and these DNA extractions were put through a PCR protocol to amplify a section of the 16S rRNA gene. 10 μ l of each PCR product was mixed with 2 μ l loading buffer and ran on a 2 % (w/v) agarose gel + 25 μ g/ml ethidium bromide alongside 5 μ l H1 hyperladder. n=5 mice per group. Exposure group refers to which compound mice were intranasally dosed with. Negative Extract 1 (NE1) is the PCR product of a DNA extraction of the medium used to perform nasal lavages. Negative extract 2 (NE2) is the PCR product of a DNA extraction of dH₂O. Negative PCR controls (N1 and N2) containing no template DNA were also included.

appear on the agarose gels. Samples were sequenced by the Genomics Service, University of Leicester, using the Ion Torrent platform.

5.5.4. Ion Torrent output and initial processing

Analysis of sequencing data was again performed with assistance from Dr. Adam Berg, Department of Genetics, University of Leicester, who developed the analysis pipeline and provided scripts. Qiime version 1.9.1 was used for initial processing (Caporaso *et al.* 2010b). The full workflow for bioinformatic analysis is displayed in Appendices 3-9. First, sequence reads were demultiplexed into sample groups according to barcodes and filtered for length (200 to 500 bp), quality (both individual scores and average scores across any 20 bp window less than 20 were removed), and additional threshold criteria (Appendix 3) (Edgar *et al.* 2011). Chimera checking was also performed to remove chimeras, hybrid sequences formed from multiple parent strains during PCR amplification (Edgar *et al.* 2011). To perform open reference operational taxonomic unit (OTU) picking, the usearch61_ref OTU picker (Edgar 2010) was used. A reference sequence set was used to determine the seeds of each cluster. OTUs were clustered based on greater than 97 % similarity of the 16S sequence, and the most abundant sequence within each OTU was elected as the reference sequence for that OTU. Uclust (Edgar 2010) was used to assign taxonomy against the Greengenes reference database (McDonald *et al.* 2012), and the PyNAST aligner (Caporaso *et al.* 2010a) was used to align OTU sequences using the Greengenes core reference alignment (DeSantis *et al.* 2006). It should be noted that no database contains all OTUs and many bacterial species are unknown. Therefore sequences which could not be matched to the database were assigned to the lowest taxonomic classification possible. An OTU table was then produced, and a phylogenetic tree was constructed with FastTree (Price *et al.* 2010). Data was converted to relative abundance for graphical presentation. This allows the major taxa to be shown, however while relative abundance is used to display data, it was not used for statistical analysis.

A total of 5,332,956 raw sequence reads were obtained from chip 1, and 4,954,436 raw sequence reads were obtained from chip 2. After initial quality checks and OTU picking, a total of 4,243,146 reads were clustered and classified for all test samples,

4,756,255 including all controls. The mean number of reads obtained for all test samples was 55,106, with a standard deviation of 13,983. OTUs only present in controls and not samples were discarded, and non-bacterial reads, accounting for ~5 % of all sequences, were removed. OTUs were then merged at family level, leaving 1,500 OTUs containing 921,062 sequences. Therefore during processing, ~90 % of raw data was discarded.

5.5.5. Elimination of contamination

A variety of 16S sequences were identified in both negative extraction controls and negative PCR controls (Figure 5-11), showing that contamination had been introduced during the preparation of samples for sequencing. Interestingly, there were no differences in the diversity of sequences between the two types of negative extraction controls (dH₂O/medium), which implied that the contamination observed was not derived from the lavage medium. Therefore these were grouped together for data presentation. *Enterobacteriaceae*, *Oxalobacteraceae*, *Chitinophagaceae*, 4389128 (an OTU grouping of Cyanobacteria), and *Rhodospirillaceae* are some of the major families identified, although there is variation between the two control sets (Figure 5-11). This contamination was surprising as no PCR products were seen on agarose gels for any controls (Section 5.5.3. Figure 5-10), and attempts were made to reduce laboratory contamination as far as possible.

On average, 2,225 (SD±2,042) sequences were obtained from each negative PCR control after initial quality checks, clustering, and classification, and the top 19 families identified represent 97 % of all sequences. In contrast, for negative extraction controls, 94 (SD±289) sequences were obtained for each sample and the top 19 families represent 80 % of all sequences. Therefore it is clear that negative extraction controls contained fewer sequences, but more diverse contamination, than negative PCR controls. This lower level of contamination was unexpected as the negative extraction controls were subjected to the same preparation steps as negative PCR controls, and had the additional prior DNA extraction step. Although far fewer reads were identified in controls in comparison to test samples (55,106 reads, SD±13,983), contamination, and potentially processing errors, appeared to be an issue within this experiment.

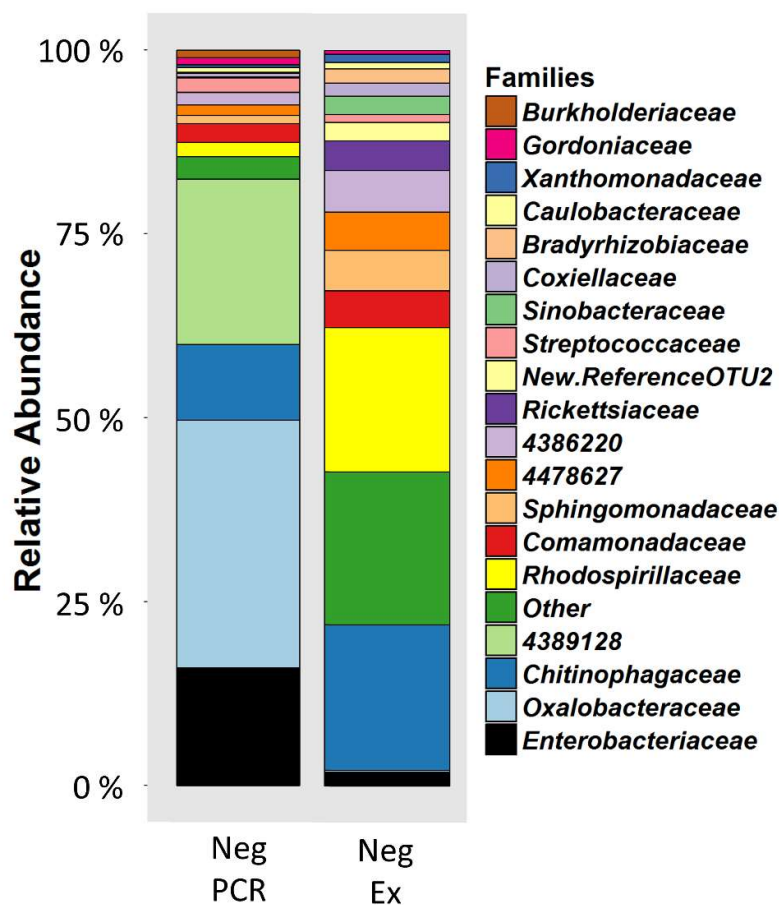


Figure 5-11. Microbiota profiles of the negative PCR reaction controls and negative extraction controls. Negative PCR controls (Neg PCR) are the sequenced products of negative/blank PCR reactions, n=6. Negative extraction controls (Neg Ex) are the sequenced products of PCR reactions of dH₂O and THY, the medium used for lavages, after DNA extraction, n = 24. Data is averaged and the 19 most abundant families are displayed, with all remaining families grouped into “Other”. Some operational taxonomic units (OTUs) could not be defined to family level. Known taxonomic groupings containing these OTUs are: 4389128-Phylum: Cyanobacteria. 4478627-Phylum: Proteobacteria, Order: Rickettsiales. 4386220-Phylum: Alphaproteobacteria, Order: Rhizobiales. New.ReferenceOTU2-Phylum: Acidobacteria, Order: Ellin6513.

Figure 5-12 shows the OTUs identified in test samples, averaged for each group. All twelve most abundant OTUs were also identified in control samples, where they were assumed to be the result of contamination. Therefore it is probable that in test samples, either the entire OTU or a proportion of these OTUs was the result of contamination. To address this issue of contamination, contaminants were removed using the data obtained from controls. First, OTUs accounting for less than 1 % of fewer than 3 control samples were removed from controls (Jervis-Bardy *et al.* 2015; Krone *et al.* 2014). This was done to prevent extremely low level OTUs in controls influencing contaminant removal. Subsequently, any OTUs present in more than 30 % of negative extraction controls were removed from test samples. Additionally, any OTUs making up greater than 1 % of sequences, in at least 30 % of negative PCR controls, were also removed from the test dataset. These different approaches were used due to the lower reads obtained from negative extraction controls, requiring a lower threshold.

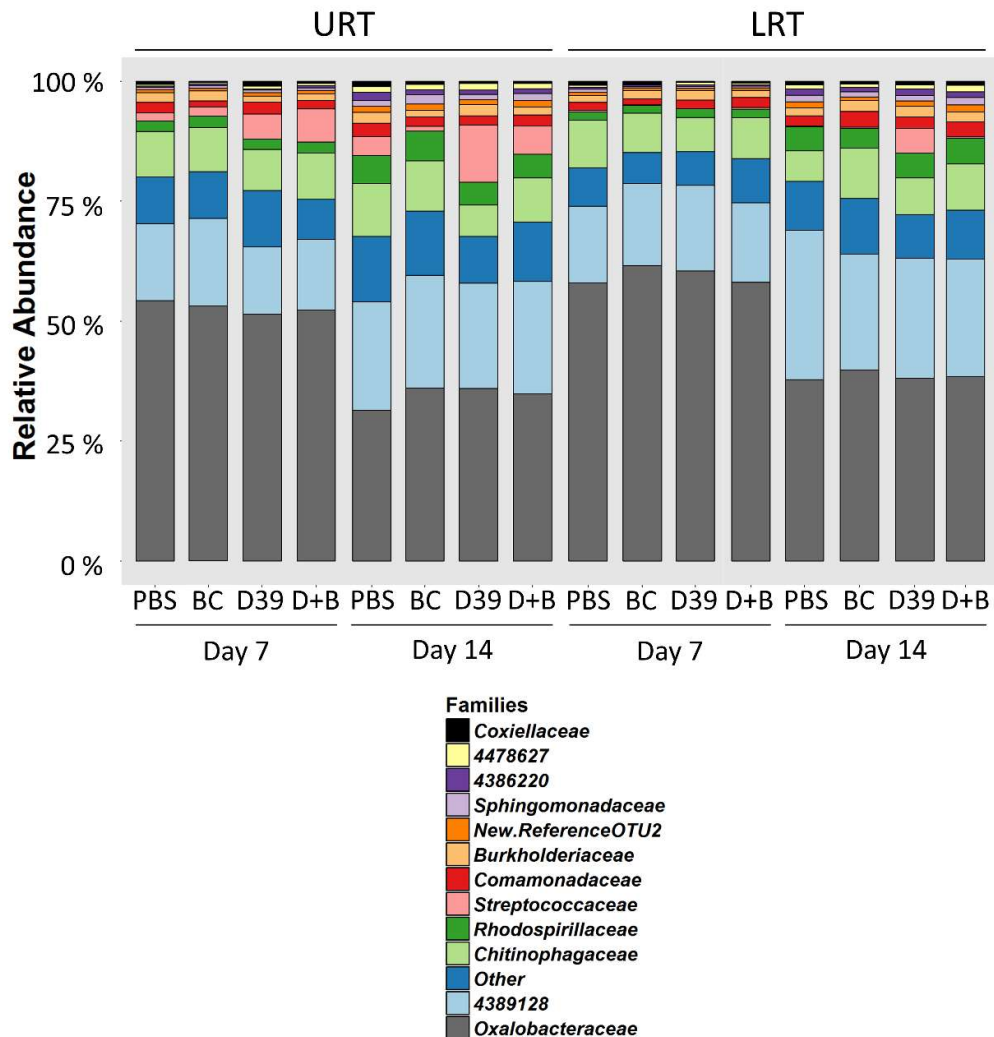


Figure 5-12. Microbiota profiles of the upper and lower respiratory tracts of mice prior to removal of contaminants. MF1 mice were intranasally inoculated with 15 μ l PBS, 7 mg/ml black carbon (BC), 6.45×10^5 CFU of *S. pneumoniae* D39 (D39), or a combination of BC and *S. pneumoniae* D39 (D+B). Nasal and bronchoalveolar lavages were performed at 7 and 14 days post-inoculation to determine the microbiota composition of the upper (URT) and lower (LRT) respiratory tracts, respectively. $n=5$ mice per group and per time-point, except for the D39 group at 14 days post-inoculation, where $n=4$. Data for mice within each group is averaged and displayed as relative abundance. The 12 most abundant families determined for all groups are displayed, with all remaining families grouped into “Other”. The full dataset was used to construct this figure prior to the removal of contaminants. Some operational taxonomic units (OTUs) could not be defined to family level. Known taxonomic groupings containing these OTUs are: 4389128-Phylum: Cyanobacteria. New.ReferenceOTU2-Phylum: Acidobacteria, Order: Ellin6513. 4386220-Phylum: Alphaproteobacteria, Order: Rhizobiales. 4478627-Phylum: Proteobacteria, Order: Rickettsiales.

5.5.6. Sequences identified

Figures 5-13 and 5-14 show the relative abundance of dominant families of test samples, averaged for each group, after subtraction of contaminants. Information about each of these families is displayed in Table 5-1. On average, 44 % (lowest 34 %, highest 56 %) of sequences are displayed as “other”, therefore the top 14 families generally make up over 50 % of sequences. The major two families present in all URT samples at both 7 and 14 days post-inoculation were *Streptococcaceae* and *Burkholderiaceae* (Figure 5-13). *Streptococcaceae* constituted 15 %, 15 %, 26 %, and 39 % of sequences of the PBS, BC, D39, and D39+BC groups at 7 days, and 21 %, 8 %, 33 %, and 33 % at 14 days, respectively. Therefore the mice inoculated with *S. pneumoniae* had the most *Streptococcaceae* at both time-points. Interestingly, the abundance of *Streptococcaceae* increased from 7 to 14 days for the PBS and D39 groups, but fell for the BC and D39+BC groups. It is also notable that there were far less *Streptococcaceae* in the BC group at the 14 day time-point compared to all other groups. Generally, there was little variation between the abundance of *Burkholderiaceae* between groups and time-points, with one exception. At 7 days, *Burkholderiaceae* contributed slightly less to the URT microbiota in the D39 group (9 %) compared to other groups (12-18 %), which corresponded with a slight increase in *Enterobacteriaceae* and *Propionibacteriaceae*. Apart from this, the 12 most abundant families following *Streptococcaceae* and *Burkholderiaceae* were fairly evenly split.

In contrast, *Streptococcaceae* were not as prevalent in the LRT (Figure 5-14). The major family identified at both 7 and 14 days was *Burkholderiaceae*, with similar levels in all groups at both time-points, but slightly more at 7 days post-inoculation. At 7 days, the remaining 12 most abundant families were fairly evenly distributed, with the notable lack of *Streptococcaceae* and corresponding slight increase in *Propionibacteriaceae* in the D39 group. At 14 days there was more variation between groups and the D39 group was the only one to contain a notable amount of *Streptococcaceae* (19 %), which was the second most abundant family.

Figures 5-15 and 5-16 again display the relative abundance of families identified in test samples, but grouped into phyla. These figures show that for all URT samples at both 7

and 14 days post-inoculation (Figure 5-15), Firmicutes and Proteobacteria were the major phyla. For mice in the D39 and D39+BC group, Firmicutes represented 30-40 % of all sequences at 7 and 14 days, which is mainly due to the presence of *Streptococcaceae*. The second most abundant phyla for these groups was Proteobacteria, containing *Burkholderiaceae*, contributing ~20 % of sequences at both time-points. In contrast, levels of Firmicutes and Proteobacteria were similar in the PBS and BC groups at both time-points, representing ~10-20 % and ~25 % of sequences, respectively.

In the LRT (Figure 5-16), Firmicutes represented a much lower proportion of sequences due to less *Streptococcaceae*. At both 7 and 14 days, Proteobacteria were the dominating phylum, making up ~30 % of sequences regardless of exposure group and time-point. This was then followed by Firmicutes, which generally constituted less than 10 % of sequences apart from in the D39 group at 14 days (~20 %) due to the presence of more *Streptococcaceae*. For all groups at both time-points, Actinobacteria represent less than ~10 % of sequences, and Acidobacteria and Cyanobacteria represent less than ~5 % of sequences combined.

Therefore overall, there were no great differences between the microbiota of any group. Neither pneumococcal colonisation nor BC inhalation, separately or in the co-inoculation condition, had any notable effect on the abundance of any family apart from *Streptococcaceae*. Furthermore, there were no overt time-dependent differences. Generally, besides the greater abundance of *Streptococcaceae* in the URT, there were also no prominent differences between the microbiota of the URT or LRT. One potentially notable exception to this is the increased representation of *Methylobacteriaceae* in the LRT of the PBS condition at 14 days, in comparison to the URT.

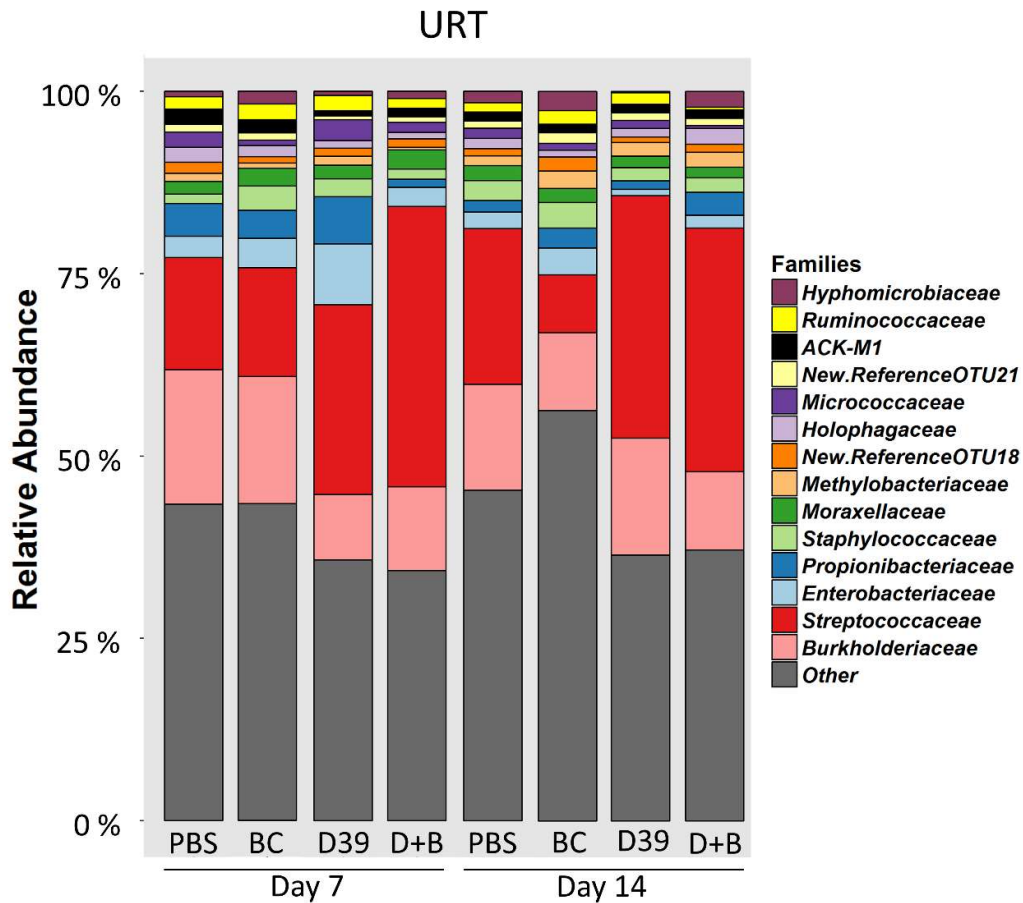


Figure 5-13. Microbiota profiles of the murine upper respiratory tract at 7 and 14 days post-inoculation. MF1 mice were intranasally inoculated with 15 μ l PBS, 7 mg/ml black carbon (BC), 6.45×10^5 CFU of *S. pneumoniae* D39 (D39), or a combination of BC and *S. pneumoniae* D39 (D+B). Nasal lavages were performed at 7 and 14 days post-inoculation to determine microbiota composition of the upper respiratory tract (URT). n=5 mice per group and per time-point, except for the D39 group at 14 days post-inoculation, where n=4. Data for mice within each group is averaged and displayed as relative abundance. The 14 most abundant families determined for all groups are displayed, with all remaining families grouped into “Other”. Some operational taxonomic units (OTUs) could not be defined to family level. Known taxonomic groupings containing these OTUs are: New.ReferenceOTU18-Phylum: Actinobacteria, Order: Gaiellaceae. New.ReferenceOTU21-Phylum: Cyanobacteria, Order: ML635J-21. ACK-M1-Phylum: Actinobacteria.

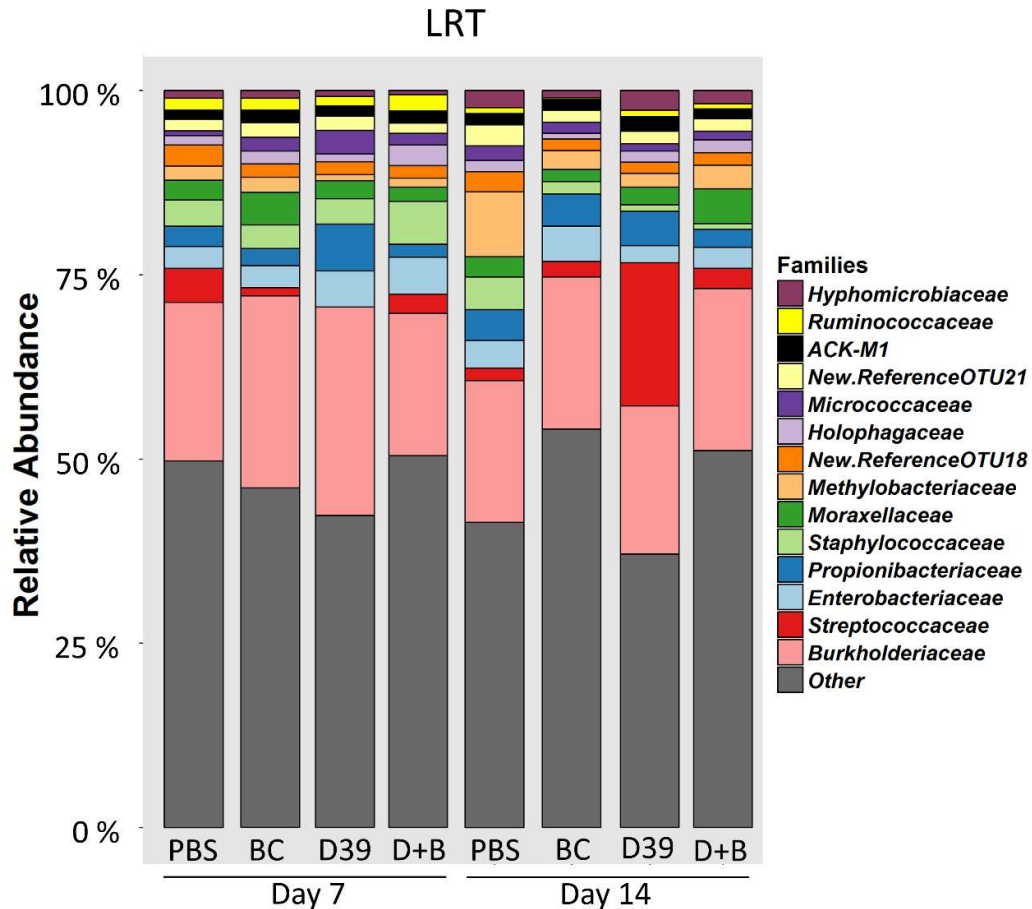


Figure 5-14. Microbiota profiles of the murine lower respiratory tract at 7 and 14 days post-inoculation. MF1 mice were intranasally inoculated with 15 μ l PBS, 7 mg/ml black carbon (BC), 6.45×10^5 CFU of *S. pneumoniae* D39 (D39), or a combination of BC and *S. pneumoniae* D39 (D+B). Bronchoalveolar lavages were performed at 7 and 14 days post-inoculation to determine microbiota composition of the lower respiratory tract (LRT). n=5 mice per group and per time-point, except for the D39 group at 14 days post-inoculation, where n=4. Data for mice within each group is averaged and displayed as relative abundance. The 14 most abundant families determined for all groups are displayed, with all remaining families grouped into “Other”. Some operational taxonomic units (OTUs) could not be defined to family level. Known taxonomic groupings containing these OTUs are: New.ReferenceOTU18-Phylum: Actinobacteria, Order: Gaiellaceae. New.ReferenceOTU21-Phylum: Cyanobacteria, Order: ML635J-21. ACK-M1-Phylum: Actinobacteria.

Table 5-1. The 14 most abundant families identified in sequencing of the murine respiratory tract microbiota, after removal of contaminants. Phyla abbreviations: Acido - Acidobacteria. Cyano –Cyanobacteria.

Phylum and Family		Gram Reaction	Notable members and typical environment	Reference
Firmicutes	<i>Streptococcaceae</i>	Positive	3 genera: <i>Streptococcus</i> (type genus), <i>Lactococcus</i> , <i>Lactovum</i> . Animal and human pathogens, including <i>S. pyogenes</i> and <i>S. pneumoniae</i> . <i>S. pneumoniae</i> D39 was inoculated into mice in the D39 and D39+BC groups in this study	(du Toit <i>et al.</i> 2014; De Vos <i>et al.</i> 2009)
	<i>Staphylococcaceae</i>	Positive	6 genera: <i>Staphylococcus</i> (type genus), <i>Gemella</i> , <i>Jeotgalicoccus</i> , <i>Macrococcus</i> , <i>Nosocomiicoccus</i> , <i>Salinicoccus</i> . Human and animal hosts. Important pathogens include <i>S. aureus</i> (human+animal), <i>S. intermedius</i> (animal) and <i>S. hyicus</i> (human+animal)	(Lory 2014)
	<i>Ruminococcaceae</i>	Positive and Negative	11 genera. Type genus: <i>Ruminococcus</i> Obligate anaerobes. Often environmental and intestinal isolates.	(De Vos <i>et al.</i> 2009)
Proteobacteria	<i>Burkholderiaceae</i>	Negative	11 genera. Type genus: <i>Burkholderia</i> . Diverse family. Mostly soil and water associated. Important pathogens include <i>B. mallei</i> and <i>B. pseudomallei</i>	(Coenye 2014; Brenner <i>et al.</i> 2005)
	<i>Enterobacteriaceae</i>	Negative	51 genera. Type genus: <i>Escherichia</i> . Very large family. Environmental (soil, water, plants, meats), animal, and human isolates (often intestinal).	(Octavia & Lan 2014; Brenner <i>et al.</i> 2010)
	<i>Moraxellaceae</i>	Negative	6 genera. Type genus: <i>Moraxella</i> Human and animal pathogens, as well as water and soil bacteria. Key pathogens include <i>M. catarrhalis</i> (human) and <i>M. bovis</i> (cattle).	(Teixeira & Merquior 2014; Brenner <i>et al.</i> 2010)

	<i>Methylobacteriaceae</i>	Negative	3 genera: <i>Methylobacterium</i> (type genus), <i>Microvirga</i> , and <i>Meganema</i> . Widely distributed in nature. Associated with soil, water, plants. Some human pathogens	(Brenner <i>et al.</i> 2005)
	<i>Hyphomicrobiaceae</i>	Negative	18 genera. Type genus: <i>Hyphomicrobium</i> . Diverse family. Avirulent. Associated with water and soil	(Oren & Xu 2014; Brenner <i>et al.</i> 2005)
Actinobacteria	<i>Propionibacteriaceae</i>	Positive	13 genera. Type genus: <i>Propionibacterium</i> Dairy isolates, skin flora, fermenting food and plant material, water, soil, and gut isolates.	(Goodfellow <i>et al.</i> 2012)
	OTU18 (Order: Gaiellales)	Negative	The novel family (Gaiellales), order (Gaiellaceae), genus, and species (<i>Gaiella occulta</i>) was described in 2011. Recovered from a deep mineral water aquifer.	(Albuquerque <i>et al.</i> 2011)
	<i>Micrococcaceae</i>	Positive	12 genera. Type genus: <i>Micrococcus</i> . Skin, respiratory tract, and air isolates. <i>M. luteus</i> is an important pathogen	(Goodfellow <i>et al.</i> 2012)
	ACK-M1		Freshwater cluster defined in 2002. No other information available.	(Zwart <i>et al.</i> 2002)
Acido	<i>Holophagaceae</i>	Negative	Only family of the order Holophagales. 2 genera: <i>Holophaga</i> (type genus) and <i>Geothrix</i> . The only <i>Holophaga</i> species was isolated from black anoxic mud. The only <i>Geothrix</i> was isolated from petroleum-contaminated aquifer sediment. Both are anaerobic.	(Fukunaga & Ichikawa 2014; Bergey 2010)
Cyano	OTU21 (Order: ML635J- 21)	Negative	Named in the Greengenes and Silva databases. No other information available.	(Soo <i>et al.</i> 2014; Quast <i>et al.</i> 2013; McDonald <i>et al.</i> 2012)

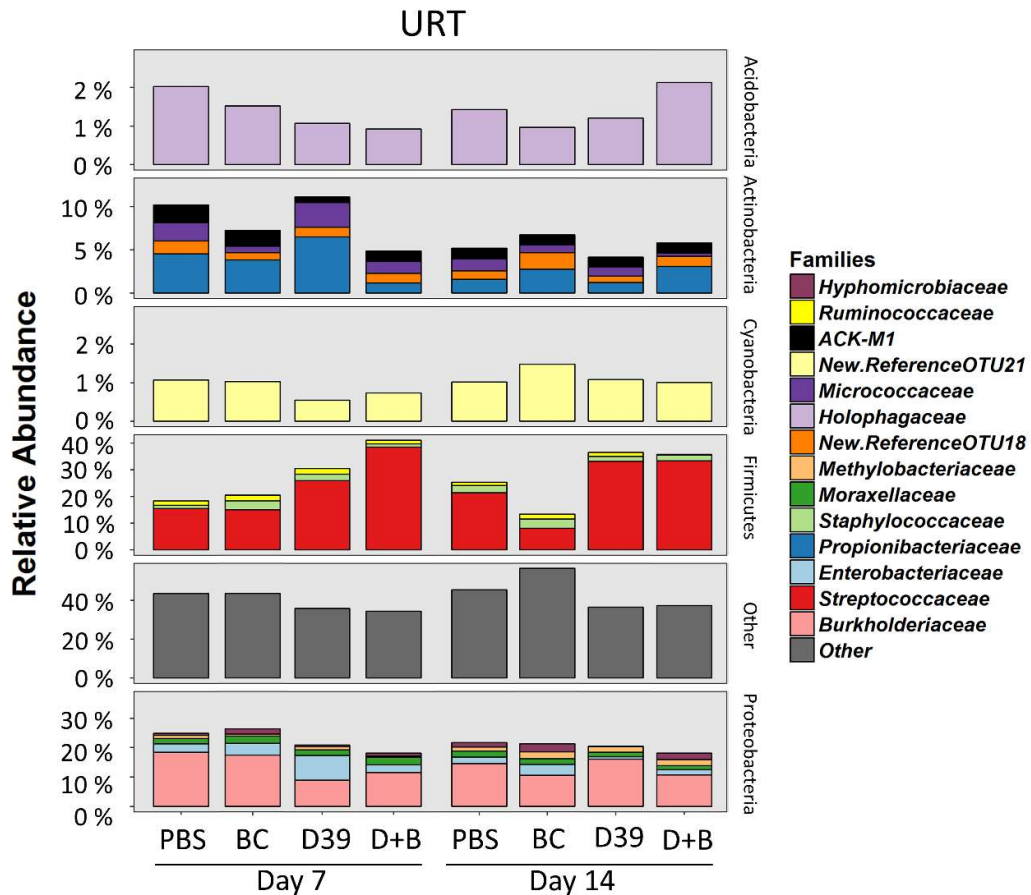


Figure 5-15. Microbiota profiles of the murine upper respiratory tract at 7 and 14 days post-inoculation, faceted by phylum. MF1 mice were intranasally inoculated with 15 μ l PBS, 7 mg/ml black carbon (BC), 6.45×10^5 CFU of *S. pneumoniae* D39 (D39), or a combination of BC and *S. pneumoniae* D39 (D+B). Nasal lavages were performed at 7 and 14 days post-inoculation to determine microbiota composition of the upper respiratory tract (URT). $n=5$ mice per group and per time-point, except for the D39 group at 14 days post-inoculation, where $n=4$. Data for mice within each group is averaged and displayed as relative abundance. The 14 most abundant families determined for all groups are displayed, with all remaining families grouped into “Other”. Some operational taxonomic units (OTUs) could not be defined to family level. Known taxonomic groupings containing these OTUs are: New.ReferenceOTU18-Phylum: Actinobacteria, Order: Gaiellaceae. New.ReferenceOTU21-Phylum: Cyanobacteria, Order: ML635J-21. ACK-M1-Phylum: Actinobacteria.

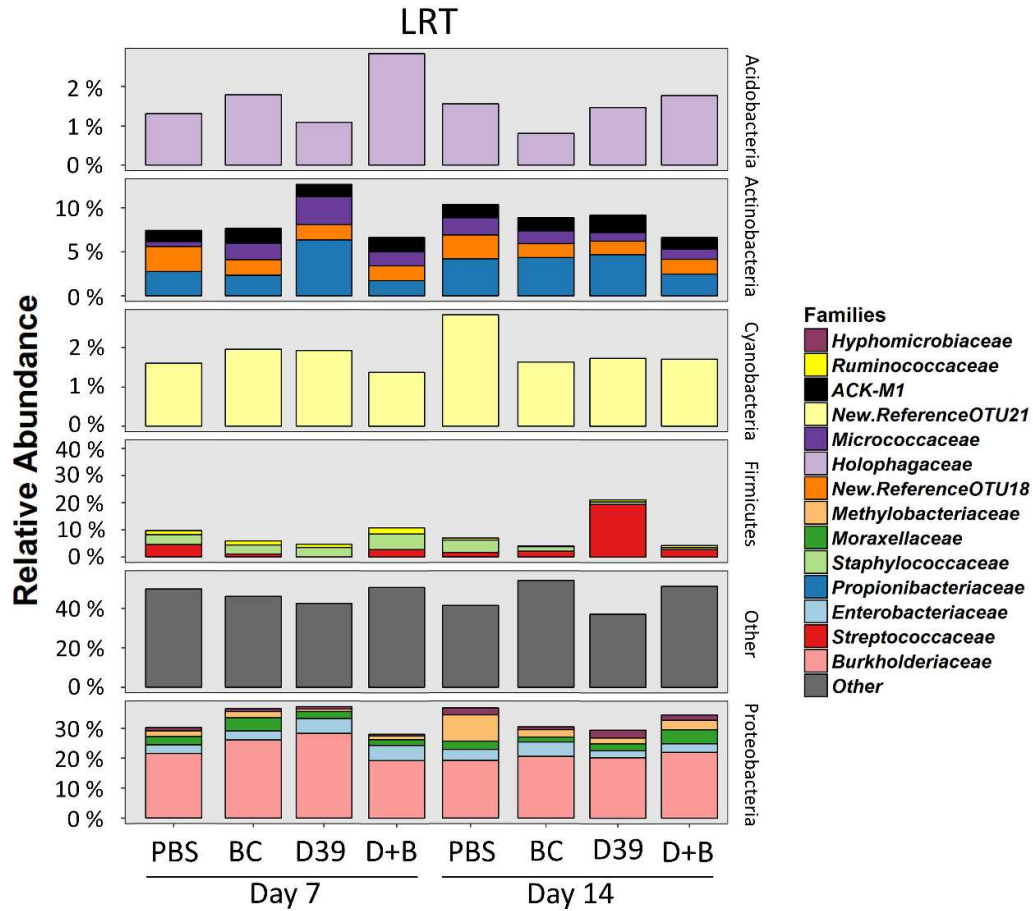


Figure 5-16. Microbiota profiles of the murine lower respiratory tract at 7 and 14 days post-inoculation, faceted by phylum. MF1 mice were intranasally inoculated with 15 μ l PBS, 7 mg/ml black carbon (BC), 6.45×10^5 CFU of *S. pneumoniae* D39 (D39), or a combination of BC and *S. pneumoniae* D39 (D+B). Bronchoalveolar lavages were performed at 7 and 14 days post-inoculation to determine microbiota composition of the lower respiratory tract (LRT). $n=5$ mice per group and per time-point, except for the D39 group at 14 days post-inoculation, where $n=4$. Data for mice within each group is averaged and displayed as relative abundance. The 14 most abundant families determined for all groups are displayed, with all remaining families grouped into “Other”. Some operational taxonomic units (OTUs) could not be defined to family level. Known taxonomic groupings containing these OTUs are: New.ReferenceOTU18-Phylum: Actinobacteria, Order: Gaiellaceae. New.ReferenceOTU21-Phylum: Cyanobacteria, Order: ML635J-21. ACK-M1-Phylum: Actinobacteria.

5.5.7. Alpha Diversity

Alpha diversity (Whittaker 1972) describes the mean diversity in a sample based on richness (the number of OTUs present) and evenness (the distribution of those OTUs). However there is danger in reducing diversity to a single value as with this metric because an apparently diverse sample may contain a high richness but an uneven distribution of OTUs, or a low richness but with an even distribution of OTUs (Purvis & Hector 2000). The experimenter may therefore draw a false negative result when comparing the diversity of these two samples, despite the samples being quite different. This means that care should be taken when comparing the diversity of samples based solely on alpha diversity. For this reason, use of multiple measures of alpha diversity provide a more robust approach than a single metric.

The Shannon index (Shannon 1948) and Simpson index of diversity (Simpson 1949) were used to assess alpha diversity of microbial communities, results of which are given in Figure 5-17. For these indices, the greater the value calculated, the more diverse a community is. It is clear that there is a high degree of correlation in the results from both formulae. In general, there is more variation in alpha diversity within some groups compared to others. For example the alpha diversity of the URT microbiota of mice in the D39+BC is more varied than other groups, at both 7 and 14 days post-inoculation. However, there were no significant differences ($p>0.05$) between any groups in the URT or LRT at either time-point, using either index. Therefore it appears that inhalation of BC, colonisation of *S. pneumoniae* D39, and the co-inoculation of BC and pneumococci, had no effect on alpha diversity of the respiratory tract microbiota in this colonisation assay.

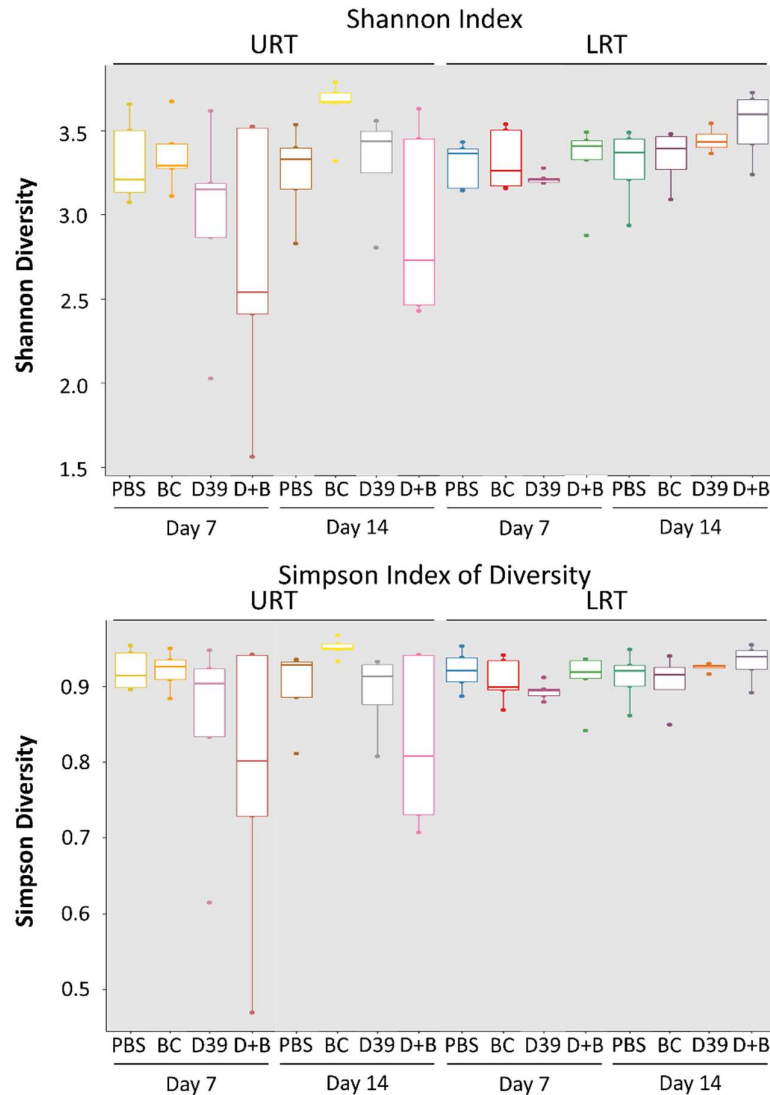


Figure 5-17. Alpha diversity analysis. MF1 mice were intranasally inoculated with 15 μ l PBS, 7 mg/ml black carbon (BC), 6.45×10^5 CFU of *S. pneumoniae* D39 (D39), or a combination of BC and *S. pneumoniae* D39 (D+B). Nasal and bronchoalveolar lavages were performed at 7 and 14 days post-inoculation to determine microbiota composition of the upper (URT) and lower (LRT) respiratory tracts, respectively. $n=5$ mice per group and per time-point, except for the D39 group at 14 days post-inoculation, where $n=4$. The Shannon index and Simpson index of diversity were used to evaluate alpha diversity. The greater the index value, the more diverse the community. Shown are the 25th to 75th percentiles (boxes), with whiskers extending to the last value which falls within 1.5 x the interquartile range. A line within each box denotes the median. Outliers are displayed as extra points outside the range of whiskers. One-way ANOVA with Tukey's multiple comparisons tests were performed to test for significant differences between the PBS, BC, D39, and D39+BC groups within the URT and LRT at 7 and 14 days post-inoculation. No significant differences ($p>0.05$) were identified.

5.5.8. Beta Diversity and Non-metric Multidimensional Scaling

Beta diversity (Whittaker 1972) describes the difference in diversity between samples along gradients. Nonmetric Multidimensional Scaling (NMDS) was used to visualise the differences between data using the Bray-Curtis dissimilarity. NMDS is a distance-based approach to ordination which uses rank orders. This means that NMDS ranks the distances between samples and these ranks are used to map the samples onto an ordination (Shepard 1966). Therefore the proximity between samples reflects their similarity (Ramette 2007). To do this, the difference between the rank order of distances in the ordination and the rank order of distances in the data is calculated (the stress), and samples are presented in a way as to reduce stress to a minimum so that the presented ordination represents the data as far as possible. Additionally, NMDS makes fewer assumptions regarding the data presented, unlike other techniques such as Principal Coordinates Analysis (PCoA). NMDS is a means of visualising data, and requires input information to be in the form of a distance matrix. The Bray-Curtis dissimilarity is reported to provide robust and effective NMDS ordinations (Legendre & De Cáceres 2013; Faith *et al.* 1987), therefore the Bray-Curtis dissimilarity was chosen. Figures 5-18 and 5-19 show the NMDS analysis compressed into two arbitrary dimensions. It is important to note that neither axis of an NMDS plot are more important than another. No clustering was evident and there was no discernible difference between the PBS, BC, D39, or D39+BC groups within the URT (Figure 5-18) or LRT (Figure 5-19) at either 7 (Figure 5-13 A and 5-14 A) or 14 (Figure 5-13 B and 5-14 B) days post-inoculation.

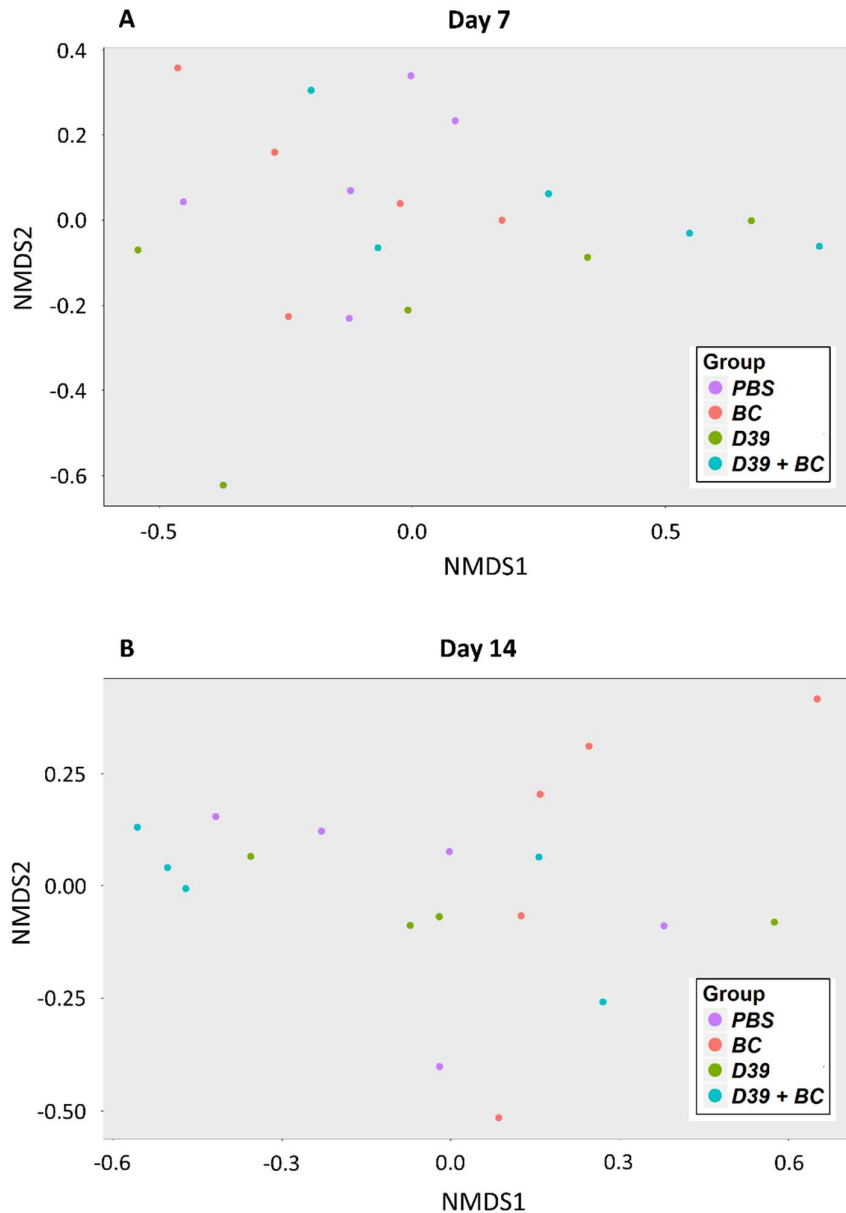


Figure 5-18. Non-metric Multidimensional Scaling (NMDS) analysis of the upper respiratory tract microbiota profiles of MF1 mice subjected to Bray-Curtis similarity coefficient transformation. 16S amplicon Ion Torrent sequencing of the upper respiratory tract of mice following intranasal inoculation of 15 μ l PBS (purple), 7 mg/ml black carbon (BC, red), 6.45×10^5 CFU of *S. pneumoniae* D39 (D39, green), or a combination of BC and *S. pneumoniae* D39 (D39+BC, blue), at 7 (A) and 14 (B) days post-inoculation. $n=5$ mice per group and per time-point, except for the D39 group at 14 days post-inoculation, where $n=4$. Axis represents the scale for similarity distance scores.

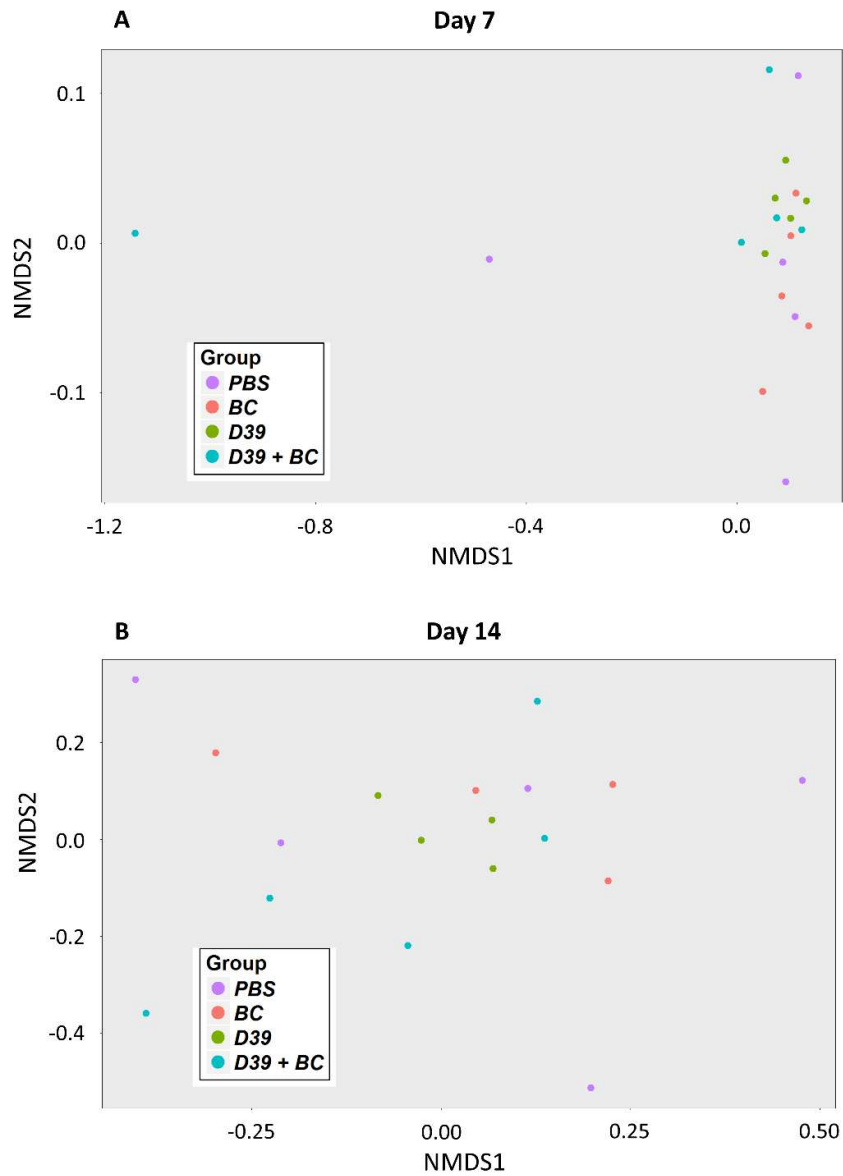


Figure 5-19. Non-metric Multidimensional Scaling (NMDS) analysis of the lower respiratory tract microbiota profiles of MF1 mice subjected to Bray-Curtis similarity coefficient transformation. 16S amplicon Ion Torrent sequencing of the lower respiratory tract of mice following intranasal inoculation of 15 μ l PBS (purple), 7 mg/ml black carbon (BC, red), 6.45×10^5 CFU of *S. pneumoniae* D39 (D39, green), or a combination of BC and *S. pneumoniae* D39 (D39+BC, blue), at 7 (A) and 14 (B) days post-inoculation. n=5 mice per group and per time-point, except for the D39 group at 14 days post-inoculation, where n=4. Axis represents the scale for similarity distance scores.

5.5.9. Statistical analysis

Phyloseq and Vegan were used to analyse data in R version 3.2.3 (Oksanen *et al.* 2016; R Core Team 2015; McMurdie & Holmes 2013). The adonis permutational multivariate analysis of variance (Anderson 2001) and betadisper (Anderson 2006; Anderson *et al.* 2006) were used to determine whether there was a significant difference between any groups, using both Bray-Curtis (Bray & Curtis 1957) and UniFrac (Lozupone *et al.* 2011; Lozupone & Knight 2005) distance matrices (Oksanen *et al.* 2016). These two distance matrices were employed to assess whether the similarity metric affected the outcome of the analysis, which it did not. The Bray-Curtis dissimilarity takes abundance into account and provides a measure of community structure. Furthermore, Bray-Curtis is not affected by differences in total abundance or the addition or lack of taxonomic groups between samples, and can recognise differences in total abundances even when relative abundances are the same. Unifrac takes abundance into account and in addition, incorporates phylogenetic information to see how related OTUs are. Betadisper acts as a counterpart to comment on the validity of an adonis result. This is because adonis tests the differences in means of groups, and betadisper compares the spread of data in these groups. A significant adonis value means that the data centroids are significantly different, and a non-significant betadisper value reinforces this by showing that the data sets being compared have a similar dispersion. Additionally, data was assessed using DESeq2 (Love *et al.* 2014), and by Multiple Testing in Phyloseq (McMurdie & Holmes 2013) to assess specific changes in abundance of families. Tests were adjusted for multiple testing using the Benjamini-Hochberg false discovery rate (FDR) correction method, to control for type I errors (Benjamini & Hochberg 1995).

No significant differences ($p > 0.05$) were identified between any group (PBS, BC, D39, D39+BC) in either the URT or LRT, at either time-point, with any test. Furthermore, no significant differences were identified between the URT and LRT, or between 7 and 14 days post-inoculation. Therefore in this study, it appears that inhalation of BC and colonisation of *S. pneumoniae* D39, separately and in conjunction with each other, had no significant effect on the respiratory tract microbiota.

5.6. Discussion

This chapter aimed to identify whether BC exposure altered respiratory tract colonisation of *S. pneumoniae*, and secondly, to assess the effects of BC exposure, pneumococcal colonisation, and BC-pneumococcal co-inhalation on the respiratory tract microbiota. Our data demonstrate that BC promotes dissemination of *S. pneumoniae*, the leading cause of bacterial pneumonia worldwide, from the URT to the LRT in an *in vivo* pneumococcal colonisation model. These data thereby demonstrate that a significant biological effect of air pollution has been overlooked. Inhalation of BC, *S. pneumoniae* D39, or the combination of D39 and BC, appeared to have no measurable effect on the microbiota of either the upper or lower respiratory tract in this initial experiment.

5.6.1. Preliminary work for the murine colonisation model

It was confirmed that up to 100 µg of BC suspended in 50 µl PBS caused no overt signs of disease in MF1 mice. It has been reported that doses of up to 500 µg BC in 50 µl can be tolerated by this mouse strain (Tellabati *et al.* 2010), therefore these results were expected. At 7 days post-inoculation, BC had been taken up by alveolar macrophages (AM) in the high-dose group (100 µg BC in 50 µl PBS) and collections of BC-loaded AM could be seen. Carbon-loaded AM have been recovered from the lungs of people naturally exposed to normal levels of air pollution, particularly in the developing world, and this phenotype has been reproduced both *in vivo* and *in vitro* using a variety of exposure protocols to BC and PM (Rylance *et al.* 2015; Zhao *et al.* 2012; Tellabati *et al.* 2010; Fullerton *et al.* 2009; Lundborg *et al.* 2007; Zhou & Kobzik 2007; Renwick 2004). Therefore this preliminary work showed the expected response to BC inhalation. Interestingly however, past research has reported variation in the observed effects of PM and BC, with some studies identifying no pathological effects (Tuan *et al.* 2015; Guarnieri *et al.* 2015; MacIntyre *et al.* 2014; Zhou & Kobzik 2007; Anderson *et al.* 2001; Yang *et al.* 2001). In contrast to the high-dose group, the majority of BC had been eliminated from the low-dose group (5 µg BC in 50 µl PBS) but at 7 days post-inoculation, no carbon-loaded AM were observed. It is possible that particles in this

group were cleared by mucociliary clearance, as this is a major particle clearance mechanism, whereas this may not have been sufficient for the high-dose group (Thurston & Lippmann 2015).

The objective of the *in vivo* work described in this thesis was to allow the assessment of the effect of BC on pneumococcal colonisation. Animal passaging is routinely performed prior to murine assays in order to standardise strain virulence (Canvin *et al.* 1995). Passaging selects for bacteria which are able to cause septicaemia, and there are distinct patterns of gene expression associated with recovering pneumococci from the blood compared to the lungs (Oggioni *et al.* 2006). Therefore it was decided to perform this work with non-passaged pneumococci as the predisposition of the bacterial population towards a septicaemia causing phenotype was not desired.

As pneumococci primarily colonise the nasopharynx (Shak *et al.* 2013b; Simell *et al.* 2012; Hogberg *et al.* 2007), inoculation procedures were required to restrict inoculation of BC and pneumococci to the URT and promote nasopharyngeal colonisation. Intranasal inoculation with 1×10^5 - 1×10^7 CFU of *S. pneumoniae* D39 in 10 μ l PBS has been reported to be sufficient to achieve nasopharyngeal colonisation but avoid spread of pneumococci to the lungs (Krone *et al.* 2014; Richards *et al.* 2010; Ogunniyi *et al.* 2007). However, a larger volume was desired for the work described in this thesis to allow a greater dose of BC to be used, but dose volume can directly influence the outcome of intranasal inoculation. Haste *et al.* (2014) has shown that increasing an intranasal dose volume from 20 to 50 μ l, whilst maintaining the total amount of pneumococci suspended in this volume, resulted in an increase in mortality (Haste *et al.* 2014). This effect was due to the upper airways being physically unable to accommodate larger volumes of liquid, causing the inoculum to be displaced to the LRT (Haste *et al.* 2014; Miller *et al.* 2012). Similarly, intranasal inoculation volumes of 10, 20, 50, and 100 μ l of *Francisella tularensis* show that increasing the volume increases the proportion of bacteria which reach the LRT (Miller *et al.* 2012). A preliminary assay showed that an inoculation volume of 15 μ l, containing 5×10^5 CFU *S. pneumoniae* D39, resulted in URT colonisation without detectable levels of pneumococci being inoculated into the LRT (Figure 5-5), therefore this volume was chosen for the colonisation experiment.

5.6.2. BC causes pneumococci to spread to the LRT

The major result of this work is that inhalation of *S. pneumoniae* in the presence of BC promoted dissemination of bacteria to the LRT by 7 days post-inoculation. *S. pneumoniae* is carried asymptomatically in the nasopharynx in up to 88 % of children and up to 20 % of adults (Wyllie *et al.* 2014; Shak *et al.* 2013b; Mook-kanamori *et al.* 2011; Lanie *et al.* 2007; Hussain *et al.* 2005; Bogaert *et al.* 2004) and notably, nasopharyngeal colonisation is required prior to pneumococcal disease (Simell *et al.* 2012; Weiser 2010). This data shows, for the first time, that BC causes *S. pneumoniae* to shift from URT colonisation to dissemination into the LRT, which could be a key factor in how air pollutants cause LRT infections. Transfer to the LRT may provide pneumococci with the opportunity to cause invasive LRT diseases such as pneumonia, and could explain why BC/PM exposure is associated with LRT infections such as pneumonia, and exacerbations of chronic infectious diseases such as asthma and COPD (Brugha & Grigg 2014; MacIntyre *et al.* 2014; Qiu *et al.* 2014; Darrow *et al.* 2014; WHO 2014d; Gittins *et al.* 2013; Janssen *et al.* 2012; WHO 2007).

Interestingly, no signs of disease were observed in mice in this assay. There are two potential hypotheses for why this lack of disease occurred. Firstly, although BC increased the spread of bacteria to the LRT and thereby provided an increased potential to cause disease, it may be that the susceptibility of the host to infection is a defining factor in the outcome of dissemination. Indeed, it is known that PM exposure more adversely affects certain populations than others, including women (Guo *et al.* 2013; Hoek *et al.* 2013; Taylor & Nakai 2012), particularly post-menopausal and pregnant women (Mannucci *et al.* 2015; Miller *et al.* 2007), the elderly over 65 years old (Mannucci *et al.* 2015; Ostro *et al.* 2014; Guo *et al.* 2013), children under 5 years old (Martinelli *et al.* 2013; Taylor & Nakai 2012), those from socially deprived backgrounds (Morelli *et al.* 2016; Hoek *et al.* 2013), the immunocompromised, and those with prior illnesses such as COPD (Faustini *et al.* 2012) and Cystic Fibrosis (CF) (Psoter *et al.* 2015). Alternatively, BC exposure conditions may need to be optimised. In reality, humans are exposed to atmospheric BC over weeks, months, and years. Therefore repeated dosing with BC may be a more realistic exposure model. Indeed,

repeated exposure to cigarette smoke has been shown to exacerbate its effect on bacterial phenotypes (Antunes *et al.* 2012). It is also worth noting that the BC concentration used in this research was based on results from the *in vitro* work described in this thesis, preliminary *in vivo* work, and concentrations used in previous research (Jackson *et al.* 2012a; Tellabati *et al.* 2010). However this concentration far exceeds atmospheric PM concentrations (Section 1.1.4). Although atmospheric PM concentrations and personal PM exposure can be estimated, the concentration of BC deposited on the surface of the respiratory tract at any one time has not been characterised. This is partially because not all PM deposits in the respiratory tract, there is interpersonal variation in inspiration flow rate and volume, and the host continually attempts to clear BC from the surface of the respiratory tract (Thurston & Lippmann 2015; Kelly & Fussell 2012; Heal *et al.* 2012; Peters *et al.* 2006; Briant & Lippmann 1993; Briant & Lippmann 1992). Therefore, future work may advance on this research by exposing mice to aerosolised BC (Noël *et al.* 2015; Jackson *et al.* 2012a; Jackson *et al.* 2012b; Gallagher *et al.* 2003; Yin *et al.* 2003; Yin *et al.* 2002) at a concentration matching atmospheric conditions over a longer time period. This may potentiate the colonisation phenotype and could be associated with the development of disease.

It is interesting that the BC-induced dispersion of pneumococci to the LRT was a transient effect, as there were no pneumococci present in the LRT at 14 days. In a previous study, rats exposed to diesel exhaust particles and later challenged with *L. monocytogenes* displayed an initial increase in bacterial load in comparison to controls not exposed to PM, however bacteria were subsequently cleared by a strong T cell-mediated immune response (Yin *et al.* 2003; Yin *et al.* 2002). This was characterised by the increased secretion of IL-2, IL-6, and interferon- γ (IFN- γ), and increased CD4⁺ and CD8⁺ cell counts. This infection profile is similar to the present study, whereby BC transiently increased pneumococcal penetration into the LRT but bacteria were cleared by 14 days post-inoculation. PM and BC alter cytokine expression systemically (Longhin *et al.* 2016; Wang *et al.* 2015; Mannucci *et al.* 2015; Kumar *et al.* 2015; Cho *et al.* 2014; Zhao *et al.* 2012; Yin *et al.* 2002), therefore the increase in pneumococci recovered from the LRT may be due to altered immune system functioning caused by BC, reducing the ability of the host to clear bacteria. The transient presence of

pneumococci in the lungs could have therefore been due to the recovered ability of the immune system to clear these bacteria once BC had been cleared from the respiratory tract. In order to determine if this is a potential explanation for the transient spread of pneumococci to the lungs, future work could repeat this colonisation assay but in addition could evaluate key host factors which PM and BC are known to affect, including cytokine expression and immune effector cell recruitment (Longhin *et al.* 2016; Wang *et al.* 2015; Mannucci *et al.* 2015; Kumar *et al.* 2015; Cho *et al.* 2014; Zhao *et al.* 2014; Zhao *et al.* 2012; Yin *et al.* 2002), and phagocytic activity (Rylance *et al.* 2015; Zhao *et al.* 2012; Tellabati *et al.* 2010; Lundborg *et al.* 2007; Zhou & Kobzik 2007; Renwick 2004). The potential future work previously described, using repeated BC doses, may also inform on whether a “recovered” immune system was responsible for clearance of pneumococci from the LRT.

Furthermore, only four of the five mice inoculated with D39 and BC were found to have pneumococci in the LRT. It is interesting that there was a low variation in the CFUs recovered within these four mice (3.55-3.9 Log₁₀ CFU/ml), but no pneumococci were recovered from the fifth mouse. This could be due to the genetic variation of the outbred MF1 strain used, implying that the effect of BC on human populations may be defined not only by individual exposure, but by specific genetic traits. The colonisation assay could be independently repeated in order to determine whether these results are due to genetic variation or an experimental outlier.

Although pneumococci were found in the LRT of mice at 7 days post-inoculation with D39 and BC, histology showed no signs of pathology. However, any signs of pathology may have subsided by 7 days post-exposure. Future work could repeat this colonisation assay but complete a quantification of bacterial load and histological analysis of the lungs at intermediate time-points between exposure and 7 days. This may provide more information on when LRT colonisation occurs and whether it is associated with any immediate signs of pathological significance.

It is notable that BC was absent from all URT tissue sections. It is known that insoluble particles which deposit in the URT are carried to the larynx after deposition, and are then swallowed (Lippmann 2014; Southam *et al.* 2002). Therefore it is possible that BC

was cleared from the URT via the gastrointestinal system prior to histological analysis. This could have been assessed through further histopathological analysis however it is likely that it would be difficult to detect the clearance of BC into the gastrointestinal system as it would gradually occur over time. Furthermore, histopathological analysis is a terminal procedure and experimental time-points were chosen to fit in with the principles of the 3R's (replacement, reduction, refinement). The observed rapid BC clearance lends further weight to the hypothesis that repeated BC exposure may exacerbate the observed BC-associated phenotype of increased pneumococcal colonisation, and could be associated with the development of disease.

Interestingly, the data from this colonisation assay are in stark contrast to the only previous investigation into the effect of BC on pneumococcal virulence in an *in vivo* model (Tellabati *et al.* 2010). In the study by Tellabati *et al.* (2010), pre-exposure to BC significantly reduced murine mortality associated with a subsequent pneumococcal infection. However there are key differences between these assays. In Tellabati's study mice received two doses of 500 µg BC in 50 µl prior to being inoculated with pneumococci. BC is known to cause inflammation and oxidative stress (Xie *et al.* 2010; Folkmann *et al.* 2009; Yang *et al.* 2009; Renwick 2004; Gallagher *et al.* 2003), be taken up by AM, and reduce the ability of macrophages to kill bacteria (Rylance *et al.* 2015; Zhao *et al.* 2012; Tellabati *et al.* 2010; Lundborg *et al.* 2007; Zhou & Kobzik 2007; Renwick 2004). Therefore in the study by Tellabati *et al.* (2010), BC was inoculated directly into the lungs to exert these effects on the host prior to the pneumococcal challenge. Interestingly, the protective effect of BC in this study was thought to be the result of BC causing oxidative stress which in turn stimulated the recruitment of neutrophils, protecting against the subsequent pneumococcal challenge (Tellabati *et al.* 2010). Furthermore the dose volume and concentration used in Tellabati's study are known to cause pneumonia (Haste *et al.* 2014; Miller *et al.* 2012). Indeed, this is exactly what was observed in the study by Tellabati *et al.* (2010) in the control group. Therefore Tellabati's work assessed the development of pneumonia in a host pre-exposed to BC, whereas the work described in this thesis assessed the effect of BC on pneumococcal colonisation.

5.6.3. Potential mechanisms for the BC-induced spread of pneumococci to the lungs

The mechanisms by which BC induced the spread of pneumococci to the LRT were not elucidated in the current study. Therefore it is unknown what effect BC had on bacteria. I hypothesise that BC enhanced URT colonisation of *S. pneumoniae*, resulting in a greater subsequent dispersion of bacteria to the LRT. Consequently the presence of bacteria in the lungs observed in this assay may be an indirect effect due to increased colonisation. Alternatively it is possible that BC acts as a signal inducing *S. pneumoniae* to disperse and spread.

To investigate these potential mechanisms, future work could assess the transcriptome of colonising bacteria, for example using RNA-Seq, to assess the differences between colonisation in the presence and absence of BC. This may be difficult *in vivo* due to the low number of bacteria present in colonisation, therefore an *in vitro* model whereby pneumococci are allowed to colonise airway epithelial cells may be a more suitable method to use in combination with RNA-Seq (Baddal *et al.* 2015; Pettigrew *et al.* 2014; Jorth *et al.* 2013). Alternatively, specific targets could be assessed by qRT-PCR *in vivo*. As biofilm formation is a key aspect of pneumococcal nasopharyngeal colonisation, and BC has been shown to alter biofilm formation *in vitro* in Chapters 3 and 4, a potential investigative target is the pneumococcal two-component regulatory system 11, which is upregulated in response to cigarette smoke condensate, increasing biofilm formation (Feldman & Anderson 2013; Mutepe *et al.* 2013; Goldstein-Daruech *et al.* 2011). Future work could also assess nasopharyngeal biofilm formation using SEM (Marks *et al.* 2012a). This would allow the determination of whether bacteria in the co-exposure group displayed an enhanced biofilm and colonisation phenotype. Additionally, host factors may be involved. PM and steel welding fumes increase pneumococcal adhesion to airway epithelial cells by increasing host expression of platelet-activating factor receptor (PAFr) and causing oxidative stress (Suri *et al.* 2015; Mushtaq *et al.* 2011). Therefore it may be useful to investigate expression of key adhesion molecules on host cells in the URT.

An alternative explanation for the observation of pneumococci in the LRT is that a proportion of the inoculum was inoculated directly into the LRT, and that BC enhanced pneumococcal survival in the co-exposure condition in comparison to pneumococci inoculated alone. Methodology was optimised to ensure the inoculation volume used restricted the inoculum to the URT. However it is possible that although no pneumococci were detected in the bronchoalveolar lavage fluid of mice in preliminary work (Section 5.3), some pneumococci may have been inoculated in to the LRT but fallen below the detection threshold. Therefore it is possible that in the colonisation assay, a total number of bacteria less than this detection threshold was inoculated into the LRT, along with BC in the co-exposure condition. Future work could repeat intranasal dosing with D39 and BC and immediately cull mice to check that no BC had penetrated to the LRT using a histological analysis of the lungs. However, there is evidence that this hypothesis may not be true and this future work may not be required. No BC was detected in the LRT at 7 days post-inoculation, but in optimisation work (Section 5.2), any BC inoculated into the lungs persisted for at least a week, even with a dose as low as 5 µg total BC. There was also no evidence of a BC-associated inflammatory response, or BC-loaded AM.

Another hypothesis for the observed presence of pneumococci in the LRT in the co-exposure condition is that pneumococci attached to BC particles, and BC acted as a carrier taking bacteria to the lungs. Therefore this hypothesis assumes this is a physical effect, not due to a biological interaction. However there are multiple reasons why this is unlikely to be the case. BC and D39 were mixed immediately prior to inoculation, there was no incubation period, therefore pneumococci and BC would need to attach to each other immediately. Furthermore, the inoculating dose was either fully restricted to the URT, or some may have penetrated into the LRT, both of which have been discussed in this section. However as the inoculum was well mixed to fully disperse bacteria and BC throughout the liquid, if some of the dose was inoculated into the LRT this would have contained bacteria and BC, and is simply a result of the inoculation method. In addition, as mentioned in the previous paragraph, no BC was detected in the LRT and the inoculation volume was designed to restrict dosing to the URT, indicating

that it is unlikely that inoculation into the LRT occurred. Therefore the observed effect of BC on pneumococcal colonisation is likely to be a biological effect.

Therefore, in this study, BC caused pneumococci to spread to the LRT. This may support the hypothesis that the LRT infections associated with PM exposure are in part due to effects on bacteria. However it is not known what proportion of this dispersion is due to direct effects of BC on the bacteria, and what is caused by the bacterial response to a BC-exposed host.

5.6.4. The effect of pneumococcal colonisation and BC inhalation on the respiratory tract microbiota

In the work presented in this chapter, pneumococcal colonisation and the inhalation of BC were found to have no measurable significant effect on the respiratory tract microbiota. No overt clustering and no significant differences in alpha or beta diversity, or in the representation of specific families, were identified in relation to any exposure condition. However, subtle differences in the microbiota of different groups were observed, as described in Section 5.5.6.

Only one study has previously investigated the effect of pneumococcal colonisation on the respiratory tract microbiota. Krone *et al.* (2014) found that 7 days after inoculation with a colonising dose of *S. pneumoniae*, there was no significant alteration in bacterial diversity of the URT, correlating with the results of the investigation described in this chapter. Interestingly however, Krone *et al.* (2014) did identify a significant difference in diversity 3 days after pneumococcal inoculation, indicating that microbiota alterations occurred but were transient. This suggests that the time points chosen in the current assay may have been too long after inoculation to observe these initial temporary changes in microbial diversity. Future work could repeat this colonisation assay and assess the microbiota at 3 days post-inoculation to determine whether this time-point would be more informative.

It has been shown that the number of anaerobic bacteria in the rat oropharynx significantly increased with daily exposure to a combination of PM₁₀, SO₂, NO₂, and

CO, for one and thirty days (Xiao *et al.* 2013). However there was no change detected in the number of viable aerobic bacteria. This is the only previous investigation into the effect of PM on the respiratory tract microbiota. Therefore it may have been expected that BC would have altered the microbial diversity of the murine respiratory tract in the current investigation. Importantly however, there are key differences between these studies which could be the basis of the different findings. These differences include the form of air pollution used, the differences in exposure model, and the method of assessment. Xiao *et al.* (2013) used PM₁₀ collected in Shenyang, China, combined with other gaseous pollutants, and although the use of collected PM may be more realistic than use of components such as BC, there is important temporal and spatial variation in PM as described in Section 1.1. As Xiao *et al.* (2013) did not characterise the PM used, it is not known how this relates to PM at any other location or at any other time. As BC is a major component of PM found worldwide, BC investigations may provide data which can be more clearly extrapolated to all areas containing BC pollution. In addition, Xiao *et al.* (2013) only assessed the total number of bacterial colonies recovered on two types of agar plates after incubation in anaerobic and aerobic conditions. Therefore only bacteria culturable in these conditions were assessed. Furthermore, no assessment of diversity was performed and no data is presented by Xiao *et al.* (2013) to show which bacteria were recovered at any taxonomic level. Therefore although the work presented in this chapter did not identify a change in bacterial diversity, previous work has also not reported on the effect of PM on the microbial diversity of the respiratory tract. This may suggest the requirement for further investigation and the need for a critical analysis of the methodologies employed, as described in Section 5.6.6.

5.6.5. The composition of the murine respiratory tract microbiota

As discussed before (Section 5.6.2), pneumococcal inoculation resulted in significantly more pneumococci in the URT at both time-points in comparison to mice in the PBS and BC groups (Figure 5-6). Correlating with this, mice in the D39 and D39+BC groups were identified to have more *Streptococcaceae* in the URT than mice in the PBS and BC groups, at both time-points. Notably, mice in the D39+BC group had more

Streptococcaceae than the D39 group. However, there was no significant difference between any groups, indicating that pneumococci did not have an overt effect on the overall abundance of *Streptococcaceae*. Furthermore, groups which received an inoculation of pneumococci did not always have the greatest abundance of *Streptococcaceae*, which were recovered from almost all mice in all conditions. These results show that additional members of the *Streptococcaceae* family were naturally present in the murine respiratory tract besides the inoculated *S. pneumoniae* D39.

No significant differences were identified between the diversity of the URT or LRT, correlating with previous research (Dickson & Huffnagle 2015; Dickson *et al.* 2014; Morris *et al.* 2013; Charlson *et al.* 2011). Furthermore, no significant time-related differences were identified. The majority of families identified in the murine respiratory tract have been previously reported to be members of this microbiota (Thevaranjan *et al.* 2016; Krone *et al.* 2014; Barfod *et al.* 2013). Some of these families were expected and have been repeatedly identified as major components of this microbiota, including *Streptococcaceae*, *Staphylococcaceae*, and *Micrococcaceae*. Many other families identified have also been previously found to be more minor components of the microbiota of this environment, including *Ruminococcaceae*, *Burkholderia*, *Enterobacteriaceae*, *Moraxella*, *Propionibacteriaceae*, *Hyphomicrobiaceae*, and Cyanobacteria (Thevaranjan *et al.* 2016; Krone *et al.* 2014; Barfod *et al.* 2013). However previous research has not consistently identified all these families in the murine respiratory tract. For example, while *Ruminococcaceae* and *Enterococcaceae* have been identified in the murine URT in one study (Krone *et al.* 2014), they were exclusively isolated from the vaginal or caecal microbiota in another (Barfod *et al.* 2013).

The most surprising families identified were *Methylobacteriaceae*, *Holophagaceae*, the new reference OTU18, and ACK-M1 (a freshwater isolate within Actinobacteria), which to my knowledge have never been identified as associated with the murine respiratory tract. Information about each of these families is provided in Table 5-1. Specifically, OTU18 is an OTU within the order Gaillales. This novel family was described in 2011, and so far the only species within this family has been isolated from a deep mineral water aquifer (Albuquerque *et al.* 2011). Similarly, only two species

within the *Holophagaceae* family have ever been described, isolated either from black anoxic mud or petroleum-contaminated aquifer sediment (Fukunaga & Ichikawa 2014; Bergey 2010). These families were identified in mice in all conditions, therefore could imply that there are key members the respiratory tract which are as yet unappreciated. An alternative and potentially more likely explanation is that these families are result of contamination or errors in grouping and taxonomy, discussed in Section 5.6.6.

5.6.6. Limitations of microbiota assessment, and potential sources of bias and error

One limitation of the work described in this chapter is that rarefaction curves were not presented. Rarefaction curves plot the number of OTUs identified against sequencing depth, and therefore allow the demonstration of whether samples have been sequenced to a suitable depth, based on the plateau of the curves. These would have been a useful tool to establish the effectiveness of sequencing in this investigation.

As described, pneumococcal colonisation and BC inhalation were not observed to cause any significant alterations in the murine respiratory tract microbiota in this research. Therefore in this case, these data do not support the hypothesis that BC-induced microbiota dysbiosis contributes to PM-associated disease. However, there are a variety of factors which indicate that these findings have been influenced by the methodologies employed. Firstly, repeated BC exposure may be required to observe biological changes in the microbiota. Furthermore, any alterations induced by the single BC dose may have subsided by 7 days post-inoculation. Future work may therefore consider repeated BC doses and assessment closer to initial inoculation. In addition, multiple potential limitations and sources of bias are described in the literature related to the sequencing of microbial communities. These include, but are not limited to, contamination, operator error, the method of DNA extraction, PCR amplification, choice of sequencing platform, and bioinformatic analysis (Kunin *et al.* 2010; Wintzingerode *et al.* 1997). Some issues related to DNA extraction protocol choice have been discussed, namely the choice of DNA extraction protocol (Section 5.5.1). This section details some of the salient remaining issues not yet covered.

5.6.6.1. Contamination

This investigation into the respiratory tract microbiota was impacted by the issue of contamination, however controls were used to elucidate both the level and diversity of this contamination. Contaminating microbial DNA is a serious current issue in microbial ecology that can both hinder research and lead to the interpretation of false associations between specific microbes and ecological niches or disease states (Jervis-Bardy *et al.* 2015; Laurence *et al.* 2014; Salter *et al.* 2014; Lazarevic *et al.* 2014). Initial sequencing of the naïve murine respiratory tract to test ion torrent protocols revealed that *Oxalobacteraceae* was the dominant family identified. However, *Oxalobacteraceae* and several of the other major families identified are known contaminants of FastDNA prep kits, including *Methylobacteriaceae*, *Ruminococcaceae*, *Burkholderiaceae*, *Comamonadaceae*, *Phyllobacteriaceae*, *Enterobacteraceae*, and *Bacteroidaceae* (Salter *et al.* 2014). The issue of contamination arising from DNA extraction kits has been described in Section 5.5.1, and the most appropriate kits were chosen to limit this issue. Contaminating microbial DNA can also be introduced through molecular biology grade water (Keki *et al.* 2013; Bohus *et al.* 2011; Shen *et al.* 2006; Kulakov *et al.* 2002; Mcalister *et al.* 2002; McFeters *et al.* 1993) and PCR reagents (Newsome *et al.* 2004; Grahn *et al.* 2003; Corless *et al.* 2000; Tanner *et al.* 1998; Wintzingerode *et al.* 1997; Maiwald *et al.* 1994; Rand & Houck 1990). Indeed, *Ralstonia* in particular are also known to be contaminants found in ultrapure water (Kulakov *et al.* 2002; Mcalister *et al.* 2002), such as that used for 16S PCR reactions (Section 2.9.2). Therefore it was not clear whether contamination had arisen entirely from the extraction kits used, or from alternative, or even multiple, sources.

This initial sequencing data informed the development of two types of control measures for further microbiota investigations. Firstly, laboratory contamination was limited as far as possible (Section 5.5.3), and secondly, contaminating OTUs were elucidated through the sequencing of bacteria-free control samples. A variety of bacterial families were classified in the sequencing of these controls, therefore it appeared that the methods introduced to limit contamination were not entirely effective. However some contamination was expected as it is unlikely to be possible to completely prevent

contamination during preparation of samples for sequencing (Jervis-Bardy *et al.* 2015), and it is worth noting that test samples contained at least over an order of magnitude more reads than the controls. Controls were therefore used as the basis for a contaminant removal procedure. Contaminant removal was performed at the OTU level prior to grouping. Otherwise errors could be introduced by eliminating taxa containing some contaminant OTUs but also genuine OTUs.

The most stringent approach to contaminant removal would have been to remove all OTUs found in controls from test data (Jervis-Bardy *et al.* 2015). This was not done for the data described in this thesis as with this approach, extremely rare OTUs in control samples would have been removed even if these OTUs were genuine major components of the test data. Furthermore, this approach would have removed all *Streptococcaceae* and it was known that at least a portion of *Streptococcaceae* identified in the URT of mice in the D39 and D39+BC groups was a real component of the microbiota. The contaminant removal procedure was therefore based on an empirical approach, and two thresholds of contaminant removal were employed based on the level of contamination in each set of controls.

With this contaminant removal procedure, entire OTUs were removed from test samples. However it is possible that some of these OTUs may have contained genuine reads in addition to reads due to contamination. Future work may therefore employ an approach which allows the interpretation of what proportion of each OTU is the result of contamination. Oligotyping may be suitable for this by distinguishing closely related but distinct bacteria which have been clustered into the same OTU, potentially allowing the discrimination of contaminant sequences from genuine sequences (Eren *et al.* 2013). Oligotyping uses highly variable sites in 16S RNA gene sequences to determine whether all sequences clustered into an OTU are from the same source, and is able to distinguish subpopulations within a single OTU.

It was surprising that negative extraction controls contained less sequences than negative PCR controls, as negative extraction controls were subjected to the same preparation protocols as PCR controls, and had the additional DNA extraction step. A potential reason for this could be inhibition of PCR amplification. PCR inhibition is a

particular issue during amplification of low DNA samples, preventing rare sequences from being amplified. In the work described here, if the contamination observed arose from the laboratory and PCR reagents, but inhibitory factors were introduced from the DNA extraction kit, this may have prevented contamination in these samples reaching an equivalent amplification level. This would therefore explain the fewer sequences obtained in the negative extraction controls. It has been reported that DNA extractions with FastDNA kits are ineffective at removing PCR inhibitors (Dineen *et al.* 2010; Jiang *et al.* 2005), however to my knowledge it has not been suggested that the kits themselves are a source of inhibitory substances.

5.6.6.2. Extracting microbial DNA from lavages

Host DNA can interfere with the accurate assessment of microbiota with a low bacterial content, such as the respiratory tract. This is because host DNA can present issues during PCR amplification, resulting in sampling bias due to competitive and inhibitory interactions (Jervis-Bardy *et al.* 2015; Salter *et al.* 2014). Therefore although it is possible to perform microbiota analyses using DNA extracted from tissue samples, and this method has the advantage of potentially recovering more bacterial DNA than lavages, microbial DNA in the starting material is overwhelmed by host DNA which may have a negative impact on the investigation. Therefore lavages were chosen for this investigation.

It is possible that by using lavages in this investigation of a microbiota containing low numbers of bacteria, too few bacteria may have been recovered to have sufficient power to observe statistically significant differences in data, even if biological changes were observed. Therefore future work may advance on the research presented here by extracting DNA from nasal tissue and lung samples, and separating microbial and host DNA prior to amplification. This would therefore avoid the stated issues with PCR bias. As eukaryotic DNA is methylated at CpGs, whereas methylation at these sites in bacteria is rare, host and microbial DNA can be separated based on these methylation differences (Feehery *et al.* 2013). A protocol has been described whereby a modified MBD2 protein has been constructed which binds to Protein A, thereby allowing attachment to Protein A-bound magnetic beads (Feehery *et al.* 2013). The methyl-CpG

domain of human MBD2 protein binds specifically to CpG methylated DNA, therefore the user is able to extract CpG methylated DNA from a sample mixture. This allows the removal of eukaryotic DNA from a sample of mixed eukaryotic and microbial DNA. Furthermore, any remaining host sequences can be removed during processing of data in the QIIME pipeline (Caporaso *et al.* 2010b).

5.6.6.3. PCR amplification

An assumption of the work described is that PCR amplification was able to amplify all sequences present at equivalent efficiencies. This assumes that all DNA sequences were equally accessible for primer binding, primers bound to all sequences with the same efficiency, and all sequences were representatively amplified with equal efficiency (Wintzingerode *et al.* 1997). However this may not have been the case.

The 16S rRNA gene is found in all bacteria, containing nine hypervariable regions that are separated by highly conserved fragments, as shown in Figure 2-4 (Section 2.9.2). Mutations accumulate in the 16S hypervariable regions over time, separating diverged bacterial taxa, and therefore allow the 16S rRNA sequence to be used for taxonomic identification. The conserved regions are important in folding of the RNA molecule, and so are under a strong negative selection pressure, and therefore can be used as primer annealing sites. The universal primers used in the research described in this thesis bind in these conserved regions, however purposefully contained degeneracies in order to amplify all DNA, which may have influenced primer binding (Wintzingerode *et al.* 1997). Furthermore, primers may not be entirely universal as conserved regions are highly, but not absolutely, conserved (Sipos *et al.* 2007; Baker *et al.* 2003; Schmalenberger *et al.* 2001). Although this is worth consideration, in reality it may not be an issue as only ~70 % identity is required for successful primer annealing and amplification (Baker *et al.* 2003).

5.6.6.4. Data processing

After the sequencing reactions, careful processing of data is required in order to avoid distortions of data and false interpretations of associations (Jervis-Bardy *et al.* 2015;

Weiss *et al.* 2014). It is worth noting that it is possible that during deconvolution of reads based on barcodes, sequences from test samples may have been incorrectly matched to control barcodes. Therefore the assumed contamination in control samples discussed in Section 5.6.6.1 may not have been entirely due to true contamination, but a failure of processing.

OTUs are assigned taxonomy based on the most abundant sequence, and therefore poor clustering can impact later data analysis (Nguyen *et al.* 2016; Konstantinidis & Tiedje 2005). Open reference OTU picking has been reported to perform better than closed reference and *de novo* OTU picking, in that it is able to efficiently eliminate non-bacterial reads and retain unclassified bacterial reads (Jervis-Bardy *et al.* 2015).

Therefore open reference OTU picking was employed. A 97 % sequence identity was used to group OTUs as this the commonly accepted threshold (Nguyen *et al.* 2016; Jervis-Bardy *et al.* 2015; Konstantinidis & Tiedje 2005; Stackebrandt & Goebel 1994). However, it is becoming apparent that this threshold may not always be accurate (Rossi-Tamisier *et al.* 2015). Two distinct species may have a 16S similarity greater than 97 % and so may be incorrectly grouped together (Rossi-Tamisier *et al.* 2015; Fournier & Raoult 2009; Konstantinidis & Tiedje 2005; Kulakov *et al.* 2002). One study of note found that 57 % of species within human-associated genera had a 16S rRNA sequence similarity rate ≥ 98.7 % with another species in the same genus (Rossi-Tamisier *et al.* 2015). For example 26 distinct species of *Rickettsia* have 16S gene sequence similarity values over 99 % (Fournier & Raoult 2009). These species are maintained as separate due to differences in pathogenicity and other characteristics. Furthermore, there may be sequence variability among the multiple copies of 16 rRNA genes (Konstantinidis & Tiedje 2005; Wang *et al.* 1997). For example *E. coli* K12 16S sequences can differ by 5 % in certain regions (Eren *et al.* 2013). Therefore strict use of the 97 % threshold described can both combine multiple species into one OTU, and divide one bacterial species into multiple OTUs depending on the 16S rRNA copy analysed. It is worth noting that the lack of a clear definition of a species is why the term OTU is used in microbiota analysis rather than species.

In this study, the primers used amplified a fragment of the 16S rRNA gene across two hypervariable regions; V1 and V2 (Figure 2-4, Section 2.9.2). Importantly, choice of

the hypervariable regions amplified impacts the success of classification. V2 has been described as one of the most suitable regions for distinguishing bacteria to genus level, with one of the lowest classification error rates of all hypervariable sequences (Chakravorty *et al.* 2007; Wang *et al.* 2007). In addition, V1 has been shown to be particularly good at distinguishing between Staphylococcal species (Chakravorty *et al.* 2007). However, sequencing over the hypervariable 16S regions rather than the full length can lead to mischaracterisation of samples, and it has been reported that up to 10 % of examined V3 and V6 sequences map to multiple full-length rRNA sequences (Huse *et al.* 2008). Therefore an alternative approach would be the use of whole genome shotgun sequencing, however this carries its own financial, technical, and processing considerations (Ranjan *et al.* 2016).

5.6.7. Conclusions

BC causes dissemination of pneumococci from the upper to the lower respiratory tract. This dissemination may provide the opportunity to cause disease in a susceptible host, which may contribute to the established association between PM and lower respiratory tract infections. Additionally, this effect may be exacerbated by repeated BC exposure. Interestingly, BC exposure and pneumococcal colonisation were not observed to affect the respiratory tract microbiota in this initial investigation. However, it is recognised that there are a variety of limitations in the work described, which may have hindered the observation of a biological effect.

Chapter 6. Final Discussion

Particulate matter (PM) is a major component of air pollution which is associated with both causing and aggravating multiple cardiorespiratory diseases, including acute respiratory tract infections (WHO 2014d; WHO 2007), asthma (Deng *et al.* 2015; Brauer *et al.* 2007; Brauer *et al.* 2002), and Chronic Obstructive Pulmonary Disease (COPD) (Xu *et al.* 2016; Cortez-Lugo *et al.* 2015; Qiu *et al.* 2014; Darrow *et al.* 2014). However despite the fact that bacteria are directly responsible for respiratory infections (Shak *et al.* 2013b; Vernatter & Pirofski 2013; Porto *et al.* 2013; Park *et al.* 2013; Edwards *et al.* 2012; Mook-kanamori *et al.* 2011) and may cause exacerbations of asthma and COPD (Erkan *et al.* 2008; Pelaia *et al.* 2006), there has been extremely limited research into the direct effect of PM on bacteria (Adedeji *et al.* 2004). Therefore two hypotheses were tested in this project. The first hypothesis was that Black Carbon (BC) alters the ability of respiratory tract bacteria to colonise or cause disease. To address this hypothesis, it was split into 2 questions; 1, Does BC affect growth, the activity of extracellular virulence factors, or biofilm formation of *S. aureus* or *S. pneumoniae*? and 2, Does BC affect respiratory tract colonisation by *S. pneumoniae in vivo*? The second hypothesis that was tested in this project was that BC alters the diversity of the respiratory tract microbiota.

Figure 6-1 shows a summary of the factors identified to be affected by BC in this investigation, as well as potential additional factors which could be involved, based on the observations made. In short, BC was found to alter growth and biofilm formation of *S. pneumoniae* and *S. aureus* (addressing question 1), and colonisation of *S. pneumoniae* strain D39 (addressing question 2). Therefore, in agreement with the first hypothesis, BC was found to alter the ability of respiratory tract bacteria to colonise a host, as well as affect factors known to be involved in colonisation and virulence. Pneumococcal colonisation, inhalation of BC, and co-inhalation of pneumococci and BC were found to have no effect on the respiratory tract microbiota, therefore the second hypothesis could not be answered. However, multiple limitations were encountered in microbiota investigations, as discussed in Section 5.6.6.

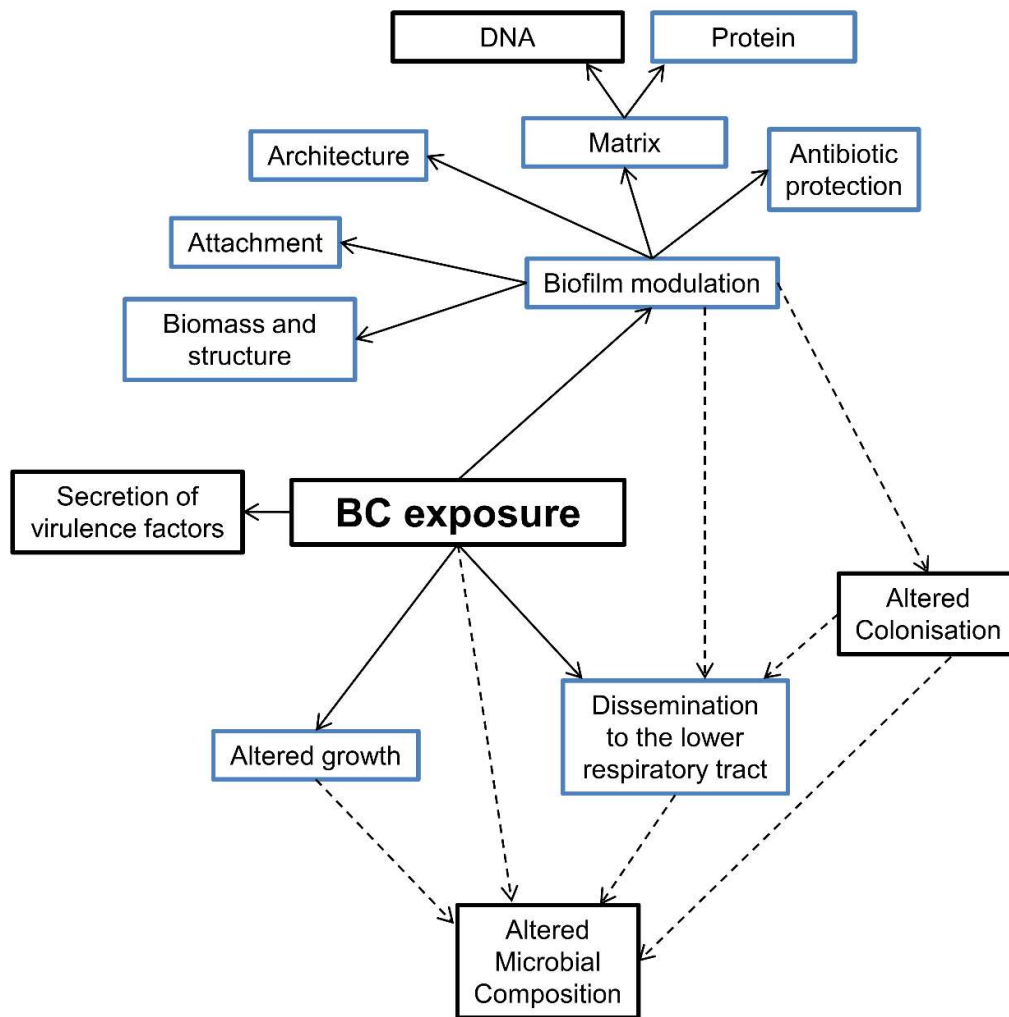


Figure 6-1. Proposed effects of black carbon (BC) on bacteria. Blue boxes indicate factors determined to be altered by BC in this project. Black boxes indicate factors which were not revealed to be altered by BC, however further investigation and/or method development may be required. Dashed lines indicate potential hypothesised effects.

The key result of this research is that BC induced the spread of pneumococci from the URT to the LRT in a murine colonisation model. This induction of pneumococcal dissemination may be a previously unknown mechanism by which PM exposure results in increased lower respiratory tract infection and disease (Brugha & Grigg 2014; MacIntyre *et al.* 2014; Qiu *et al.* 2014). Therefore these results address the overarching issue this research intended to examine, that bacteria may also be affected by PM exposure and contribute towards the PM-disease association.

Biofilm formation is a necessary step in pneumococcal colonisation of the nasopharynx, and colonisation is required prior to pneumococcal infection (Gilley & Orihuela 2014; Blanchette-cain *et al.* 2013; Marks *et al.* 2012a; Domenech *et al.* 2012; Sanchez *et al.* 2011; Munoz-Elias *et al.* 2008). Therefore I proposed that in the murine colonisation investigation described in Chapter 5, BC altered biofilm formation in the URT, resulting in the subsequent increased dissemination of bacteria. Unfortunately, *S. pneumoniae* D39 was used in the *in vivo* colonisation assay, but the structure of D39 biofilms formed with BC was not assessed by SEM or TEM, as was performed for other strains (Sections 4.2 and 4.3). This was due to degradation of biofilms formed by this strain during processing for microscopy, as described in Chapter 4. To address whether BC alters biofilm formation of strain D39, Section 4.9.1 describes future work which could be employed to assess *in vitro* biofilm formation with a lysine-acetate-based formaldehyde-glutaraldehyde ruthenium red-osmium (LRR) fixation procedure, which has been shown to preserve biofilms formed by encapsulated microscopy better than standard techniques (Marks *et al.* 2012a; Hammerschmidt *et al.* 2005). Alternatively, Section 5.6.3 describes methods to assess nasopharyngeal biofilm formation *in vivo* by removing the URT and directly imaging pneumococcal biofilms in this site by SEM (Marks *et al.* 2012a). These investigations would allow the assessment of whether the BC-induced alteration of pneumococcal colonisation *in vivo* is, at least in part, due to altered biofilm formation.

Although the structure of biofilms formed by pneumococcal strain D39 was not evaluated in this project, biofilms formed by strain PR201 were. Biofilms of this strain formed in the presence of BC were significantly thicker than controls, and displayed a honeycomb structure characteristic of nasopharyngeal biofilms (Marks *et al.* 2012a).

This structure has only ever been previously reported to be reproduced *in vitro* on surfaces coated with epithelial cells (Marks *et al.* 2012a). It was therefore hypothesised in Chapter 4 that because BC caused abiotic *in vitro* biofilms of PR201 to emulate the structure of *in vivo* biofilms, these effects may be exaggerated *in vivo*, whereby larger and more complex biofilms may be formed. This altered biofilm formation may therefore affect colonisation and subsequent bacterial dispersal.

S. aureus biofilms formed in the presence of BC were found to have BC-associated protrusions from their surfaces. It was hypothesised in Chapter 4 that these protrusions are the cause of the significant increase in loosely-adherent bacteria in SH1000 BC-biofilms, in comparison to control biofilms, in that these protrusions may readily detach from the main biofilm structure. The hypothesised mechanism responsible for the dissemination of pneumococci in the *in vivo* work described also relates to altered biofilm formation during colonisation. Therefore it may be interesting for future work to repeat this colonisation assay with *S. aureus*, assessing both bacterial burden and biofilm formation.

Interestingly, BC was found to alter biofilm architecture, thickness, matrix composition, and antibiotic tolerance of all strains investigated, but effects varied between strains. These parameters were investigated because alterations in these factors would impact bacterial colonisation, survival, and dissemination *in vivo*. This is because biofilm structure affects mechanisms of dispersal, such as sloughing (the detachment of large clumps of biofilm cells at one time) (Petrova & Sauer 2016; Kaplan 2010). Furthermore, the extracellular matrix provides a scaffold for biofilm formation and is a major protective component of biofilms (De la Fuente-Nunez *et al.* 2013; Archer *et al.* 2011; Kiedrowski & Horswill 2011; Flemming & Wingender 2010). Alterations in antibiotic tolerance would impact the outcome of antibiotic treatment, thereby potentially altering microbial diversity. In addition, alterations in antibiotic tolerance may alter the ability of colonised biofilms to seed infection, due to the enhanced resistance of biofilms to eradication.

Microbiota dysbiosis is strongly associated with disease states, causing inflammation and exacerbating respiratory diseases including asthma and COPD (Salami & Marsland

2015; Dickson *et al.* 2014). Importantly, the observed intra- and inter-species variation implies that BC may alter the respiratory tract microbiota by differentially impacting different species or strains. Therefore the induction of microbiota dysbiosis may be a mechanism by which PM exposure is associated with disease. In the initial investigation described in this thesis however, inhalation of BC, *S. pneumoniae* D39, or the combination of D39 and BC, did not appear to alter the respiratory tract microbiota. This observation is not consistent with the hypothesis presented for this work, but the multiple factors described in Section 5.6.6 may have prevented a definitive conclusion from being reached.

An improved method for assessment of the respiratory tract microbiota is therefore required for future investigations. Section 5.6 discussed potential improvements that could be employed in microbiota investigations, the most salient of which would be the use of samples with a greater microbial biomass, and an improved procedure for the elucidation and removal of contamination. A major limitation of the investigation described was the issue of contamination with extraneous microbial DNA. This is known to be a particular problem for sequence based investigations of microbiota containing a low bacterial density, due to the swamping of real microbial sequences with contaminating DNA (Salter *et al.* 2014). Use of a greater microbial biomass may be beneficial as this would allow a lower PCR cycle number to be employed, potentially limiting the impact of low-level contamination, and also providing more power for statistical calculations. As described in Section 5.6.6, extracting DNA from nasal and lung tissue samples, followed by removal of methylated host DNA (Feehery *et al.* 2013), may provide samples with a greater concentration of bacterial DNA in comparison to DNA extracted from lavage fluid. In addition, removing host DNA prevents this affecting PCR amplification, where it can cause sampling bias due to competitive and inhibitory interactions (Jervis-Bardy *et al.* 2015; Salter *et al.* 2014).

In this project, contaminating OTUs were identified through use of bacteria-free control samples. OTUs present in these controls were then removed from test data if they violated certain threshold criteria, as explained in Section 5.5.5. However it is possible that as entire OTUs which violated the contaminant removal procedure were removed from test samples, some of these OTUs may have contained genuine reads in addition

to reads from contamination. An improvement on this contaminant removal procedure would be to use an approach which allow the interpretation what proportion of an OTU is due to contamination. Oligotyping may be suitable for this purpose and is discussed in Section 5.6.6. Oligotyping would allow the differentiation of closely related but distinct bacteria clustered into the same OTU, potentially allowing contaminant sequences to be separated from genuine sequences clustered in the same OTU (Eren *et al.* 2013).

The work described in this thesis has shown the potential importance of the overlooked effect of BC on bacteria, and the role these interactions may have in the association between PM exposure and disease. However as this was an initial investigation, there are limitations to the experiments described, a number of unanswered questions, and key areas of future research. Specific advances on each experiment have been discussed in each chapter where appropriate. In the rest of this chapter, overarching issues and considerations for future work will be addressed.

6.1. Limitations of investigations in this project

This thesis has presented data to show that BC has direct effects on *S. pneumoniae* and *S. aureus*. The BC used in this project was purchased from Sigma-Aldrich (UK) in order to standardise the work performed, however the purity of this BC was not checked. It is therefore possible that the results obtained may have been influenced by, or due to, trace contaminants which were not elucidated. It would have been beneficial to check the full composition of the BC, for example by LC-MS, to determine whether additional chemical components were present which may have been responsible for any of the observed phenotypes. In addition, PM is known to contain biological components, including viable bacteria, fragments of bacteria, and bacterial products such as endotoxins (Section 1.6). After the stock solution of BC was made, sterility was checked by plating onto LA, BHI agar, and 5 % (v/v) Horse Blood Agar, and inoculating 1 ml of the stock into 10 ml LB, BHI, THB, THY, TSB. These plates and media were then incubated at 37 °C in air, both statically and shaking at 200 *rpm*, and statically in 5 % (v/v) CO₂. In all cases, no viable bacteria were recovered. However in addition to checking for sterility, the assessment of whether any endotoxin was present

in the stock may have been useful in order to determine whether additional non-viable bacterial components were present which may have influenced results. A common method of endotoxin assessment is the Limulus Amebocyte Lysate (LAL) assay, which reacts with endotoxin to produce a colour change which can be read in a plate reader (Brune *et al.* 2016). Samples can then be compared to a standard curve of endotoxin to determine the concentration present in the test sample, and can detect levels as low as 0.01 ng endotoxin per ml. This would have been a simple assay to perform on the stock BC solution to check for biological contamination.

In this project, BC concentrations were based on previous research into the effects of BC on the host, as well as research into the effects of other pollutants on bacteria (Suraju *et al.* 2015; Vesterdal *et al.* 2012; Tellabati *et al.* 2010). However a notable limitation to this work was that these concentrations do not model real-world BC exposure. Atmospheric concentrations of BC in the UK range from 1 to 7 $\mu\text{g}/\text{m}^3$, with an average of 1.6 $\mu\text{g}/\text{m}^3$ (Butterfield *et al.* 2015), equating to 1.6×10^{-6} $\mu\text{g}/\text{ml}$. Therefore the concentrations of BC employed in this project (10-100 $\mu\text{g}/\text{ml}$), equate to 10,000-100,000 mg/m^3 , far exceeding atmospheric levels. However, atmospheric BC is inhaled over long time periods, with constant deposition on the surface of the respiratory tract. Therefore single high dose suspensions, such as those used in this project, are typically used to model this long-term exposure (Suraju *et al.* 2015; Vesterdal *et al.* 2012; Tellabati *et al.* 2010). To advance on this work, future *in vivo* investigations could expose mice to BC concentrations more closely resembling atmospheric concentrations, using repeated doses over time (Larcombe *et al.* 2014). However, this would come at an increased cost due to housing mice for longer time periods.

An additional limitation of the research described is that BC was prepared in an aqueous solution, whereas in reality PM exposure occurs by inhalation. It has been shown that the effect of PM on the murine immune system varies depending on whether mice are exposed to an inhaled aerosol or a liquid suspension (Larcombe *et al.* 2014; Jackson *et al.* 2012b). For example, in the research by Larcombe *et al.* (2014), DEPs caused pulmonary inflammation and altered lung function with both exposure protocols, however aerosolised particles displayed a stronger dose-response relationship. In contrast, in the investigation by Jackson *et al.* (2012b), inhaled BC

caused DNA strand breaks, whereas instilled BC had no effect. To address this, future work could employ an inhalation protocol whereby mice are exposed to aerosolised BC at concentrations which model atmospheric concentrations. This protocol would thereby address both the issue of particle concentration and that of the exposure method. For this, mice could be placed in a chamber to inhale aerosolised BC for set periods. Indeed this exposure model has been used in past research investigating the effects of particles on inflammation, DNA strand breaks, markers for oxidative stress, and susceptibility to infection (Noël *et al.* 2015; Jackson *et al.* 2012b; Gallagher *et al.* 2003; Yin *et al.* 2003; Yin *et al.* 2002). It should be noted that inhalation exposure is more expensive and more technically difficult than liquid instillation, and requires specific equipment, therefore was not used in this project.

6.2. Additional future research

PM is a complex pollutant mixture including many components in addition to BC, as described in Section 1.1 (Kelly & Fussell 2012; Air Quality Expert Group 2012; Air Quality Expert Group 2005). It is possible that the different PM components will either act synergistically, or will affect bacteria in diverse ways, with the overall impact being a combination of the effects of these components. To address this, both additional individual components of PM and collected atmospheric PM could be investigated in the future. Use of different PM components would inform on the effects each of these components have on bacteria, and how these effects may be associated with disease. These investigations may therefore have the potential to advise on PM policy by reducing emission of the most harmful components of air pollution. Indeed, existing PM policy attempts to reduce overall PM exposure and advise on changes in regulation which may reduce the most harmful PM components (Heal *et al.* 2012; Air Quality Expert Group 2012; Air Quality Expert Group 2005).

Importantly, the intra- and inter-species differential impact observed may have currently overlooked wider implications than those considered in this project. Bacteria are central to many biological processes and as PM pollution is a global issue, PM could affect bacteria in many ecological niches. Indeed, air pollution is found globally therefore PM may affect bacteria in terrestrial, freshwater, and marine environments,

and on any air-surface interface of humans and animals including the respiratory tract and skin. Therefore future work could expand on this project and assess the effect of PM on key bacteria of other environments, as well as further investigating respiratory tract bacteria.

6.3. Conclusions

BC was found to directly affect bacteria of the respiratory tract in *in vitro* investigations, and promoted pneumococcal dissemination to the LRT. Consequently, this research establishes a new paradigm; that the detrimental impact of particulate pollutants on human health may not just be due to direct effects on the host, but may also stem from effects on bacteria. This research demonstrates that a significant biological effect of air pollution may have been overlooked, and that the impact of BC on bacteria must be considered in future research. As a concentration dependent effect of BC was observed in growth and biofilm assays, these data would suggest that individual exposure should be reduced as far as possible to limit effects of BC, agreeing with existing PM policy (Janssen *et al.* 2012; Air Quality Expert Group 2012; WHO 2006a; Air Quality Expert Group 2005).

Appendices

Appendix 1. UK cities breaching the World Health Organisation annual mean guidelines for PM₁₀ in 2013 (WHO 2016)

City	Annual mean concentration of PM ₁₀ (µg/m ³)
EASTBOURNE	21
GLASGOW	23
LEEDS	22
LONDON	22
NOTTINGHAM	21
OXFORD	21
PORT TALBOT	14
SCUNTHORPE	22
SOUTHAMPTON	21
STANFORD-LE-HOPE	24

Appendix 2. UK cities breaching the World Health Organisation annual mean guidelines for PM_{2.5} in 2013 (WHO 2016)

City	Annual mean concentration of PM_{2.5} (µg/m³)	City	Annual mean concentration of PM_{2.5} (µg/m³)
ARMAGH	14	NOTTINGHAM	12
BELFAST	12	OXFORD	14
BIRKENHEAD	11	PLYMOUTH	12
BIRMINGHAM	14	PORT TALBOT	14
BRIGHTON	11	PORTSMOUTH	14
BRISTOL	13	PRESTONPANS	12
CARDIFF	14	SALFORD	12
CARLISLE	12	SALTASH	15
CHEPSTOW	14	SCUNTHORPE	11
EASTBOURNE	15	SOUTHAMPTON	16
GLASGOW	16	SOUTHEND-ON-SEA	15
LEAMINGTON SPA	15	STANFORD-LE-HOPE	11
LEEDS	15	STOCKTON-ON-TEES	14
LIVERPOOL	12	SUNDERLAND	14
LONDON	15	SWANSEA	12
LONDONDERRY	11	THURROCK	14
MANCHESTER	13	WARRINGTON	14
MIDDLESBROUGH	11	WIGAN	13
NEWPORT	13	YORK	12
NORWICH	13		

Appendix 3. Initial processing of ion torrent data from main investigation.

#Initial processing was performed in Qiime version 1.9.1 running on Linux

```
convert_fastaqual_fastq.py -c fastq_to_fastaqual -f
R_2012_12_20_08_51_33_user_LU1-68-ALB_SH1_011215.fastq -o Shane1
convert_fastaqual_fastq.py -c fastq_to_fastaqual -f
R_2012_12_21_08_14_56_user_LU1-69-ALB_SH2_021215.fastq -o Shane2
```

#Renamed .fna and .qual files to Shane1 and Shane2

```
split_libraries.py -m Shane_Mapping_Chip1.txt -f Shane1.fna -q
Shane1.qual -o split_Library_output_Shane1/ -z truncate_only --
reverse_primer_mismatches 5 -w 20 -s 20 -n 1 -c -e 0 -M 2 -H 5 -a 2 -l
200 -L 500 -b variable_length
split_libraries.py -m Shane_Mapping_Chip2.txt -f Shane2.fna -q
Shane2.qual -o split_Library_output_Shane2/ -z truncate_only --
reverse_primer_mismatches 5 -w 20 -s 20 -n 10000000 -c -e 0 -M 2 -H 5
-a 2 -l 200 -L 500 -b variable_length
```

#Provides trimmed sequence files in the output folders which are then renamed as Shane1Final.fna and Shane2Final.fna and combined/concatenated

```
cat Shane1Final.fna Shane2Final.fna > ShaneCombined.fna
```

```
identify_chimeric_seqs.py -i ShaneCombined.fna -m usearch61 -o
usearch_checked_chimeras_Shane/ -r 97_otus.fasta
```

```
filter_fasta.py -f ShaneCombined.fna -o
ShaneCombinedSeqs_chimeras_filtered.fna -s
usearch_checked_chimeras_Shane/chimeras.txt -n
```

```
pick_open_reference_otus.py -i
$HOME/ShaneCombinedSeqs_chimeras_filtered.fna -r $HOME/97_otus.fasta -
o $HOME/openref_usearch_Shane/ -s 0.1 -m usearch61 --min_otu_size 1
```

#Rename otu_table_mc1_w_tax_no_pynast_failures.biom to Shane.biom

```
summarize_taxa.py -i Shane.biom -o Shane_taxa/
```

#Create a tree to allow use of Unifrac

```
make_phylogeny.py -i rep_set_aligned.fasta -o Shane_rep_phylo.tre
```

#Convert biom to text to allow editing and input to phyloseq

```
biom convert -i Shane.biom -o Shane_final_otu_table.txt --to-tsv --
header-key taxonomy
```

#Edit table in Excel as follows:

#Copy and split 'taxonomy' column of OTU table using semi-colon as delimiter and insert extra columns next to each level of taxonomy. Copy '#OTU ID' column to column 1 so it sits to the left of 'k__Bacteria' in column 'A'

```
=IF(ISBLANK(C3), " p__"&A3, C3)
=IF(ISBLANK(E3), " c__"&A3, E3)
=IF(F3=" c__", " c__"&A3, F3)
=IF(ISBLANK(H3), " o__"&A3, H3)
=IF(I3=" o__", " o__"&A3, I3)
=IF(ISBLANK(K3), " f__"&A3, K3)
=IF(L3=" f__", " f__"&A3, L3)
=IF(ISBLANK(N3), " g__"&A3, N3)
=IF(O3=" g__", " g__"&A3, O3)
=IF(ISBLANK(Q3), " s__"&A3, Q3)
=IF(R3=" s__", " s__"&A3, R3)
```

#Copy and paste relevant columns to adjacent columns

```
=B3&" ";"&C3&" ";"&D3&" ";"&E3&" ";"&F3&" ";"&G3&" ";"&H3
```

#Rename Taxonomy to Consensus Lineage, ensure no spaces in taxonomy, paste merged column back over 'taxonomy' and save new table as tab-delimited.txt named Shane_OTU_for_Phyloseq.txt.

#Combine 2 mapping files to create Shane_Master_Mapping.txt

#Now have the following: Shane_rep_phylo.tre; Shane_Master_Mapping.txt ; and Shane_OTU_for_Phyloseq.txt

#Entering R and creating environment for phyloseq analysis

```
source("http://bioconductor.org/biocLite.R")
biocLite("phyloseq")
install.packages("devtools")
library("devtools")
install_github("phyloseq", "joey711")
biocLite("BiocUpgrade")
install.packages("ape")
install.packages("ade4")
install.packages("doParallel")
install.packages("foreach")
install.packages("ggplot2")
install.packages("igraph")
install.packages("picante")
install.packages("plyr")
install.packages("RJSONIO")
install.packages("scales")
install.packages("testthat")
install.packages("vegan")
install.packages("extrafont")
library(extrafont)
font_import()
loadfonts(device="win")
```

#Check status with the following:

```

sessionInfo()
library()

#Begin phyloseq analysis

require(phyloseq)

otufilename <-
"C:/Users/Shane/Desktop/IonTorrent/Shane_OTU_for_Phyloseq.txt"

mapfilename <-
"C:/Users/Shane/Desktop/IonTorrent/Shane_Master_Mapping.txt"

treefilename <- "C:/Users/Shane/Desktop/IonTorrent/Shane_rep_phylo.tre"

ShaneAll <- import_qiime(otufilename=otufilename, mapfilename=mapfilename,
treefilename=treefilename)

rank_names(ShaneAll)

tax_table(ShaneAll) <- tax_table(ShaneAll)[,-8]

rank_names(ShaneAll)
sample_sums(ShaneAll)
mean(sample_sums(ShaneAll))
min(sample_sums(ShaneAll))
max(sample_sums(ShaneAll))
sd(sample_sums(ShaneAll))

#Prune taxa from the OTU table that are in zero samples, and remove non bacterial counts, and
rename to SAW (Shane All Working)

SAW <- prune_taxa(taxa_sums(ShaneAll)>0, ShaneAll)
SAW <- subset_taxa(SAW, Kingdom=="Bacteria")

write.table(otu_table(SAW), file =
"C:/Users/Shane/Desktop/IonTorrent/SAW_otu.txt", append = FALSE, quote
= TRUE, sep = " ", eol = "\n", na = "NA", dec = ".", row.names = TRUE,
col.names = TRUE)

write.table(tax_table(SAW), file =
"C:/Users/Shane/Desktop/IonTorrent/SAW_tax.txt", append = FALSE, quote
= TRUE, sep = " ", eol = "\n", na = "NA", dec = ".", row.names = TRUE,
col.names = TRUE)

#Check object details

SAW
# phyloseq-class experiment-level object
#otu_table() OTU Table: [ 7817 taxa and 120 samples ]
#sample_data() Sample Data: [ 120 samples by 11 sample variables
]
#tax_table() Taxonomy Table: [ 7817 taxa by 7 taxonomic ranks ]
#phy_tree() Phylogenetic Tree: [ 7817 tips and 7606 internal nodes
]

#Split into timepoints and sites, and also extract controls

```

```

SAW_Day7 <- subset_samples(SAW, Time %in% c("Day 7"))
SAW_Day14 <- subset_samples(SAW, Time %in% c("Day 14"))
SAW_Lung <- subset_samples(SAW, Group %in% c("Lung"))
SAW_Naso <- subset_samples(SAW, Group %in% c("Naso"))
SAW_Controls <- subset_samples(SAW, Combi %in% c("Controls"))

#Merge at family level for sensible comparisons and data representation in bar charts

SAW_fam <- tax_glom(SAW, taxrank="Family")
SAW_Day7_fam <- tax_glom(SAW_Day7, taxrank="Family")
SAW_Day14_fam <- tax_glom(SAW_Day14, taxrank="Family")
SAW_Lung_fam <- tax_glom(SAW_Lung, taxrank="Family")
SAW_Naso_fam <- tax_glom(SAW_Naso, taxrank="Family")
SAW_Controls_fam <- tax_glom(SAW_Controls, taxrank="Family")

#And remove controls from the time sets

SAW_Day7_fam_no_controls <- subset_samples(SAW_Day7_fam, Group %in%
c("Naso", "Lung"))
SAW_Day14_fam_no_controls <- subset_samples(SAW_Day14_fam, Group %in%
c("Naso", "Lung"))

#So sets are:

SAW
SAW_Day7_fam
SAW_Day14_fam
SAW_Lung_fam
SAW_Naso_fam
SAW_Controls_fam
SAW_Day7_fam_no_controls
SAW_Day14_fam_no_controls

#Rename and prune taxa and samples that are zero

S7F <- prune_taxa(taxa_sums(SAW_Day7_fam)>0, SAW_Day7_fam)
S7F <- prune_samples(sample_sums(S7F)>0, S7F)
S14F <- prune_taxa(taxa_sums(SAW_Day14_fam)>0, SAW_Day14_fam)
S14F <- prune_samples(sample_sums(S14F)>0, S14F)
SLF <- prune_taxa(taxa_sums(SAW_Lung_fam)>0, SAW_Lung_fam)
SLF <- prune_samples(sample_sums(SLF)>0, SLF)
SNF <- prune_taxa(taxa_sums(SAW_Naso_fam)>0, SAW_Naso_fam)
SNF <- prune_samples(sample_sums(SNF)>0, SNF)
SCF <- prune_taxa(taxa_sums(SAW_Controls_fam)>0, SAW_Controls_fam)
SCF <- prune_samples(sample_sums(SCF)>0, SCF)
S7Fnc <- prune_taxa(taxa_sums(SAW_Day7_fam_no_controls)>0,
SAW_Day7_fam_no_controls)
S7Fnc <- prune_samples(sample_sums(S7Fnc)>0, S7Fnc)
S14Fnc <- prune_taxa(taxa_sums(SAW_Day14_fam_no_controls)>0,
SAW_Day14_fam_no_controls)
S14Fnc <- prune_samples(sample_sums(S14Fnc)>0, S14Fnc)

#Then transform sample counts to relative abundance

S7F_RA <- transform_sample_counts(S7F, function(x){x/sum(x)})
S14F_RA <- transform_sample_counts(S14F, function(x){x/sum(x)})
SLF_RA <- transform_sample_counts(SLF, function(x){x/sum(x)})

```

```

SNF_RA <- transform_sample_counts(SNF, function(x) {x/sum(x)})
SCF_RA <- transform_sample_counts(SCF, function(x) {x/sum(x)})
S7Fnc_RA <- transform_sample_counts(S7Fnc, function(x) {x/sum(x)})
S14Fnc_RA <- transform_sample_counts(S14Fnc, function(x) {x/sum(x)})
#The following object (SAW_Controls) has all OTUs for all the control samples only
SAW_Controls

#Remove taxa that have a sum of zero

SAW_Controls_edit1 <- prune_taxa(taxa_sums(SAW_Controls)>0,
SAW_Controls)

#Convert to relative abundance

SAW_Controls_edit2 <- transform_sample_counts(SAW_Controls_edit1,
function(x) {x/sum(x)})

sample_sums(SAW_Controls_edit2)

SAW_Controls_edit3 <- prune_samples(sample_sums(SAW_Controls_edit2)>0,
SAW_Controls_edit2)

SAW_Controls_edit3_PCRs <- subset_samples(SAW_Controls_edit3, Group
%in% c("Negative"))

SAW_Controls_edit3_Blanks <- subset_samples(SAW_Controls_edit3, Group
%in% c("Blank"))

SAW_Controls_edit3_EColi <- subset_samples(SAW_Controls_edit3, Group
%in% c("EColi"))

SAW_Controls_edit3_PCRs_edit <- filter_taxa(SAW_Controls_edit3_PCRs,
function(x) sum(x > 0.01) > (0.3*length(x)), TRUE)

SAW_Controls_edit3_Blanks_edit <-
filter_taxa(SAW_Controls_edit3_Blanks, function(x) sum(x > 0) >
(0.3*length(x)), TRUE)

SAW_Controls_edit3_EColi_edit <- filter_taxa(SAW_Controls_edit3_EColi,
function(x) sum(x > 0.01) > (0.3*length(x)), TRUE)

ControlTaxaNames1 <- taxa_names(SAW_Controls_edit3_PCRs_edit)
ControlTaxaNames2 <- taxa_names(SAW_Controls_edit3_Blanks_edit)
ControlTaxaNames3 <- taxa_names(SAW_Controls_edit3_EColi_edit)

RemoveTaxaNames <- c(ControlTaxaNames1, ControlTaxaNames2,
ControlTaxaNames3)

RemoveTaxaNames <- unique(RemoveTaxaNames)

SAW_Controls_contaminant_taxa <- prune_taxa(RemoveTaxaNames,
SAW_Controls_edit3)

ContaminantFamilyNames <-
tax_table(SAW_Controls_contaminant_taxa)[,"Family"]

```

```

ContaminantFamilyNames <- as.vector(ContaminantFamilyNames)

ContaminantFamilyNames <- unique(ContaminantFamilyNames)

ContaminantFamilyNames <-
ContaminantFamilyNames[!ContaminantFamilyNames %in%
"Enterobacteriaceae"]

SAW_test <- subset_taxa(SAW, !(Family %in% c(ContaminantFamilyNames)))

#SAW_test contains all the samples but none of the contaminant families

#S7F is SAW_Day7_fam
#S14F is SAW_Day14_fam
#SLF is SAW_Lung_fam
#SNF is SAW_Naso_fam
#SCF is SAW_Controls_fam
#S7Fnc is SAW_Day7_fam_no_controls
#S14Fnc is SAW_Day14_fam_no_controls

#All of the above also have an RA version which is the relative abundance e.g. S7F_RA

#Create a full SAW object, without controls, for the final ordinations

SAW_fam_no_controls <- subset_samples(SAW_fam, Group %in%
c("Naso", "Lung"))

SAWFNC <- SAW_fam_no_controls

#And a relative abundance set for graphs

SAWFNC_RA <- transform_sample_counts(SAWFNC, function(x){x/sum(x)})

SAW_test_Day7 <- subset_samples(SAW_test, Time %in% c("Day 7"))
SAW_test_Day14 <- subset_samples(SAW_test, Time %in% c("Day 14"))
SAW_test_Lung <- subset_samples(SAW_test, Group %in% c("Lung"))
SAW_test_Naso <- subset_samples(SAW_test, Group %in% c("Naso"))

SAW_test_fam <- tax_glom(SAW_test, taxrank="Family")
SAW_test_Day7_fam <- tax_glom(SAW_test_Day7, taxrank="Family")
SAW_test_Day14_fam <- tax_glom(SAW_test_Day14, taxrank="Family")
SAW_test_Lung_fam <- tax_glom(SAW_test_Lung, taxrank="Family")
SAW_test_Naso_fam <- tax_glom(SAW_test_Naso, taxrank="Family")

#And remove control samples from the first 3 sets

SAW_test_fam_no_controls <- subset_samples(SAW_test_fam, Group %in%
c("Naso", "Lung"))
SAW_test_Day7_fam_no_controls <- subset_samples(SAW_test_Day7_fam,
Group %in% c("Naso", "Lung"))
SAW_test_Day14_fam_no_controls <- subset_samples(SAW_test_Day14_fam,
Group %in% c("Naso", "Lung"))
SAW_test_fam <- prune_taxa(taxa_sums(SAW_test_fam)>0, SAW_test_fam)
SAW_test_fam <- prune_samples(sample_sums(SAW_test_fam)>0,
SAW_test_fam)

```

```

SAWTFNC <- SAW_test_fam_no_controls
SAWTFNC <- prune_taxa(taxa_sums(SAWTFNC)>0, SAWTFNC)
SAWTFNC <- prune_samples(sample_sums(SAWTFNC)>0, SAWTFNC)
ST7F <- SAW_test_Day7_fam
ST7F <- prune_taxa(taxa_sums(ST7F)>0, ST7F)
ST7F <- prune_samples(sample_sums(ST7F)>0, ST7F)
ST14F <- SAW_test_Day14_fam
ST14F <- prune_taxa(taxa_sums(ST14F)>0, ST14F)
ST14F <- prune_samples(sample_sums(ST14F)>0, ST14F)
STLF <- SAW_test_Lung_fam
STLF <- prune_taxa(taxa_sums(STLF)>0, STLF)
STLF <- prune_samples(sample_sums(STLF)>0, STLF)
STNF <- SAW_test_Naso_fam
STNF <- prune_taxa(taxa_sums(STNF)>0, STNF)
STNF <- prune_samples(sample_sums(STNF)>0, STNF)
STFNc <- SAW_test_fam_no_controls
STFNc <- prune_taxa(taxa_sums(STFNc)>0, STFNc)
STFNc <- prune_samples(sample_sums(STFNc)>0, STFNc)
ST7FNc <- SAW_test_Day7_fam_no_controls
ST7FNc <- prune_taxa(taxa_sums(ST7FNc)>0, ST7FNc)
ST7FNc <- prune_samples(sample_sums(ST7FNc)>0, ST7FNc)
ST14FNc <- SAW_test_Day14_fam_no_controls
ST14FNc <- prune_taxa(taxa_sums(ST14FNc)>0, ST14FNc)
ST14FNc <- prune_samples(sample_sums(ST14FNc)>0, ST14FNc)

SAWTFNC_RA <- transform_sample_counts(SAWTFNC, function(x){x/sum(x)})
ST7F_RA <- transform_sample_counts(ST7F, function(x){x/sum(x)})
ST14F_RA <- transform_sample_counts(ST14F, function(x){x/sum(x)})
STLF_RA <- transform_sample_counts(STLF, function(x){x/sum(x)})
STNF_RA <- transform_sample_counts(STNF, function(x){x/sum(x)})
STFNc_RA <- transform_sample_counts(STFNc, function(x){x/sum(x)})
ST7FNc_RA <- transform_sample_counts(ST7FNc, function(x){x/sum(x)})
ST14FNc_RA <- transform_sample_counts(ST14FNc, function(x){x/sum(x)})

SAWCE3F <- tax_glom(SAW_Controls_edit3, taxrank="Family")
SAWCE3F_RA <- transform_sample_counts(SAWCE3F, function(x){x/sum(x)})

SAWTFNC_RA

Nasoday7_RA <- subset_samples(STNF_RA, Time %in% c("Day 7"))
Nasoday14_RA <- subset_samples(STNF_RA, Time %in% c("Day 14"))
Lungday7_RA <- subset_samples(STLF_RA, Time %in% c("Day 7"))
Lungday14_RA <- subset_samples(STLF_RA, Time %in% c("Day 14"))

ND7RA <- Nasoday7_RA
ND14RA <- Nasoday14_RA
LD7RA <- Lungday7_RA
LD14RA <- Lungday14_RA

```

Appendix 4. Construction of relative abundance bar charts.

```
write.table(otu_table(SAW_fam), file =
"C:/Users/Shane/Desktop/IonTorrent/SAW_fam_otu.txt", append = FALSE,
quote = TRUE, sep = " ", eol = "\n", na = "NA", dec = ".", row.names =
TRUE, col.names = TRUE)
```

```
write.table(tax_table(SAW_fam), file =
"C:/Users/Shane/Desktop/IonTorrent/SAW_fam_tax.txt", append = FALSE,
quote = TRUE, sep = " ", eol = "\n", na = "NA", dec = ".", row.names =
TRUE, col.names = TRUE)
```

#Starting with SAWFNC_RA, the full set of samples, scaled proportionally, but without controls

```
myTaxa_SAWFNC_RA_1 <- names(sort(taxa_sums(SAWFNC_RA), decreasing =
TRUE)[1:12])
```

```
SAWFNC_RA_head <- prune_taxa(myTaxa_SAWFNC_RA_1, SAWFNC_RA)
```

```
sum(taxa_sums(SAWFNC_RA_head))/sum(taxa_sums(SAWFNC_RA))
```

```
myTaxa_SAWFNC_RA_2 <- names(sort(taxa_sums(SAWFNC_RA), decreasing =
TRUE)[13:ntaxa(SAWFNC_RA)])
```

```
SAWFNC_RA_top13 <- merge_taxa(SAWFNC_RA, myTaxa_SAWFNC_RA_2)
```

```
tax_table(SAWFNC_RA_top13)
```

```
tax_table(SAWFNC_RA_top13)[4,2:5] <- "Other"
```

```
myTaxa_SAWFNC_RA_3 <- names(sort(taxa_sums(SAWFNC_RA_top13),
decreasing = TRUE))
```

```
SAWFNC_RA_List <- tapply(sample_names(SAWFNC_RA_top13),
get_variable(SAWFNC_RA_top13, "Combi2"), c)
```

```
CombiSAWFNC_RA_top13 <- lapply(SAWFNC_RA_List, prune_samples,
SAWFNC_RA_top13)
```

```
CombiOTUtable <- lapply(CombiSAWFNC_RA_top13, otu_table)
```

```
CombiAvg <- lapply(CombiOTUtable, rowMeans)
```

```
pooledOTUtable <- t(do.call(rbind, CombiAvg))
```

```
pooledOTUtable <-
```

```
data.frame(OTU=row.names(pooledOTUtable),pooledOTUtable)
```

```
TT <- tax_table(SAWFNC_RA_top13)
```

```
TT <- TT[, which(apply(!apply(TT, 2, is.na), 2, any))]
```

```
tdf <- data.frame(TT, OTU = taxa_names(SAWFNC_RA_top13))
```

```
pOTUtax <- merge(pooledOTUtable, tdf, by.x = "OTU")
```

```
write.table(pOTUtax,
```

```
file="C:/Users/Shane/Desktop/IonTorrent/pOTUtaxSAWFNC_RA_top13.txt",
append = FALSE, quote = TRUE, sep = " ", eol = "\n", na = "NA", dec =
".", row.names = TRUE, col.names = TRUE)
```

```

pOTU <- data.frame(pOTUtax, SeqTotal = rowSums(pOTUtax[,2:17])
pOTU

write.table(pOTU,
file="C:/Users/Shane/Desktop/IonTorrent/pOTUSAWFNC_RA_top13.txt",
append = FALSE, quote = TRUE, sep = " ", eol = "\n", na = "NA", dec =
".", row.names = TRUE, col.names = TRUE)

levels(pOTU$Family)
pOTU <- pOTU[order(pOTU$SeqTotal, decreasing=TRUE) , ]
tempFamilyLevels <- as.vector(pOTU$Family)
tempFamilyLevels
levels(pOTU$Family)
pOTU$Family <- factor(pOTU$Family, levels=c(tempFamilyLevels))
levels(pOTU$Family)

require("reshape2")
require("ggplot2")
require("scales")
require("grid")

pOTU.family <- pOTU[,c(2:17,22)]
melt.family <- melt(pOTU.family,id.vars="Family")
colnames(melt.family)[2] <- "Groups"
agg.family <- aggregate(.~Family+Groups, melt.family, sum)

pOTU
tempforbar1 <- as.vector(pOTU$Family)
tempforbar2 <- as.vector(pOTU$Phylum)

named.pos <- tempforbar2
names(named.pos) <- tempforbar1
agg.family$Phylum <- named.pos[agg.family$Family]

ShaneP1 <- ggplot(agg.family,aes(x=Groups,y=value,fill=Family)) +
  geom_bar(stat="identity",position="fill")

ShaneP1 <-
ggplot(agg.family,aes(x=Groups,y=value,fill=Family,width=0.7)) +
  geom_bar(stat="identity",position="stack",colour="black")

install.packages("extrafont")
library(extrafont)
loadfonts(device="win")

ShaneP1_testing <- ShaneP1 + theme(text = element_text(family =
"Helvetica", size=12))

ShaneP1_testing <- ShaneP1 + theme(text = element_text(family =
"Vrinda", size=12))

ShaneP1 <- ShaneP1 + theme(text = element_text(family = "Helvetica",
size=12))

ShaneP1 <- ShaneP1 + scale_y_continuous(labels = percent_format()+
  xlab("Groups") +
  ylab("Relative Abundance"))

```

```

ShaneP1 <- ShaneP1 +
  theme(axis.title.x = element_text(face="bold",size=rel(1.2)),
        axis.text.x = element_text(angle=45, face="bold", colour =
"black", size=rel(1.2), vjust=1, hjust=1),
        axis.text.y = element_text(colour = "black", size=rel(1.2)),
        axis.title.y = element_text(face="bold", size=rel(1.2)))

ShaneP1 <- ShaneP1 + theme(panel.background =
element_rect(fill="grey90"),
        panel.grid.major = element_blank(),
        panel.grid.minor = element_blank())

ShaneP1 <- ShaneP1 + guides(fill = guide_legend(reverse = TRUE))

levels(agg.family$Groups)

ShaneP1 <- ShaneP1 + scale_x_discrete(limits=c("X7.PBS.N",
"X14.PBS.N", "X7.BC.N", "X14.BC.N", "X7.D39.N", "X14.D39.N",
"X7.D39...BC.N", "X14.D39...BC.N", "X7.PBS.L", "X14.PBS.L",
"X7.BC.L", "X14.BC.L", "X7.D39.L", "X14.D39.L", "X7.D39...BC.L",
"X14.D39...BC.L"),
        labels=c("PBS-7-N", "PBS-14-N", "BC-7-N", "BC-14-N", "D39-
7-N", "D39-14-N", "D39+BC-7-N", "D39+BC-14-N", "PBS-7-L", "PBS-14-L",
"BC-7-L", "BC-14-L", "D39-7-L", "D39-14-L", "D39+BC-7-L", "D39+BC-14-
L"))

Barchart13colours <- c("#696969", "#a6cee3", "#1f78b4", "#b2df8a",
"#33a02c", "#fb9a99", "#e31a1c", "#fdbf6f", "#ff7f00", "#cab2d6",
"#6a3d9a", "#ffff99", "#000000")

ShaneP1 <- ShaneP1 + scale_fill_manual(values = c(Barchart13colours))

ShaneP1 <- ShaneP1 + scale_fill_manual(values = c(Barchart13colours),
name="Families")

ShaneP1 <- ShaneP1 + theme(axis.text=element_text(size=rel(1.2)),
axis.title=element_text(size=rel(1.3)),
legend.text=element_text(size=rel(1.2), face="bold.italic"),
legend.title=element_text(size=rel(1.3), face="bold"))

ggsave(filename="ShaneP1.png", ShaneP1, width = 16, height = 9, dpi =
250)
require(Cairo)
print(ShaneP1)
dev.print(cairo_pdf, "ShaneP1.pdf")

ShaneP1Facet <- ShaneP1 + facet_grid(Phylum ~ ., scales="free_y")

ShaneP1Facet <- ShaneP1Facet + theme(strip.text.y =
element_text(size=rel(0.8), face="bold"), axis.text.y =
element_text(size=rel(0.65), face="plain"), axis.text.x =
element_text(size=rel(1.2), face="bold")) + theme(panel.border =
element_rect(colour="black", fill="NA"))

ggsave(filename="ShaneP1Facet.png", ShaneP1Facet, width = 16, height =
9, dpi = 250)
require(Cairo)

```

```
print(ShaneP1Facet)
dev.print(cairo_pdf, "ShaneP1Facet.pdf")
```

```
CombiOTUtable <- NULL
CombiAvg <- NULL
pooledOTUtable <- NULL
TT <- NULL
tdf <- NULL
pOTUtax <- NULL
pOTU <- NULL
pOTU.family <- NULL
melt.family <- NULL
agg.family <- NULL
tempFamilyLevels<- NULL
tempforbar1 <- NULL
tempforbar2 <- NULL
named.pos <- NULL
names(named.pos) <- NULL
```

#Script is essentially identical for other bar chart designations except for the number of otus included and sample/group names

Appendix 5. Statistical analysis of ion torrent data – alpha diversity.

```
SAW_fam_for_alpha <- SAW_fam
SFFA <- SAW_fam_for_alpha
SAW_test_fam_for_alpha <- SAW_test_fam
STFFA <- SAW_test_fam_for_alpha

SAW_fam_no_controls <- subset_samples(SAW_fam, Group %in% c("Naso",
"Lung"))
SAW_fam_no_controls_for_alpha <- subset_samples(SAW_fam_no_controls,
Time %in% c("Day 7", "Day 14"))
SFNCFA <- SAW_fam_no_controls_for_alpha
SAW_test_fam_no_controls <- subset_samples(SAW_test_fam, Group %in%
c("Naso", "Lung"))
SAW_test_fam_no_controls_for_alpha <-
subset_samples(SAW_test_fam_no_controls, Time %in% c("Day 7", "Day
14"))
STFNCFA <- SAW_test_fam_no_controls_for_alpha

#Process and rarefy

SFNCFA <- prune_taxa(taxa_sums(SFNCFA)>0,SFNCFA)

SFNCFA <- prune_samples(sample_sums(SFNCFA)>5000,SFNCFA)

min(sample_sums(SFNCFA))

SFNCFA.rar <- rarefy_even_depth(SFNCFA, sample.size =
min(sample_sums(SFNCFA)), rngseed = FALSE, replace = TRUE, trimOTUs =
TRUE)

alpha_meas <- c("Observed", "Shannon", "Simpson", "InvSimpson")

SFNCFA.rar.rich <- estimate_richness(SFNCFA.rar, split = TRUE,
measures = alpha_meas)

write.table(SFNCFA.rar.rich, file =
"C:/Users/Adam/Desktop/SFNCFA.rar.rich.txt", append = FALSE, quote =
TRUE, sep = " ", eol = "\n", na = "NA", dec = ".", row.names = TRUE,
col.names = TRUE)

colourCount <- length(unique(get_variable(SFNCFA.rar, "Combi")))

getPalette <- colorRampPalette(brewer.pal(9, "Set1"))

SFNCFA_plot <- plot_richness(SFNCFA.rar, x = "Combi", color = "Combi",
measures = c("Simpson", "Shannon")) + scale_colour_manual(values =
getPalette(colourCount)) + geom_boxplot()

SFNCFA_plot <- SFNCFA_plot + theme(text = element_text(size=16),
panel.background = element_rect(fill='grey90', colour='black'),
panel.grid.major = element_blank(), panel.grid.minor =
element_blank())

levels(sample_data(SFNCFA.rar)$Combi)
```

```
SFNCFA_plot <- SFNCFA_plot +
scale_x_discrete(limits=c("NPE", "NPL", "NCE", "NCL", "NSE", "NSL", "NSCE",
"NSCL", "LPE", "LPL", "LCE", "LCL", "LSE", "LSL", "LSCE", "LSCL"),
labels=c("PBS-7-N", "PBS-14-N", "BC-7-N", "BC-14-N", "D39-
7-N", "D39-14-N", "D39+BC-7-N", "D39+BC-14-N", "PBS-7-L", "PBS-14-L",
"BC-7-L", "BC-14-L", "D39-7-L", "D39-14-L", "D39+BC-7-L", "D39+BC-14-
L"))
```

```
SFNCFA_plot <- SFNCFA_plot +
scale_colour_manual(values=getPalette(colourCount),
breaks=c("NPE", "NPL", "NCE", "NCL", "NSE", "NSL", "NSCE",
"NSCL", "LPE", "LPL", "LCE", "LCL", "LSE", "LSL", "LSCE", "LSCL"),
labels=c("PBS-7-N", "PBS-14-N", "BC-7-N", "BC-14-N",
"D39-7-N", "D39-14-N", "D39+BC-7-N", "D39+BC-14-N", "PBS-7-L", "PBS-
14-L", "BC-7-L", "BC-14-L", "D39-7-L", "D39-14-L", "D39+BC-7-L",
"D39+BC-14-L"))
```

```
SFNCFA_plot <- SFNCFA_plot + theme(axis.title.x =
element_text(face="bold", size=rel(1.2)),
axis.text.x = element_text(angle=45, face="bold", colour =
"black", size=rel(1.2), vjust=1, hjust=1),
axis.text.y = element_text(colour = "black", size=rel(1.2)),
axis.title.y = element_text(face="bold", size=rel(1.2))) +
xlab("Groups") + guides(colour=FALSE) +
theme(plot.margin=unit(c(1,1,1,1), "cm"))
```

```
ggsave(filename="SFNCFA_plot.png", SFNCFA_plot, width = 16, height = 9,
dpi = 250)
require(Cairo)
print(SFNCFA_plot)
dev.print(cairo_pdf, "SFNCFA_plot.pdf")
```

#Procedure for STFNCFA is identical

```
sample_data(SFFA)$AlphaGroups <- c("7-BC-N", "14-PBS-N", "Blank", "7-BC-
N", "7-D39+BC-L", "14-D39-N", "14-D39+BC-L", "14-BC-N", "14-D39+BC-L", "14-
PBS-L", "7-D39-N", "14-D39-L", "7-PBS-N", "14-D39-L", "14-D39-L", "14-BC-
L", "14-BC-L", "14-D39+BC-L", "14-D39-N", "14-D39+BC-N", "14-BC-L", "7-BC-
L", "7-BC-L", "14-D39+BC-N", "EColi", "EColi", "14-BC-L", "7-D39+BC-
L", "EColi", "EColi", "7-PBS-N", "7-BC-L", "7-D39+BC-N", "14-BC-N", "7-D39-
N", "7-D39+BC-L", "14-D39-N", "7-D39+BC-N", "7-BC-N", "Neg PCR", "7-BC-
N", "Neg PCR", "14-PBS-N", "7-D39-L", "7-PBS-L", "7-D39-N", "14-PBS-L", "14-
D39-N", "7-PBS-L", "7-D39-N", "7-PBS-L", "7-PBS-L", "7-D39-L", "14-PBS-
N", "14-D39+BC-L", "7-BC-L", "14-PBS-N", "14-D39+BC-N", "7-PBS-N", "7-
D39+BC-L", "7-D39+BC-N", "7-D39+BC-L", "7-D39-L", "7-PBS-L", "7-PBS-N", "7-
D39-L", "14-PBS-N", "14-D39+BC-L", "14-PBS-L", "14-D39+BC-N", "14-D39-
L", "14-D39-L", "14-BC-N", "14-PBS-L", "14-PBS-L", "7-D39+BC-N", "7-PBS-
N", "7-D39+BC-N", "Neg PCR", "14-D39-N", "14-D39+BC-N", "7-BC-L", "7-D39-
N", "14-BC-N", "7-BC-N", "7-D39-L", "Neg
PCR", "EColi", "EColi", "Blank", "EColi", "EColi", "14-BC-N", "Neg
PCR", "EColi", "Neg
PCR", "EColi", "Blank", "Blank", "Blank", "Blank", "Blank", "14-BC-
L",
"Blank", "Blank", "Blank", "Blank", "Blank", "Blank", "Blank", "Blank", "Blank", "Blank",
"Blank", "Blank", "Blank", "Blank", "Blank", "Blank", "Blank")
```

```
alpha_meas <- c("Observed", "Shannon", "Simpson", "InvSimpson")
```

```

SFFA.rich <- estimate_richness(SFFA, split = TRUE, measures =
alpha_meas)

write.table(SFFA.rich, file = "C:/Users/Adam/Desktop/SFFA.rich.txt",
append = FALSE, quote = TRUE, sep = " ", eol = "\n", na = "NA", dec =
".", row.names = TRUE, col.names = TRUE)

colourCount <- length(unique(get_variable(SFFA, "AlphaGroups")))

getPalette <- colorRampPalette(brewer.pal(9, "Set1"))

SFFA_plot <- plot_richness(SFFA, x = "AlphaGroups", color =
"AlphaGroups", measures = c("Simpson", "Shannon")) +
scale_colour_manual(values = getPalette(colourCount)) + geom_boxplot()

SFFA_plot <- SFFA_plot + theme(text = element_text(size=16),
panel.background = element_rect(fill='grey90', colour='black'),
panel.grid.major = element_blank(), panel.grid.minor =
element_blank())

SFFA_plot <- SFFA_plot +
scale_x_discrete(limits=c("7-PBS-N", "14-PBS-N", "7-BC-N", "14-BC-N", "7-
D39-N", "14-D39-N", "7-D39+BC-N", "14-D39+BC-N", "7-PBS-L", "14-PBS-L", "7-
BC-L", "14-BC-L", "7-D39-L", "14-D39-L", "7-D39+BC-L", "14-D39+BC-
L", "Blank", "EColi", "Neg PCR"), labels=c("PBS-7-N", "PBS-14-N", "BC-7-
N", "BC-14-N", "D39-7-N", "D39-14-N", "D39+BC-7-N", "D39+BC-14-N",
"PBS-7-L", "PBS-14-L", "BC-7-L", "BC-14-L", "D39-7-L", "D39-14-L",
"D39+BC-7-L", "D39+BC-14-L", "Blanks", "E.Coli", "Neg PCR"))

SFFA_plot <- SFFA_plot +
scale_colour_manual(values=getPalette(colourCount), breaks=c("7-PBS-
N", "14-PBS-N", "7-BC-N", "14-BC-N", "7-D39-N", "14-D39-N", "7-D39+BC-
N", "14-D39+BC-N", "7-PBS-L", "14-PBS-L", "7-BC-L", "14-BC-L", "7-D39-
L", "14-D39-L", "7-D39+BC-L", "14-D39+BC-L", "Blank", "EColi", "Neg
PCR"), labels=c("PBS-7-N", "PBS-14-N", "BC-7-N", "BC-14-N", "D39-7-N",
"D39-14-N", "D39+BC-7-N", "D39+BC-14-N", "PBS-7-L", "PBS-14-L", "BC-7-
L", "BC-14-L", "D39-7-L", "D39-14-L", "D39+BC-7-L", "D39+BC-14-L",
"Blanks", "E.Coli", "Neg PCR"))

SFFA_plot <- SFFA_plot + theme(axis.title.x =
element_text(face="bold", size=rel(1.2)),
axis.text.x = element_text(angle=45, face="bold", colour =
"black", size=rel(1.2), vjust=1, hjust=1),
axis.text.y = element_text(colour = "black", size=rel(1.2)),
axis.title.y = element_text(face="bold", size=rel(1.2))) +
xlab("Groups") + guides(colour=FALSE) +
theme(plot.margin=unit(c(1,1,1,1), "cm"))

ggsave(filename="SFFA_plot.png", SFFA_plot, width = 16, height = 9, dpi
= 250)
require(Cairo)
print(SFFA_plot)
dev.print(cairo_pdf, "SFFA_plot.pdf")

```

#Procedure for STFFA is as above

Appendix 6. Beta diversity and ordinations.

#SAW_fam is the set object with all samples included; SAWFNC is the same set without controls; SAWTFNC (or STFNC) is the family level object with contaminant otus removed and without control samples

```
SF <- SAW_fam

SFo <- prune_samples(sample_sums(SF)>0, SF)
SFo_full <- transform_sample_counts(SFo, function(x){x/sum(x)})

SFo_edit <- filter_taxa(SFo_full, function(x) sum(x > 0.01) > 3, TRUE)
SFo_edit <- transform_sample_counts(SFo_edit, function(x){x/sum(x)})

SF.ord <- ordinate(SFo_full, "NMDS", "bray")

ShaneOrdP1 <- plot_ordination(SFo_full, SF.ord, type = "taxa", color =
"Phylum")

ShaneOrdP1 <- ShaneOrdP1 + geom_point(size = 2.5)

ShaneOrdP1 <- ShaneOrdP1 + theme(panel.grid.major = element_blank(),
panel.grid.minor = element_blank(), panel.border =
element_rect(fill=NA, size=0.5, linetype = "solid", colour = "black"),
legend.background = element_rect(fill=NA, size=0.5, linetype="solid",
colour="black"))

ShaneOrdP1 <- ShaneOrdP1 + theme(legend.title =
element_text(size=rel(1.3), face="bold"),
legend.text = element\_text(size=rel(1.3), face="bold.italic"),
axis.title.x = element_text(face="bold",size=rel(1.3)),
axis.text.x = element_text(face="bold", colour = "black",
size=rel(1.2)),
axis.text.y = element_text(face="bold", colour = "black",
size=rel(1.2)),
axis.title.y = element_text(face="bold", size=rel(1.3)))

SF.orda <- ordinate(SFo_edit, "NMDS", "bray")

ShaneOrdP1a <- plot_ordination(SFo_edit, SF.orda, type = "taxa", color
= "Phylum")

ShaneOrdP1a <- ShaneOrdP1a + geom_point(size = 4)

ShaneOrdP1a <- ShaneOrdP1a + theme(panel.grid.major = element_blank(),
panel.grid.minor = element_blank(), panel.border =
element_rect(fill=NA, size=0.5, linetype = "solid", colour = "black"),
legend.background = element_rect(fill=NA, size=0.5, linetype="solid",
colour="black"))

ShaneOrdP1a <- ShaneOrdP1a + theme(legend.title =
element_text(size=rel(1.3), face="bold"),
legend.text = element\_text(size=rel(1.3), face="bold.italic"),
axis.title.x = element_text(face="bold",size=rel(1.3)),
axis.text.x = element_text(face="bold", colour = "black",
size=rel(1.2)),
```

```
        axis.text.y = element_text(face="bold", colour = "black",
size=rel(1.2)),
        axis.title.y = element_text(face="bold", size=rel(1.3)))

ggsave(filename="ShaneOrdP1.png", ShaneOrdP1, width = 16, height = 9,
dpi = 250)
require(Cairo)
print(ShaneOrdP1)
dev.print(cairo_pdf, "ShaneOrdP1.pdf")

ggsave(filename="ShaneOrdP1a.png", ShaneOrdP1a, width = 16, height =
9, dpi = 250)
require(Cairo)
print(ShaneOrdP1a)
dev.print(cairo_pdf, "ShaneOrdP1a.pdf")

#Other ordinations do not differ significantly enough to warrant inclusion of script
```

Appendix 7. Statistical analysis of ion torrent data – Adonis and betadisper.

#Test adonis and betadisper on scaled beta diversity i.e. Bray Curtis of RA - Nasoday7, Nasoday14, Lungday7, Lungday14, STLF, and STNF, ST7FNc, ST14FNc, and SAWTF. Can use versions of objects from ordinations

```
SAWTFo
STLFO
STNFO
ST7FO
ST14FO
Nasoday7o
Nasoday14o
Lungday7o
Lungday14o
```

#Adonis tests differences in means of the groups; betadisper tests differences in dispersion of the groups; anosim is similar to adonis but more likely to provide false positives

```
SAWTFo.bdlist <- phyloseq::distance(SAWTFo, "bray")
SAWTFo.udist <- phyloseq::distance(SAWTFo, "unifrac", weighted=TRUE)

SAWTFo.bdlist <- phyloseq::distance(SAWTFo, "bray")
SAWTFo.udist <- phyloseq::distance(SAWTFo, "unifrac", weighted=TRUE)

adonis.bd.Combi <- adonis(SAWTFo.bdlist~Combi,
as(sample_data(SAWTFo), "data.frame"))
adonis.ud.Combi <- adonis(SAWTFo.udist~Combi,
as(sample_data(SAWTFo), "data.frame"))
betadisper.bd.Combi <- betadisper(SAWTFo.bdlist,
sample_data(SAWTFo)$Combi)
betadisper.ud.Combi <- betadisper(SAWTFo.udist,
sample_data(SAWTFo)$Combi)
anosim.bd.Combi <- anosim(SAWTFo.bdlist, sample_data(SAWTFo)$Combi)
anosim.ud.Combi <- anosim(SAWTFo.udist, sample_data(SAWTFo)$Combi)

save1 <- adonis.bd.Combi
save2 <- anova(betadisper.bd.Combi)
save3 <- permutest(betadisper.bd.Combi, pairwise = TRUE)
save4 <- TukeyHSD(betadisper.bd.Combi)

save5 <- adonis.ud.Combi
save6 <- anova(betadisper.ud.Combi)
save7 <- permutest(betadisper.ud.Combi, pairwise = TRUE)
save8 <- TukeyHSD(betadisper.ud.Combi)

save1
save2
save3
save4
save5
save6
save7
save8
```

#All results copied and saved as "SAWTFo_adonis_and_betadisper.txt"

```
save1 <- NULL
save2 <- NULL
save3 <- NULL
save4 <- NULL
```

```
save5 <- NULL
save6 <- NULL
save7 <- NULL
save8 <- NULL
```

#All others follow exactly the same format - unifracs included alongside Bray-Curtis to test that choice of metric is not influencing outcome

Nasoday7o, Nasoday14o, Lungday7o, Lungday14o

```
Nasoday7 <- subset_samples(STNF, Time %in% c("Day 7"))
Nasoday14 <- subset_samples(STNF, Time %in% c("Day 14"))
Lungday7 <- subset_samples(STLF, Time %in% c("Day 7"))
Lungday14 <- subset_samples(STLF, Time %in% c("Day 14"))
```

```
Nasoday7o <- prune_taxa(taxa_sums(Nasoday7)>0, Nasoday7)
Nasoday14o <- prune_taxa(taxa_sums(Nasoday14)>0, Nasoday14)
Lungday7o <- prune_taxa(taxa_sums(Lungday7)>0, Lungday7)
Lungday14o <- prune_taxa(taxa_sums(Lungday14)>0, Lungday14)
```

```
Naso7A <- subset_samples(Nasoday7o, Combi %in% c("NPE", "NCE"))
Naso7B <- subset_samples(Nasoday7o, Combi %in% c("NPE", "NSE"))
Naso7C <- subset_samples(Nasoday7o, Combi %in% c("NPE", "NSCE"))
```

```
Naso14A <- subset_samples(Nasoday14o, Combi %in% c("NPL", "NCL"))
Naso14B <- subset_samples(Nasoday14o, Combi %in% c("NPL", "NSL"))
Naso14C <- subset_samples(Nasoday14o, Combi %in% c("NPL", "NSCL"))
```

```
Lung7A <- subset_samples(Lungday7o, Combi %in% c("LPE", "LCE"))
Lung7B <- subset_samples(Lungday7o, Combi %in% c("LPE", "LSE"))
Lung7C <- subset_samples(Lungday7o, Combi %in% c("LPE", "LSCE"))
```

```
Lung14A <- subset_samples(Lungday14o, Combi %in% c("LPL", "LCL"))
Lung14B <- subset_samples(Lungday14o, Combi %in% c("LPL", "LSL"))
Lung14C <- subset_samples(Lungday14o, Combi %in% c("LPL", "LSCL"))
```

Appendix 8. Statistical analysis of ion torrent data – Multiple testing in Phyloseq.

```
SAWTFo

SAWTFO_for_mt <- filter_taxa(SAWTFo, function(x) var(x) > 1e-05, TRUE)

SAWTFo.fwer.table1 <- mt(SAWTFo_for_mt, "Group")

SAWTFo.fwer.table2 <- mt(SAWTFo_for_mt, "Time")

SAWTFo.fwer.table3 <- mt(SAWTFo_for_mt, test="f", "Subgroup")
#Then save the tables
write.table(SAWTFo.fwer.table1,
file="C:/Users/Shane/Desktop/IonTorrent/SAWTFo.fwer.table1.txt",
append = FALSE, quote = TRUE, sep = " ", eol = "\n", na = "NA", dec =
".", row.names = TRUE, col.names = TRUE)

write.table(SAWTFo.fwer.table2,
file="C:/Users/Shane/Desktop/IonTorrent/SAWTFo.fwer.table2.txt",
append = FALSE, quote = TRUE, sep = " ", eol = "\n", na = "NA", dec =
".", row.names = TRUE, col.names = TRUE)

write.table(SAWTFo.fwer.table3,
file="C:/Users/Shane/Desktop/IonTorrent/SAWTFo.fwer.table3.txt",
append = FALSE, quote = TRUE, sep = " ", eol = "\n", na = "NA", dec =
".", row.names = TRUE, col.names = TRUE)

SAWTFo.fwer.table1$FDR <- p.adjust(c(SAWTFo.fwer.table1[, "rawp"]),
method = c("fdr"))

SAWTFo.fdr.table4 <- subset(SAWTFo.fwer.table1, FDR < 0.05)

SAWTFo.fwer.table2$FDR <- p.adjust(c(SAWTFo.fwer.table2[, "rawp"]),
method = c("fdr"))

SAWTFo.fdr.table5 <- subset(SAWTFo.fwer.table2, FDR < 0.05)

SAWTFo.fwer.table3$FDR <- p.adjust(c(SAWTFo.fwer.table3[, "rawp"]),
method = c("fdr"))

SAWTFo.fdr.table6 <- subset(SAWTFo.fwer.table3, FDR < 0.05)

write.table(SAWTFo.fdr.table4,
file="C:/Users/Shane/Desktop/IonTorrent/SAWTFo.fdr.table4.txt", append
= FALSE, quote = TRUE, sep = " ", eol = "\n", na = "NA", dec = ".",
row.names = TRUE, col.names = TRUE)

write.table(SAWTFo.fdr.table5,
file="C:/Users/Shane/Desktop/IonTorrent/SAWTFo.fdr.table5.txt", append
= FALSE, quote = TRUE, sep = " ", eol = "\n", na = "NA", dec = ".",
row.names = TRUE, col.names = TRUE)

write.table(SAWTFo.fdr.table6,
file="C:/Users/Shane/Desktop/IonTorrent/SAWTFo.fdr.table6.txt", append
= FALSE, quote = TRUE, sep = " ", eol = "\n", na = "NA", dec = ".",
row.names = TRUE, col.names = TRUE)
```

Appendix 9. Statistical analysis of ion torrent data – DeSeq2.

```
SAW_test_fam_for_DESeq2 <-  
prune_samples(sample_sums(SAW_test_fam)>1000, SAW_test_fam)  
  
STFFD <- SAW_test_fam_for_DESeq2  
  
STFFD <- subset_samples(STFFD, Time %in% c("Day 7", "Day 14"))  
  
STFFD <- subset_samples(STFFD, Group %in% c("Naso", "Lung"))  
  
STFFD <- prune_taxa(taxa_sums(STFFD)>0,STFFD)  
  
SDS1 <- ShaneDeSeq1 <- phyloseq_to_deseq2(STFFD, ~ Group)  
SDS1$Group <- relevel(SDS1$Group, ref="Naso")  
  
SDS2 <- ShaneDeSeq2 <- phyloseq_to_deseq2(STFFD, ~ Time)  
SDS2$Time <- relevel(SDS2$Time, ref="Day 7")  
  
SDS3 <- ShaneDeSeq3 <- phyloseq_to_deseq2(STFFD, ~ Combi)  
SDS3$Combi <- relevel(SDS3$Combi, ref="NPE")  
  
SDS1a <- DESeq(SDS1, test="Wald", fitType="parametric")  
  
res <- results(SDS1a, cooksCutoff = FALSE)  
resOrdered <- res[order(res$padj),]  
alpha <- 0.1  
sigtab <- res[which(res$padj < alpha), ]  
sigtab <- cbind(as(sigtab, "data.frame"),  
as(tax_table(STFFD)[rownames(sigtab), ], "matrix"))  
head(sigtab)  
sigtabOrdered1 <- sigtab[order(sigtab$padj),]  
  
write.table(sigtabOrdered1,  
file="C:/Users/Shane/Desktop/IonTorrent/DEseq.Group.txt", append =  
FALSE, quote = TRUE, sep = " ", eol = "\n", na = "NA", dec = ".",  
row.names = TRUE, col.names = TRUE)  
  
SDS2a <- DESeq(SDS2, test="Wald", fitType="parametric")  
  
res <- results(SDS2a, cooksCutoff = FALSE)  
resOrdered <- res[order(res$padj),]  
alpha <- 0.1  
sigtab <- res[which(res$padj < alpha), ]  
sigtab <- cbind(as(sigtab, "data.frame"),  
as(tax_table(STFFD)[rownames(sigtab), ], "matrix"))  
head(sigtab)  
sigtabOrdered2 <- sigtab[order(sigtab$padj),]  
  
write.table(sigtabOrdered2,  
file="C:/Users/Shane/Desktop/IonTorrent/DEseq.Time.txt", append =  
FALSE, quote = TRUE, sep = " ", eol = "\n", na = "NA", dec = ".",  
row.names = TRUE, col.names = TRUE)  
  
SDS3a <- DESeq(SDS3, test="Wald", fitType="parametric")
```

```

NPEvNCE <- results(SDS3a, contrast=c("Combi", "NPE", "NCE"))
NPEvNSE <- results(SDS3a, contrast=c("Combi", "NPE", "NSE"))
NPEvNSCE <- results(SDS3a, contrast=c("Combi", "NPE", "NSCE"))
NCEvNSE <- results(SDS3a, contrast=c("Combi", "NCE", "NSE"))
NCEvNSCE <- results(SDS3a, contrast=c("Combi", "NCE", "NSCE"))
NSEvNSCE <- results(SDS3a, contrast=c("Combi", "NSE", "NSCE"))

LPEvLCE <- results(SDS3a, contrast=c("Combi", "LPE", "LCE"))
LPEvLSE <- results(SDS3a, contrast=c("Combi", "LPE", "LSE"))
LPEvLSCE <- results(SDS3a, contrast=c("Combi", "LPE", "LSCE"))
LCEvLSE <- results(SDS3a, contrast=c("Combi", "LCE", "LSE"))
LCEvLSCE <- results(SDS3a, contrast=c("Combi", "LCE", "LSCE"))
LSEvLSCE <- results(SDS3a, contrast=c("Combi", "LSE", "LSCE"))

NPLvNCL <- results(SDS3a, contrast=c("Combi", "NPL", "NCL"))
NPLvNSL <- results(SDS3a, contrast=c("Combi", "NPL", "NSL"))
NPLvNSCL <- results(SDS3a, contrast=c("Combi", "NPL", "NSCL"))
NCLvNSL <- results(SDS3a, contrast=c("Combi", "NCL", "NSL"))
NCLvNSCL <- results(SDS3a, contrast=c("Combi", "NCL", "NSCL"))
NSLvNSCL <- results(SDS3a, contrast=c("Combi", "NSL", "NSCL"))

LPLvLCL <- results(SDS3a, contrast=c("Combi", "LPL", "LCL"))
LPLvLSL <- results(SDS3a, contrast=c("Combi", "LPL", "LSL"))
LPLvLSCL <- results(SDS3a, contrast=c("Combi", "LPL", "LSCL"))
LCLvLSL <- results(SDS3a, contrast=c("Combi", "LCL", "LSL"))
LCLvLSCL <- results(SDS3a, contrast=c("Combi", "LCL", "LSCL"))
LSLvLSCL <- results(SDS3a, contrast=c("Combi", "LSL", "LSCL"))

LPEvLPL <- results(SDS3a, contrast=c("Combi", "LPE", "LPL"))
LCEvLCL <- results(SDS3a, contrast=c("Combi", "LCE", "LCL"))
LSEvLSL <- results(SDS3a, contrast=c("Combi", "LSE", "LSL"))
LSCEvLSCL <- results(SDS3a, contrast=c("Combi", "LSCE", "LSCL"))

NPEvNPL <- results(SDS3a, contrast=c("Combi", "NPE", "NPL"))
NCEvNCL <- results(SDS3a, contrast=c("Combi", "NCE", "NCL"))
NSEvNSL <- results(SDS3a, contrast=c("Combi", "NSE", "NSL"))
NSCEvNSCL <- results(SDS3a, contrast=c("Combi", "NSCE", "NSCL"))

```

Appendix 10. Analysis for preliminary ion torrent test.

```
#Processed files in Qiime and created a combined otu table/tax table and mapping file

require(phyloseq)

otufilename1 <- "C:/Users/Adam/Desktop/Shane
Prelim/Shane_prelim_for_Phyloseq.txt"

mapfilename1 <- "C:/Users/Adam/Desktop/Shane
Prelim/Shane_prelim_mapping.txt"

ShanePrelim <- import_qiime(otufilename=otufilename1,
mapfilename=mapfilename1)

rank_names(ShanePrelim)

sample_sums(ShanePrelim)

ShanePrelim_fam <- tax_glom(ShanePrelim, taxrank="Family")

MPF <- ShanePrelim_fam

#MPF stands for Mouse Preliminary Family

MPF_RA <- transform_sample_counts(MPF, function(x){x/sum(x)})

MPF_RA_f <- filter_taxa(MPF_RA, function(x) sum(x > 0.01) > 5, TRUE)

write.table(otu_table(MPF_RA), file = "C:/Users/Adam/Desktop/Shane
Prelim/MPF_RA_otu.txt", append = FALSE, quote = TRUE, sep = " ", eol =
"\n", na = "NA", dec = ".", row.names = TRUE, col.names = TRUE)

write.table(tax_table(MPF_RA), file = "C:/Users/Adam/Desktop/Shane
Prelim/MPF_RA_tax.txt", append = FALSE, quote = TRUE, sep = " ", eol =
"\n", na = "NA", dec = ".", row.names = TRUE, col.names = TRUE)

#Manual inspection of the tables leads to selection of the top 20 families with the remaining
families being merged into an other category

myTaxa_MPF_RA_1 <- names(sort(taxa_sums(MPF_RA), decreasing =
TRUE)[1:19])
myTaxa_MPF_RA_2 <- names(sort(taxa_sums(MPF_RA), decreasing =
TRUE)[20:ntaxa(MPF_RA)])

MPF_RA_top20 <- merge_taxa(MPF_RA, myTaxa_MPF_RA_2)

#Identify the new merged OTU which has numerous 'NA' entries in the tax_table, and then
replace with 'Other'

tax_table(MPF_RA_top20)
tax_table(MPF_RA_top20)[14,2:5] <- "Other"

myTaxa_MPF_RA_3 <- names(sort(taxa_sums(MPF_RA_top20), decreasing =
TRUE))
```

```

Temp123 <- as.data.frame(otu_table(MPF_RA_top20))
Temp456 <- as.data.frame(tax_table(MPF_RA_top20))
Temp123 <- data.frame(Temp123, SeqTotal = rowSums(Temp123[,1:15]))
Temp123 <- data.frame(Temp123, Temp456$Family)
colnames(Temp123)[17] <- "Family"
Temp123 <- Temp123[order(Temp123$SeqTotal, decreasing=TRUE) ,]
Temp789 <- as.vector(Temp123$Family)

MPF_RA_top20

MPFRat20df <- psmelt(MPF_RA_top20)

Temp01 <- as.vector(sample_data(ShanePrelim)$Description)

levels(MPFRat20df$Description)

MPFRat20df$Description <- factor(MPFRat20df$Description, levels =
c(Temp01))

ShanePrelimBar1 <- ggplot(MPFRat20df[order(MPFRat20df$Family),],
aes(x=Description, y=Abundance, fill=Family)) +
  geom_bar(stat = "identity", color = "black", width=0.7)

ShanePrelimBar2 <- ShanePrelimBar1 + facet_grid(Phylum ~ .,
scales="free_y")
ShanePrelimBar3 <- ShanePrelimBar1 + facet_wrap(~Family,
scales="free_y")

ShanePrelimBar1 <- ShanePrelimBar1 +
  theme(axis.title.x = element_text(face="bold", size=rel(1.2)),
axis.text.x = element_text(colour = "black", face="bold",
size=rel(1.2)),
axis.text.y = element_text(colour = "black", size=rel(1.2)),
axis.title.y = element_text(face="bold", size=rel(1.2))) +
  xlab("Mouse Samples")+
  ylab("Relative Abundance")+
  scale_y_continuous(labels = percent_format())

#Change aspects of legend

ShanePrelimBar1 <- ShanePrelimBar1 + scale_fill_discrete(name =
"Families")

ShanePrelimBar1 <- ShanePrelimBar1 +
  theme(legend.title = element_text(size=rel(1.2), face="bold"),
legend.text = element\_text(size=rel(1.2), face="bold"))

ShanePrelimBar1 <- ShanePrelimBar1 + guides(fill =
guide_legend(reverse = TRUE))

ggsave(filename="ShanePrelimBar1.png", ShanePrelimBar1, width = 16,
height = 9, dpi = 250)
require(Cairo)
print(ShanePrelimBar1)
dev.print(cairo_pdf, "ShanePrelimBar1.pdf")

ShanePrelimBar2 <- ShanePrelimBar2 +

```

```

        theme(panel.border = element_rect(size=0.7,
linetype="solid", fill=NA, color="black"))

ShanePrelimBar2 <- ShanePrelimBar2 + guides(fill =
guide_legend(reverse = TRUE))

ShanePrelimBar2 <- ShanePrelimBar2 +
  theme(panel.background = element_rect(fill = "grey90"),
        panel.grid.major.x = element_blank(),
        panel.grid.major.y = element_line(colour = "white",
linetype="dashed", size=0.2),
        panel.grid.minor = element_blank(),
        axis.title.x = element_text(colour = "black", face="bold",
size=rel(1.2)),
        axis.text.x = element_text(colour = "black", face="bold",
size=rel(1.2)),
        axis.text.y = element_text(colour = "black", face = "bold",
size=rel(1.2)),
        axis.title.y = element_text(colour = "black", face="bold",
size=rel(1.2)),
        strip.text = element_text(colour = "black", face="bold",
size=rel(1.2))) +
  xlab("Mouse Samples")+
  ylab("Relative Abundance")+
  scale_fill_discrete(name = "Families") +
  theme(legend.title = element_text(size=rel(1.4),
face="bold"),
        legend.text = element_text(size=rel(1.2), face="bold")) +
  scale_y_continuous(labels = percent_format())

ggsave(filename="ShanePrelimBar2.png", ShanePrelimBar2, width = 16,
height = 9, dpi = 250)
require(Cairo)
print(ShanePrelimBar2)
dev.print(cairo_pdf, "ShanePrelimBar2.pdf")

ShanePrelimBar3 <- ShanePrelimBar3 +
  theme(panel.background = element_rect(fill = "grey90"),
        panel.grid.major.x = element_blank(),
        panel.grid.major.y = element_line(colour = "white",
linetype="dashed", size=0.2),
        panel.grid.minor = element_blank(),
        axis.title.x = element_text(colour = "black", face="bold",
size=rel(1.2)),
        axis.text.x = element_text(angle=270, colour = "black",
face="bold", hjust=1),
        axis.text.y = element_text(colour = "black", face = "bold",
size=rel(1.2)),
        axis.title.y = element_text(colour = "black", face="bold",
size=rel(1.2)),
        strip.text = element_text(colour = "black", face="bold",
size=rel(1))) +
  xlab("Mouse Samples")+
  ylab("Relative Abundance")+
  scale_y_continuous(labels = percent_format()) +
  guides(fill=FALSE)

ShanePrelimBar3 <- ShanePrelimBar3 +

```

```

        theme(axis.text.x = element_text(hjust=0.5, vjust=0.4))

ShanePrelimBar3 <- ShanePrelimBar3 +
theme(plot.margin=unit(c(5,5,5,5), units="mm"))

ggsave(filename="ShanePrelimBar3.png", ShanePrelimBar3, width = 16,
height = 9, dpi = 250)
require(Cairo)
print(ShanePrelimBar3)
dev.print(cairo_pdf, "ShanePrelimBar3.pdf")
ShanePrelim

write.table(otu_table(ShanePrelim), file =
"C:/Users/Adam/Desktop/Shane Prelim/ShanePrelim_otu.txt", append =
FALSE, quote = TRUE, sep = " ", eol = "\n", na = "NA", dec = ".",
row.names = TRUE, col.names = TRUE)

write.table(tax_table(ShanePrelim), file =
"C:/Users/Adam/Desktop/Shane Prelim/ShanePrelim_tax.txt", append =
FALSE, quote = TRUE, sep = " ", eol = "\n", na = "NA", dec = ".",
row.names = TRUE, col.names = TRUE)

ShanePrelim

ShanePrelim1 <- prune_taxa(taxa_sums(ShanePrelim) > 0, ShanePrelim)

ShanePrelim1PrunedEvenDepthMin <- rarefy_even_depth(ShanePrelim1,
sample.size = min(sample_sums(ShanePrelim1)), rngseed = FALSE,
replace = TRUE, trimOTUs = TRUE)

SPPEDM <- ShanePrelim1PrunedEvenDepthMin

alpha_meas <- c("Observed", "Chaol", "ACE", "Shannon", "Simpson",
"InvSimpson")

ShanePrelimAlphaDiv <- estimate_richness(SPPEDM, split = TRUE,
measures = alpha_meas)

Temp001 <- as.vector(sample_data(SPPEDM)$Description)

sample_data(SPPEDM)$X.SampleID <-
factor(sample_data(SPPEDM)$X.SampleID, levels = c(Temp001))

ShanePrelimAlphaDivPlot <- plot_richness(SPPEDM, x="X.SampleID",
colour="X.SampleID", measures = c("Chaol", "Shannon"))

ShanePrelimAlphaDivPlot$data

ShanePrelimAlphaDivPlot$data$samples

ShanePrelimAlphaDivPlot <- ShanePrelimAlphaDivPlot +
geom_point(size=4)

ShanePrelimAlphaDivPlot <- ShanePrelimAlphaDivPlot +
xlab("Samples") +

```

```

        theme(panel.background =
element_rect(fill="grey90"),
        panel.grid.major = element_blank(),
        panel.grid.minor = element_blank(),
        axis.title.x = element_text(face="bold",size=14),
        axis.title.y = element_text(face="bold",size=14),
axis.text.y = element_text(colour="black", size=13),
axis.text.x = element_text(angle=30, colour="black", size=13, vjust=0,
hjust=0.5))

ShanePrelimAlphaDivPlot <- ShanePrelimAlphaDivPlot +
guides(colour=FALSE)

ggsave(filename="ShanePrelimAlphaDivPlot.png",
ShanePrelimAlphaDivPlot, width = 16, height = 9, dpi = 250)
require(Cairo)
print(ShaneP1)
dev.print(cairo_pdf, "ShanePrelimAlphaDivPlot.pdf")

```

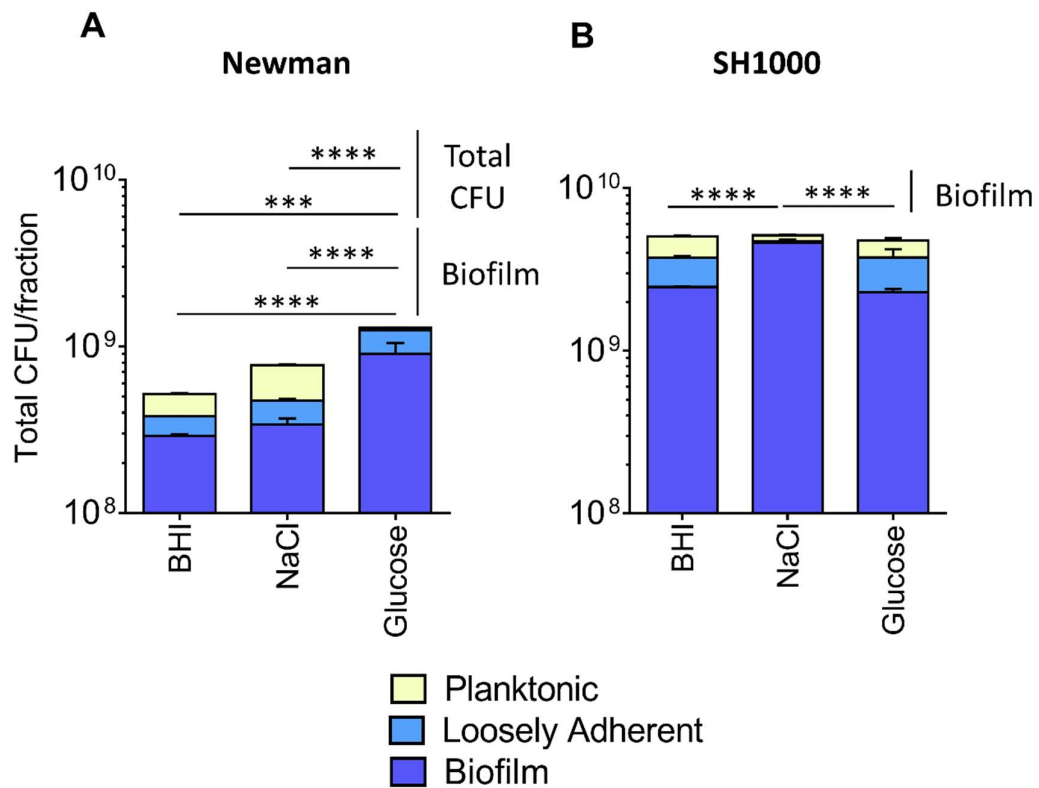
Appendix 11. Full sequences of 334R and 8F primers used in this study. Tm 53°C. Underlined sequences are required for recognition by the ion torrent system. Barcodes are displayed in bold. 16s primer sequences are displayed in italics.

Primer Name	Sequence 5'-3'
8F-1	<u>CCATCTCATCCCTGCGTGTCTCCGACTCAGCTAAGGTAACGATAGAGTTTGATCCTGGCTCAG</u>
8F-2	<u>CCATCTCATCCCTGCGTGTCTCCGACTCAGTAAGGAGAACGATAGAGTTTGATCCTGGCTCAG</u>
8F-3	<u>CCATCTCATCCCTGCGTGTCTCCGACTCAGAAGAGGATTCGATAGAGTTTGATCCTGGCTCAG</u>
8F-4	<u>CCATCTCATCCCTGCGTGTCTCCGACTCAGTACCAAGATCGATAGAGTTTGATCCTGGCTCAG</u>
8F-5	<u>CCATCTCATCCCTGCGTGTCTCCGACTCAGCAGAAGGAACGATAGAGTTTGATCCTGGCTCAG</u>
8F-6	<u>CCATCTCATCCCTGCGTGTCTCCGACTCAGCTGCAAGTTCGATAGAGTTTGATCCTGGCTCAG</u>
8F-7	<u>CCATCTCATCCCTGCGTGTCTCCGACTCAGTTCGTGATTCGATAGAGTTTGATCCTGGCTCAG</u>
8F-8	<u>CCATCTCATCCCTGCGTGTCTCCGACTCAGTTCGATAACGATAGAGTTTGATCCTGGCTCAG</u>
8F-9	<u>CCATCTCATCCCTGCGTGTCTCCGACTCAGTGAGCGGAACGATAGAGTTTGATCCTGGCTCAG</u>
8F-10	<u>CCATCTCATCCCTGCGTGTCTCCGACTCAGCTGACCGAACGATAGAGTTTGATCCTGGCTCAG</u>
8F-11	<u>CCATCTCATCCCTGCGTGTCTCCGACTCAGTCCCTCGAATCGATAGAGTTTGATCCTGGCTCAG</u>
8F-12	<u>CCATCTCATCCCTGCGTGTCTCCGACTCAGTAGGTGGTTCGATAGAGTTTGATCCTGGCTCAG</u>
8F-13	<u>CCATCTCATCCCTGCGTGTCTCCGACTCAGTCTAACGGACGATAGAGTTTGATCCTGGCTCAG</u>
8F-14	<u>CCATCTCATCCCTGCGTGTCTCCGACTCAGTTGGAGTGTCGATAGAGTTTGATCCTGGCTCAG</u>
8F-15	<u>CCATCTCATCCCTGCGTGTCTCCGACTCAGTCTAGAGGTCGATAGAGTTTGATCCTGGCTCAG</u>
8F-16	<u>CCATCTCATCCCTGCGTGTCTCCGACTCAGTCTGGATGACGATAGAGTTTGATCCTGGCTCAG</u>

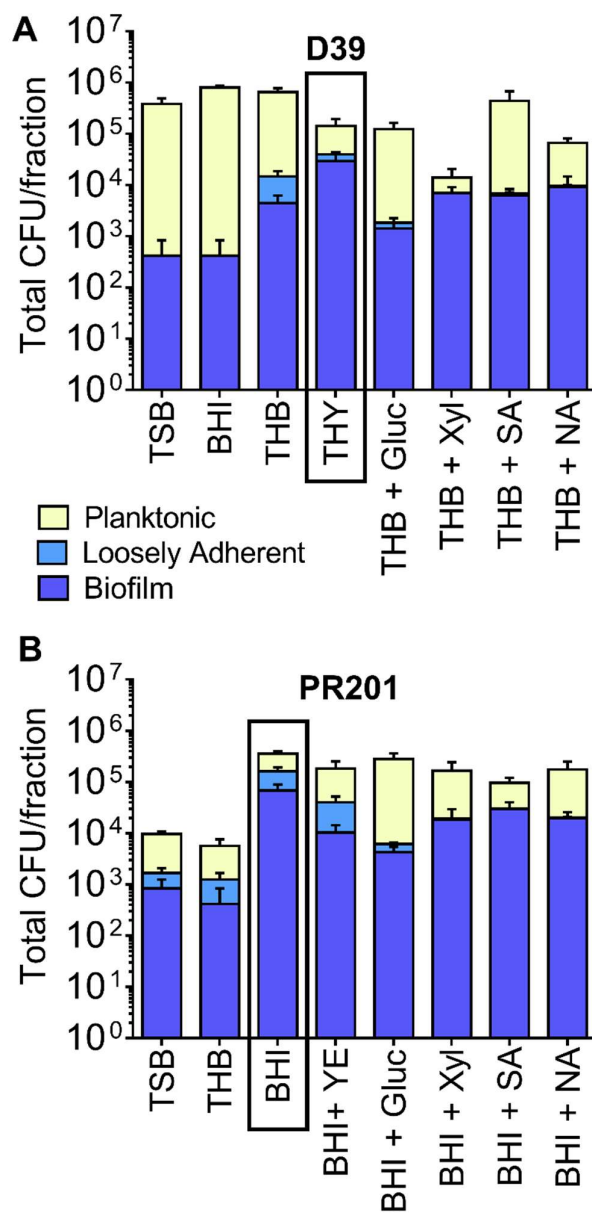
8F-17	<u>CCATCTCATCCCTGCGTGTCTCCGACTCAGTCTATTCGTCGATAGAGTTTGATCCTGGCTCAG</u>
8F-18	<u>CCATCTCATCCCTGCGTGTCTCCGACTCAGAGGCAATTGCGATAGAGTTTGATCCTGGCTCAG</u>
8F-19	<u>CCATCTCATCCCTGCGTGTCTCCGACTCAGTTAGTCGGACGATAGAGTTTGATCCTGGCTCAG</u>
8F-20	<u>CCATCTCATCCCTGCGTGTCTCCGACTCAGCAGATCCATCGATAGAGTTTGATCCTGGCTCAG</u>
8F-21	<u>CCATCTCATCCCTGCGTGTCTCCGACTCAGTCGCAATTACGATAGAGTTTGATCCTGGCTCAG</u>
8F-22	<u>CCATCTCATCCCTGCGTGTCTCCGACTCAGTTCGAGACGCGATAGAGTTTGATCCTGGCTCAG</u>
8F-23	<u>CCATCTCATCCCTGCGTGTCTCCGACTCAGTGCCACGAACGATAGAGTTTGATCCTGGCTCAG</u>
8F-24	<u>CCATCTCATCCCTGCGTGTCTCCGACTCAGAACCTCATTTCGATAGAGTTTGATCCTGGCTCAG</u>
8F-25	<u>CCATCTCATCCCTGCGTGTCTCCGACTCAGCCTGAGATACGATAGAGTTTGATCCTGGCTCAG</u>
8F-26	<u>CCATCTCATCCCTGCGTGTCTCCGACTCAGTTACAACCTCGATAGAGTTTGATCCTGGCTCAG</u>
8F-27	<u>CCATCTCATCCCTGCGTGTCTCCGACTCAGAACCATCCGCGATAGAGTTTGATCCTGGCTCAG</u>
8F-28	<u>CCATCTCATCCCTGCGTGTCTCCGACTCAGATCCGGAATCGATAGAGTTTGATCCTGGCTCAG</u>
8F-29	<u>CCATCTCATCCCTGCGTGTCTCCGACTCAGTCGACCACTCGATAGAGTTTGATCCTGGCTCAG</u>
8F-30	<u>CCATCTCATCCCTGCGTGTCTCCGACTCAGCGAGGTTATCGATAGAGTTTGATCCTGGCTCAG</u>
8F-31	<u>CCATCTCATCCCTGCGTGTCTCCGACTCAGTCCAAGCTGCGATAGAGTTTGATCCTGGCTCAG</u>
8F-32	<u>CCATCTCATCCCTGCGTGTCTCCGACTCAGTCTTACACACGATAGAGTTTGATCCTGGCTCAG</u>
8F-33	<u>CCATCTCATCCCTGCGTGTCTCCGACTCAGTTCTCATTGAACGATAGAGTTTGATCCTGGCTCAG</u>
8F-34	<u>CCATCTCATCCCTGCGTGTCTCCGACTCAGTCGCATCGTTCGATAGAGTTTGATCCTGGCTCAG</u>
8F-35	<u>CCATCTCATCCCTGCGTGTCTCCGACTCAGTAAGCCATTGTCGATAGAGTTTGATCCTGGCTCAG</u>

8F-36	<u>CCATCTCATCCCTGCGTGTCTCCGACTCAGAAGGAATCGTCGATAGAGTTTGATCCTGGCTCAG</u>
8F-37	<u>CCATCTCATCCCTGCGTGTCTCCGACTCAGCTTGAGAATGTCGATAGAGTTTGATCCTGGCTCAG</u>
8F-38	<u>CCATCTCATCCCTGCGTGTCTCCGACTCAGTGGAGGACGGACGATAGAGTTTGATCCTGGCTCAG</u>
8F-39	<u>CCATCTCATCCCTGCGTGTCTCCGACTCAGTAACAATCGGCGATAGAGTTTGATCCTGGCTCAG</u>
8F-40	<u>CCATCTCATCCCTGCGTGTCTCCGACTCAGCTGACATAATCGATAGAGTTTGATCCTGGCTCAG</u>
8F-41	<u>CCATCTCATCCCTGCGTGTCTCCGACTCAGTTCCACTTCGCGATAGAGTTTGATCCTGGCTCAG</u>
8F-42	<u>CCATCTCATCCCTGCGTGTCTCCGACTCAGAGCACGAATCGATAGAGTTTGATCCTGGCTCAG</u>
8F-43	<u>CCATCTCATCCCTGCGTGTCTCCGACTCAGCTTGACACCGCGATAGAGTTTGATCCTGGCTCAG</u>
8F-44	<u>CCATCTCATCCCTGCGTGTCTCCGACTCAGTTGGAGGCCAGCGATAGAGTTTGATCCTGGCTCAG</u>
8F-45	<u>CCATCTCATCCCTGCGTGTCTCCGACTCAGTGGAGCTTCCTCGATAGAGTTTGATCCTGGCTCAG</u>
8F-46	<u>CCATCTCATCCCTGCGTGTCTCCGACTCAGTCAGTCCGAACGATAGAGTTTGATCCTGGCTCAG</u>
8F-47	<u>CCATCTCATCCCTGCGTGTCTCCGACTCAGTAAGGCAACCACGATAGAGTTTGATCCTGGCTCAG</u>
8F-48	<u>CCATCTCATCCCTGCGTGTCTCCGACTCAGTTCTAAGAGACGATAGAGTTTGATCCTGGCTCAG</u>
8F-49	<u>CCATCTCATCCCTGCGTGTCTCCGACTCAGTCCTAACATAACGATAGAGTTTGATCCTGGCTCAG</u>
8F-50	<u>CCATCTCATCCCTGCGTGTCTCCGACTCAGCGGACAATGGCGATAGAGTTTGATCCTGGCTCAG</u>
8F-51	<u>CCATCTCATCCCTGCGTGTCTCCGACTCAGTTGAGCCTATTCGATAGAGTTTGATCCTGGCTCAG</u>
8F-52	<u>CCATCTCATCCCTGCGTGTCTCCGACTCAGCCGCATGGAACGATAGAGTTTGATCCTGGCTCAG</u>
8F-53	<u>CCATCTCATCCCTGCGTGTCTCCGACTCAGCTGGCAATCCTCGATAGAGTTTGATCCTGGCTCAG</u>
8F-54	<u>CCATCTCATCCCTGCGTGTCTCCGACTCAGCCGGAGAATCGCGATAGAGTTTGATCCTGGCTCAG</u>

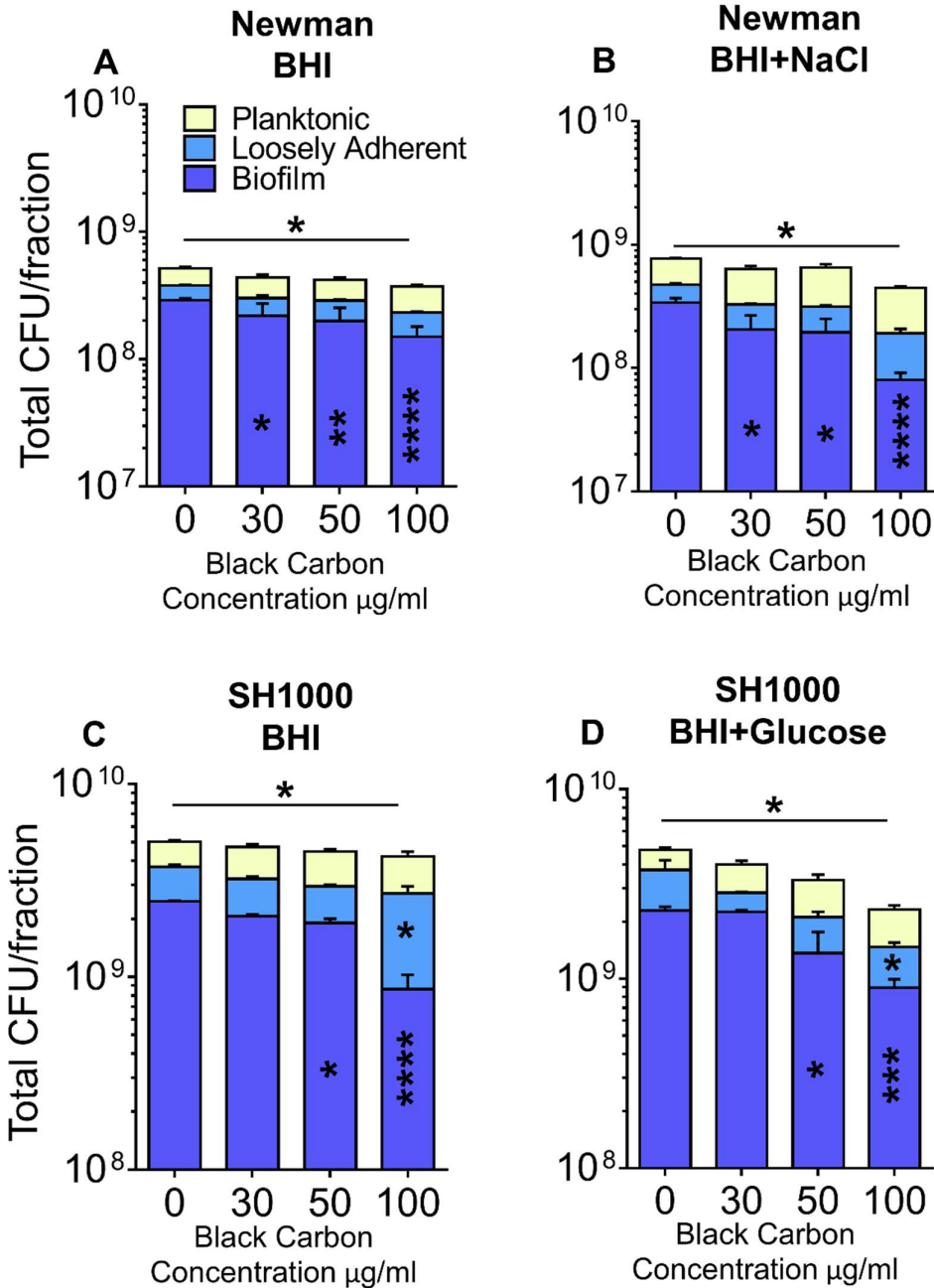
8F-55	<u>CCATCTCATCCCTGCGTGTCTCCGACTCAGTCCACCTCCTCGATAGAGTTTGATCCTGGCTCAG</u>
8F-56	<u>CCATCTCATCCCTGCGTGTCTCCGACTCAGCAGCATTAAATTCGATAGAGTTTGATCCTGGCTCAG</u>
8F-57	<u>CCATCTCATCCCTGCGTGTCTCCGACTCAGTCTGGCAACGGCGATAGAGTTTGATCCTGGCTCAG</u>
8F-58	<u>CCATCTCATCCCTGCGTGTCTCCGACTCAGTCCTAGAACACGATAGAGTTTGATCCTGGCTCAG</u>
8F-59	<u>CCATCTCATCCCTGCGTGTCTCCGACTCAGTCCTTGATGTTTCGATAGAGTTTGATCCTGGCTCAG</u>
8F-60	<u>CCATCTCATCCCTGCGTGTCTCCGACTCAGTCTAGCTCTTCGATAGAGTTTGATCCTGGCTCAG</u>
334R	CCACTACGCCTCCGCTTTCCTCTCTATGGGCAGTCGGTGATTGCCTCCCGTAGGAGTCTG



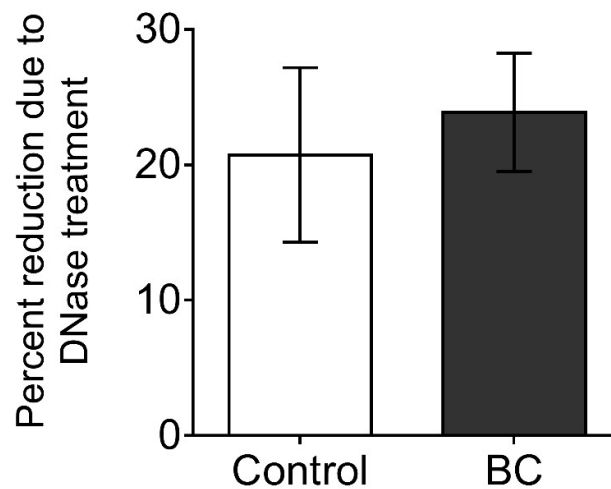
Appendix 12. Biofilm formation of *S. aureus* in various environmental conditions. *S. aureus* Newman (A) and SH1000 (B) were allowed to form biofilms in BHI, BHI supplemented with 4 % (w/v) NaCl, and BHI supplemented with 1 % (w/v) Glucose. $n \geq 3$. Error bars represent +1 SEM. Two-way ANOVA with Tukey's multiple comparisons tests were performed to determine significance, significant results compared to the control condition are denoted with ** ($p \leq 0.001$) or **** ($p \leq 0.0001$).



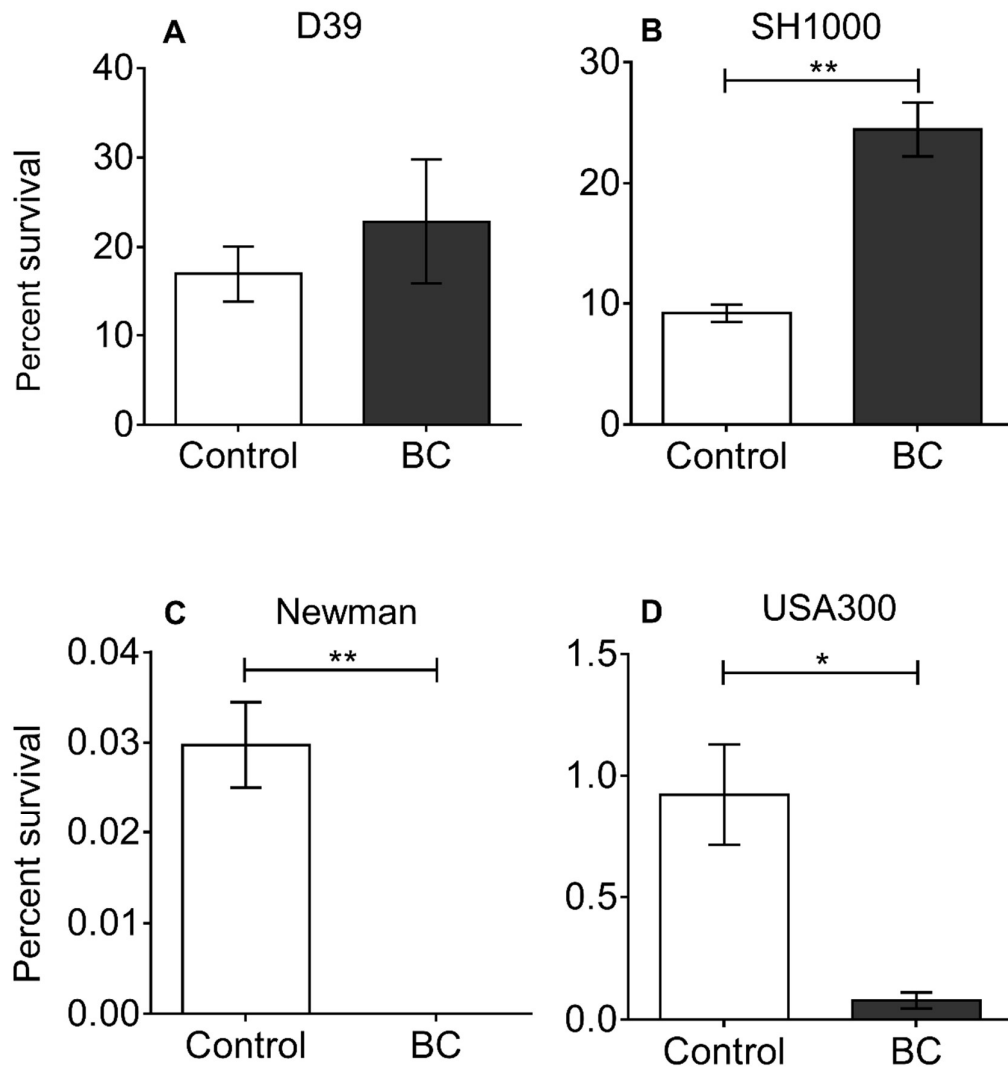
Appendix 13. Biofilm formation of *S. pneumoniae* in various environmental conditions. *S. pneumoniae* D39 (A) and PR201 (B) were allowed to form biofilms in three media (TSB, THB, and BHI) both un-supplemented and supplemented with 0.5 % yeast extract (YE), 1 % glucose (Gluc), 0.5 % xylitol (Xyl), 3 $\mu\text{g}/\text{ml}$ sialic acid (SA), and 10 $\mu\text{g}/\text{ml}$ N-acetyl mannosamine (NA). Media supplementation was tested with both single supplements and combinations of Gluc+Xly, Gluc+SA, and Gluc+NA. The three base media and certain supplemented conditions are displayed. Boxes show the medium promoting greatest biofilm formation. It should be noted that in the biofilm fraction, the lower threshold of accurate detection was 1.25×10^3 bacteria. $n \geq 3$. Error bars represent +1 SEM. Two-way ANOVA with Tukey's multiple comparisons tests were performed to determine significance. No significant differences were identified between the amount of biofilm bacteria.



Appendix 14. Examples showing the consistency of the effect of BC on biofilm formation in different environmental conditions. *S. aureus* Newman (A+B) and SH1000 (C+D) were allowed to form biofilms in the presence or absence of 30-100 µg/ml black carbon (BC) in different media: BHI, BHI + 4 % (w/v) NaCl (BHI+NaCl), and BHI + 1 % (w/v) Glucose (BHI+Gluc). n=3. Error bars represent +1 SEM. Two-way ANOVA with Tukey's multiple comparisons tests were used to determine significance, significant results compared to the control condition are denoted with * (p≤0.05), ** (p≤0.01), or **** (p≤0.0001).



Appendix 15. Percent reduction in SH1000 biofilm viability due to DNaseI degradation. *S. aureus* SH1000 was allowed to form biofilms in the presence (black bar) or absence (white bar) of 100 µg/ml black carbon (BC) for 24 hours. Planktonic and loosely-adherent bacteria were then removed, and biofilms were exposed to 140 U/ml DNaseI for 2 hours. After incubation, planktonic and loosely adherent bacteria were removed and discarded, and the remaining biofilm bacteria were quantified. The percent reduction in biofilm viability after DNaseI exposure was then calculated in comparison to biofilms incubated with the same medium but without DNaseI. n=3. Error bars represent ± 1 SEM. T-tests were performed to determine significance between the two conditions, no significant difference ($p>0.05$) was identified between the two conditions.



Appendix 16. Antibiotic tolerance of control and BC-formed biofilms displayed as percentage survival. *S. pneumoniae* D39 (A) and *S. aureus* SH1000 (B), Newman (C), and USA300 (D) were allowed to form biofilms in the presence (black) or absence (white) of 100 µg/ml black carbon (BC) for 24 hours. Planktonic and loosely-adherent bacteria were then removed, and biofilms were exposed to either 50 mg/ml oxacillin (*S. aureus*) in 2 % (w/v) NaCl, or 500 µg/ml gentamicin (*S. pneumoniae*) for 3 hours. After incubation, planktonic and loosely adherent bacteria were removed and discarded, and the remaining biofilm bacteria were quantified. Percent survival after antibiotic exposure was calculated in comparison to biofilms incubated with the same medium but without antibiotics. n=3. Error bars represent ± 1 SEM. T-tests were performed to determine significance between the two conditions, significant results are denoted with ** (p<0.01).

Bibliography

- Abdi-Ali, A., Mohammadi-Mehr, M. & Agha Alaei, Y., 2006. Bactericidal activity of various antibiotics against biofilm-producing *Pseudomonas aeruginosa*. *International Journal of Antimicrobial Agents*, 27(3), pp.196–200.
- Abraham, N.M. & Jefferson, K.K., 2012. *S. aureus* clumping factor B mediates biofilm formation in the absence of calcium. *Microbiology (United Kingdom)*, 158(6), pp.1504–1512.
- Adedeji, A. *et al.*, 2004. Effect of PM₁₀ on *H. influenzae* and *S. pneumoniae*. *Thorax*, 59(6), pp.543–543.
- Agarwal, A. & Jain, A., 2013. Glucose & Sodium chloride induced biofilm production & ica operon in clinical isolates of staphylococci. *Indian Journal of Medical Research*, 138(AUG), pp.262–266.
- Air Quality Expert Group, 2005. *Particulate Matter in the United Kingdom*. London
- Air Quality Expert Group, 2012. *Fine Particulate Matter (PM_{2.5}) in the United Kingdom*. London
- Albuquerque, L. *et al.*, 2011. *Gaiella occulta* gen. nov., sp. nov., a novel representative of a deep branching phylogenetic lineage within the class Actinobacteria and proposal of *Gaiellaceae* fam. nov. and *Gaiellales* ord. nov. *Systematic and Applied Microbiology*, 34(8), pp.595–599.
- Alghamdi, M.A. *et al.*, 2014. Microorganisms associated particulate matter: A preliminary study. *Science of the Total Environment*, 479-480(1), pp.109–116.
- Almirall, J., Blanquer, J. & Bello, S., 2014. Community-acquired pneumonia among smokers. *Archivos de bronconeumología*, 50(6), pp.250–4.
- Anderson, H.R. *et al.*, 2001. Particulate matter and daily mortality and hospital admissions in the west midlands conurbation of the United Kingdom: associations with fine and coarse particles, black smoke and sulphate. *Occupational and environmental medicine*, 58(8), pp.504–510.
- Anderson, J.O., Thundiyil, J.G. & Stolbach, A., 2012. Clearing the Air: A Review of the Effects of Particulate Matter Air Pollution on Human Health. *Journal of Medical Toxicology*, 8(2), pp.166–175.
- Anderson, M.J., 2001. A new method for non-parametric multivariate analysis of variance. *Austral Ecology*, 26, pp.32–46.
- Anderson, M.J., 2006. Distance-based tests for homogeneity of multivariate dispersions. *Biometrics*, 62(1), pp.245–253.

- Anderson, M.J., Ellingsen, K.E. & McArdle, B.H., 2006. Multivariate dispersion as a measure of beta diversity. *Ecology Letters*, 9(6), pp.683–693.
- Andersson, D.I. & Hughes, D., 2014. Microbiological effects of sublethal levels of antibiotics. *Nature reviews. Microbiology*, 12(7), pp.465–78.
- Antunes, M.B. *et al.*, 2012. Molecular Basis of Tobacco-Induced Bacterial Biofilms: An In Vitro Study. *Otolaryngology -- Head and Neck Surgery*, 147(5), pp.876–884.
- Archer, N.K. *et al.*, 2011. *S. aureus* biofilms: properties, regulation, and roles in human disease. *Virulence*, 2(2150-5608), pp.445–459.
- Avery, O.T., Macleod, C.M. & McCarty, M., 1944. Studies on the Chemical Nature of the Substance Inducing Transformation of Pneumococcal Types: Induction of Transformation By a Desoxyribonucleic Acid Fraction Isolated From Pneumococcus Type Iii. *The Journal of experimental medicine*, 79(2), pp.137–58.
- Aztatzi-Aguilar, O.G. *et al.*, 2015. Acute and subchronic exposure to air particulate matter induces expression of angiotensin and bradykinin-related genes in the lungs and heart: Angiotensin-II type-I receptor as a molecular target of particulate matter exposure. *Particle and Fibre Toxicology*, 12(1), p.17.
- Baddal, B. *et al.*, 2015. Dual RNA-seq of nontypeable *Haemophilus influenzae* and host cell transcriptomes reveals novel insights into host-pathogen cross talk. *mBio*, 6(6).
- Bagaitkar, J. *et al.*, 2011. Tobacco smoke augments *Porphyromonas gingivalis*-*Streptococcus gordonii* biofilm formation. *PloS one*, 6(11), p.e27386.
- Baker, G.C., Smith, J.J. & Cowan, D.A., 2003. Review and re-analysis of domain-specific 16S primers. *Journal of Microbiological Methods*, 55(3), pp.541–555.
- Baker, J.P., 2009. *Iron and copper homeostasis in S. aureus*. Univeristy of Leicester.
- Baker, J. *et al.*, 2010. Copper Stress Induces a Global Stress Response in *S. aureus* and Represses *sae* and *agr* Expression and Biofilm Formation. *Applied and Environmental Microbiology*, 76(1), pp.150–160.
- Balachandran, P. *et al.*, 2001. The autolytic enzyme *lytA* of *S. pneumoniae* is not responsible for releasing pneumolysin. *Journal of Bacteriology*, 183(10), pp.3108–3116.
- Baldoni, D. *et al.*, 2009. Linezolid alone or combined with rifampin against methicillin-resistant *S. aureus* in experimental foreign-body infection. *Antimicrobial Agents and Chemotherapy*, 53(3), pp.1142–1148.

- Balm, M.N. *et al.*, 2013. Progression from new methicillin-resistant *S. aureus* colonisation to infection: an observational study in a hospital cohort. *BMC infectious diseases*, 13(1), p.491.
- Bardiau, M. *et al.*, 2014. Associations between properties linked with persistence in a collection of *S. aureus* isolates from bovine mastitis. *Veterinary Microbiology*, 169(1-2), pp.74–79.
- Barfod, K.K. *et al.*, 2013. The murine lung microbiome in relation to the intestinal and vaginal bacterial communities. *BMC microbiology*, 13, p.303.
- Bartoszewicz, M. *et al.*, 2007. Penetration of a selected antibiotic and antiseptic into a biofilm formed on orthopedic steel implants. *Ortopedia Traumatologia Rehabilitacja*, 9(3), pp.310–318.
- Beamish, L.A., Osornio-Vargas, A.R. & Wine, E., 2011. Air pollution: An environmental factor contributing to intestinal disease. *Journal of Crohn's and Colitis*, 5(4), pp.279–286.
- Beck, J.M., Young, V.B. & Huffnagle, G.B., 2012. The microbiome of the lung. *Translational Research*, 160(4), pp.258–266.
- Beelen, R. *et al.*, 2014. Effects of long-term exposure to air pollution on natural-cause mortality: An analysis of 22 European cohorts within the multicentre ESCAPE project. *The Lancet*, 383(9919), pp.785–795.
- Belenky, P. *et al.*, 2015. Bactericidal Antibiotics Induce Toxic Metabolic Perturbations that Lead to Cellular Damage. *Cell Reports*, 13(5), pp.968–980.
- Benjamini, Y. & Hochberg, Y., 1995. Controlling the False Discovery Rate : A Practical and Powerful Approach to Multiple Testing. *Journal of the Royal Statistical Society*, 57(1), pp.289–300.
- Bentley, S.D. *et al.*, 2006. Genetic analysis of the capsular biosynthetic locus from all 90 pneumococcal serotypes. *PLoS Genetics*, 2(3), pp.0262–0269.
- Benton, K.A., Paton, J.C. & Briles, D.E., 1997. Differences in virulence for mice among *S. pneumoniae* strains of capsular types 2, 3, 4, 5, and 6 are not attributable to differences in pneumolysin production. *Infection and Immunity*, 65(4), pp.1237–1244.
- Bergey, D.H., 2010. *Bergey's Manual of Systematic Bacteriology - Vol 4: Bacteroidetes*.
- Bergmann, S. & Hammerschmidt, S., 2006. Versatility of pneumococcal surface proteins. *Microbiology*, 152(2), pp.295–303.

- Berry, A.M. *et al.*, 1999. Comparative virulence of *S. pneumoniae* strains with insertion-duplication, point, and deletion mutations in the pneumolysin gene. *Infection and Immunity*, 67(2), pp.981–985.
- Bien, J., Sokolova, O. & Bozko, P., 2011. Characterization of Virulence Factors of *S. aureus*: Novel Function of Known Virulence Factors That Are Implicated in Activation of Airway Epithelial Proinflammatory Response. *Journal of pathogens*, 2011, p.601905.
- Bind, M.-A. *et al.*, 2016. Quantile Regression Analysis of the Distributional Effects of Air Pollution on Blood Pressure, Heart Rate Variability, Blood Lipids, and Biomarkers of Inflammation in Elderly American Men: The Normative Aging Study. *Environmental health perspectives*, (April 2015).
- Blanchette-cain, K. *et al.*, 2013. *S. pneumoniae* Biofilm Formation Is Strain Dependent, Multifactorial, and Associated with Reduced Invasiveness and Immunoreactivity during Colonization. *mBio*, 4(4), pp.1–11.
- Bogaardt, C., van Tonder, A.J. & Brueggemann, A.B., 2015. Genomic analyses of pneumococci reveal a wide diversity of bacteriocins - including pneumocyclicin, a novel circular bacteriocin. *BMC genomics*, 16(1), p.554.
- Bogaert, D. *et al.*, 2001. Pneumococcal carriage in children in the Netherlands: A molecular epidemiological study. *Journal of Clinical Microbiology*, 39(9), pp.3316–3320.
- Bogaert, D., De Groot, R. & Hermans, P.W.M., 2004. *S. pneumoniae* colonisation: The key to pneumococcal disease. *Lancet Infectious Diseases*, 4(3), pp.144–154.
- Bogaert, D. *et al.*, 2011. Variability and Diversity of Nasopharyngeal Microbiota in Children: A Metagenomic Analysis. *PLoS ONE*, 6(2), p.e17035.
- Bohus, V. *et al.*, 2011. Bacterial communities in an ultrapure water containing storage tank of a power plant. *Acta Microbiol Immunol Hung*, 58(4), pp.371–382.
- Bond, T.C. *et al.*, 2007. Historical emissions of black and organic carbon aerosol from energy-related combustion, 1850-2000. *Global Biogeochemical Cycles*, 21(2).
- Boogaard, H. *et al.*, 2013. Respiratory effects of a reduction in outdoor air pollution concentrations. *Epidemiology (Cambridge, Mass.)*, 24(5), pp.753–61.
- Bowers, E.F. & Jeffries, L.R., 1955. Optochin in The Identification of *Str. pneumoniae*. , pp.58–60.
- Brauer, M. *et al.*, 2002. Air pollution from traffic and the development of respiratory infections and asthmatic and allergic symptoms in children. *American Journal of Respiratory and Critical Care Medicine*, 166(8), pp.1092–1098.

- Brauer, M. *et al.*, 2007. Air pollution and development of asthma, allergy and infections in a birth cohort. *European Respiratory Journal*, 29(5), pp.879–888.
- Bray, J.R. & Curtis, J.T., 1957. An Ordination of the Upland Forest Communities of Southern Wisconsin. *Ecological Monographs*, 27(4), p.325.
- Brenner, D.J., Krieg, N.R. & Staley, J.T., 2005. *Bergey's Manual of Systematic Bacteriology - Vol 2: The Proteobacteria. Part C The Alpha-, Beta-, Delta-, and Epsilonproteobacteria*,
- Brenner, D.J., Krieg, N.R. & Staley, J.T., 2010. *Bergey's Manual of Systematic Bacteriology - Vol 2: The Proteobacteria Part B -The Gammaproteobacteria*.
- Briant, J.K. & Lippmann, M., 1992. Particle transport through a hollow canine airway cast by high-frequency oscillatory ventilation. *Exp Lung Res.*, 18(3), pp.385–407.
- Briant, J.K. & Lippmann, M., 1993. Aerosol Bolus Transport through a Hollow Airway Cast by Steady Flow in Different Gases. *Aerosol Science and Technology*, 19(1), pp.27–39.
- Brogden, K.A., Guthmiller, J.M. & Taylor, C.E., 2005. Human polymicrobial infections. *Lancet*, 365(9455), pp.253–255.
- Brook, I., 1999. Bacterial Interference. *Critical Reviews in Microbiology*, 25(3), pp.155–172.
- Brook, R.D., 2004. Air Pollution and Cardiovascular Disease: A Statement for Healthcare Professionals From the Expert Panel on Population and Prevention Science of the American Heart Association. *Circulation*, 109(21), pp.2655–2671.
- Brook, I., 2011. The Impact of Smoking on Oral and Nasopharyngeal Bacterial Flora. *Journal of Dental Research*, 90(6), pp.704–710.
- Brugha, R. & Grigg, J., 2014. Urban air pollution and respiratory infections. *Paediatric Respiratory Reviews*, 15(2), pp.194–199.
- Brune, K.D., *et al.* 2016. Plug-and-Display: decoration of Virus-Like Particles via isopeptide bonds for modular immunization. *Scientific Reports*, 6: 19234.
- Brunekreef, B. & Forsberg, B., 2005. Epidemiological evidence of effects of coarse airborne particles on health. *European Respiratory Journal*, 26(2), pp.309–318.
- Bui, L.M.G., Turnidge, J.D. & Kidd, S.P., 2015. The induction of *S. aureus* biofilm formation or Small Colony Variants is a strain-specific response to host-generated chemical stresses. *Microbes and Infection*, 17(1), pp.77–82.

- Butterfield, D. *et al.*, 2015. *2014 Annual Report for the UK Black Carbon Network*. National Physical Laboratory. Middlesex, UK.
- Cai, X. *et al.*, 2016. Short-term effects of atmospheric particulate matter on myocardial infarction: a cumulative meta-analysis. *Environmental Science and Pollution Research*, 23(7), pp.6139–6148.
- Caiazza, N.C. & O’Toole, G.A., 2003. Alpha-toxin is required for biofilm formation by *S. aureus*. *Journal of Bacteriology*, 185(10), pp.3214–3217.
- Calix, J.J. *et al.*, 2012. Biochemical, genetic, and serological characterization of two capsule subtypes among *S. pneumoniae* serotype 20 strains: Discovery of a new pneumococcal serotype. *Journal of Biological Chemistry*, 287(33), pp.27885–27894.
- Camilli, R., Pantosti, A. & Baldassarri, L., 2011. Contribution of serotype and genetic background to biofilm formation by *S. pneumoniae*. *European Journal of Clinical Microbiology and Infectious Diseases*, 30(1), pp.97–102.
- Canvin, J.R. *et al.*, 1995. The role of pneumolysin and autolysin in the pathology of pneumonia and septicemia in mice infected with a type 2 pneumococcus. *The Journal of infectious diseases*, 172(1), pp.119–23.
- Cao, C. *et al.*, 2014. Inhalable microorganisms in Beijing’s PM_{2.5} and PM₁₀ pollutants during a severe smog event. *Environmental Science and Technology*, 48(3), pp.1499–1507.
- Caporaso, J.G., Bittinger, K., *et al.*, 2010a. PyNAST: A flexible tool for aligning sequences to a template alignment. *Bioinformatics*, 26(2), pp.266–267.
- Caporaso, J.G., Kuczynski, J., *et al.*, 2010b. QIIME allows analysis of high-throughput community sequencing data. *Nature methods*, 7(5), pp.335–6.
- Carmen, J.C. *et al.*, 2004. Ultrasonic-enhanced gentamicin transport through colony biofilms of *Pseudomonas aeruginosa* and *Escherichia coli*. *Journal of Infection and Chemotherapy*, 10(4), pp.193–199.
- Carrolo, M. *et al.*, 2010. Prophage spontaneous activation promotes DNA release enhancing biofilm formation in *S. pneumoniae*. *PLoS ONE*, 5(12).
- Casillas-Ituarte, N.N. *et al.*, 2012. Dissociation rate constants of human fibronectin binding to fibronectin-binding proteins on living *S. aureus* isolated from clinical patients. *Journal of Biological Chemistry*, 287(9), pp.6693–6701.
- Cattaneo, R. *et al.*, 2010. Association of marine viral and bacterial communities with reference black carbon particles under experimental conditions: an analysis with scanning electron, epifluorescence and confocal laser scanning microscopy. *FEMS Microbiology Ecology*, 74(2), pp.382–396.

- Catterall, J.R., 1999. *S. pneumoniae*. *Thorax*, pp.929–937.
- Cerca, N., Brooks, J.L. & Jefferson, K.K., 2008. Regulation of the intercellular adhesin locus regulator (icaR) by SarA, ??B, and IcaR in *S. aureus*. *Journal of Bacteriology*, 190(19), pp.6530–6533.
- Chaignon, P. *et al.*, 2007. Susceptibility of staphylococcal biofilms to enzymatic treatments depends on their chemical composition. *Applied Microbiology and Biotechnology*, 75(1), pp.125–132.
- Chakravorty, S. *et al.*, 2007. A detailed analysis of 16S ribosomal RNA gene segments for the diagnosis of pathogenic bacteria. *Journal of Microbiological Methods*, 69(2), pp.330–339.
- Chang, X. *et al.*, 2015. Association of fine particles with respiratory disease mortality: a meta-analysis. *Archives of environmental & occupational health*, 70(2), pp.98–101.
- Chao, Y. *et al.*, 2015. *S. pneumoniae* biofilm formation and dispersion during colonization and disease. *Frontiers in cellular and infection microbiology*, 4(January), p.194.
- Charlson, E.S. *et al.*, 2011. Topographical continuity of bacterial populations in the healthy human respiratory tract. *American Journal of Respiratory and Critical Care Medicine*, 184(8), pp.957–963.
- Chaudhuri, N. *et al.*, 2012. Diesel Exhaust Particle Exposure In Vitro Alters Monocyte Differentiation and Function. *PLoS ONE*, 7(12), p.e51107.
- Chertow, D.S. & Memoli, M.J., 2013. Bacterial coinfection in influenza: a grand rounds review. *JAMA*, 309(3), pp.275–82.
- Chen *et al.* 2012. Association of particulate air pollution with daily mortality: the China Air Pollution and Health Effects Study. *American Journal of Epidemiology*. 175(11), 1173-81.
- Cho, D.Y. *et al.*, 2014. Air pollutants cause release of hydrogen peroxide and interleukin-8 in a human primary nasal tissue culture model. *International Forum of Allergy and Rhinology*, 4(12), pp.966–971.
- Choi, H., Yang, Z. & Weisshaar, J.C., 2015. Single-cell, real-time detection of oxidative stress induced in *Escherichia coli* by the antimicrobial peptide CM15. *Proceedings of the National Academy of Sciences*, p.201417703.
- Chuang, K.-J. *et al.*, 2007. The Effect of Urban Air Pollution on Inflammation, Oxidative Stress, Coagulation, and Autonomic Dysfunction in Young Adults. *American Journal of Respiratory and Critical Care Medicine*, 176(4), pp.370–376.

- Clancy, L. *et al.*, 2002. Effect of air-pollution control on death rates in Dublin, Ireland: An intervention study. *Lancet*, 360(9341), pp.1210–1214.
- Clifford, H.D., Perks, K.L. & Zosky, G.R., 2015. Geogenic PM₁₀ exposure exacerbates responses to influenza infection. *Science of the Total Environment*, 533, pp.275–282.
- CLSI, 2015. *Performance Standards for Antimicrobial Susceptibility Testing; Twenty-Fifth Informational Supplement*,
- Coenye, T., 2014. The Family Burkholderiaceae. In *The Prokaryotes: Alphaproteobacteria and Betaproteobacteria*. pp. 759–776.
- Cofala, J. *et al.*, 2007. Scenarios of global anthropogenic emissions of air pollutants and methane until 2030. *Atmospheric Environment*, 41(38), pp.8486–8499.
- Cohen, R. *et al.*, 1997. Change in nasopharyngeal carriage of *S. pneumoniae* resulting from antibiotic therapy for acute otitis media in children. *The Pediatric infectious disease journal*, 16(6), pp.555–60.
- Cohen, R. *et al.*, 1999. One dose ceftriaxone vs. ten days of amoxicillin/clavulanate therapy for acute otitis media: clinical efficacy and change in nasopharyngeal flora. *The Pediatric infectious disease journal*, 18(5), pp.403–9.
- COMEAP, 2009. *Long-Term Exposure to Air Pollution: Effect on Mortality*, Committee on the Medical Effects of Air Pollutants.
- Conlon, K.M., Humphreys, H. & O’Gara, J.P., 2002. Regulation of icaR gene expression in *Staphylococcus epidermidis*. *FEMS Microbiology Letters*, 216(2), pp.171–177.
- Corless, C.E. *et al.*, 2000. Contamination and sensitivity issues with a real-time universal 16s rRNA PCR. *Journal of Clinical Microbiology*, 38(5), pp.1747–1752.
- Cortez-Lugo, M. *et al.*, 2015. Effect of Personal Exposure to PM_{2.5} on Respiratory Health in a Mexican Panel of Patients with COPD. *International Journal of Environmental Research and Public Health*, 12(9), pp.10635–10647
- Costa, A.R. *et al.*, 2013. *S. aureus* virulence factors and disease. *Microbial pathogens and strategies for combating them: science, technology and education*, pp.702–710.
- Costello, S. *et al.*, 2016. Incident Ischemic Heart Disease After Long-Term Occupational Exposure to Fine Particulate Matter: Accounting for 2 Forms of Survivor Bias. *American Journal of Epidemiology*.
- Costerton, J.W., Stewart, P.S. & Greenberg, E.P., 1999. Bacterial biofilms: a common cause of persistent infections. *Science*, 284(5418), pp.1318–1322.

- Costerton, J.W., Montanaro, L. & Arciola, C.R., 2005. Biofilm in implant infections: Its production and regulation. *International Journal of Artificial Organs*, 28(11), pp.1062–1068.
- Cramton, S.E. *et al.*, 1999. The intercellular adhesion (ica) locus is present in *S. aureus* and is required for biofilm formation. *Infect. Immun.*, 67(10), pp.5427–5433.
- Croucher, N.J. & Thomson, N.R., 2010. Studying bacterial transcriptomes using RNA-seq. *Current Opinion in Microbiology*, 13(5), pp.619–624.
- Crum, N.F. *et al.*, 2004. An outbreak of conjunctivitis due to a novel unencapsulated *S. pneumoniae* among military trainees. *Clinical infectious diseases : an official publication of the Infectious Diseases Society of America*, 39(8), pp.1148–1154.
- Cruse, G. *et al.*, 2010. Human Lung Mast Cells Mediate Pneumococcal Cell Death in Response to Activation by Pneumolysin. *The Journal of Immunology*, 184(12), pp.7108–7115.
- Cucarella, C., Solano, C. & Valle, J., 2001. Bap, a *S. aureus* surface protein involved in biofilm formation. *Journal of Bacteriology*, 183(9), pp.2888–2896.
- Cue, D. *et al.*, 2009. Rbf promotes biofilm formation by *S. aureus* via repression of icaR, a negative regulator of icaADBC. *Journal of Bacteriology*, 191(20), pp.6363–6373.
- Cue, D., Lei, M.G. & Lee, C.Y., 2012. Genetic regulation of the intercellular adhesion locus in staphylococci. *Front.Cell.Infect.Microbiol.*, 2(2235-2988), p.38.
- Cue, D., Lei, M.G. & Lee, C.Y., 2013. Activation of sarX by Rbf is required for biofilm formation and icaADBC expression in *S. aureus*. *Journal of Bacteriology*, 195(7), pp.1515–1524.
- Cui, P. *et al.*, 2015. Ambient particulate matter and lung cancer incidence and mortality: A meta-analysis of prospective studies. *European Journal of Public Health*, 25(2), pp.324–329.
- Dabernat, H. *et al.*, 1998. Effects of cefixime or co-amoxiclav treatment on nasopharyngeal carriage of *S. pneumoniae* and *Haemophilus influenzae* in children with acute otitis media. *Journal of Antimicrobial Chemotherapy*, 41, pp.253–258.
- Dagan, R. *et al.*, 1998. Dynamics of pneumococcal nasopharyngeal colonization during the first days of antibiotic treatment in pediatric patients. *The Pediatric infectious disease journal*, 17(10), pp.880–5.
- Darrow, L.A. *et al.*, 2014. Air pollution and acute respiratory infections among children 0-4 years of age: An 18-year time-series study. *American Journal of Epidemiology*, 180(10), pp.968–977.

- David, M.Z. & Daum, R.S., 2010. Community-associated methicillin-resistant *S. aureus*: Epidemiology and clinical consequences of an emerging epidemic. *Clinical Microbiology Reviews*, 23(3), pp.616–687.
- De la Fuente-Nunez, C. *et al.*, 2013. Bacterial biofilm development as a multicellular adaptation: Antibiotic resistance and new therapeutic strategies. *Current Opinion in Microbiology*, 16(5), pp.580–589.
- DEFRA, 2015. *Emissions of Air Pollutants in the UK, 1970 to 2014*. Department for Environment Food & Rural Affairs.
- DEFRA, 2016. *Annual levels of PM₁₀ and Ozone in the UK, 1987 to 2015*. Department for Environment Food & Rural Affairs.
- DeLeo, F.R. *et al.*, 2010. Community-associated methicillin-resistant *S. aureus*. *The Lancet*, 375(9725), pp.1557–1568.
- Deng, Q. *et al.*, 2015. Effects of early life exposure to outdoor air pollution and indoor renovation on childhood asthma in China. *Building and Environment*, 93(P1), pp.84–91.
- DeSantis, T.Z. *et al.*, 2006. Greengenes, a chimera-checked 16S rRNA gene database and workbench compatible with ARB. *Applied and Environmental Microbiology*, 72(7), pp.5069–5072.
- Dickson, R.P., Erb-Downward, J.R. & Huffnagle, G.B., 2014. The Role of the Bacterial Microbiome in Lung Disease. *Expert review of respiratory medicine*, 7(3), pp.245–257.
- Dickson, R.P. & Huffnagle, G.B., 2015. The Lung Microbiome: New Principles for Respiratory Bacteriology in Health and Disease. *PLOS Pathogens*, 11(7), p.e1004923.
- Diederer, B.M.W. & Kluytmans, J.A.J.W., 2006. The emergence of infections with community-associated methicillin resistant *S. aureus*. *Journal of Infection*, 52(3), pp.157–168.
- Dineen, S.M. *et al.*, 2010. An evaluation of commercial DNA extraction kits for the isolation of bacterial spore DNA from soil. *Journal of Applied Microbiology*, 109(6), pp.1886–1896.
- Dinges, M.M., Orwin, P.M. & Schlievert, P.M., 2000. Exotoxins of *S. aureus*. 13(1), pp.16–34.
- Domenech, M., García, E. & Moscoso, M., 2012. Biofilm formation in *S. pneumoniae*. *Microbial Biotechnology*, 5(4), pp.455–465.

- Domenech, M. *et al.*, 2013. Biofilm Formation Avoids Complement Immunity and Phagocytosis of *S. pneumoniae*. *Infection and Immunity*, 81(7), pp.2606–2615.
- Dominici, F. *et al.*, 2015. Chemical composition of fine particulate matter and life expectancy: in 95 US counties between 2002 and 2007. *Epidemiology*, 26, pp.556–564.
- Donlan, R.M. & Costerton, J.W., 2002. Biofilms: Survival mechanisms of clinically relevant microorganisms. *Clinical Microbiology Reviews*, 15(2), pp.167–193.
- Dons, E. *et al.*, 2012. Personal exposure to Black Carbon in transport microenvironments. *Atmospheric Environment*, 55, pp.392–398.
- Durai, R., Ng, P.C.H. & Hoque, H., 2010. Methicillin-Resistant *S. aureus*: An Update. *AORN Journal*, 91(5), pp.599–609.
- Duthie, E.S. & Lorenz, L.L., 1952. Staphylococcal coagulase; mode of action and antigenicity. *Journal of general microbiology*, 6(1-2), pp.95–107.
- Dykstra, M.J. & Reuss, L.E., 2003. *Biological Electron Microscopy* 2nd ed., Springer US.
- Dziedziatkowska, M., Hill, R. & Hansen, K.C., 2014. GeLC-MS/MS Analysis of Complex Protein Mixtures. *Methods Mol Biol*, 1156, pp.53–66.
- ECDC (European Centre for Disease Prevention and Control), 2015. *Antimicrobial Resistance surveillance in Europe 2014. Annual report of the European Antimicrobial Resistance Surveillance Network (EARS-Net)*, Stockholm.
- Edgar, R.C., 2010. Search and clustering orders of magnitude faster than BLAST. *Bioinformatics*, 26(19), pp.2460–2461.
- Edgar, R.C. *et al.*, 2011. UCHIME improves sensitivity and speed of chimera detection. *Bioinformatics*, 27(16), pp.2194–2200.
- Edwards, A.M.M., Massey, R.C.C. & Clarke, S.R.R., 2012. Molecular mechanisms of *S. aureus* nasopharyngeal colonization. *Molecular Oral Microbiology*, 27(1), pp.1–10.
- Enright, M.C. *et al.*, 2000. Multilocus sequence typing for characterization of methicillin-resistant and methicillin-susceptible clones of *S. aureus*. *Journal of Clinical Microbiology*, 38(3), pp.1008–1015.
- Eren, A.M. *et al.*, 2013. Oligotyping: Differentiating between closely related microbial taxa using 16S rRNA gene data. *Methods in Ecology and Evolution*, 4(12), pp.1111–1119.

- Erkan, L. *et al.*, 2008. Role of bacteria in acute exacerbations of chronic obstructive pulmonary disease. *International journal of chronic obstructive pulmonary disease*, 3(3), pp.463–7.
- EUCAST (European Committee on Antimicrobial Susceptibility Testing), 2015. *Clinical breakpoints database*. Available at: http://www.eucast.org/ast_of_bacteria/.
- Faith, D.P., Minchin P. R., Belbin L., 1987. Compositional dissimilarity as a robust measure of ecological distance. *Vegetatio*, 69, pp.57–68.
- Fang, S.C. *et al.*, 2012. Residential black carbon exposure and circulating markers of systemic inflammation in elderly males: The normative aging study. *Environmental Health Perspectives*, 120(5), pp.674–680.
- Faustini, A. *et al.*, 2012. Short-term effects of air pollution in a cohort of patients with chronic obstructive pulmonary disease. *Epidemiology (Cambridge, Mass.)*, 23(6), pp.861–79.
- Feehery, G.R. *et al.*, 2013. A Method for Selectively Enriching Microbial DNA from Contaminating Vertebrate Host DNA. *PLoS ONE*, 8(10).
- Feil, E.J. *et al.*, 2003. How clonal is *S. aureus*? *Journal of Bacteriology*, 185(11), pp.3307–3316.
- Feldman, C. & Anderson, R., 2011. Bacteraemic pneumococcal pneumonia: Current therapeutic options. *Drugs*, 71(2), pp.131–153.
- Feldman, C. & Anderson, R., 2013. Cigarette smoking and mechanisms of susceptibility to infections of the respiratory tract and other organ systems. *Journal of Infection*, 67(3), pp.169–184.
- Fernández Guerrero, M.L. *et al.*, 2009. Endocarditis caused by *S. aureus*: A reappraisal of the epidemiologic, clinical, and pathologic manifestations with analysis of factors determining outcome. *Medicine*, 88(1), pp.1–22.
- Fitzpatrick, F., Humphreys, H. & O’Gara, J.P., 2005. Evidence for icaADBC-independent biofilm development mechanism in methicillin-resistant *S. aureus* clinical isolates. *Journal of Clinical Microbiology*, 43(4), pp.1973–1976.
- Fitzpatrick, F., Humphreys, H. & P, O.J., 2006. Environmental regulation of biofilm development in methicillin-resistant and methicillin-susceptible *S. aureus* clinical isolates. *Journal of Hospital Infection*, 62(1), pp.119–120.
- Flemming, H. & Wingender, J., 2010. The biofilm matrix. *Nature reviews. Microbiology*, 8(9), pp.623–33.

- Folkmann, J.K. *et al.*, 2009. Oxidatively Damaged DNA in Rats Exposed by Oral Gavage to C60 Fullerenes and Single-Walled Carbon Nanotubes. *Environmental Health Perspectives*, 117(5), pp.703–708.
- Foster, T.J. *et al.*, 2014. Adhesion, invasion and evasion: the many functions of the surface proteins of *S. aureus*. *Nat.Rev.Microbiol.*, 12(1740-1534 (Electronic)), pp.49–62.
- Fournier, P.E. & Raoult, D., 2009. Current knowledge on phylogeny and taxonomy of rickettsia spp. *Annals of the New York Academy of Sciences*, 1166, pp.1–11.
- Fowler, V.G. *et al.*, 1997. Role of echocardiography in evaluation of patients with *S. aureus* bacteremia: experience in 103 patients. *Journal of the American College of Cardiology*, 30(4), pp.1072–1078.
- Fowler, V.G. *et al.*, 2005. *S. aureus* endocarditis: a consequence of medical progress. *JAMA*, 293(24), pp.3012–21.
- Frank, D.N. *et al.*, 2010. The human nasal microbiota and *S. aureus* carriage. *PloS one*, 5(5), p.e10598.
- Franzetti, A. *et al.*, 2011. Seasonal variability of bacteria in fine and coarse urban air particulate matter. *Applied Microbiology and Biotechnology*, 90(2), pp.745–753.
- Fukunaga, Y. & Ichikawa, N., 2014. The Class Holophagaceae. In *The Prokaryotes: Other Major Lineages of Bacteria and The Archaea*. pp. 683–687.
- Fullerton, D.G. *et al.*, 2009. Domestic smoke exposure is associated with alveolar macrophage particulate load. *Tropical Medicine and International Health*, 14(3), pp.349–354.
- Fux, C.A., Wilson, S. & Stoodley, P., 2004. Detachment Characteristics and Oxacillin Resistance of *Staphylococcus aureus* Biofilm Emboli in an In Vitro Catheter Infection Model. *Journal of Bacteriology*, 186(14), pp.4486–4491.
- Gallagher, J. *et al.*, 2003. Formation of 8-oxo-7,8-dihydro-2'-deoxyguanosine in rat lung DNA following subchronic inhalation of carbon black. *Toxicology and Applied Pharmacology*, 190(3), pp.224–231.
- Gandolfi, I. *et al.*, 2015. Spatio-temporal variability of airborne bacterial communities and their correlation with particulate matter chemical composition across two urban areas. *Applied Microbiology and Biotechnology*, pp.4867–4877.
- Gangamma, S., 2014. Characteristics of airborne bacteria in Mumbai urban environment. *Science of the Total Environment*, 488-489(1), pp.70–74.

- García-Rodríguez, J.Á. & Fresnadillo Martínez, M.J., 2002. Dynamics of nasopharyngeal colonization by potential respiratory pathogens. *J.Antimicrob.Chemother.* Suppl S(0305-7453 (Print)), pp.59–73.
- Gardete, S. & Tomasz, A., 2014. Mechanisms of vancomycin resistance in *S. aureus*. *The Journal of clinical investigation*, 124(7), pp.2836–40.
- Garmendia, J., Morey, P. & Bengoechea, J.A., 2012. Impact of cigarette smoke exposure on host-bacterial pathogen interactions. *European Respiratory Journal*, 39(2), pp.467–477.
- Gerber, A. *et al.*, 2015. Tobacco smoke particles and indoor air quality (ToPIQ-II) - a modified study protocol and first results. *Journal of occupational medicine and toxicology (London, England)*, 10, p.5.
- Gilan, I. & Sivan, A., 2013. Effect of proteases on biofilm formation of the plastic-degrading actinomycete *Rhodococcus ruber* C208. *FEMS Microbiology Letters*, 342(1), pp.18–23.
- Gilley, R.P. & Orihuela, C.J., 2014. Pneumococci in biofilms are non-invasive: implications on nasopharyngeal colonization. *Frontiers in cellular and infection microbiology*, 4(November), p.163.
- Gittins, M. *et al.*, 2013. Has the short-term effect of black smoke exposure on pneumonia mortality been underestimated because hospitalisation is ignored: findings from a case-crossover study. *Environmental Health*, 12(1), p.97.
- Glauert, A.M. & Lewis, P.R., 2014. *Biological Specimen Preparation for Transmission Electron Microscopy* A. M. Glauert, ed., London: Portland Press Ltd.
- Goeminne, P.C. *et al.*, 2013. Impact of air pollution on cystic fibrosis pulmonary exacerbations: A case-crossover analysis. *Chest*, 143(4), pp.946–954.
- Goldstein-Daruech, N. *et al.*, 2011. Tobacco Smoke Mediated Induction of Sinonasal Microbial Biofilms. *PLoS ONE*, 6(1), p.e15700.
- Goodfellow, M. *et al.*, 2012. *Bergey's Manual of Systematic Bacteriology - Vol 5: The Actinobacteria, Part A*.
- Gou, H. *et al.*, 2016. Assessment of microbial communities in PM₁ and PM₁₀ of Urumqi during winter. *Environmental Pollution*, 214, pp.202–210.
- Gould, F.K. *et al.*, 2012. Guidelines for the diagnosis and antibiotic treatment of endocarditis in adults: a report of the Working Party of the British Society for Antimicrobial Chemotherapy. *The Journal of antimicrobial chemotherapy*, 67(2), pp.269–89.

- Graff, D.W. *et al.*, 2009. Exposure to concentrated coarse air pollution particles causes mild cardiopulmonary effects in healthy young adults. *Environmental Health Perspectives*, 117(7), pp.1089–1094.
- Grahn, N. *et al.*, 2003. Identification of mixed bacterial DNA contamination in broad-range PCR amplification of 16S rDNA V1 and V3 variable regions by pyrosequencing of cloned amplicons. *FEMS Microbiology Letters*, 219(1), pp.87–91.
- Gritzfeld, J.F. *et al.*, 2014. Density and duration of experimental human pneumococcal carriage. *Clinical Microbiology and Infection*, 20(12), pp.O1145–O1151.
- Gu, B. *et al.*, 2013. The emerging problem of linezolid-resistant *Staphylococcus*. *Journal of Antimicrobial Chemotherapy*, 68(1), pp.4–11.
- Gu, J. *et al.*, 2015. Personal day-time exposure to ultrafine particles in different microenvironments. *International journal of hygiene and environmental health*, 218(2), pp.188–195.
- Gualdi, L. *et al.*, 2012. Regulation of neuraminidase expression in *S. pneumoniae*. *BMC microbiology*, 12(1), p.200.
- Guarnieri, M. *et al.*, 2015. Lung function in rural guatemalan women before and after a chimney stove intervention to reduce wood smoke exposure: results from the randomized exposure study of pollution indoors and respiratory effects and chronic respiratory effects of early childhood. *Chest*, 148(5), pp.1184–92.
- Guiral, S. *et al.*, 2005. Competence-programmed predation of noncompetent cells in the human pathogen *S. pneumoniae*: Genetic requirements. *Proceedings of the National Academy of Sciences of the United States of America*, 102(24), pp.8710–8715.
- Guo, Y. *et al.*, 2013. The burden of air pollution on years of life lost in Beijing, China, 2004–08: retrospective regression analysis of daily deaths. *BMJ (Clinical research ed.)*, 347(dec09_7), p.f7139.
- Gupta, A.K., Lyons, D.C.A. & Rosen, T., 2015. New and emerging concepts in managing and preventing community-associated methicillin-resistant *S. aureus* infections. *International Journal of Dermatology*, 54(11), pp.1226–1232.
- Hall-Stoodley, L. *et al.*, 2006. Direct detection of bacterial biofilms on the middle-ear mucosa of children with chronic otitis media. *JAMA*, 296(2), pp.202–11.
- Hall-Stoodley, L. *et al.*, 2008. Characterization of biofilm matrix, degradation by DNase treatment and evidence of capsule downregulation in *S. pneumoniae* clinical isolates. *BMC microbiology*, 8, p.173.

- Hammerschmidt, S. *et al.*, 2005. Illustration of pneumococcal polysaccharide capsule during adherence and invasion of epithelial cells. *Infection and Immunity*, 73(8), pp.4653–4667.
- Hammoud, A. *et al.*, 2010. Decreased sperm motility is associated with air pollution in Salt Lake City. *Fertility and Sterility*, 93(6), pp.1875–1879.
- Hansen, A.B. *et al.*, 2016. Long-term exposure to fine particulate matter and incidence of diabetes in the Danish Nurse Cohort. *Environment International*, 91, pp.243–250.
- Harrod, K.S., 2004. Inhaled Diesel Engine Emissions Reduce Bacterial Clearance and Exacerbate Lung Disease to *Pseudomonas aeruginosa* Infection In Vivo. *Toxicological Sciences*, 83(1), pp.155–165.
- Harvey, R.M. *et al.*, 2011. Pneumolysin with Low Hemolytic Activity Confers an Early Growth Advantage to *S. pneumoniae* in the Blood. *Infection and Immunity*, 79(10), pp.4122–4130.
- Haste, L. V *et al.*, 2014. Development and Characterisation of a Long Term Murine Model of *S. pneumoniae* Infection of the Lower Airways. *Infection and immunity*, 82(May), pp.3289–3298.
- Hava, D.L., LeMieux, J. & Camilli, A., 2003. From nose to lung: The regulation behind *S. pneumoniae* virulence factors. *Molecular Microbiology*, 50(4), pp.1103–1110.
- Hayre, J. *et al.*, 2012. Optimization of a direct spectrophotometric method to investigate the kinetics and inhibition of sialidases. *BMC Biochemistry*, 13(1), p.19.
- He, T. *et al.*, 2016. Ambient air pollution and years of life lost in Ningbo, China. *Scientific Reports*, 6, p.22485.
- Heal, M.R., Kumar, P. & Harrison, R.M., 2012. Particles, air quality, policy and health. *Chemical Society reviews*, 41(19), pp.6606–6630.
- Heinrich, J. *et al.*, 2003. Endotoxin in fine (PM_{2.5}) and coarse (PM_{2.5-10}) particle mass of ambient aerosols. A temporo-spatial analysis. *Atmospheric Environment*, 37(26), pp.3659–3667.
- Hoa, M. *et al.*, 2009. Demonstration of nasopharyngeal and middle ear mucosal biofilms in an animal model of acute otitis media. *Annals of Otolology, Rhinology and Laryngology*, 118(4), pp.292–298.
- Hoek, G. *et al.*, 2002. Association between mortality and indicators of traffic-related air pollution in the Netherlands: A cohort study. *Lancet*, 360(9341), pp.1203–1209.

- Hoek, G. *et al.*, 2013. Long-term air pollution exposure and cardio- respiratory mortality: a review. *Environmental Health: A Global Access Science Source*, 12(1), p.43.
- Hoffmann, B. *et al.*, 2009. Chronic residential exposure to particulate matter air pollution and systemic inflammatory markers. *Environmental Health Perspectives*, 117(8), pp.1302–1308.
- Hogberg, L. *et al.*, 2007. Age- and serogroup-related differences in observed durations of nasopharyngeal carriage of penicillin-resistant pneumococci. *Journal of Clinical Microbiology*, 45(3), pp.948–952.
- Hoover, S.E. *et al.*, 2015. A new quorum sensing system (TprA/PhrA) for *S. pneumoniae* D39 that regulates a lantibiotic biosynthesis gene cluster. *Molecular Microbiology*, 97(2), pp.229–43.
- Horsburgh, M.J. *et al.*, 2002. SigmaB modulates virulence determinant expression and stress resistance: Characterization of a functional rsbU strain derived from *S. aureus* 8325-4. *Journal of Bacteriology*, 184(19), pp.5457–5467.
- Houston, P. *et al.*, 2011. Essential role for the major autolysin in the fibronectin-binding protein-mediated *S. aureus* biofilm phenotype. *Infection and Immunity*, 79(3), pp.1153–1165.
- Hu, C. *et al.*, 2012. Functional characterization of lipase in the pathogenesis of *S. aureus*. *Biochemical and Biophysical Research Communications*, 419(4), pp.617–620.
- Huang, R. *et al.*, 2014. Effects of nicotine on *Streptococcus gordonii* growth, biofilm formation, and cell aggregation. *Applied and Environmental Microbiology*, 80(23), pp.7212–7218.
- Huang, S.S. *et al.*, 2008. Strain-relatedness of methicillin-resistant *S. aureus* isolates recovered from patients with repeated infection. *Clinical infectious diseases : an official publication of the Infectious Diseases Society of America*, 46, pp.1241–1247.
- Huang, Y.J. *et al.*, 2013. The Role of the Lung Microbiome in Health and Disease. A National Heart, Lung, and Blood Institute Workshop Report. *American Journal of Respiratory and Critical Care Medicine*, 187(12), pp.1382–1387.
- Huse, S.M. *et al.*, 2008. Exploring microbial diversity and taxonomy using SSU rRNA hypervariable tag sequencing. *PLoS Genetics*, 4(11).
- Huseby, M. *et al.*, 2007. Structure and biological activities of beta toxin from *S. aureus*. *Journal of Bacteriology*, 189(23), pp.8719–8726.

- Huseby, M.J. *et al.*, 2010. Beta toxin catalyzes formation of nucleoprotein matrix in staphylococcal biofilms. *Proceedings of the National Academy of Sciences of the United States of America*, 107(32), pp.14407–12.
- Hussain, M. *et al.*, 2005. A longitudinal household study of *S. pneumoniae* nasopharyngeal carriage in a UK setting. *Epidemiology and Infection*, 133(5), pp.891–8.
- Hwang, B.F. *et al.*, 2015. Relationship between exposure to fine particulates and ozone and reduced lung function in children. *Environmental Research*, 137, pp.382–390.
- Invernizzi, G. *et al.*, 2004. Particulate matter from tobacco versus diesel car exhaust: an educational perspective. *Tobacco control*, 13(3), pp.219–221.
- Invernizzi, G. *et al.*, 2011. Measurement of black carbon concentration as an indicator of air quality benefits of traffic restriction policies within the ecopass zone in Milan, Italy. *Atmospheric Environment*, 45(21), pp.3522–3527.
- Ishii, K. & Akira, S., 2006. Innate immune recognition of, and regulation by, DNA. *Trends in Immunology*, 27(11), pp.525–532.
- Ito, T. *et al.*, 2009. Classification of staphylococcal cassette chromosome mec (SCCmec): Guidelines for reporting novel SCCmec elements. *Antimicrobial Agents and Chemotherapy*, 53(12), pp.4961–4967.
- Iwase, T. *et al.*, 2010. *Staphylococcus epidermidis* Esp inhibits *S. aureus* biofilm formation and nasal colonization. *Nature*, 465(1476-4687 (Electronic)), pp.346–349.
- Jackson, P., Hougaard, K.S., Vogel, U., *et al.*, 2012a. Exposure of pregnant mice to carbon black by intratracheal instillation: Toxicogenomic effects in dams and offspring. *Mutation Research/Genetic Toxicology and Environmental Mutagenesis*, 745(1-2), pp.73–83.
- Jackson, P., Hougaard, K.S., Boisen, A.M.Z., *et al.*, 2012b. Pulmonary exposure to carbon black by inhalation or instillation in pregnant mice: Effects on liver DNA strand breaks in dams and offspring. *Nanotoxicology*, 6(5), pp.486–500.
- Jaenicke, R., 2005. Abundance of cellular material and proteins in the atmosphere. *Science (New York, N.Y.)*, 308(5718), p.73.
- Jalava, P.I. *et al.*, 2016. Chemical and microbial components of urban air PM cause seasonal variation of toxicological activity. *Environmental Toxicology and Pharmacology*, 40(2), pp.375–387.
- Janssen, N.A. *et al.*, 2012. *Health effects of black carbon*. World Health Organization. Copenhagen

- Jedrychowski, W.A. *et al.*, 2013. Intrauterine exposure to fine particulate matter as a risk factor for increased susceptibility to acute broncho-pulmonary infections in early childhood. *International Journal of Hygiene and Environmental Health*, 216(4), pp.395–401.
- Jefferson, K.K. *et al.*, 2004. The Teicoplanin-Associated Locus Regulator (TcaR) and the Intercellular Adhesin Locus Regulator (IcaR) Are Transcriptional Inhibitors of the ica Locus in *S. aureus*. *Journal of Bacteriology*, 186(8), pp.2449–2456.
- Jervis-Bardy, J. *et al.*, 2015. Deriving accurate microbiota profiles from human samples with low bacterial content through post-sequencing processing of Illumina MiSeq data. *Microbiome*, 3(1), p.19.
- Jevons, M., Coe, A. & Parker, M., 1963. Methicillin resistance in staphylococci. *Lancet*, 27(1 (7287)), pp.904–907.
- Jiang, J. *et al.*, 2005. Development of Procedures for Direct Extraction of Cryptosporidium DNA from Water Concentrates and for Relief of PCR Inhibitors. *Appl Environ Microbiol.*, 71(3), pp.1135–1141.
- Johnson, M., Cockayne, A. & Morrissey, J.A., 2008. Iron-regulated biofilm formation in *S. aureus* newman requires ica and the secreted protein Emp. *Infection and Immunity*, 76(4), pp.1756–1765.
- Jorth, P. *et al.*, 2013. Probing bacterial metabolism during infection using high-resolution transcriptomics. *Journal of Bacteriology*, 195(22), pp.4991–4998.
- Jumpstart Consortium Human Microbiome Project Data Generation Working Group, 2012. Evaluation of 16S rDNA-based community profiling for human microbiome research. *PloS one*, 7(6), p.e39315.
- Kadioglu, A., *et al.*, 2000. Host cellular immune response to pneumococcal lung infection in mice. *Infection and immunity*, 68(2), pp.492–501.
- Kadioglu, A. & Andrew, P.W., 2005. Susceptibility and resistance to pneumococcal disease in mice. *Briefings in functional genomics & proteomics*, 4(3), pp.241–247.
- Kadioglu, A. *et al.*, 2008. The role of *S. pneumoniae* virulence factors in host respiratory colonization and disease. *Nature Reviews Microbiology*, 6(4), pp.288–301.
- Kan, H. *et al.*, 2007. Differentiating the effects of fine and coarse particles on daily mortality in Shanghai, China. *Environment international*, 33(3), pp.376–84.
- Kaplan, J.B. *et al.*, 2003. Detachment of *Actinobacillus actinomycetemcomitans* biofilm cells by an endogenous beta--hexosaminidase activity. *Journal of Bacteriology*, 185(16), pp.4693–4698.

- Kaplan, J.B., 2010. Biofilm dispersal: mechanisms, clinical implications, and potential therapeutic uses. *Journal of dental research*, 89(3), 205–18.
- Kastenbauer, S. & Pfister, H.W., 2003. Pneumococcal meningitis in adults: Spectrum of complications and prognostic factors in a series of 87 cases. *Brain*, 126(5), pp.1015–1025.
- Katayama, Y. *et al.*, 2013. Beta-hemolysin promotes skin colonization by *S. aureus*. *Journal of Bacteriology*, 195(6), pp.1194–1203.
- Kavanagh, K.T., Saman, D.M. & Yu, Y., 2013. A perspective on how the United States fell behind Northern Europe in the battle against methicillin-resistant *S. aureus*. *Antimicrobial Agents and Chemotherapy*, 57(12), pp.5789–5791.
- Keki, Z. *et al.*, 2013. Application of special oligotrophic media for cultivation of bacterial communities originated from ultrapure water. *Acta Microbiol Immunol Hung*, 60(3), pp.345–357.
- Kelly, F.J. & Fussell, J.C., 2011. Air pollution and airway disease. *Clinical & Experimental Allergy*, 41(8), pp.1059–1071.
- Kelly, F.J. & Fussell, J.C., 2012. Size, source and chemical composition as determinants of toxicity attributable to ambient particulate matter. *Atmospheric Environment*, 60(0), pp.504–526.
- Kiedrowski, M.R. *et al.*, 2011. Nuclease modulates biofilm formation in community-associated methicillin-resistant *S. aureus*. *PLoS One*, 6(11), p.e26714.
- Kiedrowski, M.R. & Horswill, A.R., 2011. New approaches for treating staphylococcal biofilm infections. *Annals of the New York Academy of Sciences*, 1241(1), pp.104–121.
- Kiedrowski, M.R. *et al.*, 2014. *S. aureus* Nuc2 is a functional, surface-attached extracellular nuclease. *PLoS ONE*, 9(4).
- King, M.D. *et al.*, 2006. Emergence of community-acquired methicillin-resistant *S. aureus* USA 300 clone as the predominant cause of skin and soft-tissue infections. *Annals of Internal Medicine*, 144(5), pp.309–317.
- King, S.J., Hippe, K.R. & Weiser, J.N., 2006. Deglycosylation of human glycoconjugates by the sequential activities of exoglycosidases expressed by *S. pneumoniae*. *Molecular Microbiology*, 59(3), pp.961–974.
- Kish, L. *et al.*, 2013. Environmental Particulate Matter Induces Murine Intestinal Inflammatory Responses and Alters the Gut Microbiome. *PLoS ONE*, 8(4).

- Kjos, M. *et al.*, 2016. Expression of *S. pneumoniae* Bacteriocins Is Induced by Antibiotics via Regulatory Interplay with the Competence System. *PLOS Pathogens*, 12(2), p.e1005422.
- Kloog, I. *et al.*, 2015. Effects of airborne fine particles (PM_{2.5}) on Deep Vein Thrombosis Admissions in North Eastern United States. *Journal of Thrombosis and Haemostasis*, (January).
- Klumper, C. *et al.*, 2015. Air pollution and cytokine responsiveness in asthmatic and non-asthmatic children. *Environmental Research*, 138, pp.381–390.
- Kluytmans, J., van Belkum, A. & Verbrugh, H., 1997. Nasal carriage of *S. aureus*: epidemiology, underlying mechanisms, and associated risks. *Clinical microbiology reviews*, 10(3), pp.505–20.
- Knight, G.M. *et al.*, 2012. Shift in dominant hospital-associated methicillin-resistant *S. aureus* (HA-MRSA) clones over time. *Journal of Antimicrobial Chemotherapy*, 67(10), pp.2514–2522.
- Knight, G.M., Budd, E.L. & Lindsay, J.A., 2013. Large mobile genetic elements carrying resistance genes that do not confer a fitness burden in healthcare-associated methicillin-resistant *S. aureus*. *Microbiology (United Kingdom)*, 159(8), pp.1661–1672.
- Köck, R. *et al.*, 2010. Methicillin-resistant *S. aureus* (MRSA): burden of disease and control challenges in Europe. *Euro.Surveill*, 15(1560-7917), p.19688.
- Koedel, U., Scheld, W.M. & Pfister, H.W., 2002. Pathogenesis and pathophysiology of pneumococcal meningitis. *Lancet Infectious Diseases*, 2(12), pp.721–736.
- Koelmans, A.A. *et al.*, 2006. Black carbon: The reverse of its dark side. *Chemosphere*, 63(3), pp.365–377.
- Kogan, G. *et al.*, 2006. Biofilms of clinical strains of *Staphylococcus* that do not contain polysaccharide intercellular adhesin. *FEMS Microbiology Letters*, 255(1), pp.11–16.
- Konstantinidis, K.T. & Tiedje, J.M., 2005. Genomic insights that advance the species definition for prokaryotes. *Proceedings of the National Academy of Sciences of the United States of America*, 102(7), pp.2567–72.
- Krone, C.L. *et al.*, 2014. Respiratory Microbiota Dynamics following *S. pneumoniae* Acquisition in Young and Elderly Mice. *Infection and Immunity*, 82(4), pp.1725–1731.
- Kulakov, L.A. *et al.*, 2002. Analysis of bacteria contaminating ultrapure water in industrial systems. *Applied and Environmental Microbiology*, 68(4), pp.1548–1555.

- Kulkarni, R. *et al.*, 2012. Cigarette Smoke Increases *S. aureus* Biofilm Formation via Oxidative Stress. *Infection and immunity*, 80(11), pp.3804–3811.
- Kumar, R.K. *et al.*, 2015. Differential injurious effects of ambient and traffic-derived particulate matter on airway epithelial cells. *Respirology*, 2015(January), pp.73–79.
- Kunin, V. *et al.*, 2010. Wrinkles in the rare biosphere: Pyrosequencing errors can lead to artificial inflation of diversity estimates. *Environmental Microbiology*, 12(1), pp.118–123.
- Kurola, P. *et al.*, 2011. Effect of xylitol and other carbon sources on *S. pneumoniae* biofilm formation and gene expression in vitro. *APMIS*, 119(2), pp.135–142.
- Lanie, J.A. *et al.*, 2007. Genome Sequence of Avery’s Virulent Serotype 2 Strain D39 of *S. pneumoniae* and Comparison with That of Unencapsulated Laboratory Strain R6. *Journal of Bacteriology*, 189(1), pp.38–51.
- Larcombe, A.N. *et al.*, 2014. Route of exposure alters inflammation and lung function responses to diesel exhaust. *Inhalation toxicology*, 26(7), pp.409–418.
- Launes, C. *et al.*, 2012. Viral coinfection in children less than five years old with invasive pneumococcal disease. *The Pediatric infectious disease journal*, 31(6), pp.650–653.
- Laurence, M., Hatzis, C. & Brash, D.E., 2014. Common contaminants in next-generation sequencing that hinder discovery of low-abundance microbes. *PLoS ONE*, 9(5).
- Lazarevic, V. *et al.*, 2014. Challenges in the culture-independent analysis of oral and respiratory samples from intubated patients. *Frontiers in Cellular and Infection Microbiology*, 4, p.65.
- Lee, J.E., 2014. How and why we study the microbial world. [Online] Available at: <https://jackedwardlee.wordpress.com/2014/01/03/how-and-why-we-study-the-microbial-world/> [Accessed March 6, 2016].
- Legendre, P. & De Cáceres, M., 2013. Beta diversity as the variance of community data: Dissimilarity coefficients and partitioning. *Ecology Letters*, 16(8), pp.951–963.
- Lepeule, J. *et al.*, 2014. Long-term effects of traffic particles on lung function decline in the elderly. *American Journal of Respiratory and Critical Care Medicine*, 190(5), pp.542–548.
- Lewis, K., 2008. Multidrug tolerance of biofilms and persister cells. *Current Topics in Microbiology and Immunology*, 322, pp.107–131.

- Li, N. *et al.*, 2004. Nrf2 is a key transcription factor that regulates antioxidant defense in macrophages and epithelial cells: protecting against the proinflammatory and oxidizing effects of diesel exhaust chemicals. *Journal of immunology (Baltimore, Md. : 1950)*, 173(5), pp.3467–3481.
- Li, B. *et al.*, 2015. Personal exposure to black carbon during commuting in peak and off-peak hours in Shanghai. *Science of the Total Environment*, 524-525, pp.237–245.
- Li, Y. *et al.*, 2015. Assessing public health burden associated with exposure to ambient black carbon in the United States. , 20(8), pp.847–856.
- Li, Y. *et al.*, 2002. Novel two-component regulatory system involved in biofilm formation and acid resistance in *Streptococcus mutans*. *Journal of Bacteriology*, 184(22), pp.6333-42.
- Liang, R. *et al.*, 2014. Effect of exposure to PM_{2.5} on blood pressure: a systematic review and meta-analysis. *Journal of hypertension*, 32(11), pp.2130–41.
- Lim, Y. *et al.*, 2004. Control of Glucose- and NaCl-Induced Biofilm Formation by rbf in *S. aureus*. *Journal of Bacteriology*, 186(3), pp.722–729.
- Lindsay, J. & Holden, M., 2006. Understanding the rise of the superbug: investigation of the evolution and genomic variation of *S. aureus*. *Funct Integr Genomics*, 6(3), pp.186–201.
- Lippmann, M., 2014. Toxicological and epidemiological studies of cardiovascular effects of ambient air fine particulate matter (PM_{2.5}) and its chemical components: Coherence and public health implications. *Critical reviews in toxicology*, 44(4), pp.299–347.
- Lipsett, M.J. *et al.*, 2006. Coarse Particles and Heart Rate Variability among Older Adults with Coronary Artery Disease in the Coachella Valley, California. *Environmental Health Perspectives*, 114(8), pp.1215–1220.
- Lister, J.L. & Horswill, A.R., 2014. *S. aureus* biofilms: recent developments in biofilm dispersal. *Frontiers in cellular and infection microbiology*, 4(December), p.178.
- Liu, G.Y., 2009. Molecular Pathogenesis of *S. aureus* Infection. *Pediatr Res*, 65, pp.71–77.
- Long, C.M., Nascarella, M.A. & Valberg, P.A., 2013. Carbon black vs. black carbon and other airborne materials containing elemental carbon: Physical and chemical distinctions. *Environmental Pollution*, 181, pp.271–286.
- Longhin, E. *et al.*, 2016. Physico-chemical properties and biological effects of diesel and biomass particles. *Environmental Pollution*, pp.1–10.

- Lory, S., 2014. The Family Staphylococcaceae. In *The Prokaryotes: Firmicutes and Tenericutes*. pp. 363–366.
- Love, M.I., Anders, S. & Huber, W., 2014. Differential analysis of count data - the DESeq2 package. *Genome Biology*, 15(12), p.550.
- Lowy, F.D., 2003. Antimicrobial resistance: The example of *S. aureus*. *Journal of Clinical Investigation*, 111(9), pp.1265–1273.
- Lozupone, C. *et al.*, 2011. UniFrac: An effective distance metric for microbial community comparison. *The ISME Journal*, 5(2), pp.169–172.
- Lozupone, C. & Knight, R., 2005. UniFrac: A new phylogenetic method for comparing microbial communities. *Applied and Environmental Microbiology*, 71(12), pp.8228–8235.
- Lu, F. *et al.*, 2015. Systematic review and meta-analysis of the adverse health effects of ambient PM_{2.5} and PM₁₀ pollution in the Chinese population. *Environmental Research*, 136, pp.196–204.
- Lundborg, M. *et al.*, 2007. Aggregates of ultrafine particles modulate lipid peroxidation and bacterial killing by alveolar macrophages. *Environmental Research*, 104(2), pp.250–257.
- Luong, T.T., Lei, M.G. & Lee, C.Y., 2009. *S. aureus* Rbf activates biofilm formation in vitro and promotes virulence in a murine foreign body infection model. *Infection and Immunity*, 77(1), pp.335–340.
- MacIntyre, E.A. *et al.*, 2014. Air Pollution and Respiratory Infections during Early Childhood: An Analysis of 10 European Birth Cohorts within the ESCAPE Project. *Environmental Health Perspectives*, 122(1), pp.107–113.
- Mahalingaiah, S. *et al.*, 2016. Adult air pollution exposure and risk of infertility in the Nurses' Health Study II. *Human reproduction (Oxford, England)*, 31(3), pp.638–647.
- Maiwald, M. *et al.*, 1994. Characterization of contaminating DNA in Taq polymerase which occurs during amplification with a primer set for Legionella 5S ribosomal RNA. *Molecular and cellular probes*, 8(1), pp.11–14.
- Malachowa, N. & DeLeo, F.R., 2010. Mobile genetic elements of *S. aureus*. *Cell Mol.Life Sci.*, 67(1420-9071 (Electronic)), pp.3057–3071.
- Manco, S. *et al.*, 2006. Pneumococcal neuraminidases A and B both have essential roles during infection of the respiratory tract and sepsis. *Infection and Immunity*, 74(7), pp.4014–4020.

- Mann, E.E. *et al.*, 2009. Modulation of eDNA release and degradation affects *S. aureus* biofilm maturation. *PLoS ONE*, 4(6).
- Mannucci, P.M. *et al.*, 2015. Effects on health of air pollution: a narrative review. *Internal and Emergency Medicine*, 10(6), pp.657–662.
- De Marco, C. *et al.*, 2015. Particulate matters from diesel heavy duty trucks exhaust versus cigarettes emissions: a new educational antismoking instrument. *Multidisciplinary Respiratory Medicine*, 11(1), p.2.
- Marks, L.R., Iyer Parameswaran, G. & Hakansson, A.P., 2012a. Pneumococcal interactions with epithelial cells are crucial for optimal biofilm formation and colonization in vitro and in vivo. *Infection and Immunity*, 80(8), pp.2744–2760.
- Marks, L.R., Reddinger, R.M. & Anders, P., 2012b. High Levels of Genetic Recombination during Nasopharyngeal Carriage and Biofilm Formation in *S. pneumoniae*. *mBio*, 3(5), pp.e00200–12.
- Marks, L.R. *et al.*, 2013. Interkingdom signaling induces *S. pneumoniae* biofilm dispersion and transition from asymptomatic colonization to disease. *mBio*, 4(4), pp.e00438–13–e00438–13.
- Marques, S.C. *et al.*, 2007. Formation of Biofilms By *S. aureus* on Stainless Steel and Glass Surfaces and Its Resistance To Some Selected Chemical Sanitizers. , pp.538–543.
- Marriott, H.M., Mitchell, T.J. & Dockrell, D.H., 2008. Pneumolysin: a double-edged sword during the host-pathogen interaction. *Curr Mol Med*, 8(6), pp.497–509.
- Marshall, J.E. *et al.*, 2015. The Crystal Structure of Pneumolysin at 2.0 Å Resolution Reveals the Molecular Packing of the Pre-pore Complex. *Scientific reports*, 5(July), p.13293.
- Martin, M. *et al.*, 2003. An outbreak of conjunctivitis due to atypical *S. pneumoniae*. *The New England journal of medicine*, 348(12), pp.1112–21.
- Martinelli, N., Olivieri, O. & Girelli, D., 2013. Air particulate matter and cardiovascular disease: A narrative review. *European Journal of Internal Medicine*, 24(4), pp.295–302.
- Mazzoli-Rocha, F. *et al.*, 2010. Roles of oxidative stress in signaling and inflammation induced by particulate matter. *Cell Biology and Toxicology*, 26(5), pp.481–498..
- Mcalister, M. *et al.*, 2002. Survival and nutritional requirements of three bacteria isolated from ultrapure water. *Journal of Industrial Microbiology & Biotechnology*, 29, pp.75–82.

- McCarthy, H. *et al.*, 2015. Methicillin resistance and the biofilm phenotype in *S. aureus*. *Frontiers in cellular and infection microbiology*, 5, p.1.
- McDonald, D. *et al.*, 2012. An improved Greengenes taxonomy with explicit ranks for ecological and evolutionary analyses of bacteria and archaea. *The ISME journal*, 6(3), pp.610–8.
- McEachern, E.K. *et al.*, 2015. Analysis of the effects of cigarette smoke on staphylococcal virulence phenotypes. *Infection and Immunity*, 83(6), pp.2443–2452.
- McFeters, G.A. *et al.*, 1993. Distribution of bacteria within operating laboratory water purification systems. *Applied and Environmental Microbiology*, 59(5), pp.1410–1415.
- McMurdie, P.J. & Holmes, S., 2013. Phyloseq: An R Package for Reproducible Interactive Analysis and Graphics of Microbiome Census Data. *PLoS ONE*, 8(4).
- Mellroth, P. *et al.*, 2012. LytA, major autolysin of *S. pneumoniae*, requires access to nascent peptidoglycan. *Journal of Biological Chemistry*, 287(14), pp.11018–11029.
- Melo, J. *et al.*, 2013. *Listeria monocytogenes* dairy isolates show a different proteome response to sequential exposure to gastric and intestinal fluids. *International Journal of Food Microbiology*, 163(2-3), pp.51–63.
- Miles, A.A., Misra, S.S. & Irwin, J.O., 1938. The estimation of the bactericidal power of the blood. *The Journal of hygiene*, 38(6), pp.732–749.
- Miller, E.L. *et al.*, 2016. Diverse ecological strategies are encoded by *S. pneumoniae* bacteriocin-like peptides. *Genome biology and evolution*, 8(4), pp.1072–1090.
- Miller, K.A. *et al.*, 2007. Long-term exposure to air pollution and incidence of cardiovascular events in women. *The New England journal of medicine*, 356(5), pp.447–458.
- Miller, M.A. *et al.*, 2012. Visualization of murine intranasal dosing efficiency using luminescent *Francisella tularensis*: Effect of instillation volume and form of anesthesia. *PLoS ONE*, 7(2).
- Mitchell, T.J. *et al.*, 1997. Molecular analysis of virulence factors of *S. pneumoniae*. *Society for Applied Bacteriology symposium series*, 26, p.62S–71S.
- Moche, M. *et al.*, 2015. Time-Resolved Analysis of Cytosolic and Surface-Associated Proteins of *S. aureus* HG001 under Planktonic and Biofilm Conditions. *Journal of Proteome Research*, 14(9), pp.3804–3822.

- Mohammadi, T. *et al.*, 2005. Removal of contaminating DNA from commercial nucleic acid extraction kit reagents. *Journal of Microbiological Methods*, 61(2), pp.285–288.
- Mook-kanamori, B.B. *et al.*, 2011. Pathogenesis and Pathophysiology of Pneumococcal Meningitis. , 24(3), pp.557–591.
- Morelli, X. *et al.*, 2016. Air pollution, health and social deprivation: a fine-scale risk assessment Highlights. , 147, pp.59–70.
- Morris, A. *et al.*, 2013. Comparison of the respiratory microbiome in healthy nonsmokers and smokers. *American Journal of Respiratory and Critical Care Medicine*, 187(10), pp.1067–1075.
- Morrissey, J.A. *et al.*, 2002. Conservation, surface exposure, and in vivo expression of the Frp family of iron-regulated cell wall proteins in *S. aureus*. *Infection and Immunity*, 70(5), pp.2399–2407.
- Morton, D. & Griffiths, P., 1985. Guidelines on the recognition of pain, distress and discomfort in experimental animals and an hypothesis for assessment. *Veterinary Record*, 116(16), pp.431–436.
- Moscoso, M., García, E. & López, R., 2006. Biofilm formation by *S. pneumoniae*: Role of choline, extracellular DNA, and capsular polysaccharide in microbial accretion. *Journal of Bacteriology*, 188(22), pp.7785–7795.
- Moscoso, M., Garcia, E. & Lopez, R., 2009. Pneumococcal biofilms. *International Microbiology*, 12(2), pp.77–85.
- Müller, L. *et al.*, 2013. Diesel exhaust particles modify natural killer cell function and cytokine release. *Particle and fibre toxicology*, 10(Mic), p.16.
- Munoz-Elias, E.J. *et al.*, 2008. Isolation of *S. pneumoniae* biofilm mutants and their characterization during nasopharyngeal colonization. *Infection and Immunity*, 76(11), pp.5049–5061.
- Mushtaq, N. *et al.*, 2011. Adhesion of *S. pneumoniae* to human airway epithelial cells exposed to urban particulate matter. *Journal of Allergy and Clinical Immunology*, 127(5), pp.1236–1242.e2.
- Mustafic, H. *et al.*, 2012. Main air pollutants and myocardial infarction: a systematic review and meta-analysis. *Jama*, 307(7), pp.713–721.
- Mutepe, N.D. *et al.*, 2013. Effects of cigarette smoke condensate on pneumococcal biofilm formation and pneumolysin. *European Respiratory Journal*, 41(2), pp.392–395.

- Nel, A., 2005. Air Pollution-Related Illness: Effects of Particles. *Science*, 308(5723), pp.804–806.
- Nelson, A.L. *et al.*, 2007. Capsule enhances pneumococcal colonization by limiting mucus-mediated clearance. *Infection and Immunity*, 75(1), pp.83–90.
- Newsome, T. *et al.*, 2004. Presence of Bacterial Phage-Like DNA Sequences in Commercial Taq DNA Polymerase Reagents. *Journal of Clinical Microbiology*, 42(5), pp.2264–2267.
- Nguyen, N.-P. *et al.*, 2016. A perspective on 16S rRNA operational taxonomic unit clustering using sequence similarity. *Biofilms and Microbes*, 2.
- Ni, M. *et al.*, 2014. A review on black carbon emissions, worldwide and in China. *Chemosphere*, 107(April), pp.83–93.
- Nicholson, T.L. *et al.*, 2013. Livestock-Associated Methicillin-Resistant *S. aureus* (LA-MRSA) Isolates of Swine Origin Form Robust Biofilms. *PLoS ONE*, 8(8), pp.1–19.
- Nieuwenhuijsen, M.J. *et al.*, 2014. Air pollution and human fertility rates. *Environment International*, 70, pp.19–24.
- Nieuwenhuijsen, M.J. *et al.*, 2015. Variability in and agreement between modeled and personal continuously measured black carbon levels using novel smartphone and sensor technologies. *Environmental Science and Technology*, 49(5), pp.2977–2982.
- Nixon, G.M. *et al.*, 2001. Clinical outcome after early *Pseudomonas aeruginosa* infection in cystic fibrosis. *The Journal of pediatrics*, 138(5), pp.699–704.
- Noël, A. *et al.*, 2015. Incomplete lung recovery following sub-acute inhalation of combustion-derived ultrafine particles in mice. *Particle and Fibre Toxicology*, 13(1), p.10.
- Nwokoro, C. *et al.*, 2012. Cycling to work in London and inhaled dose of black carbon. *European Respiratory Journal*, 40(5), pp.1091–1097.
- O'Brien, K.L. *et al.*, 2009. Burden of disease caused by *S. pneumoniae* in children younger than 5 years: global estimates. *The Lancet*, 374(9693), pp.893–902.
- O'Gara, J.P., 2007. ica and beyond: Biofilm mechanisms and regulation in *Staphylococcus epidermidis* and *S. aureus*. *FEMS Microbiology Letters*, 270(2), pp.179–188.
- O'Neill, E. *et al.*, 2007. Association between methicillin susceptibility and biofilm regulation in *S. aureus* isolates from device-related infections. *Journal of Clinical Microbiology*, 45(5), pp.1379–1388.

- Octavia, S. & Lan, R., 2014. The Family Enterobacteriaceae. In *The Prokaryotes: Gammaproteobacteria*. pp. 225–286.
- Oggioni, M.R. *et al.*, 2006. Switch from planktonic to sessile life: A major event in pneumococcal pathogenesis. *Molecular Microbiology*, 61(5), pp.1196–1210.
- Ogunniyi, A.D. *et al.*, 2007. Contributions of pneumolysin, pneumococcal surface protein A (PspA), and PspC to pathogenicity of *S. pneumoniae* D39 in a mouse model. *Infection and Immunity*, 75(4), pp.1843–1851.
- Ohlwein, S. *et al.*, 2016. Air pollution and diastolic function in elderly women – Results from the SALIA study cohort. *International Journal of Hygiene and Environmental Health*.
- Oksanen, J. *et al.*, 2016. Vegan: community ecology package. *R package 2.3-3*, p.
- Oren, A. & Xu, X., 2014. The Family Hyphomicrobiaceae. In *The Prokaryotes: Alphaproteobacteria and Betaproteobacteria*. pp. 247–281.
- Ostro, B. *et al.*, 2014. The risks of acute exposure to black carbon in Southern Europe: results from the MED-PARTICLES project. *Occupational and Environmental Medicine*, (January 2016), pp.1–7.
- Palavecino, E., 2007. Clinical, epidemiological, and laboratory aspects of methicillin-resistant *S. aureus* (MRSA) infections. *Methods in molecular biology (Clifton, N.J.)*, 391, pp.1–19.
- Park, D.A. *et al.*, 2013. Impact of methicillin-resistance on mortality in children and neonates with *S. aureus* bacteremia: A meta-analysis. *Infection and Chemotherapy*, 45(2), pp.202–210.
- Park, M.K. *et al.*, 2014. Middle ear inflammation of rat induced by urban particles. *International Journal of Pediatric Otorhinolaryngology*, 78(12), pp.2193–2197.
- Parker, D. *et al.*, 2009. The NanA Neuraminidase of *S. pneumoniae* Is Involved in Biofilm Formation. *Infection and Immunity*, 77(9), pp.3722–3730.
- Patel, R.S. *et al.*, 2011. Oxidative stress is associated with impaired arterial elasticity. *Atherosclerosis*, 218(1), pp.90–95.
- Paulin, L. & Hansel, N., 2016. Particulate air pollution and impaired lung function. *F1000 Research*.
- Pearce, B.J., Iannelli, F. & Pozzi, G., 2002. Construction of new unencapsulated (rough) strains of *S. pneumoniae*. *Research in Microbiology*, 153(4), pp.243–247.

- Pelaia, G. *et al.*, 2006. Respiratory infections and asthma. *Respiratory Medicine*, 100(5), pp.775–784.
- Percival, S.L., Suleman, L. & Donelli, G., 2015. Healthcare-Associated infections, medical devices and biofilms: Risk, tolerance and control. *Journal of Medical Microbiology*, 64(4), pp.323–334.
- Peters, A. *et al.*, 2006. Translocation and potential neurological effects of fine and ultrafine particles a critical update. *Particle and fibre toxicology*, 3, p.13.
- Petrova, O.E. & Sauer, K., 2016. Escaping the biofilm in more than one way: Desorption, detachment or dispersion. *Current Opinion in Microbiology*, 30, pp.67–78.
- Pettigrew, M.M. *et al.*, 2014. Dynamic changes in the *S. pneumoniae* transcriptome during transition from biofilm formation to invasive disease upon influenza A virus infection. *Infection and Immunity*, 82(11), pp.4607–4619.
- Pettigrew, M.M. *et al.*, 2006. Variation in the presence of neuraminidase genes among *S. pneumoniae* isolates with identical sequence types. *Infection and Immunity*, 74(6), pp.3360–3365.
- PHE, 2016. *Public Health England Quarterly Epidemiological Commentary: Mandatory MRSA, MSSA and E. coli bacteraemia, and C. difficile infection data (up to October – December 2015)*.
- Philip, S. *et al.*, 2014. Global chemical composition of ambient fine particulate matter for exposure assessment. *Environmental Science and Technology*, 48(22), pp.13060–13068.
- Phipps, J.C. *et al.*, 2010. Cigarette smoke exposure impairs pulmonary bacterial clearance and alveolar macrophage complement-mediated phagocytosis of *S. pneumoniae*. *Infection and Immunity*, 78(3), pp.1214–1220.
- Polz, M.F. & Cavanaugh, C.M., 1998. Bias in template-to-product ratios in multitemplate PCR. *Applied and Environmental Microbiology*, 64(10), pp.3724–3730.
- Porto, J.P. *et al.*, 2013. Active surveillance to determine the impact of methicillin resistance on mortality in patients with bacteremia and influences of the use of antibiotics on the development of MRSA infection. *Revista da Sociedade Brasileira de Medicina Tropical*, 46(6), pp.713–718.
- Price, K.E., Greene, N.G. & Camilli, A., 2012. Export requirements of pneumolysin in *S. pneumoniae*. *Journal of Bacteriology*, 194(14), pp.3651–3660.

- Price, M.N., Dehal, P.S. & Arkin, A.P., 2010. FastTree 2 - Approximately maximum-likelihood trees for large alignments. *PLoS ONE*, 5(3).
- De Prins, S. *et al.*, 2014. Airway oxidative stress and inflammation markers in exhaled breath from children are linked with exposure to black carbon. *Environment International*, 73, pp.440–446.
- Provost, E.B. *et al.*, 2016. Short-term fluctuations in personal black carbon exposure are associated with rapid changes in carotid arterial stiffening. *Environment International*, 88, pp.228–234.
- Przyk, E.P., Held, A. & Charoud-Got, J., 2008. *Development of particulate matter certified reference materials (PM₁₀ CRMs) Final report*. JRC Scientific and Technical Reports.
- Psoter, K.J. *et al.*, 2015. Fine particulate matter exposure and initial *Pseudomonas aeruginosa* acquisition in cystic fibrosis. *Annals of the American Thoracic Society*, 12(3), pp.385–391.
- Public Health England, 2013. Voluntary reporting of *S. aureus* bacteraemia in England, Wales and Northern Ireland, 2013. Public Health England.
- Purvis, A. & Hector, A., 2000. Getting the measure of biodiversity. *Nature Insight Biodiversity*, 405(May), p.vol 405 no. 6783.
- Qin, L. *et al.*, 2013. Impaired capsular polysaccharide is relevant to enhanced biofilm formation and lower virulence in *S. pneumoniae*. *Journal of Infection and Chemotherapy*, 19(2), pp.261–271.
- Qin, Z. *et al.*, 2007. Formation and properties of in vitro biofilms of ica-negative *Staphylococcus epidermidis* clinical isolates. *Journal of Medical Microbiology*, 56(1), pp.83–93.
- Qiu, H. *et al.*, 2014. Coarse particulate matter associated with increased risk of emergency hospital admissions for pneumonia in Hong Kong. *Thorax*, 69(11), pp.1027–1033.
- Quast, C. *et al.*, 2013. The SILVA ribosomal RNA gene database project: Improved data processing and web-based tools. *Nucleic Acids Research*, 41(D1), pp.590–596.
- Quinn, G.A., Tarwater, P.M. & Cole, A.M., 2009. Subversion of interleukin-1-mediated host defence by a nasal carrier strain of *S. aureus*. *Immunology*, 128(1 PART 2).
- R Core Team, 2015. R: A Language and Environment for Statistical Computing. *R Foundation for Statistical Computing Vienna Austria*, {ISBN} 3–900051–07–0.

- Rai, P. *et al.*, 2015. *S. pneumoniae* secretes hydrogen peroxide leading to DNA damage and apoptosis in lung cells. *Proceedings of the National Academy of Sciences of the United States of America*, 112(26), pp.E3421–30.
- Ramette, A., 2007. Multivariate analyses in microbial ecology. *FEMS Microbiology Ecology*, 62(2), pp.142–160.
- Rammelkamp, C.H. & Maxon, T., 1942. Resistance of *S. aureus* to the Action of Penicillin. *Experimental Biology and Medicine*, 51 (3), pp.386–389.
- Rand, K.H. & Houck, H., 1990. Taq polymerase contains bacterial DNA of unknown origin. *Molecular and Cellular Probes*, 4(6), pp.445–450.
- Ranjan, R. *et al.*, 2016. Analysis of the microbiome: Advantages of whole genome shotgun versus 16S amplicon sequencing. *Biochemical and Biophysical Research Communications*, 469(4), pp.967–977.
- Ratner, A.J. *et al.*, 2006. Epithelial Cells Are Sensitive Detectors of Bacterial Pore-forming Toxins. *Journal of Biological Chemistry*, 281(18), pp.12994–12998.
- Reid, S.D. *et al.*, 2009. *S. pneumoniae* forms surface-attached communities in the middle ear of experimentally infected chinchillas. *The Journal of infectious diseases*, 199, pp.786–794.
- Renwick, L.C., 2004. Increased inflammation and altered macrophage chemotactic responses caused by two ultrafine particle types. *Occupational and Environmental Medicine*, 61(5), pp.442–447.
- Rice, K.C. *et al.*, 2007. The cidA murein hydrolase regulator contributes to DNA release and biofilm development in *S. aureus*. *Proceedings of the National Academy of Sciences*, 104(19), pp.8113–8118.
- Richards, L. *et al.*, 2010. The immunising effect of pneumococcal nasopharyngeal colonisation; protection against future colonisation and fatal invasive disease. *Immunobiology*, 215(4), pp.251–263.
- Richards, R.L. *et al.*, 2015. Persistent *S. aureus* isolates from two independent bacteraemia display increased bacterial fitness and novel immune evasion phenotypes. *Infection and Immunity*, 83(June), pp.IAI.00255–15.
- Riedl, M. & Diaz-Sanchez, D., 2005. Biology of diesel exhaust effects on respiratory function. *Journal of Allergy and Clinical Immunology*, 115(2), pp.221–228.
- Robertson, C.E. *et al.*, 2013. Culture-independent analysis of aerosol microbiology in a metropolitan subway system. *Applied and Environmental Microbiology*, 79(11), pp.3485–3493.

- Rosa, M.J. *et al.*, 2014. Domestic airborne black carbon levels and 8-isoprostane in exhaled breath condensate among children in New York City. *Environmental Research*, 135, pp.105–110.
- Rossi-Tamisier, M. *et al.*, 2015. Cautionary tale of using 16S rRNA gene sequence similarity values in identification of human-associated bacterial species. *International Journal of Systematic and Evolutionary Microbiology*, 65(6), pp.1929–1934.
- Rückerl, R. *et al.*, 2006. Air pollution and markers of inflammation and coagulation in patients with coronary heart disease. *American Journal of Respiratory and Critical Care Medicine*, 173(4), pp.432–441.
- Rylance, J. *et al.*, 2015. Household air pollution causes dose-dependent inflammation and altered phagocytosis in human macrophages. *American Journal of Respiratory Cell and Molecular Biology*, 52(5), pp.584–593.
- Sætterstrøm, B. *et al.*, 2012. A Method to Assess the Potential Effects of Air Pollution Mitigation on Healthcare Costs. *Journal of Environmental and Public Health*, 2012, pp.1–10.
- Safdar, N. & Bradley, E.A., 2008. The risk of infection after nasal colonization with *S. aureus*. *Am.J.Med.*, 121(1555-7162), pp.310–315.
- Salami, O. & Marsland, B.J., 2015. Has the airway microbiome been overlooked in respiratory disease? *Genome medicine*, 7(1), p.62. Available at: <http://genomemedicine.com/content/7/1/62>.
- Salim, S.Y., Kaplan, G.G. & Madsen, K.L., 2013. Air pollution effects on the gut microbiota. *Gut Microbes*, 5(2), pp.215–219.
- Salisbury, E. *et al.*, 2015. *Air Quality Pollutant Inventories for England, Scotland, Wales and Northern Ireland: 1990 – 2013*.
- Salter, S.J. *et al.*, 2014. Reagent and laboratory contamination can critically impact sequence-based microbiome analyses. *BMC Biology*, 12(1), p.87.
- Samoli, E. *et al.*, 2016. Associations of short-term exposure to traffic-related air pollution with cardiovascular and respiratory hospital admissions in London, UK. *Occupational and environmental medicine*, 26(2), pp.125–132.
- Sanabria, T.J. *et al.*, 1990. Increasing frequency of staphylococcal infective endocarditis. Experience at a university hospital, 1981 through 1988. *Archives of internal medicine*, 150(6), pp.1305–1309.

- Sanchez, C.J. *et al.*, 2010. The pneumococcal serine-rich repeat protein is an intraspecies bacterial adhesin that promotes bacterial aggregation in Vivo and in biofilms. *PLoS Pathogens*, 6(8), pp.33–34.
- Sanchez, C.J. *et al.*, 2011. *S. pneumoniae* in biofilms are unable to cause invasive disease due to altered virulence determinant production. *PLoS ONE*, 6(12).
- Sanderson, A.R., Leid, J.G. & Hunsaker, D., 2006. Bacterial biofilms on the sinus mucosa of human subjects with chronic rhinosinusitis. *The Laryngoscope*, 116(7), pp.1121–6.
- Savage, V.J., Chopra, I. & O'Neill, A.J., 2013. *S. aureus* biofilms promote horizontal transfer of antibiotic resistance. *Antimicrobial Agents and Chemotherapy*, 57(4), pp.1968–1970.
- Schleicher, N. *et al.*, 2013. Spatio-temporal variations of black carbon concentrations in the Megacity Beijing. *Environmental Pollution*, 182, pp.382–401.
- Schmalenberger, A., Schwieger, F. & Tebbe, C.C., 2001. Effect of Primers Hybridizing to Different Evolutionarily Conserved Regions of the Small-Subunit rRNA Gene in PCR-Based Microbial Community Analyses and Genetic Profiling. *Applied and Environmental Microbiology*, 67(8), pp.3557–3563.
- Schulz, M. *et al.*, 2006. Radiative forcing by aerosols as derived from the AeroCom present-day and pre-industrial simulations. *Atmospheric Chemistry and Physics*, 6(June 2016), pp.5225–5246.
- Sevillano, D. *et al.*, 2008. Beta-Lactam effects on mixed cultures of common respiratory isolates as an approach to treatment effects on nasopharyngeal bacterial population dynamics. *PLoS ONE*, 3(12), pp.1–8.
- Shah, A.S. V *et al.*, 2013. Global association of air pollution and heart failure: a systematic review and meta-analysis. *Lancet*, 382(9897), pp.1039–48.
- Shah, A.S. V *et al.*, 2015. Short term exposure to air pollution and stroke: systematic review and meta-analysis. *BMJ (Clinical research ed.)*, 350, p.h1295.
- Shah, S.D. *et al.*, 2004. Emission Rates of Particulate Matter and Elemental and Organic Carbon from In-Use Diesel Engines. *Environmental Science and Technology*, 38(9), pp.2544–2550.
- Shainheit, M.G. *et al.*, 2014. The core promoter of the capsule operon of *S. pneumoniae* is necessary for colonization and invasive disease. *Infection and Immunity*, 82(2), pp.694–705.
- Shak, J.R., Ludewick, H.P., *et al.*, 2013a. Novel role for the *S. pneumoniae* toxin pneumolysin in the assembly of biofilms. *mBio*, 4(5), pp.1–10.

- Shak, J.R., Vidal, J.E. & Klugman, K.P., 2013b. Influence of bacterial interactions on pneumococcal colonization of the nasopharynx. *Trends in Microbiology*, 21(3), pp.129–135.
- Shannon, C.E., 1948. A Mathematical Theory of Communication. *Bell System Technical Journal*, 27(3), pp.379–423.
- Shen, H., Rogelj, S. & Kieft, T.L., 2006. Sensitive, real-time PCR detects low-levels of contamination by *Legionella pneumophila* in commercial reagents. *Molecular and Cellular Probes*, 20(3-4), pp.147–153.
- Shepard, R.N., 1966. Metric structures in ordinal data. *Journal of Mathematical Psychology*, 3(2), pp.287–315.
- Shi, L. *et al.* 2016. Low-Concentration PM2.5 and Mortality: Estimating Acute and Chronic Effects in a Population-Based Study. *Environmental Health Perspectives*. 124(1), pp46-52.
- Shrestha, G., Traina, S.J. & Swanston, C.W., 2010. Black carbon's properties and role in the environment: A comprehensive review. *Sustainability*, 2(1), pp.294–320.
- Simell, B. *et al.*, 2012. The fundamental link between pneumococcal carriage and disease. *Expert review of vaccines*, 11(7), pp.841–55.
- Simpson, E.H., 1949. Measurement of Diversity. *Nature*, 163(688).
- Singh, R. *et al.*, 2010. Penetration of antibiotics through *S. aureus* and *Staphylococcus epidermidis* biofilms. *Journal of Antimicrobial Chemotherapy*, 65(9), pp.1955–1958.
- Sipos, R. *et al.*, 2007. Effect of primer mismatch, annealing temperature and PCR cycle number on 16S rRNA gene-targetting bacterial community analysis. *FEMS Microbiology Ecology*, 60(2), pp.341–350.
- Sloss, L., 2012. *Black carbon emissions in India*. US Department of State
- Smith, A.W. *et al.*, 2002. Characterization of the dihydrolipoamide dehydrogenase from *S. pneumoniae* and its role in pneumococcal infection. *Molecular Microbiology*, 44(2), pp.431–448.
- Smith, C.M. *et al.*, 2014. Respiratory syncytial virus increases the virulence of *S. pneumoniae* by binding to penicillin binding protein 1a. A new paradigm in respiratory infection. *American journal of respiratory and critical care medicine*, 190(2), pp.196–207.
- Smith, K. *et al.*, 2008. Biofilm formation by Scottish clinical isolates of *S. aureus*. *Journal of Medical Microbiology*, 57(8), pp.1018–1023.

- Smith, K.R. *et al.*, 2011. Effect of reduction in household air pollution on childhood pneumonia in Guatemala (RESPIRE): A randomised controlled trial. *The Lancet*, 378(9804), pp.1717–1726.
- Snow, S.J. *et al.*, 2014. Air pollution upregulates endothelial cell procoagulant activity via ultrafine particle-induced oxidant signaling and tissue factor expression. *Toxicological Sciences*, 140(1), pp.83–93.
- Soo, R.M. *et al.*, 2014. An expanded genomic representation of the phylum Cyanobacteria. *Genome Biology and Evolution*, 6(5), pp.1031–1045.
- Sorensen, U.B.S. *et al.*, 1988. Ultrastructural localization of capsules, cell wall polysaccharide, cell wall proteins, and F antigen in pneumococci. *Infection and Immunity*, 56(8), pp.1890–1896.
- Sorensen, U.B.S. *et al.*, 1990. Covalent linkage between the capsular polysaccharide and the cell wall peptidoglycan of *S. pneumoniae* revealed by immunochemical methods. *Microbial Pathogenesis*, 8(5), pp.325–334.
- Southam, D.S. *et al.*, 2002. Distribution of intranasal instillations in mice: effects of volume, time, body position, and anesthesia. *American journal of physiology. Lung cellular and molecular physiology*, 282(4), pp.L833–L839.
- Sowash, M.G. & Uhlemann, A.-C., 2014. Community-associated methicillin-resistant *S. aureus* case studies. *Methods in molecular biology (Clifton, N.J.)*, 1085, pp.25–69.
- Stackebrandt, E. & Goebel, B.M., 1994. Taxonomic Note: A Place for DNA-DNA Reassociation and 16S rRNA Sequence Analysis in the Present Species Definition in Bacteriology. *International Journal of Systematic Bacteriology*, 44(4), pp.846–849.
- Steenhof, M. *et al.*, 2014. Air pollution exposure affects circulating white blood cell counts in healthy subjects: the role of particle composition, oxidative potential and gaseous pollutants - the RAPTES project. *Inhal Toxicol*, 26(3), pp.141–165.
- Stefani, S. *et al.*, 2015. Insights and clinical perspectives of daptomycin resistance in *S. aureus*: A review of the available evidence. *Int.J.Antimicrob.Agents*, 46(1872-7913), pp.278–289.
- Stulik, L. *et al.*, 2014. α -hemolysin activity of methicillin-susceptible *S. aureus* predicts ventilator-associated pneumonia. *American Journal of Respiratory and Critical Care Medicine*, 190(10), pp.1139–1148.
- Sun, Q. *et al.*, 2005. Long-term air pollution exposure and acceleration of atherosclerosis and vascular inflammation in an animal model. *JAMA : the journal of the American Medical Association*, 294(23), pp.3003–3010.

- Sun, S. *et al.*, 2015. Temperature as a modifier of the effects of fine particulate matter on acute mortality in Hong Kong. *Environmental Pollution*, 205, pp.357–364.
- Sun, X. *et al.*, 2016. The associations between birth weight and exposure to fine particulate matter (PM_{2.5}) and its chemical constituents during pregnancy: A meta-analysis. *Environmental Pollution*, 211, pp.38–47.
- Suraju, M.O. *et al.*, 2015. The effects of indoor and outdoor dust exposure on the growth, sensitivity to oxidative-stress, and biofilm production of three opportunistic bacterial pathogens. *Science of The Total Environment*, 538, pp.949–958.
- Suri, R. *et al.*, 2015. Exposure to welding fumes and lower airway infection with *S. pneumoniae*. *Journal of Allergy and Clinical Immunology*, 137(2), pp.527–534.e7.
- Tanner, M.A. *et al.*, 1998. Specific ribosomal DNA sequences from diverse environmental settings correlate with experimental contaminants. *Applied and Environmental Microbiology*, 64(8), pp.3110–3113.
- Tarrant, E., 2013. *The Role of Hfq in S. aureus Gene Regulation*. University of Leicester.
- Taylor, E.T. & Nakai, S., 2012. Prevalence of Acute Respiratory Infections in Women and Children in Western Sierra Leone due to Smoke from Wood and Charcoal Stoves. *International Journal of Environmental Research and Public Health*, 9(12), pp.2252–2265.
- Teixeira, L.M. & Merquior, V.L.C., 2014. The Family Moraxellaceae. In *The Prokaryotes: Gammaproteobacteria*. pp. 443–476.
- Tellabati, A. *et al.*, 2010. Acute exposure of mice to high-dose ultrafine carbon black decreases susceptibility to pneumococcal pneumonia. *Particle and Fibre Toxicology*, 7(1), p.30.
- Tettelin, H. *et al.*, 2001. Complete Genome Sequence of a Virulent Isolate of *S. pneumoniae*. *Science*, 293(5529), pp.498–506.
- Thevaranjan, N. *et al.*, 2016. *S. pneumoniae* colonization disrupts the microbial community within the upper respiratory tract of aging mice. *Infection and Immunity*, (January), pp.IAI.01275–15.
- Thistlethwaite, G. *et al.*, 2012. *Air Quality Pollutant Inventories for England, Scotland, Wales and Northern Ireland: 1990 – 2011*. National Atmospheric Emissions Inventory.
- Thomson, E.M. *et al.*, 2015. Cytotoxic and inflammatory potential of size-fractionated particulate matter collected repeatedly within a small urban area. *Particle and Fibre Toxicology*, 12(1), p.24.

- Thurston, G. & Lippmann, M., 2015. Ambient Particulate Matter Air Pollution and Cardiopulmonary Diseases. *Seminars in Respiratory and Critical Care Medicine*, 1(212), pp.422–432.
- Tilley, S.J. *et al.*, 2005. Structural basis of pore formation by the bacterial toxin pneumolysin. *Cell*, 121(2), pp.247–256.
- du Toit, M. *et al.*, 2014. The family *Streptococcaceae*. In *The Prokaryotes: Firmicutes and Tenericutes*. pp. 367–370.
- Tormo, M.Á. *et al.*, 2005. SarA is an essential positive regulator of *Staphylococcus epidermidis* biofilm development. *Journal of Bacteriology*, 187(7), pp.2348–2356.
- Trappetti, C. *et al.*, 2009. Sialic acid: a preventable signal for pneumococcal biofilm formation, colonization, and invasion of the host. *The Journal of infectious diseases*, 199(10), pp.1497–1505.
- Trappetti, C. *et al.*, 2011. Extracellular Matrix Formation Enhances the Ability of *S. pneumoniae* to Cause Invasive Disease. *PLoS ONE*, 6(5), p.e19844.
- Trotonda, M.P. *et al.*, 2005. SarA positively controls Bap-dependent biofilm formation in *S. aureus*. *Journal of Bacteriology*, 187(16), pp.5790–5798.
- Tuan, T.S., Venâncio, T.S. & Nascimento, L.F.C., 2015. Air pollutants and hospitalization due to pneumonia among children. An ecological time series study. *Sao Paulo Medical Journal*, 133(5), pp.408–413.
- USEPA, 2012. *Report to Congress on Black Carbon*. United States Environmental Protection Agency.
- Uski, O.J. *et al.*, 2012. Acute systemic and lung inflammation in C57Bl/6J mice after intratracheal aspiration of particulate matter from small-scale biomass combustion appliances based on old and modern technologies. *Inhalation Toxicology*, 24(14), pp.952–965.
- Valentino, M.D. *et al.*, 2014. Unencapsulated *S. pneumoniae* from conjunctivitis encode variant traits and belong to a distinct phylogenetic cluster. *Nature communications*, 5(May), p.5411.
- Valle, J. *et al.*, 2012. Bap, a Biofilm Matrix Protein of *S. aureus* Prevents Cellular Internalization through Binding to GP96 Host Receptor. *PLoS Pathogens*, 8(8).
- van Belkum, A. *et al.*, 2009. Reclassification of *S. aureus* nasal carriage types. *The Journal of infectious diseases*, 199(12), pp.1820–1826.
- van de Beek, D. *et al.*, 2002. Cognitive impairment in adults with good recovery after bacterial meningitis. *The Journal of infectious diseases*, 186(7), pp.1047–52.

- van de Beek, D. *et al.*, 2004. Clinical features and prognostic factors in adults with bacterial meningitis. *The New England journal of medicine*, 351(18), pp.1849–1859.
- van Rossum, A.M.C., Lysenko, E.S. & Weiser, J.N., 2005. Host and Bacterial Factors Contributing to the Clearance of Colonization by *S. pneumoniae* in a Murine Model Host and Bacterial Factors Contributing to the Clearance of Colonization by *S. pneumoniae* in a Murine Model. *Infection and Immunity*, 73(11), pp.7718–7726.
- Varon, E. *et al.*, 2000. Impact of antimicrobial therapy on nasopharyngeal carriage of *S. pneumoniae*, *Haemophilus influenzae*, and *Branhamella catarrhalis* in children with respiratory tract infections. *Clinical Infectious Diseases*, 31(2), pp.477–81.
- Vernatter, J. & Pirofski, L., 2013. Current concepts in host-microbe interaction leading to pneumococcal pneumonia. *Current opinion in infectious diseases*, 26(3), pp.277–83.
- Vesterdal, L.K. *et al.*, 2012. Carbon black nanoparticles and vascular dysfunction in cultured endothelial cells and artery segments. *Toxicology Letters*, 214(1), pp.19–26.
- Vilcassim, M.J.R. *et al.*, 2014. Black Carbon and Particulate Matter (PM 2.5) Concentrations in New York City’s Subway Stations. *Environmental Science & Technology*, 48(24), pp.14738–14745.
- Vlachopoulos, C. *et al.*, 2005. Acute systemic inflammation increases arterial stiffness and decreases wave reflections in healthy individuals. *Circulation*, 112(14), pp.2193–2200.
- De Vos, P. *et al.*, 2009. *Bergey’s Manual of Systematic Bacteriology - Vol 3: The Firmicutes*,
- Walker, J.A. *et al.*, 1987. Molecular cloning, characterization, and complete nucleotide sequence of the gene for pneumolysin, the sulfhydryl-activated toxin of *S. pneumoniae*. *Infection and Immunity*, 55(5), pp.1184–1189.
- Wang, B. *et al.*, 2012. An environmental chamber study of the characteristics of air pollutants released from environmental tobacco smoke. *Aerosol and Air Quality Research*, 12(6), pp.1269–1281.
- Wang, C. *et al.*, 2015. PM_{2.5} and Cardiovascular Diseases in the Elderly: An Overview. *International Journal of Environmental Research and Public Health*, 12(7), pp.8187–8197.
- Wang, Q. *et al.*, 2007. Naive Bayesian classifier for rapid assignment of rRNA sequences into the new bacterial taxonomy. *Applied and Environmental Microbiology*, 73(16), pp.5261–5267.

- Wang, R. *et al.*, 2012. Black carbon emissions in China from 1949 to 2050. *Environmental Science and Technology*, 46(14), pp.7595–7603.
- Wang, R. *et al.*, 2014. Exposure to ambient black carbon derived from a unique inventory and high-resolution model. *Proceedings of the National Academy of Sciences of the United States of America*, 111(7), pp.2459–63.
- Wang, Y., Zhang, Z. & Ramanan, N., 1997. The actinomycete *Thermobispora bispora* contains two distinct types of transcriptionally active 16S rRNA genes. *Journal of Bacteriology*, 179(10), pp.3270–3276.
- Weinberger, D.M. *et al.*, 2009. Pneumococcal capsular polysaccharide structure predicts serotype prevalence. *PLoS Pathogens*, 5(6).
- Weiser, J.N., 2010. The pneumococcus: Why a commensal misbehaves. *Journal of Molecular Medicine*, 88(2), pp.97–102.
- Weisfelt, M. *et al.*, 2006. Clinical features, complications, and outcome in adults with pneumococcal meningitis: A prospective case series. *Lancet Neurology*, 5(2), pp.123–129.
- Weiss, S. *et al.*, 2014. Tracking down the sources of experimental contamination in microbiome studies. *Genome biology*, 15(12), p.564.
- Wertheim, H.F. *et al.*, 2005. The role of nasal carriage in *S. aureus* infections. *The Lancet Infectious Diseases*, 5(12), pp.751–762.
- Whittaker, R.H., 1972. Evolution and Measurement of Species Diversity. *Taxon*, 21(2), pp.213–251.
- WHO, 2006a. *Air Quality Guidelines: Global Update 2005. Report on a working group meeting, Bonn, Germany, 18-20 October 2005*. World Health Organization
- WHO, 2006b. *WHO Air quality guidelines for particulate matter, ozone, nitrogen dioxide and sulfur dioxide*. Geneva: World Health Organization.
- WHO, 2007. *Analysis of estimates of the environmental attributable fraction by disease*. p. 33-56. World Health Organization.
- WHO, 2012. *Public Health and Environment*. [Online] Available at: http://www.who.int/phe/health_topics/outdoorair/en/ [Accessed April 19, 2016].
- WHO, 2013. *Health Effects of Particulate Matter: Policy implications for countries in eastern Europe, Caucasus and central Asia*. World Health Organization.

- WHO, 2014a. *7 Million Deaths Annually Linked To Air Pollution*. [Online] Available at: <http://www.who.int/mediacentre/news/releases/2014/air-pollution/en/> [Accessed April 19, 2016].
- WHO, 2014b. *Annual mean concentrations of fine particulate matter (PM_{2.5}) in urban areas (ug/m³), 2014*. [Online] Available at: http://www.who.int/gho/phe/outdoor_air_pollution/exposure/en/ [Accessed December 6, 2015]
- WHO, 2014c. *Antimicrobial resistance: global report on surveillance*. World Health Organization
- WHO, 2014d. *Burden of disease from Ambient Air Pollution for 2012*. World Health Organization
- WHO, 2014e. Exposure to particulate matter with an aerodynamic diameter of 10 µm or less (PM₁₀) in urban areas, 2008–2013. *Global Health Observatory Map Gallery*. Available at: http://gamapserver.who.int/mapLibrary/Files/Maps/Global_pm10_countries.png.
- WHO, 2014f. Exposure to particulate matter with an aerodynamic diameter of 2.5 µm or less (PM_{2.5}) in urban areas, 2008–2013. *Global Health Observatory Map Gallery*. Available at: http://gamapserver.who.int/mapLibrary/Files/Maps/Global_pm25_countries.png.
- WHO, 2016. *Ambient Air Pollution Database*. Available at: http://www.who.int/phe/health_topics/outdoorair/databases/cities/en/
- Wiese, S. *et al.*, 2007. Protein labeling by iTRAQ: A new tool for quantitative mass spectrometry in proteome research. *Proteomics*, 7(3), pp.340–350.
- Wintzingerode, F., Göbel, U.B. & Stackebrandt, E., 1997. Determination of microbial diversity in environmental samples: pitfalls of PCR-based analysis. *FEMS Microbiol. Rev.*, 21, pp.213–229.
- WMO/IGAC, 2012. *GAW Report No. 205 WMO/IGAC Impacts of Megacities on Air Pollution and Climate*,
- Wyllie, A.L. *et al.*, 2014. *S. pneumoniae* in saliva of Dutch primary school children. *PLoS ONE*, 9(7).
- Xiao, C. *et al.*, 2013. The effect of air pollutants on the microecology of the respiratory tract of rats. *Environmental toxicology and pharmacology*, 36(2), pp.588–94.
- Xie, S.-H. *et al.*, 2010. DNA damage and oxidative stress in human liver cell L-02 caused by surface water extracts during drinking water treatment in a waterworks in China. *Environmental and molecular mutagenesis*, 51(3), pp.229–235.

- Xu, G. *et al.*, 2008. Structure of the catalytic domain of *S. pneumoniae* sialidase NanA. *Acta Crystallographica Section F: Structural Biology and Crystallization Communications*, 64(9), pp.772–775.
- Xu, G. *et al.*, 2011. Three *S. pneumoniae* sialidases: Three different products. *Journal of the American Chemical Society*, 133(6), pp.1718–1721.
- Xu, Q. *et al.*, 2016. Fine Particulate Air Pollution and Hospital Emergency Room Visits for Respiratory Disease in Urban Areas in Beijing, China, in 2013. *Plos One*, 11(4), p.e0153099.
- Yamaguchi, N. *et al.*, 2014. Changes in the Airborne Bacterial Community in Outdoor Environments following Asian Dust Events. *Microbes and Environments*, 29(1), pp.82–88.
- Yang, H. *et al.*, 2009. Comparative study of cytotoxicity, oxidative stress and genotoxicity induced by four typical nanomaterials: The role of particle size, shape and composition. *Journal of Applied Toxicology*, 29(1), pp.69–78.
- Yang, H.M. *et al.*, 2001. Diesel exhaust particles suppress macrophage function and slow the pulmonary clearance of *Listeria monocytogenes* in rats. *Environmental Health Perspectives*, 109(5), pp.515–521.
- Yeatts, K. *et al.*, 2007. Coarse Particulate Matter (PM_{2.5-10}) Affects Heart Rate Variability, Blood Lipids, and Circulating Eosinophils in Adults with Asthma. *Environmental Health Perspectives*, 115(5), pp.709–714.
- Yin, H., Xu, L. & Cai, Y., 2015. Monetary Valuation of PM₁₀-Related Health Risks in Beijing China: The Necessity for PM₁₀ Pollution Indemnity. *International Journal of Environmental Research and Public Health*, 12(8), pp.9967–9987.
- Yin, X.J. *et al.*, 2002. Alteration of pulmonary immunity to *Listeria monocytogenes* by diesel exhaust particles (DEPs). I. Effects of DEPs on early pulmonary responses. *Environmental Health Perspectives*, 110(11), pp.1105–1111.
- Yin, X.J. *et al.*, 2003. Alteration of pulmonary immunity to *Listeria monocytogenes* by diesel exhaust particles (DEPs). II. Effects of DEPs on T-cell-mediated immune responses in rats. *Environmental Health Perspectives*, 111(4), pp.524–530.
- Ying, Z. *et al.*, 2015. Exposure to concentrated ambient particulate matter induces reversible increase of heart weight in spontaneously hypertensive rats. *Particle and fibre toxicology*, 12(1), p.1.
- You, R. *et al.*, 2015. Nanoparticulate carbon black in cigarette smoke induces DNA cleavage and Th17-mediated emphysema. *eLife*, 4(October2015).
- Yue, J. *et al.*, 2014. Linezolid versus vancomycin for skin and soft tissue infections. *Evidence-Based Child Health*, 9(1), pp.103–166.

- Yun, Y. *et al.*, 2014. Environmentally determined differences in the murine lung microbiota and their relation to alveolar architecture. *PLoS ONE*, 9(12).
- Zanobetti, A. & Schwartz, J., 2009. The effect of fine and coarse particulate air pollution on mortality: A national analysis. *Environmental Health Perspectives*, 117(6), pp.898–903.
- Zecconi, A. & Scali, F., 2013. *S. aureus* virulence factors in evasion from innate immune defenses in human and animal diseases. *Immunology Letters*, 150(1-2), pp.12–22.
- Zeka, A., Zanobetti, A., & Schwartz, J., 2005. Short term effects of particulate matter on cause specific mortality: effects of lags and modification by city characteristics. *Occupational and environmental medicine*, 62(10), pp.718–25.
- Zhang, Y. *et al.*, 2015. Short-Term Effects of Fine Particulate Matter and Temperature on Lung Function among Healthy College Students in Wuhan, China. *International journal of environmental research and public health*, 12(7), pp.7777–93.
- Zhao, C. *et al.*, 2012. Involvement of TLR2 and TLR4 and Th1/Th2 shift in inflammatory responses induced by fine ambient particulate matter in mice. *Inhalation Toxicology*, 24(13), pp.918–927.
- Zhou, H. & Kobzik, L., 2007. Effect of concentrated ambient particles on macrophage phagocytosis and killing of *S. pneumoniae*. *American Journal of Respiratory Cell and Molecular Biology*, 36(4), pp.460–465.
- Zhao, H. *et al.*, 2014. Exposure to particular matter increases susceptibility to respiratory *S. aureus* infection in rats via reducing pulmonary natural killer cells. *Toxicology*, 325, pp.180–188.
- Zhao, X. & Drlica, K., 2014. Reactive oxygen species and the bacterial response to lethal stress. *Current Opinion in Microbiology*, 21, pp.1–6.
- Zhou, M. *et al.*, 2015. Smog episodes, fine particulate pollution and mortality in China. *Environmental Research*, 136, pp.396–404.
- Zwart, G. *et al.*, 2002. Typical freshwater bacteria: An analysis of available 16S rRNA gene sequences from plankton of lakes and rivers. *Aquatic Microbial Ecology*, 28(2), pp.141–155.